

國立交通大學

土木工程學系

博士論文

三維電磁彈性迴轉體與楔形體奇異性分析

Singularity Analyses of Three-Dimensional
Magneto-Electro-Elastic Bodies of Revolution and Wedges

研究生：胡政甯

指導教授：黃炯憲 博士

中華民國一百零二年六月

三維電磁彈性迴轉體與楔形體奇異性分析

Singularity Analyses of Three-Dimensional Magneto-Electro-Elastic Bodies of Revolution and Wedges

研 究 生：胡政甯
指 導 教 授：黃炯憲 博士

Student: Cheng-Ning Hu
Advisor: Dr. Chiung-Shiann Huang



Submitted to Department of Civil Engineering
College of Engineering
National Chiao Tung University
in Partial Fulfillment of the Requirements
for the Degree of
Doctor of Philosophy
in
Civil Engineering

June 2013

HsinChu, Taiwan, Republic of China

中華民國一百零二年六月

三維電磁彈性迴轉體與楔形體奇異性分析

研究生：胡政甯

指導教授：黃炯憲 博士

國立交通大學土木工程學系博士班

摘 要

由於電磁彈性 (magneto-electro-elastic, MEE) 或壓電 (piezoelectric) 材料擁有將機械能與電磁能以及機械能與電能相互轉換的特性，因此被廣泛應用於高科技之電子設備。為了對於智能元件的優化設計以及進行相關破壞分析，則需通盤了解由幾何形狀所引致之電磁彈奇異性行為。本研究主要目標為建立電磁彈性迴轉體與楔形體之三維電磁彈奇異性漸近解。透過特徵函數展開法配合級數解直接求解於以位移、電勢與磁勢表示的三維力平衡與馬克斯威爾 (Maxwell) 方程組之漸近解。假設電磁彈性材料為橫向等向性 (transversely isotropic) 材料，其極化方向毋須平行於迴轉體之旋轉軸或是垂直於楔形體之中平面 (mid-plane)，如此將造成面外與面內之位移、電場與磁場彼此複雜之耦合關係，導致求解之困難度。在已發表的文獻中對於迴轉體或楔形體之分析，大多基於平面應變之假設，而本研究並未做任何之簡化與假設以建立迴轉體或楔形體於尖角處之漸近解。根據漸近解，將探討有關於極化方向、幾何形狀、材料種類與邊界條件對於電磁彈性與壓電迴轉體與楔形體奇異性階數之影響。其中迴轉體與楔形體可為單一電磁彈性材料 ($\text{BaTiO}_3\text{-CoFe}_2\text{O}_4$) 或壓電材料 (PZT-4 與 PZT-6B) 以及電磁彈性/各向同性彈性材料 ($\text{BaTiO}_3\text{-CoFe}_2\text{O}_4/\text{Si}$)、電磁彈性/壓電材料 ($\text{BaTiO}_3\text{-CoFe}_2\text{O}_4/\text{PZT-4}$ 或 $\text{BaTiO}_3\text{-CoFe}_2\text{O}_4/\text{PZT-6B}$)、雙電磁彈性材料 ($\text{BaTiO}_3\text{-CoFe}_2\text{O}_4(V_I^{(1)} = 50\%)/\text{BaTiO}_3\text{-CoFe}_2\text{O}_4(V_I^{(2)} = 20\%)$)、壓電/各向同性彈性材料 (PZT-4/Si 或 PZT-6B/Si) 或雙壓電材料 (PZT-4/PZT-6B)。

關鍵詞：奇異性、迴轉體、楔形體、電磁彈性材料、壓電材料

Singularity Analyses of Three-Dimensional Magneto-Electro-Elastic Bodies of Revolution and Wedges

Student: Cheng-Ning Hu

Advisor: Dr. Chiung-Shiann Huang

Department of Civil Engineering
National Chiao Tung University

ABSTRACT

Magneto-electro-elastic (MEE) materials and piezoelectric material are able to exchange mechanical, electric, and magnetic forms of energy among themselves and have been widely used in electronic devices. A comprehensive understanding of the magneto-electro-elastic singularities induced by geometry is valuable in optimizing the design of MEE components and analyzing their failures. The main purpose of this research is to establish three-dimensional asymptotic solutions for magneto-electro-elastic singularities in bodies of revolution and wedges. The solutions are obtained by combining an eigenfunction expansion approach with the power series solution method to solve three-dimensional equilibrium equations and Maxwell's equations in terms of mechanical displacement components and electric and magnetic potentials. Assume the MEE material is transversely isotropic, its polarization direction is not necessarily parallel to the axis of revolution of a body of revolution or normal to the mid-plane of a wedge. Therefore, the in-plane components of displacement, electric, and magnetic fields are generally coupled with their out-of-plane components, which causes difficulties in finding the solution. The analyses of bodies of revolution and wedges in the published literature are based on generalized plane strain assumption. However, the proposed method makes no simplification or assumption to construct the asymptotic solutions at vertex of bodies of revolution and wedges. The developed solutions are further employed to examine the effects of the direc-

tion of polarization, the configuration, the material components and boundary conditions on the orders of the MEE singularities in bodies of revolution and wedges that comprise a single MEE material ($\text{BaTiO}_3\text{-CoFe}_2\text{O}_4$) or a single piezoelectric material (PZT-4 and PZT-6B) and bonded MEE/isotropic elastic ($\text{BaTiO}_3\text{-CoFe}_2\text{O}_4/\text{Si}$), MEE/piezoelectric ($\text{BaTiO}_3\text{-CoFe}_2\text{O}_4/\text{PZT-4}$ or $\text{BaTiO}_3\text{-CoFe}_2\text{O}_4/\text{PZT-6B}$), MEE/MEE($\text{BaTiO}_3\text{-CoFe}_2\text{O}_4(V_I^{(1)} = 50\%)/\text{BaTiO}_3\text{-CoFe}_2\text{O}_4(V_I^{(2)} = 20\%)$), piezoelectric/isotropic elastic (PZT-4/Si 或 PZT-6B/Si), or piezoelectric/piezoelectric (PZT-4/PZT-6B) materials.

Keywords: singularity, body of revolution, wedge, magneto-electro-elastic material, piezoelectric material



致 謝

感謝恩師 黃炯憲教授於博士班四年來的指導，於過程中看見老師對於學術的嚴謹態度，以及對於研究品質之要求，心中敬佩不已。對於計算力學領域可我說是半路出家，若非老師耐心指引研究方向，相信無法完成本篇論文以及多篇期刊，於此獻上最誠摯的謝意。

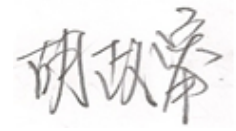
感謝我的啟蒙老師 陳誠直教授於碩士班及博士班前期的指導，陳老師給了我很多學習機會，也教導我許多關於實務操作上的知識及方法。雖然最後沒有由老師的門下畢業，但老師對我的影響絕對是相當深刻，致上最由衷的感謝。

口試期間，感謝 吳致平教授、胡宣德教授、交通大學土木系劉俊秀教授、洪士林教授與郭心怡教授於百忙之中擔任口試委員，並細心審閱且提供許多寶貴的建議與指正，使本論文更臻完備。

感謝 明儒學長、威智學長、連杰學長與交交學長，在這多年的研究路途中給予我無論在課業及生活上許多協助，希望各位學長在研究或工作上都能順心。感謝研究所同學明昌、紀勳、建霖與博士班學弟政億，認識你們真好，很懷念同甘共苦的日子。感謝我可愛的學弟璿至、俞燦、煒銘、孟暉、岳勳、顯嘉以及同學嘉儀，永遠不會忘記每個瘋狂的夜晚，真的讓我的研究生涯「多采多姿」，希望大家在各自崗位繼續努力，我們友誼長存。感謝研究室的博士班夥伴靖俞，真的當了很久的同學，在這祝福你一切順利。

謹將本文獻給我最敬愛的父母以及最疼愛我的奶奶，謝謝您們無悔的付出與多年來對我的關愛與支持，讓我在沒有後顧之憂的環境下完成學業，感恩之情已溢乎文字所能表達。最後，感謝女友怡瑤體諒，伴我度過漫長研究生涯，有你的生活真的很開心，使我未曾感到絲毫寂寞。曾經幫助過我的人實在太多，族繁不

及備載，若有疏漏，還望請見諒。再次感謝大家，願與各位分享畢業時刻的喜悅及榮耀。



2013/6/21 工二館 406



目 錄

中文摘要.....	i
英文摘要.....	ii
致謝.....	iv
目錄.....	vi
圖目錄.....	ix
表目錄.....	xii
符號表.....	xiii
第一章 緒論.....	1
1.1 前言.....	1
1.2 研究背景及動機.....	1
1.2.1 壓電效應.....	2
1.2.2 壓電材料.....	2
1.2.3 電磁彈性材料.....	2
1.3 文獻回顧.....	3
1.3.1 彈性楔形體之應力奇異性.....	3
1.3.2 壓電楔形體之電彈奇異性.....	5
1.3.3 電磁彈性楔形體之應力奇異性.....	6
1.3.4 彈性迴轉體之應力奇異性.....	7
1.3.5 壓電迴轉體之應力奇異性.....	7
1.4 研究目的.....	7
1.5 研究方法.....	8

1.6 研究內容	8
第二章 三維電磁彈性迴轉體之奇異性	10
2.1 電磁彈性力學本構方程式	10
2.2 三維力平衡方程式與馬克斯威爾方程式	12
2.3 電磁彈性迴轉體於尖角處之漸近解.....	16
2.4 電磁彈性迴轉體之邊界條件與連續條件	28
2.5 壓電迴轉體於尖角處之漸近解	30
2.6 壓電迴轉體之邊界條件與連續條件.....	35
第三章 電磁彈性迴轉體奇異性之結果與討論	36
3.1 迴轉體奇異性漸近解之驗證.....	36
3.2 壓電迴轉體奇異性結果與討論	37
3.2.1 單一壓電材料迴轉體	37
3.2.2 雙壓電材料迴轉體.....	38
3.2.3 壓電/彈性材料 Si 迴轉體.....	40
3.3 電磁彈迴轉體奇異性結果與討論	41
3.3.1 單一電磁彈性材料迴轉體.....	41
3.3.2 雙電磁彈性材料迴轉體	42
3.3.3 電磁彈性/彈性材料 Si 迴轉體	44
3.3.4 電磁彈性/壓電材料迴轉體.....	45
第四章 三維電磁彈性楔形體之奇異性	49
4.1 電磁彈楔形體於尖角處之漸近解	49
4.2 電磁彈性楔形體之邊界條件與連續條件	56
4.3 壓電楔形體於尖角處之漸近解	57
4.4 壓電楔形體之邊界條件與連續條件.....	59

第五章 電磁彈楔形體奇異性之結果與討論	60
5.1 楔形體奇異性漸近解之驗證	60
5.2 壓電楔形體奇異性結果與討論	61
5.2.1 單一壓電材料楔形體	61
5.2.2 雙壓電材料楔形體	62
5.2.3 壓電/彈性材料 Si 楔形體	64
5.3 電磁彈楔形體奇異性結果與討論	65
5.3.1 單一電磁彈性材料楔形體	65
5.3.2 雙電磁彈性材料楔形體	66
5.3.3 電磁彈性/彈性材料 Si 楔形體	68
5.3.4 電磁彈性/壓電材料楔形體	69
第六章 結論與建議	72
6.1 結論	72
6.2 建議	73
參考文獻	74
附錄 A：座標系統轉換	131
附錄 B：以位移、電勢與磁勢表示應力、電位移與磁感應強度	133
附錄 C：式 (4.3) 之變係數	135
個人簡歷	137

圖 目 錄

圖 1.1	幾何或材料不連續示意圖	85
圖 1.2	材料可能缺陷示意圖	85
圖 2.1	含尖角之雙材料旋轉體	86
圖 2.2	迴轉體幾何形狀	86
圖 2.3	圓柱 (r, Z) 與尖角 (ρ, ξ) 座標系統	87
圖 2.4	迴轉體子域 $\xi \in [\xi_0, \xi_n]$	87
圖 3.1	單 PZT-4 壓電迴轉體 λ_1 隨 θ 之變化	88
圖 3.2	單 PZT-6B 壓電迴轉體 λ_1 隨 θ 之變化	88
圖 3.3	不同邊界條件下單 PZT-4 迴轉體 λ_1 隨 β 之變化	89
圖 3.4	不同邊界條件下單 PZT-6B 迴轉體 λ_1 隨 β 之變化	89
圖 3.5	雙壓電迴轉體 $\text{Re}[\lambda_1]$ 隨 θ 之變化	90
圖 3.6	不同邊界條件下雙壓電迴轉體 $\text{Re}[\lambda_1]$ 之變化	91
圖 3.7	壓電材料/Si 迴轉體 $\text{Re}[\lambda_1]$ 隨 θ 之變化	92
圖 3.8	不同邊界條件下壓電材料/Si 迴轉體 $\text{Re}[\lambda_1]$ 隨 β 之變化	93
圖 3.9	單 $\text{BaTiO}_3\text{-CoFe}_2\text{O}_4$ 迴轉體 λ_1 隨 θ 之變化	94
圖 3.10	不同邊界條件下單 $\text{BaTiO}_3\text{-CoFe}_2\text{O}_4$ 迴轉體 λ_1 隨 β 之變化	95
圖 3.11	雙 $\text{BaTiO}_3\text{-CoFe}_2\text{O}_4$ 迴轉體 λ_1 隨 θ 之變化	96
圖 3.12	不同邊界條件下雙 $\text{BaTiO}_3\text{-CoFe}_2\text{O}_4$ 迴轉體 $\text{Re}[\lambda_1]$ 隨 β 之變化	97
圖 3.13	$\text{BaTiO}_3\text{-CoFe}_2\text{O}_4/\text{Si}$ 迴轉體 λ_1 隨 θ 之變化	98
圖 3.14	不同邊界條件下 $\text{BaTiO}_3\text{-CoFe}_2\text{O}_4/\text{Si}$ 迴轉體 $\text{Re}[\lambda_1]$ 隨 β 之變化	99
圖 3.15	$\text{BaTiO}_3\text{-CoFe}_2\text{O}_4/\text{PZT-4}$ 迴轉體 $\text{Re}[\lambda_1]$ 隨 θ 之變化	100

圖 3.16	BaTiO ₃ -CoFe ₂ O ₄ /PZT-6B 迴轉體 $\text{Re}[\lambda_1]$ 隨 θ 之變化	101
圖 3.17	不同邊界條件下 BaTiO ₃ -CoFe ₂ O ₄ /PZT-4 迴轉體 $\text{Re}[\lambda_1]$ 隨 β 之變化	102
圖 3.18	不同邊界條件下 BaTiO ₃ -CoFe ₂ O ₄ /PZT-6B 迴轉體 $\text{Re}[\lambda_1]$ 隨 β 之變化	103
圖 4.1	楔形體示意圖	104
圖 4.2	楔形體 (r, θ) 座標系統	104
圖 4.3	楔形體子域 $\theta \in [\theta_0, \theta_n]$	105
圖 4.4	楔形體幾何示意圖	105
圖 5.1	不同邊界條件下單壓電材料楔形體 λ_1 隨 β 之變化	106
圖 5.2	不同邊界條件下單壓電材料楔形體 $\text{Re}[\lambda_1]$ 隨 γ 之變化	107
圖 5.3	不同邊界條件下單壓電材料楔形體 $\text{Re}[\lambda_1]$ 隨 θ 之變化	108
圖 5.4	不同邊界條件下雙壓電材料楔形體 $\text{Re}[\lambda_1]$ 隨 β 之變化	109
圖 5.5	不同邊界條件下雙壓電材料楔形體 $\text{Re}[\lambda_1]$ 隨 γ 之變化	110
圖 5.6	不同邊界條件下雙壓電材料楔形體 $\text{Re}[\lambda_1]$ 隨 θ 之變化	111
圖 5.7	不同邊界條件下壓電材料/Si 楔形體 $\text{Re}[\lambda_1]$ 隨 β 之變化	112
圖 5.8	不同邊界條件下壓電材料/Si 楔形體 $\text{Re}[\lambda_1]$ 隨 γ 之變化	113
圖 5.9	不同邊界條件下壓電材料/Si 楔形體 $\text{Re}[\lambda_1]$ 隨 θ 之變化	114
圖 5.10	不同邊界條件下單 BaTiO ₃ -CoFe ₂ O ₄ 楔形體 λ_1 隨 β 之變化	115
圖 5.11	不同邊界條件下單 BaTiO ₃ -CoFe ₂ O ₄ 楔形體 $\text{Re}[\lambda_1]$ 隨 γ 之變化	116
圖 5.11	不同邊界條件下單 BaTiO ₃ -CoFe ₂ O ₄ 楔形體 $\text{Re}[\lambda_1]$ 隨 γ 之變化	117
圖 5.12	不同邊界條件下單 BaTiO ₃ -CoFe ₂ O ₄ 楔形體 $\text{Re}[\lambda_1]$ 隨 θ 之變化	118
圖 5.13	不同邊界條件下雙 BaTiO ₃ -CoFe ₂ O ₄ 楔形體 $\text{Re}[\lambda_1]$ 隨 β 之變化	119
圖 5.14	不同邊界條件下雙 BaTiO ₃ -CoFe ₂ O ₄ 楔形體 $\text{Re}[\lambda_1]$ 隨 γ 之變化	120
圖 5.15	不同邊界條件下雙 BaTiO ₃ -CoFe ₂ O ₄ 楔形體 $\text{Re}[\lambda_1]$ 隨 θ 之變化	121
圖 5.16	不同邊界條件下 BaTiO ₃ -CoFe ₂ O ₄ /Si 楔形體 $\text{Re}[\lambda_1]$ 隨 β 之變化	122
圖 5.17	不同邊界條件下 BaTiO ₃ -CoFe ₂ O ₄ /Si 楔形體 $\text{Re}[\lambda_1]$ 隨 γ 之變化	123

圖 5.18	不同邊界條件下 BaTiO ₃ -CoFe ₂ O ₄ /Si 楔形體 $\text{Re}[\lambda_1]$ 隨 θ 之變化	124
圖 5.19	不同邊界條件下 BaTiO ₃ -CoFe ₂ O ₄ /PZT-4 楔形體 $\text{Re}[\lambda_1]$ 隨 β 之變化 .	125
圖 5.20	不同邊界條件下 BaTiO ₃ -CoFe ₂ O ₄ /PZT-6B 楔形體 $\text{Re}[\lambda_1]$ 隨 β 之變化	126
圖 5.21	不同邊界條件下 BaTiO ₃ -CoFe ₂ O ₄ /PZT-4 楔形體 $\text{Re}[\lambda_1]$ 隨 γ 之變化 .	127
圖 5.22	不同邊界條件下 BaTiO ₃ -CoFe ₂ O ₄ /PZT-6B 楔形體 $\text{Re}[\lambda_1]$ 隨 γ 之變化	128
圖 5.23	不同邊界條件下 BaTiO ₃ -CoFe ₂ O ₄ /PZT-4 楔形體 $\text{Re}[\lambda_1]$ 隨 θ 之變化 . .	129
圖 5.24	不同邊界條件下 BaTiO ₃ -CoFe ₂ O ₄ /PZT-6B 楔形體 $\text{Re}[\lambda_1]$ 隨 θ 之變化 .	130



表 目 錄

表 3.1	材料性質	82
表 3.2	壓電迴轉體之 $\text{Re}[\lambda_1]$ 收斂性分析	83
表 5.1	壓電楔形體之 $\text{Re}[\lambda_1]$ 收斂性分析	84



符 號 表

$\bar{X}, \bar{Y}, \bar{Z}$	材料卡氏座標系統
\bar{Z}	極化方向
X, Y, Z	幾何卡氏座標系統
γ	幾何卡氏座標 Z 軸與材料卡氏座標 \bar{Z} 之夾角
$\bar{\sigma}_{ij}$	材料之卡氏座標系統之應力
$\bar{\epsilon}_{ij}$	材料卡氏座標系統之應變
\bar{D}_i	材料卡氏座標系統之電位移
\bar{B}_i	材料卡氏座標系統之磁感應強度
\bar{E}_i	材料卡氏座標系統之電場
\bar{H}_i	材料卡氏座標系統之磁場
$[\bar{c}], [\bar{e}], [\bar{d}], [\bar{\eta}], [\bar{\mu}], [\bar{g}]$	材料卡氏座標系統之材料係數
r, θ, Z	圓柱座標系統
σ_{ij}	圓柱座標系統之應力
ϵ_{ij}	圓柱座標系統之應變
D_i	圓柱座標系統之電位移
B_i	圓柱座標系統之磁感應強度
E_i	圓柱座標系統之電場
H_i	圓柱座標系統之磁場
$[c], [e], [d], [\eta], [\mu], [g]$	圓柱座標系統之材料係數
u_i^*, ϕ^*, ψ^*	圓柱座標系統之位移分量、電勢與磁勢
ρ, ξ	迴轉體於某 θ 剖面之座標系統

$\hat{U}_n^{(i)}, \hat{V}_n^{(i)}, \hat{W}_n^{(i)}, \hat{\Phi}_n^{(i)}, \hat{\Psi}_n^{(i)}$

式 (2.9) 中 (ρ, ξ) 系統下假設之位移、電勢與磁勢函數

λ_m

特徵值

$\hat{A}_0^{(i)}, \hat{A}_1^{(i)}, \hat{B}_0^{(i)}, \hat{B}_1^{(i)},$

$\hat{C}_0^{(i)}, \hat{C}_1^{(i)}, \hat{D}_0^{(i)}, \hat{D}_1^{(i)},$

各子域待定常數

$\hat{E}_0^{(i)}, \hat{E}_1^{(i)}$

$\lambda_1 - 1$

電磁彈奇異性階數

$\hat{U}_n^{(i)}, \hat{V}_n^{(i)}, \hat{W}_n^{(i)}, \hat{\Phi}_n^{(i)}, \hat{\Psi}_n^{(i)}$

式 (4.1) 中 (r, θ, Z) 系統下假設之位移、電勢與磁勢函數



第一章 緒論

1.1 前言

智能材料的出現為科學及工程領域開啟了新的一頁，其中以壓電 (piezoelectric) 材料最為常見，其具有將電能與機械能互相轉換之特性，由於如此特殊的性質，在如今科技快速發展的時代中被廣泛應用於精密之儀器以及智慧型結構中。因科學家於材料科學領域上不斷努力研究，電磁彈性 (magneto-electro-elastic, MEE) 材料也漸被推廣於世。存於自然界中之電磁彈性材料之電磁耦合係數過小而無法進行實際之應用，因此近年來許多科學家致力於人工之電磁彈性材料之發展，盼提升電磁耦合係數，增加電磁彈性材料之實用性。大部分常見的智慧型材料多為脆性材料，例如較早期出現人造之壓電陶瓷 (PZT) 當受到外力作用時極易產生破壞，因此許多專家學者紛紛投入壓電材料之破壞力學研究，建立其破壞理論基礎。電磁彈性材料類似於壓電材料多為脆性，因此有必要進一步了解相關之破壞行為，為元件設計及優化上建構更為完整之參考依據。

1.2 研究背景及動機

智慧型材料的發展在近代扮演著非常重要的角色，於目前各項工業中為不可或缺的重要技術之一，許多精密儀器中採用壓電材料製成之元件。雖說電磁彈性材料之使用不如壓電材料廣泛，但其電磁彈耦合特性亦有部分層面之應用，特別為致動器 (actuators) 與感測器 (sensors) 的運用。為了對於精密儀器中智能元件的優化設計以及進行相關之破壞分析，因此了解由幾何形狀所引致之電磁彈奇異性行為為非常重要之課題。以下先就壓電材料與電磁彈性材料進行簡單的了解。

1.2.1 壓電效應

西元 1880 年由居禮 (Curie) 兄弟發現石英晶體中之壓電效應 (piezoelectricity)，透過實驗得知石英晶體不同方向之切割面或是於不同方向施加外力均會造成不同之壓電效應。壓電效應導因於材料受到外加之電能或是機械能使得晶格內原子重新排列。其可分為正壓電 (direct piezoelectric effects) 與逆壓電效應 (inverse piezoelectric effects) 兩種。正壓電效應為當材料承受一機械外力時，該外力使材料變形導致晶體內部電荷產生位移，因此材料正負電荷分布改變而造成極化 (electric polarization) 現象，稱正壓電效應，該效應可用於發展感測器；反言之，壓電材料表面被施加某方向之電場時，材料除了出現極化現象外，亦朝電場方向產生應變與變位，此稱為逆壓電效應，可以利用該特性製成致動器。

1.2.2 壓電材料

材料是否具備壓電效應通常取決於材料本身晶體之形式。一般來說，晶體結構若有對稱中心則無壓電效應，反之若無對稱中心之晶體則有壓電效應。

目前較為常見的壓電材料為壓電陶瓷以及由壓電陶瓷 (PZT) 與壓電複合材料，壓電陶瓷為典型之脆性材料，對於外力承載之韌性相當低，所以常因製造或設計過程中之缺陷造成應力或電荷集中於尖端處，以致壓電陶瓷元件失去應有的功能或甚至斷裂破壞。壓電複合材料則為兩種材料以上複合而成，根據不同之複合材料，可製造出較為柔軟之人工壓電材料，以改善壓電陶瓷易碎之性質。雖說如此，壓電陶瓷仍為使用最完廣泛之壓電材料。

1.2.3 電磁彈性材料

自然界中所存之天然電磁彈性材料之電磁耦合係數過低，造成實際應用不易，故科學家轉投以製造人工之電磁彈性材料，人工電磁彈性材料為壓電—壓磁之複合物，關於

壓電—壓磁複合物的發展，於西元 1972 年 van Suchtelen[1] 提出壓電—壓磁複合材料擁有電磁彈耦合效應，該耦合效應式於單相之壓電或壓磁材料中所未見的。西元 1974 年 van dan Boomgaard 等人 [2] 與 van Run 等人 [3] 利用實驗量測證明 $\text{BaTiO}_3\text{-CoFe}_2\text{O}_4$ 壓電—壓磁複合材料，存在良好之電磁耦合效應。西元 1981 年 Bracke 與 van Vliet[4] 發表了利用電磁彈性材料所製成的傳導器，因此許多有關於電磁彈性材料力學與磁電的耦合效應的理論及技術相繼而生，但如今電磁彈性材料之使用廣泛程度尚不如壓電材料。

1.3 文獻回顧

由過去經驗或理論上可知於一般彈性材料中奇異點總為應力集中處，並常為破壞之起始點。當進行電磁彈性材料分析時於奇異點除了應力集中外亦有可能造成電力或磁力集中，而使得較彈性材料更佳容易產生破壞。所以本研究將建立奇異點處之漸近解，探討不同幾何形狀以及極化方向對電磁彈性材料之奇異性階數之影響，藉此了解可能產生之電磁彈奇異行為。一般來說，電磁彈性元件安裝於儀器中時，元件間總會造成材料以及幾何形狀之不連續 (圖 1.1)；或者材料本身具有類似裂縫或凹口之缺陷 (圖 1.2)，均可能造成材料或器材之使用壽命縮短。其奇異行為與楔形體及迴轉體相同，故本研究將以這兩種幾何形態作為分析之模型。

1.3.1 彈性楔形體之應力奇異性

至目前為止已有相當多的文獻對於彈性楔形體之應力奇異性進行探討。許多學者將彈性楔形體分析簡化為二維之問題，對於楔形體面內 (in-plane) 與面外 (anti-plane) 行為進行討論。有關於楔形體面內奇異性行為之研究，由 Williams[5] 首先對於各向等向性 (isotropic) 之彈性扇形板由於邊界條件所引致之應力奇異性行為探討，其研究結果顯示於不同邊界條件以及扇形角變化時均會呈現不同之應力奇異性階數。因為探討的問題以板作為出發點，故後續許多研究均以平面應變或應力作為假設，忽略了板厚度

方向應變或應力分量對於奇異性行為的影響，如 Williams[6] 分析不同邊界條件於 180 度以下之扇形板面內 (in-plane) 尖端奇異性，由結果可知道在混合的邊界條件 (一側為 clamped，另一側為 free) 下之應力奇異性較兩側邊界條件一致的情況下強烈。除了單一材料之楔形體，亦有學者對於複合材料楔形體進行討論，因為複合材料楔形體為兩種材料以上所組成，因此在兩材料之連結處為一材料不連續面，亦有可能於材料不連續面之尖端點造成應力集中而產生奇異性行為。Hartranft 與 Sih[7] 利用特徵函數展開法探討三維之裂縫問題，另外提出該方法可利用於楔形體問題。Bogy 與 Wang[8] 分析於雙等向性彈性材料楔形體，指出應力奇異性階數與材料性質及楔形體角度息息相關；Bogy[9] 提出當雙彈性材料楔形體於兩邊界受到表面 tractions 作用時，於楔形體尖端之應力異性階數與材料性質以及楔形體之幾何形狀有關，與 Bogy 與 Wang[8] 提出之結果一致。Dempsey 與 Sinclair[10] 延續 Dempsey 與 Sinclair[11] 之方法，根據 Airy stress function，使用變數分離法推導出當 $r \rightarrow 0$ 時奇異性形態 $O(r^{-\lambda} \ln r)$ ，其中 r 為與奇異點之距離，另指出奇異性階數是根據於材料種類數量而定。之後專家學者 [12-21] 亦針對楔形體應力奇異性進行相關之探討，所得結果如同 Bogy 與 Wang[8] 所提出之楔形體材料種類與幾何形狀均對於應力奇異性有顯著之影響。

亦有學者對於彈性楔形體面外奇異性行為進行研究。Ma 與 Hour[22] 分析雙異向性 (anisotropic) 材料之面外應變之問題，根據結果發現面外奇異性階數總為實數，該結論與面內問題有相當大的不同。Kargarnovin 等 [23] 與 Shahani[24] 分別討論有限之等向性與異向性材料楔形體面外奇異性行為。Xie 與 Chaudhuri[25] 亦配合特徵函數展開法探討雙材料板承受面外 (antiplane) 剪力或彎矩時於界面間之奇異性問題。此外，各家學者基於各種板理論 [26-31]，例如古典板理論、Reissner 理論、三階薄板、一階剪力變形板理論以及 Mindlin 理論等，對於單一或多材料彈性楔形體之應力奇異性做進一步之探討。

若以彈性材料之性質分類，可分為等向性材料與異向性材料。於已發表的文獻中對於各向等向性材料楔形體奇異性行為研究 [5-14, 25-31] 已有相當深入之探討。Ting 與

Chou[16] 於極座標系統下分析異向性材料楔形體之奇異性，亦推導出當 $r \rightarrow 0$ 時，奇異性擁有 $r^{-\xi} F(r, \theta)$ 之形態，其中 ξ 為一複數 (complex)，也證明了於異向性材料裂縫尖端之奇異性階數為 0.5 與一般等向性材料一致；[17–22, 32–34] 亦針對異向性楔形體進行分析，結論類似於各向等向性材料楔形體，奇異性階數會根據幾何形狀與材料種類性質而變化，此外材料之纖維方向亦會造成影響。

1.3.2 壓電楔形體之電彈奇異性

一般來說壓電材料被假設為側向等向性材料 (transversely isotropic material)，其極化方向被定義為垂直於材料等向性平面，側向等且在通常假設平行某幾何之主軸。因此，奇異性分析通常建構於廣義平面應變或變位之假設上，Xu 與 Rajapakse[35] 利用 extended Lekhnitskii's formulation 分析任意極化方向之單一或多材料壓電楔形體之壓電奇異性為一平面問題，提出極化方不影響考量裂縫時的奇異性，另外根據數值結果顯示楔形體角度、極化方向、材料種類以及邊界或是界面條件均會導致壓電奇異性的變化；Chen 等人 [36] 亦利用 extended Lekhnitskii's formulation 進行極化方向為徑向、環向與軸向之壓電楔形體奇異性分析，得到與 Xu 與 Rajapakse[35] 相同的結論。Hwu 與 Ikeda[37] 延伸對於異向性材料分析時採用之 Stroh formulation 分析於不同邊界條件下含尖角或裂縫壓電材料之奇異性行為。Chue 與 Chen[38] 基於廣義平面變位 (generalized plane deformation) 之假設分析雙壓電材料與壓電材料/彈性材料楔形體奇異性問題，同樣的也提出了楔形體角度、極化方向、材料種類以及雙材料界面間的連續條件，均會影響於尖端附近之電彈奇異性階數。Sosa 與 Pack[39] 利用特徵函數展開法分析極化方向為面外方向之壓電材料三維之半無限裂縫之問題，其結果證明了於裂縫尖端附近會產生 $1/\sqrt{r}$ 之奇異性行為，其中 r 為距離尖端之半徑長度。Chue 與 Chen[40] 使用 Mellin 轉換分析雙壓電材料楔形體面外之奇異性問題，發現雙材料壓電楔形體之面外電彈奇異性階數可能為複數，該結論與雙彈性材料楔形體面外應力奇異性階數總為實數的結論相反；另外也提出在單一壓電楔形體之電彈奇異性階數總為實數，

除非該單一壓電楔形體之邊界條件為 C-D 則可能產生複數之電彈奇異性階數 (Chue 與 Chen[40] 中定義 C 為 traction free 與 electrically open ; D 為 clamped 與 electrically open)。Scherzer 與 Kuna[41] 結合特徵函數展開法與有限元素法分析裂縫相關問題，說明了若利用標準之有限元素法分析壓電材料裂縫問題時，在材料裂縫尖端是無法得到正確之解。Chen 等人 [42] 利用 ad hoc 一維有限元素法 (或稱 hypoparametric 有限元素法) 分析極化方向為任意方向之壓電/彈性材料楔形體之奇異性行為，提出影響電彈奇異性階數可能的原因有彈性材料之纖維方向、壓電材料之極化方向以及楔型板之幾何角度。Shang 與 Kitamura[43] 根據 Wang 與 Zheng[44] 所提出對於壓電材料之 modified general solution，探討壓電薄片黏結於一彈性基材 (幾何形狀參考圖 1.1) 時其交界處可能產生之奇異性行為，提出強烈的奇異性為材料的差異以及幾何形狀所引致的。歸納上述學者之分析結果可知壓電楔形體可能因楔形體角度、極化方向、材料種類以及邊界或是界面條件導致電彈奇異性的變化。

1.3.3 電磁彈性楔形體之應力奇異性

相較於彈性或壓電楔形體已有大量研究，目前僅有少數的文獻對於電磁彈性材料楔形體尖端之電磁彈奇異性行為進行探討。Liu 與 Chue[45] 根據 Chue 與 Chen[38] 廣義平面變位之假設分析雙電磁彈性材料楔形體，利用 Mellin 轉換推導出特徵方程式以求得奇異性階數，顯示電磁彈性奇異性階數與由彈性、壓電楔形體求得之奇異性階數迥異。Sue 等人 [46] 利用 complex potential function 與特徵函數展開法，考量於面內電場與磁場以及面外變位之情況下，討論雙電磁彈性複合楔形體尖端之電磁彈性奇異性行為，根據數值結果分析得到由於電磁彈性效應可能造成其奇異性階數為複數，該情況類似於壓電材料，不如彈性材料之奇異性階數總為實數。Liu [47] 更進一步延伸 Liu 與 Chue[45] 所得之結果，考量於空氣中之電場與磁場對於多材料楔形體尖端應力奇異性之影響，其中電磁彈性材料的極化方向均被假設平行於幾何形狀的某主軸。

1.3.4 彈性迴轉體之應力奇異性

對於彈性迴轉體可假設軸對稱進行分析。Zak[48] 分析迴轉體於不連續處之奇異性，根據數值結果可知道奇異性階數落於 0 與 1 之間；Ting 等人 [49] 推導出含裂縫或缺口之側向等向性材料承受軸對稱變形時特徵方程式。另外，在不考慮軸對稱之假設下，Huang 與 Leissa[50] 對於迴轉體之鄰近 V 型凹口處進行漸近分析，直接求解於三維力平衡方程式，將問題簡化為特徵值問題，並配合邊界條件以建立 3-D sharp corner displacement functions；Huang 與 Leissa[51] 延續 Huang 與 Leissa[50] 之方法，拓展至分析雙彈性材料迴轉體之應力奇異性，透過特徵方程式求得應力奇異性階數，亦建立了於雙材料交界處尖角附近之漸近位移及應力場。

1.3.5 壓電迴轉體之應力奇異性

Li 等人 [52] 仍基於軸對稱之假設，延伸 Ting 等人 [49] 之方法建構軸對稱壓電材料迴轉體之解以探討雙壓電材料界面之電彈奇異性，其結果顯示若忽略壓電效應則奇異性階數會有明顯不同；Xu 與 Mutoh[53] 亦根據軸對稱假設分析雙壓電材料迴轉體，以特徵方程式求得奇異性階數，其發現當承受扭矩作用時，壓電與介電常數均對奇異性沒有任何影響。目前尚未有關於電磁彈性迴轉體電磁彈性材料奇異性行為之研究文獻。

1.4 研究目的

本研究旨在建立三維電磁彈性迴轉體與楔形體於尖端處之三維漸近解，以探討其電磁彈奇異性。雖然已有相當多的文獻探有關於迴轉體與楔形體奇異性之問題，但大多進行了平面化之假設，例如：Xu 與 Ragapakse[35]、Chen[36] 以及 Hwu 與 Ikeda[37] 基於廣義平面應變假設，分析壓電楔形體問題；Chue 與 Chen[33] 以及 Liu 與 Chue[45] 廣義平面應變假設，分析壓電與電磁彈楔形體問題。於該假設下處理平面內 (in-plane) 或平面外 (out-of-plane) 極化方向的問題是有效的；若極化方向為空間中任意方向時，

則平面內與平面外的位移與電磁場會相互耦合，因此在處理的過程中會增加許多困難處。故本研究以三維電磁彈性理論做為基礎，不做任何之簡化與假設，對於極化方向為空間中任意方向之電磁彈性迴轉體與楔形體奇異性行為，做進一步之探討及瞭解。

1.5 研究方法

假設壓電材料以及電磁彈性材料為卡氏座標下之橫向等向性材料，但極化方向無必然與描述幾何之主軸相互平行。為求分析上之便利性將座標轉換至圓柱座標系統後，於本研究中考量電磁彈迴轉體之極化方向未必於幾何旋轉軸平行，故過去文獻中提及以軸對稱之假設對於迴轉體進行分析之方式是無法成立的；在楔形體的問題中，同樣因極化方向可為空間中任意方向，其造成平面內外奇異性行為相互耦合，則無法單純以平面應變或平面應力作為假設對於楔形體問題進行解析。

以三維電磁彈性理論為出發點，利用特徵函數展開法 (eigenfunction expansion approach) 並結合級數法 (power series technique) 對以彈性位移 (mechanical displacement)、電勢 (electric potential) 與磁勢 (magnetic potential) 表示之三維力平衡方程式與馬克斯威爾方程式建立電磁彈奇異性漸近解。將針對單一電磁彈性材料、單一壓電材料、電磁彈性/壓電材料、電磁彈性/電磁彈性 (彼此擁有不同的 volume fraction)、雙壓電材料、壓電/各向同性彈性材料與電磁彈性/各向同性彈性材料進行分析，並對極化方向、材料類型與邊界條件對奇異性階數所造成的影響進行探討。

1.6 研究內容

有別於許多文獻中利用二維之電磁彈性之理論分析奇異性問題。本研究將利用特徵函數展開法，結合級數解之技巧建立於電磁彈迴轉體與楔形體尖角處之電磁彈奇異性漸近解。該漸近解為直接求解於三維力平衡方程式與馬克斯威爾方程式，並無做任何簡化至平面問題之假設。藉以分析於不同之邊界條件、材料性質、幾何形狀以及極化方

向與幾何座標軸不一致之情況下電磁彈奇異性之變化。

本文架構：

第一章、緒論

內容為研究背景及動機、文獻回顧、研究方法與研究方法之闡述。

第二章、三維電磁彈性迴轉體之奇異性

於迴轉體幾何狀態下，從三維力平衡方程式與馬克斯威爾方程式出發，推導於幾何或材料不連續處之漸近解。

第三章、電磁彈性迴轉體奇異性之結果與討論

方法之驗證與進行收斂性分析。探討因材料特性、邊界條件、幾何形狀與極化方法等參數改變對於電磁彈性迴轉體之最小電磁彈奇異性階數 λ_1 值之影響。

第四章、三維電磁彈性楔形體之奇異性

於楔形體幾何狀態下，從三維力平衡方程式與馬克斯威爾方程式出發，推導於幾何或材料不連續處之漸近解。

第五章、電磁彈性楔形體奇異性之結果與討論

方法之驗證與進行收斂性分析。探討因材料特性、邊界條件、幾何形狀與極化方法等參數改變對於電磁彈性楔形體之最小電磁彈奇異性階數 λ_1 值之影響。

第六章、結論與建

總結研究中電磁彈性迴轉體與楔形體因各參數變化對於電磁彈奇異性之影響；並建議於未來可進一步之研究。

第二章 三維電磁彈性迴轉體之奇異性

於本研究中所謂「電磁彈性」與「壓電」被定義為電、磁與彈性系統以及電與彈性系統間之線性交互作用，關於壓電固體之壓電線性理論方程式可參考 Rogacheva[54] 與 Ikeda[55]；而電磁彈性固體之電磁彈性線性理論方程式可參考 Nan[56]、Benveniste[57] 以及 Li 與 Dunn[58, 59]。

2.1 電磁彈性力學本構方程式

根據圖 2.1，一電磁彈材料之迴轉體被定義於卡氏座標系統 (X, Y, Z) 下，其中 Z 軸為迴轉體之迴轉軸亦為幾何對稱軸。一般而言，電磁彈性材料被假設為橫向等向性 (transversely isotropic) 材料，並設定該材料於 $\bar{X} - \bar{Y}$ 平面上之性質為均質，令其極化軸為 \bar{Z} 軸垂直於 $\bar{X} - \bar{Y}$ 平面，同時與 Z 軸含一夾角 γ 。在卡氏座標 $(\bar{X}, \bar{Y}, \bar{Z})$ 系統，橫向等向性之電磁彈性材料的本構方程式 (constitutive equations) 可表示如下：

$$\{\bar{\sigma}\} = [\bar{c}] \{\bar{\varepsilon}\} - [\bar{e}]^T \{\bar{E}\} - [\bar{d}]^T \{\bar{H}\}, \quad (2.1a)$$

$$\{\bar{D}\} = [\bar{e}] \{\bar{\varepsilon}\} + [\bar{\eta}] \{\bar{E}\} + [\bar{g}] \{\bar{H}\}, \quad (2.1b)$$

$$\{\bar{B}\} = [\bar{d}] \{\bar{\varepsilon}\} + [\bar{g}] \{\bar{E}\} + [\bar{\mu}] \{\bar{H}\}, \quad (2.1c)$$

其中 $\bar{\sigma}_{ij}$ 、 $\bar{\varepsilon}_{ij}$ 、 \bar{D}_i 、 \bar{B}_i 、 \bar{E}_i 與 $\bar{H}_i (i, j = \bar{X}, \bar{Y}, \bar{Z})$ 分別為應力、應變、電位移、磁感應強度、電場與磁場分量；彈性係數 $[\bar{c}]$ 、壓電係數 $[\bar{e}]$ 、壓磁係數 $[\bar{d}]$ 、介電常數 $[\bar{\eta}]$ ，導磁係數 $[\bar{\mu}]$ 以及電磁耦合係數 $[\bar{g}]$ 如下：

$$[\bar{c}] = \begin{bmatrix} \bar{c}_{11} & \bar{c}_{12} & \bar{c}_{13} & 0 & 0 & 0 \\ \bar{c}_{12} & \bar{c}_{11} & \bar{c}_{13} & 0 & 0 & 0 \\ \bar{c}_{13} & \bar{c}_{13} & \bar{c}_{33} & 0 & 0 & 0 \\ 0 & 0 & 0 & \bar{c}_{44} & 0 & 0 \\ 0 & 0 & 0 & 0 & \bar{c}_{44} & 0 \\ 0 & 0 & 0 & 0 & 0 & \frac{\bar{c}_{11}-\bar{c}_{12}}{2} \end{bmatrix}, [\bar{e}] = \begin{bmatrix} 0 & 0 & 0 & 0 & \bar{e}_{15} & 0 \\ 0 & 0 & 0 & \bar{e}_{15} & 0 & 0 \\ \bar{e}_{31} & \bar{e}_{31} & \bar{e}_{33} & 0 & 0 & 0 \end{bmatrix},$$

$$[\bar{d}] = \begin{bmatrix} 0 & 0 & 0 & 0 & \bar{d}_{15} & 0 \\ 0 & 0 & 0 & \bar{d}_{15} & 0 & 0 \\ \bar{d}_{31} & \bar{d}_{31} & \bar{d}_{33} & 0 & 0 & 0 \end{bmatrix}, [\bar{\eta}] = \begin{bmatrix} \bar{\eta}_{11} & 0 & 0 \\ 0 & \bar{\eta}_{11} & 0 \\ 0 & 0 & \bar{\eta}_{33} \end{bmatrix}, [\bar{\mu}] = \begin{bmatrix} \bar{\mu}_{11} & 0 & 0 \\ 0 & \bar{\mu}_{11} & 0 \\ 0 & 0 & \bar{\mu}_{33} \end{bmatrix},$$

$$[\bar{g}] = \begin{bmatrix} \bar{g}_{11} & 0 & 0 \\ 0 & \bar{g}_{11} & 0 \\ 0 & 0 & \bar{g}_{33} \end{bmatrix}.$$



由於極化方向軸 (\bar{Z} 軸) 與幾何座標系統之 Z 軸未必平行，於是將 $(\bar{X}, \bar{Y}, \bar{Z})$ 轉換至 (X, Y, Z) 座標系統。考量於分析過程中的便利性，再將 (X, Y, Z) 轉換至圓柱座標 (r, θ, Z) 系統，此時電磁彈性材料的本構方程式可被改寫為

$$\{\sigma\} = [c] \{\varepsilon\} - [e]^T \{E\} - [d]^T \{H\}, \quad (2.2a)$$

$$\{D\} = [e] \{\varepsilon\} + [\eta] \{E\} + [g] \{H\}, \quad (2.2b)$$

$$\{B\} = [d] \{\varepsilon\} + [g] \{E\} + [\mu] \{H\}, \quad (2.2c)$$

類似前段所敘述的，其中 σ_{ij} 、 ε_{ij} 、 D_i 、 B_i 、 E_i 與 H_i ($i, j = r, \theta, Z$) 分別為圓柱座標系統下的應力、應變、電位移、磁感應強度、電場與磁場分量；經座標系統轉換後，材料性質分別改變為

$$[c] = \begin{bmatrix} c_{11} & c_{12} & c_{13} & c_{14} & c_{15} & c_{16} \\ c_{12} & c_{22} & c_{23} & c_{24} & c_{25} & c_{26} \\ c_{13} & c_{23} & c_{33} & c_{34} & c_{35} & c_{36} \\ c_{14} & c_{24} & c_{34} & c_{44} & c_{45} & c_{46} \\ c_{15} & c_{25} & c_{35} & c_{45} & c_{55} & c_{56} \\ c_{16} & c_{26} & c_{36} & c_{46} & c_{56} & c_{66} \end{bmatrix}, [e] = \begin{bmatrix} e_{11} & e_{12} & e_{13} & e_{14} & e_{15} & e_{16} \\ e_{21} & e_{22} & e_{23} & e_{24} & e_{25} & e_{26} \\ e_{31} & e_{32} & e_{33} & e_{34} & e_{35} & e_{36} \end{bmatrix},$$

$$[d] = \begin{bmatrix} d_{11} & d_{12} & d_{13} & d_{14} & d_{15} & d_{16} \\ d_{21} & d_{22} & d_{23} & d_{24} & d_{25} & d_{26} \\ d_{31} & d_{32} & d_{33} & d_{34} & d_{35} & d_{36} \end{bmatrix}, [\eta] = \begin{bmatrix} \eta_{11} & \eta_{12} & \eta_{13} \\ \eta_{12} & \eta_{22} & \eta_{23} \\ \eta_{13} & \eta_{23} & \eta_{33} \end{bmatrix}, [\mu] = \begin{bmatrix} \mu_{11} & \mu_{12} & \mu_{13} \\ \mu_{12} & \mu_{22} & \mu_{23} \\ \mu_{13} & \mu_{23} & \mu_{33} \end{bmatrix},$$

$$[g] = \begin{bmatrix} g_{11} & g_{12} & g_{13} \\ g_{12} & g_{22} & g_{23} \\ g_{13} & g_{23} & g_{33} \end{bmatrix},$$



此時材料性質 $[c]$ 、 $[e]$ 、 $[d]$ 、 $[\eta]$ 、 $[\mu]$ 以及 $[g]$ 已成為 γ 與 θ 的函數。座標轉換的詳細過程可參考附錄 A。

2.2 三維力平衡方程式與馬克斯威爾方程式

於圓柱座標 (r, θ, z) 系統下，三維力平衡方程式與馬克斯威爾方程式可表示為

$$\frac{\partial \sigma_{rr}}{\partial r} + \frac{1}{r} \frac{\partial \sigma_{r\theta}}{\partial \theta} + \frac{\partial \sigma_{rz}}{\partial z} + \frac{(\sigma_{rr} - \sigma_{\theta\theta})}{r} = f_r + \rho^* \frac{\partial^2 u_r^*}{\partial t^2}, \quad (2.3a)$$

$$\frac{\partial \sigma_{r\theta}}{\partial r} + \frac{1}{r} \frac{\partial \sigma_{\theta\theta}}{\partial \theta} + \frac{\partial \sigma_{\theta z}}{\partial z} + 2 \frac{\sigma_{r\theta}}{r} = f_\theta + \rho^* \frac{\partial^2 u_\theta^*}{\partial t^2}, \quad (2.3b)$$

$$\frac{\partial \sigma_{rz}}{\partial r} + \frac{1}{r} \frac{\partial \sigma_{\theta z}}{\partial \theta} + \frac{\partial \sigma_{zz}}{\partial z} + \frac{\sigma_{rz}}{r} = f_z + \rho^* \frac{\partial^2 u_z^*}{\partial t^2}, \quad (2.3c)$$

$$\frac{1}{r} \frac{\partial (rD_r)}{\partial r} + \frac{1}{r} \frac{\partial D_\theta}{\partial \theta} + \frac{\partial D_z}{\partial z} = f_e, \quad (2.3d)$$

$$\frac{1}{r} \frac{\partial (rB_r)}{\partial r} + \frac{1}{r} \frac{\partial B_\theta}{\partial \theta} + \frac{\partial B_z}{\partial z} = f_m, \quad (2.3e)$$

其中 ρ^* 為材料密度； $f_i (i = r, \theta, z)$ 、 f_e 與 f_m 分別為體力 (body force)、自由電荷密度以及自由磁荷密度， t 為時間。本研究中不考慮體力與自由電荷密度；另外，根據電磁學式(2.3e) 被稱為高斯磁定律，該定律表示空間中不存在磁單極子，故宇宙中並不存在「磁荷」此種物質，所以磁通量為零，則可知 $f_m = 0$ 。於式 (2.2) 中之應變、電場及磁場可以位移分量、電勢與磁勢表示如下

$$\begin{aligned} \varepsilon_{rr} &= \frac{\partial u_r^*}{\partial r}, \quad \varepsilon_{\theta\theta} = \left(\frac{1}{r} \frac{\partial u_\theta^*}{\partial \theta} + \frac{u_r^*}{r} \right), \quad \varepsilon_{zz} = \frac{\partial u_z^*}{\partial z}, \quad \varepsilon_{\theta z} = \left(\frac{\partial u_\theta^*}{\partial z} + \frac{1}{r} \frac{\partial u_z^*}{\partial \theta} \right), \\ \varepsilon_{zr} &= \left(\frac{\partial u_z^*}{\partial r} + \frac{\partial u_r^*}{\partial z} \right), \quad \varepsilon_{r\theta} = \left(\frac{1}{r} \frac{\partial u_r^*}{\partial \theta} + \frac{\partial u_\theta^*}{\partial r} - \frac{u_\theta^*}{r} \right), \\ E_r &= -\frac{\partial \phi^*}{\partial r}, \quad E_\theta = -\frac{1}{r} \frac{\partial \phi^*}{\partial \theta}, \quad E_z = -\frac{\partial \phi^*}{\partial z}, \\ H_r &= -\frac{\partial \psi^*}{\partial r}, \quad H_\theta = -\frac{1}{r} \frac{\partial \psi^*}{\partial \theta}, \quad H_z = -\frac{\partial \psi^*}{\partial z} \end{aligned} \quad (2.4)$$

利用式 (2.4)，應力 σ_{ij} 、電位移 D_i 及磁感應強度 B_i 可分別以位移分量 u_i^* 、電勢 ϕ^* 與磁勢 ψ^* 來表示，其關係式可參考附錄 B。三維力平衡方程式與馬克斯威爾方程式亦可以位移分量 u_i^* 、電勢 ϕ^* 與磁勢 ψ^* 表示成

$$\begin{aligned} & \left[c_{11} \frac{\partial^2}{\partial r^2} + \left(\frac{c_{66}}{r^2} \right) \frac{\partial^2}{\partial \theta^2} + c_{55} \frac{\partial^2}{\partial z^2} + \left(\frac{2c_{16}}{r} \right) \frac{\partial^2}{\partial r \partial \theta} + 2c_{15} \frac{\partial^2}{\partial r \partial z} + \left(\frac{2c_{56}}{r} \right) \frac{\partial^2}{\partial \theta \partial z} + \left(c_{11} \right. \right. \\ & \quad \left. \left. + \frac{\partial c_{16}}{\partial \theta} \right) \frac{\partial}{r \partial r} + \left(\frac{\partial c_{66}}{\partial \theta} \right) \frac{\partial}{r^2 \partial \theta} + \left(c_{15} + \frac{\partial c_{56}}{\partial \theta} \right) \frac{\partial}{r \partial z} + \left(-c_{22} + \frac{\partial c_{26}}{\partial \theta} \right) \frac{1}{r^2} - \rho^* \frac{\partial^2}{\partial t^2} \right] u_r^* \\ & + \left[c_{16} \frac{\partial^2}{\partial r^2} + \left(\frac{c_{26}}{r^2} \right) \frac{\partial^2}{\partial \theta^2} + c_{45} \frac{\partial^2}{\partial z^2} + (c_{12} + c_{66}) \frac{\partial^2}{r \partial r \partial \theta} + (c_{14} + c_{56}) \frac{\partial^2}{\partial r \partial z} + (c_{25} + c_{46}) \right. \\ & \quad \left. \times \frac{\partial^2}{r \partial \theta \partial z} + \left(-c_{26} + \frac{\partial c_{66}}{\partial \theta} \right) \frac{\partial}{r \partial r} + \left(-c_{22} - c_{66} + \frac{\partial c_{26}}{\partial \theta} \right) \frac{\partial}{r^2 \partial \theta} + \left(c_{14} - c_{24} - c_{56} + \frac{\partial c_{46}}{\partial \theta} \right) \right. \\ & \quad \left. \times \frac{\partial}{r \partial z} + \left(c_{26} - \frac{\partial c_{66}}{\partial \theta} \right) \frac{1}{r^2} \right] u_\theta^* + \left[c_{15} \frac{\partial^2}{\partial r^2} + \left(\frac{c_{46}}{r^2} \right) \frac{\partial^2}{\partial \theta^2} + c_{35} \frac{\partial^2}{\partial z^2} + (c_{14} + c_{56}) \frac{\partial^2}{r \partial r \partial \theta} \right. \\ & \quad \left. + (c_{13} + c_{55}) \frac{\partial^2}{\partial r \partial z} + (c_{36} + c_{45}) \frac{\partial^2}{r \partial \theta \partial z} + \left(c_{15} - c_{25} + \frac{\partial c_{56}}{\partial \theta} \right) \frac{\partial}{r \partial r} + \left(-c_{24} + \frac{\partial c_{46}}{\partial \theta} \right) \frac{\partial}{r^2 \partial \theta} \right. \\ & \quad \left. + \left(c_{13} - c_{23} + \frac{\partial c_{36}}{\partial \theta} \right) \frac{\partial}{r \partial z} \right] u_z^* + \left[e_{11} \frac{\partial^2}{\partial r^2} + \left(\frac{e_{26}}{r^2} \right) \frac{\partial^2}{\partial \theta^2} + e_{35} \frac{\partial^2}{\partial z^2} + (e_{16} + e_{21}) \frac{\partial^2}{r \partial r \partial \theta} \right. \\ & \quad \left. + (e_{15} + e_{31}) \frac{\partial^2}{\partial r \partial z} + (e_{25} + e_{36}) \frac{\partial^2}{r \partial \theta \partial z} + \left(e_{11} - e_{12} + \frac{\partial e_{16}}{\partial \theta} \right) \frac{\partial}{r \partial r} + \left(-e_{22} + \frac{\partial e_{26}}{\partial \theta} \right) \frac{\partial}{r^2 \partial \theta} \right. \\ & \quad \left. + (e_{15} + e_{31}) \frac{\partial^2}{\partial r \partial z} + (e_{25} + e_{36}) \frac{\partial^2}{r \partial \theta \partial z} + \left(e_{11} - e_{12} + \frac{\partial e_{16}}{\partial \theta} \right) \frac{\partial}{r \partial r} + \left(-e_{22} + \frac{\partial e_{26}}{\partial \theta} \right) \frac{\partial}{r^2 \partial \theta} \right. \\ & \quad \left. + \left(e_{31} - e_{32} + \frac{\partial e_{36}}{\partial \theta} \right) \frac{\partial}{r \partial z} \right] \phi^* + \left[d_{11} \frac{\partial^2}{\partial r^2} + \left(\frac{d_{26}}{r^2} \right) \frac{\partial^2}{\partial \theta^2} + d_{35} \frac{\partial^2}{\partial z^2} + (d_{16} + d_{21}) \frac{\partial^2}{r \partial r \partial \theta} \right. \end{aligned}$$

$$\begin{aligned}
& + (d_{15} + d_{31}) \frac{\partial^2}{\partial r \partial z} + (d_{25} + d_{36}) \frac{\partial^2}{r \partial \theta \partial z} + \left(d_{11} - d_{12} + \frac{\partial d_{16}}{\partial \theta} \right) \frac{\partial}{r \partial r} + \left(-d_{22} + \frac{\partial d_{26}}{\partial \theta} \right) \\
& \times \frac{\partial}{r^2 \partial \theta} + \left(d_{31} - d_{32} + \frac{\partial d_{36}}{\partial \theta} \right) \frac{\partial}{r \partial z} \Big] \psi^* = 0, \tag{2.5a}
\end{aligned}$$

$$\begin{aligned}
& \left[c_{16} \frac{\partial^2}{\partial r^2} + \left(\frac{c_{26}}{r^2} \right) \frac{\partial^2}{\partial \theta^2} + c_{45} \frac{\partial^2}{\partial z^2} + (c_{12} + c_{66}) \frac{\partial^2}{r \partial r \partial \theta} + (c_{14} + c_{56}) \frac{\partial^2}{\partial r \partial z} + (c_{25} + c_{46}) \frac{\partial^2}{r \partial \theta \partial z} \right. \\
& + \left(2c_{16} + c_{26} + \frac{\partial c_{12}}{\partial \theta} \right) \frac{\partial}{r \partial r} + \left(c_{22} + c_{66} + \frac{\partial c_{26}}{\partial \theta} \right) \frac{\partial}{r^2 \partial \theta} + \left(c_{24} + 2c_{56} + \frac{\partial c_{25}}{\partial \theta} \right) \frac{\partial}{r \partial z} \\
& + \left(c_{26} + \frac{\partial c_{22}}{\partial \theta} \right) \frac{1}{r^2} \Big] u_r^* + \left[c_{66} \frac{\partial^2}{\partial r^2} + \left(\frac{c_{22}}{r^2} \right) \frac{\partial^2}{\partial \theta^2} + c_{44} \frac{\partial^2}{\partial z^2} + \left(\frac{2c_{26}}{r} \right) \frac{\partial^2}{\partial r \partial \theta} + 2c_{46} \frac{\partial^2}{\partial r \partial z} \right. \\
& + 2c_{24} \frac{\partial^2}{r \partial \theta \partial z} + \left(c_{66} + \frac{\partial c_{26}}{\partial \theta} \right) \frac{\partial}{r \partial r} + \left(\frac{\partial c_{22}}{\partial \theta} \right) \frac{\partial}{r^2 \partial \theta} + \left(c_{46} + \frac{\partial c_{24}}{\partial \theta} \right) \frac{\partial}{r \partial z} + \left(-c_{66} - \frac{\partial c_{26}}{\partial \theta} \right) \\
& \times \frac{1}{r^2} - \rho^* \frac{\partial^2}{\partial t^2} \Big] u_\theta^* + \left[c_{56} \frac{\partial^2}{\partial r^2} + \left(\frac{c_{24}}{r^2} \right) \frac{\partial^2}{\partial \theta^2} + c_{34} \frac{\partial^2}{\partial z^2} + (c_{25} + c_{46}) \frac{\partial^2}{r \partial r \partial \theta} + (c_{36} + c_{45}) \right. \\
& \times \frac{\partial^2}{\partial r \partial z} + (c_{23} + c_{44}) \frac{\partial^2}{r \partial \theta \partial z} + \left(2c_{56} + \frac{\partial c_{25}}{\partial \theta} \right) \frac{\partial}{r \partial r} + \left(c_{46} + \frac{\partial c_{24}}{\partial \theta} \right) \frac{\partial}{r^2 \partial \theta} + \left(2c_{36} + \frac{\partial c_{23}}{\partial \theta} \right) \\
& + \left(2c_{36} + \frac{\partial c_{23}}{\partial \theta} \right) \frac{\partial}{r \partial z} \Big] u_z^* + \left[e_{16} \frac{\partial^2}{\partial r^2} + \left(\frac{e_{22}}{r^2} \right) \frac{\partial^2}{\partial \theta^2} + e_{34} \frac{\partial^2}{\partial z^2} + (e_{12} + e_{26}) \frac{\partial^2}{r \partial r \partial \theta} \right. \\
& + (e_{14} + e_{36}) \frac{\partial^2}{\partial r \partial z} + (e_{24} + e_{32}) \frac{\partial^2}{r \partial \theta \partial z} + \left(2e_{16} + \frac{\partial e_{12}}{\partial \theta} \right) \frac{\partial}{r \partial r} + \left(e_{26} + \frac{\partial e_{22}}{\partial \theta} \right) \frac{\partial}{r^2 \partial \theta} \\
& + \left(2e_{36} + \frac{\partial e_{32}}{\partial \theta} \right) \frac{\partial}{r \partial z} \Big] \phi^* + \left[d_{16} \frac{\partial^2}{\partial r^2} + \left(\frac{d_{22}}{r^2} \right) \frac{\partial^2}{\partial \theta^2} + d_{34} \frac{\partial^2}{\partial z^2} + (d_{12} + d_{26}) \frac{\partial^2}{r \partial r \partial \theta} \right. \\
& + \left[d_{16} \frac{\partial^2}{\partial r^2} + \left(\frac{d_{22}}{r^2} \right) \frac{\partial^2}{\partial \theta^2} + d_{34} \frac{\partial^2}{\partial z^2} + (d_{12} + d_{26}) \frac{\partial^2}{r \partial r \partial \theta} + (d_{14} + d_{36}) \frac{\partial^2}{\partial r \partial z} + (d_{24} + d_{32}) \right. \\
& \times \frac{\partial^2}{r \partial \theta \partial z} + \left(2d_{16} + \frac{\partial d_{12}}{\partial \theta} \right) \frac{\partial}{r \partial r} + \left(d_{26} + \frac{\partial d_{22}}{\partial \theta} \right) \frac{\partial}{r^2 \partial \theta} + \left(2d_{36} + \frac{\partial d_{32}}{\partial \theta} \right) \frac{\partial}{r \partial z} \Big] \psi^* = 0, \tag{2.5b}
\end{aligned}$$

$$\begin{aligned}
& \left[c_{15} \frac{\partial^2}{\partial r^2} + \left(\frac{c_{46}}{r^2} \right) \frac{\partial^2}{\partial \theta^2} + c_{35} \frac{\partial^2}{\partial z^2} + (c_{14} + c_{56}) \frac{\partial^2}{r \partial r \partial \theta} + (c_{13} + c_{55}) \frac{\partial^2}{\partial r \partial z} + (c_{36} + c_{45}) \frac{\partial^2}{r \partial \theta \partial z} \right. \\
& + \left(c_{15} + c_{25} + \frac{\partial c_{14}}{\partial \theta} \right) \frac{\partial}{r \partial r} + \left(c_{24} + \frac{\partial c_{46}}{\partial \theta} \right) \frac{\partial}{r^2 \partial \theta} + \left(c_{23} + c_{55} + \frac{\partial c_{45}}{\partial \theta} \right) \frac{\partial}{r \partial z} + \left(\frac{\partial c_{24}}{\partial \theta} \right) \frac{1}{r^2} \Big] u_r^* \\
& + \left[c_{56} \frac{\partial^2}{\partial r^2} + \left(\frac{c_{24}}{r^2} \right) \frac{\partial^2}{\partial \theta^2} + c_{34} \frac{\partial^2}{\partial z^2} + (c_{25} + c_{46}) \frac{\partial^2}{r \partial r \partial \theta} + (c_{36} + c_{45}) \frac{\partial^2}{\partial r \partial z} + (c_{23} + c_{44}) \right. \\
& \times \frac{\partial^2}{r \partial \theta \partial z} + \left(\frac{\partial c_{46}}{\partial \theta} \right) \frac{\partial}{r \partial r} + \left(-c_{46} + \frac{\partial c_{24}}{\partial \theta} \right) \frac{\partial}{r^2 \partial \theta} + \left(-c_{36} + c_{45} + \frac{\partial c_{44}}{\partial \theta} \right) \frac{\partial}{r \partial z} + \left(-\frac{\partial c_{46}}{\partial \theta} \right) \\
& \times \frac{1}{r^2} \Big] u_\theta^* + \left[c_{55} \frac{\partial^2}{\partial r^2} + \left(\frac{c_{44}}{r^2} \right) \frac{\partial^2}{\partial \theta^2} + c_{33} \frac{\partial^2}{\partial z^2} + \left(\frac{2c_{45}}{r} \right) \frac{\partial^2}{\partial r \partial \theta} + 2c_{35} \frac{\partial^2}{\partial r \partial z} + \left(\frac{2c_{34}}{r} \right) \frac{\partial^2}{\partial \theta \partial z} \right. \\
& + \left(c_{55} + \frac{\partial c_{45}}{\partial \theta} \right) \frac{\partial}{r \partial r} + \left(\frac{\partial c_{44}}{\partial \theta} \right) \frac{\partial}{r^2 \partial \theta} + \left(c_{35} + \frac{\partial c_{34}}{\partial \theta} \right) \frac{\partial}{r \partial z} - \rho^* \frac{\partial^2}{\partial t^2} \Big] u_z^* + \left[e_{15} \frac{\partial^2}{\partial r^2} + \left(\frac{e_{24}}{r^2} \right) \right.
\end{aligned}$$

$$\begin{aligned}
& \times \frac{\partial^2}{\partial \theta^2} + e_{33} \frac{\partial^2}{\partial z^2} + (e_{14} + e_{25}) \frac{\partial^2}{r \partial r \partial \theta} + (e_{13} + e_{35}) \frac{\partial^2}{\partial r \partial z} + (e_{23} + e_{34}) \frac{\partial^2}{r \partial \theta \partial z} + \left(e_{15} + \frac{\partial e_{14}}{\partial \theta} \right) \\
& \times \frac{\partial}{r \partial r} + \left(\frac{\partial e_{24}}{\partial \theta} \right) \frac{\partial}{r^2 \partial \theta} + \left(e_{35} + \frac{\partial e_{34}}{\partial \theta} \right) \frac{\partial}{r \partial z} \Big] \phi^* + \left[d_{15} \frac{\partial^2}{\partial r^2} + \left(\frac{d_{24}}{r^2} \right) \frac{\partial^2}{\partial \theta^2} + d_{33} \frac{\partial^2}{\partial z^2} \right. \\
& + (d_{14} + d_{25}) \frac{\partial^2}{r \partial r \partial \theta} + (d_{13} + d_{35}) \frac{\partial^2}{\partial r \partial z} + (d_{23} + d_{34}) \frac{\partial^2}{r \partial \theta \partial z} + \left(d_{15} + \frac{\partial d_{14}}{\partial \theta} \right) \frac{\partial}{r \partial r} + \left(\frac{\partial d_{24}}{\partial \theta} \right) \\
& \left. \times \frac{\partial}{r^2 \partial \theta} + \left(d_{35} + \frac{\partial d_{34}}{\partial \theta} \right) \frac{\partial}{r \partial z} \right] \psi^* = 0, \tag{2.5c}
\end{aligned}$$

$$\begin{aligned}
& \left[e_{11} \frac{\partial^2}{\partial r^2} + \left(\frac{e_{26}}{r^2} \right) \frac{\partial^2}{\partial \theta^2} + e_{35} \frac{\partial^2}{\partial z^2} + (e_{16} + e_{21}) \frac{\partial^2}{r \partial r \partial \theta} + (e_{15} + e_{31}) \frac{\partial^2}{\partial r \partial z} + (e_{25} + e_{36}) \frac{\partial^2}{r \partial \theta \partial z} \right. \\
& + \left(e_{11} + e_{12} + \frac{\partial e_{21}}{\partial \theta} \right) \frac{\partial}{r \partial r} + \left(e_{22} + \frac{\partial e_{26}}{\partial \theta} \right) \frac{\partial}{r^2 \partial \theta} + \left(e_{15} + e_{32} + \frac{\partial e_{25}}{\partial \theta} \right) \frac{\partial}{r \partial z} + \left(\frac{\partial e_{22}}{\partial \theta} \right) \frac{1}{r^2} \Big] u_r^* \\
& + \left[e_{16} \frac{\partial^2}{\partial r^2} + \left(\frac{e_{22}}{r^2} \right) \frac{\partial^2}{\partial \theta^2} + e_{34} \frac{\partial^2}{\partial z^2} + (e_{12} + e_{26}) \frac{\partial^2}{r \partial r \partial \theta} + (e_{14} + e_{36}) \frac{\partial^2}{\partial r \partial z} + (e_{24} + e_{32}) \right. \\
& \times \frac{\partial^2}{r \partial \theta \partial z} + \left(\frac{\partial e_{26}}{\partial \theta} \right) \frac{\partial}{r \partial r} + \left(-e_{26} + \frac{\partial e_{22}}{\partial \theta} \right) \frac{\partial}{r^2 \partial \theta} + \left(e_{14} - e_{36} + \frac{\partial e_{24}}{\partial \theta} \right) \frac{\partial}{r \partial z} + \left(-\frac{\partial e_{26}}{\partial \theta} \right) \\
& \left. \times \frac{1}{r^2} \right] u_\theta^* + \left[e_{15} \frac{\partial^2}{\partial r^2} + \left(\frac{e_{24}}{r^2} \right) \frac{\partial^2}{\partial \theta^2} + e_{33} \frac{\partial^2}{\partial z^2} + (e_{14} + e_{25}) \frac{\partial^2}{r \partial r \partial \theta} + (e_{13} + e_{35}) \frac{\partial^2}{\partial r \partial z} \right. \\
& + (e_{23} + e_{34}) \frac{\partial^2}{r \partial \theta \partial z} + \left(e_{15} + \frac{\partial e_{25}}{\partial \theta} \right) \frac{\partial}{r \partial r} + \left(\frac{\partial e_{24}}{\partial \theta} \right) \frac{\partial}{r^2 \partial \theta} + \left(e_{13} + \frac{\partial e_{23}}{\partial \theta} \right) \frac{\partial}{r \partial z} \Big] u_z^* \\
& - \left[\eta_{11} \frac{\partial^2}{\partial r^2} + \left(\frac{\eta_{22}}{r^2} \right) \frac{\partial^2}{\partial \theta^2} + \eta_{33} \frac{\partial^2}{\partial z^2} + \left(\frac{2\eta_{12}}{r} \right) \frac{\partial^2}{\partial r \partial \theta} + 2\eta_{13} \frac{\partial^2}{\partial r \partial z} + \left(\frac{2\eta_{23}}{r} \right) \frac{\partial^2}{\partial \theta \partial z} \right. \\
& + \left(\eta_{11} + \frac{\partial \eta_{12}}{\partial \theta} \right) \frac{\partial}{r \partial r} + \left(\frac{\partial \eta_{22}}{\partial \theta} \right) \frac{\partial}{r^2 \partial \theta} + \left(\eta_{13} + \frac{\partial \eta_{23}}{\partial \theta} \right) \frac{\partial}{r \partial z} \Big] \phi^* - \left[g_{11} \frac{\partial^2}{\partial r^2} + \left(\frac{g_{22}}{r^2} \right) \frac{\partial^2}{\partial \theta^2} \right. \\
& + g_{33} \frac{\partial^2}{\partial z^2} + \left(\frac{2g_{12}}{r} \right) \frac{\partial^2}{\partial r \partial \theta} + 2g_{13} \frac{\partial^2}{\partial r \partial z} + \left(\frac{2g_{23}}{r} \right) \frac{\partial^2}{\partial \theta \partial z} + \left(g_{11} + \frac{\partial g_{12}}{\partial \theta} \right) \frac{\partial}{r \partial r} + \left(\frac{\partial g_{22}}{\partial \theta} \right) \\
& \left. \times \frac{\partial}{r^2 \partial \theta} + \left(g_{13} + \frac{\partial g_{23}}{\partial \theta} \right) \frac{\partial}{r \partial z} \right] \psi^* = 0, \tag{2.5d}
\end{aligned}$$

$$\begin{aligned}
& \left[d_{11} \frac{\partial^2}{\partial r^2} + \left(\frac{d_{26}}{r^2} \right) \frac{\partial^2}{\partial \theta^2} + d_{35} \frac{\partial^2}{\partial z^2} + (d_{16} + d_{21}) \frac{\partial^2}{r \partial r \partial \theta} + (d_{15} + d_{31}) \frac{\partial^2}{\partial r \partial z} + (d_{25} + d_{36}) \frac{\partial^2}{r \partial \theta \partial z} \right. \\
& + \left(d_{11} + d_{12} + \frac{\partial d_{21}}{\partial \theta} \right) \frac{\partial}{r \partial r} + \left(d_{22} + \frac{\partial d_{26}}{\partial \theta} \right) \frac{\partial}{r^2 \partial \theta} + \left(d_{15} + d_{32} + \frac{\partial d_{25}}{\partial \theta} \right) \frac{\partial}{r \partial z} + \left(\frac{\partial d_{22}}{\partial \theta} \right) \\
& \left. \times \frac{1}{r^2} \right] u_r^* + \left[d_{16} \frac{\partial^2}{\partial r^2} + \left(\frac{d_{22}}{r^2} \right) \frac{\partial^2}{\partial \theta^2} + d_{34} \frac{\partial^2}{\partial z^2} + (d_{12} + d_{26}) \frac{\partial^2}{r \partial r \partial \theta} + (d_{14} + d_{36}) \frac{\partial^2}{\partial r \partial z} \right. \\
& + (d_{24} + d_{32}) \frac{\partial^2}{r \partial \theta \partial z} + \left(\frac{\partial d_{26}}{\partial \theta} \right) \frac{\partial}{r \partial r} + \left(-d_{26} + \frac{\partial d_{22}}{\partial \theta} \right) \frac{\partial}{r^2 \partial \theta} + \left(d_{14} - d_{36} + \frac{\partial d_{24}}{\partial \theta} \right) \frac{\partial}{r \partial z} \\
& + \left(-d_{26} + \frac{\partial d_{22}}{\partial \theta} \right) \frac{\partial}{r^2 \partial \theta} + \left(d_{14} - d_{36} + \frac{\partial d_{24}}{\partial \theta} \right) \frac{\partial}{r \partial z} + \left(-\frac{\partial d_{26}}{\partial \theta} \right) \frac{1}{r^2} \Big] u_\theta^* + \left[d_{15} \frac{\partial^2}{\partial r^2} \right. \\
& \left. + \left(\frac{d_{24}}{r^2} \right) \frac{\partial^2}{\partial \theta^2} + d_{33} \frac{\partial^2}{\partial z^2} + (d_{14} + d_{25}) \frac{\partial^2}{r \partial r \partial \theta} + (d_{13} + d_{35}) \frac{\partial^2}{\partial r \partial z} + (d_{23} + d_{34}) \frac{\partial^2}{r \partial \theta \partial z} \right.
\end{aligned}$$

$$\begin{aligned}
& + \left(d_{15} + \frac{\partial d_{25}}{\partial \theta} \right) \frac{\partial}{r \partial r} + \left(\frac{\partial d_{24}}{\partial \theta} \right) \frac{\partial}{r^2 \partial \theta} + \left(d_{13} + \frac{\partial d_{23}}{\partial \theta} \right) \frac{\partial}{r \partial z} \Big] u_z^* - \left[g_{11} \frac{\partial^2}{\partial r^2} + \left(\frac{g_{22}}{r^2} \right) \right. \\
& \times \frac{\partial^2}{\partial \theta^2} + g_{33} \frac{\partial^2}{\partial z^2} + \left(\frac{2g_{12}}{r} \right) \frac{\partial^2}{\partial r \partial \theta} + 2g_{13} \frac{\partial^2}{\partial r \partial z} + \left(\frac{2g_{23}}{r} \right) \frac{\partial^2}{\partial \theta \partial z} + \left(g_{11} + \frac{\partial g_{12}}{\partial \theta} \right) \frac{\partial}{r \partial r} \\
& + \left(\frac{\partial g_{22}}{\partial \theta} \right) \frac{\partial}{r^2 \partial \theta} + \left(g_{13} + \frac{\partial g_{23}}{\partial \theta} \right) \frac{\partial}{r \partial z} \Big] \phi^* - \left[\mu_{11} \frac{\partial^2}{\partial r^2} + \left(\frac{\mu_{22}}{r^2} \right) \frac{\partial^2}{\partial \theta^2} + \mu_{33} \frac{\partial^2}{\partial z^2} + \left(\frac{2\mu_{12}}{r} \right) \right. \\
& \times \frac{\partial^2}{\partial r \partial \theta} + 2\mu_{13} \frac{\partial^2}{\partial r \partial z} + \left(\frac{2\mu_{23}}{r} \right) \frac{\partial^2}{\partial \theta \partial z} + \left(\mu_{11} + \frac{\partial \mu_{12}}{\partial \theta} \right) \frac{\partial}{r \partial r} + \left(\frac{\partial \mu_{22}}{\partial \theta} \right) \frac{\partial}{r^2 \partial \theta} + \left(\mu_{13} \right. \\
& \left. + \frac{\partial \mu_{23}}{\partial \theta} \right) \frac{\partial}{r \partial z} \Big] \psi^* = 0, \tag{2.5e}
\end{aligned}$$

考慮自由振動，位移分量、電勢與磁勢可表示成

$$u_r^* = u_r(r, \theta, Z) e^{i\omega t} \tag{2.6a}$$

$$u_\theta^* = u_\theta(r, \theta, Z) e^{i\omega t} \tag{2.6b}$$

$$u_z^* = u_z(r, \theta, Z) e^{i\omega t} \tag{2.6c}$$

$$\phi^* = \phi(r, \theta, Z) e^{i\omega t} \tag{2.6d}$$

$$\psi^* = \psi(r, \theta, Z) e^{i\omega t} \tag{2.6e}$$

其中 ω 為角頻率。



2.3 電磁彈性迴轉體於尖角處之漸近解

隨著極化方向的改變，迴轉體任一 θ 剖面擁有不同之奇異性強度，為了求取迴轉體於尖角處之漸近解，對於圖 2.2 之幾何形狀進行分析。於分析上之便利性，於某 θ 平面下，根據圖 2.3 將座標系統 (r, Z) 轉換至 (ρ, ξ) 系統，其轉換關係為

$$\rho = \sqrt{(r-R)^2 + Z^2}, \quad \xi = \tan^{-1} \left(\frac{-Z}{r-R} \right), \quad r-R = \rho \cos \xi \text{ 與 } Z = -\rho \sin \xi \tag{2.7}$$

利用式 (2.6) 與 (2.7)，三維力平衡方程式與馬克斯威爾方程式可改寫為

$$\begin{aligned}
& \left\{ (c_{11}L_1 + c_{55}L_3 + 2c_{15}L_5) + \left[\left(c_{11} + \frac{\partial c_{16}}{\partial \theta} + 2c_{16} \frac{\partial}{\partial \theta} \right) L_2 + \left(c_{15} + \frac{\partial c_{56}}{\partial \theta} + 2c_{56} \frac{\partial}{\partial \theta} \right) \right. \right. \\
& \left. \left. \times L_4 \right] + s^2 \left[-c_{22} + \frac{\partial c_{26}}{\partial \theta} + c_{66} \frac{\partial^2}{\partial \theta^2} + \frac{\partial c_{66}}{\partial \theta} \frac{\partial}{\partial \theta} \right] - \omega^2 \rho^* \right\} u_r + \left\{ (c_{16}L_1 + c_{45}L_3 \right.
\end{aligned}$$

$$\begin{aligned}
& + (c_{14} + c_{56}) L_5) + s \left[\left(-c_{26} + \frac{\partial c_{66}}{\partial \theta} + (c_{12} + c_{66}) \frac{\partial}{\partial \theta} \right) L_2 + \left(c_{14} - c_{24} - c_{56} \right. \right. \\
& \left. \left. + \frac{\partial c_{46}}{\partial \theta} + (c_{25} + c_{46}) \frac{\partial}{\partial \theta} \right) L_4 + s^2 \left[c_{26} - \frac{\partial c_{66}}{\partial \theta} + c_{26} \frac{\partial^2}{\partial \theta^2} + \left(-c_{22} - c_{66} + \frac{\partial c_{26}}{\partial \theta} \right) \right. \right. \\
& \left. \left. \times \frac{\partial}{\partial \theta} \right] \right\} u_\theta + \left\{ (c_{15} L_1 + c_{35} L_3 + (c_{13} + c_{55}) L_5) + s \left[\left(c_{15} - c_{25} + \frac{\partial c_{56}}{\partial \theta} + (c_{14} + c_{56}) \right. \right. \right. \\
& \left. \left. \times \frac{\partial}{\partial \theta} \right) L_2 + \left(c_{13} - c_{23} + \frac{\partial c_{36}}{\partial \theta} + (c_{36} + c_{46}) \frac{\partial}{\partial \theta} \right) L_4 \right] + s^2 \left[\left(-c_{24} + \frac{\partial c_{46}}{\partial \theta} \right) \frac{\partial}{\partial \theta} \right. \\
& \left. \left. + c_{46} \frac{\partial^2}{\partial \theta^2} \right] \right\} u_z + \left\{ (e_{11} L_1 + e_{35} L_3 + (e_{15} + e_{31}) L_5) + s \left[\left(e_{11} - e_{12} \frac{\partial e_{16}}{\partial \theta} + (e_{16} \right. \right. \right. \\
& \left. \left. + e_{21}) \frac{\partial}{\partial \theta} \right) L_2 + \left(e_{31} - e_{32} + \frac{\partial e_{36}}{\partial \theta} + (e_{26} + e_{36}) \frac{\partial}{\partial \theta} \right) L_4 \right] + s^2 \left[\left(-e_{22} + \frac{\partial e_{26}}{\partial \theta} \right) \right. \\
& \left. \left. \times \frac{\partial}{\partial \theta} + e_{26} \frac{\partial^2}{\partial \theta^2} \right] \right\} \phi + \left\{ (d_{11} L_1 + d_{35} L_3 + (d_{15} + d_{31}) L_5) + s \left[\left(d_{11} - d_{12} \frac{\partial d_{16}}{\partial \theta} \right. \right. \right. \\
& \left. \left. + (d_{16} + d_{21}) \frac{\partial}{\partial \theta} \right) L_2 + \left(d_{31} - d_{32} + \frac{\partial d_{36}}{\partial \theta} + (d_{25} + d_{36}) \frac{\partial}{\partial \theta} \right) L_4 \right] + s^2 \left[\left(-d_{22} \right. \right. \\
& \left. \left. + \frac{\partial d_{26}}{\partial \theta} \right) \frac{\partial}{\partial \theta} + d_{26} \frac{\partial^2}{\partial \theta^2} \right] \right\} \psi = 0, \tag{2.8a}
\end{aligned}$$

$$\begin{aligned}
& \left\{ (c_{16} L_1 + c_{45} L_3 + (c_{14} + c_{56}) L_5) + s \left[\left(2c_{16} + c_{26} + \frac{\partial c_{12}}{\partial \theta} + (c_{12} + c_{66}) \frac{\partial}{\partial \theta} \right) L_2 + \left(c_{24} \right. \right. \right. \\
& \left. \left. + 2c_{56} + \frac{\partial c_{25}}{\partial \theta} + (c_{25} + c_{46}) \frac{\partial}{\partial \theta} \right) L_4 \right] + s^2 \left[\left(c_{26} + \frac{\partial c_{22}}{\partial \theta} + c_{26} \frac{\partial^2}{\partial \theta^2} \right) + \left(c_{22} + c_{66} \right. \right. \\
& \left. \left. + \frac{\partial c_{26}}{\partial \theta} \right) \frac{\partial}{\partial \theta} \right] \right\} u_r + \left\{ (c_{66} L_1 + c_{44} L_3 + 2c_{46} L_5) + s \left[\left(c_{66} + \frac{\partial c_{26}}{\partial \theta} + 2c_{26} \frac{\partial}{\partial \theta} \right) L_2 \right. \right. \\
& \left. \left. + \left(c_{46} + \frac{\partial c_{24}}{\partial \theta} + 2c_{24} \frac{\partial}{\partial \theta} \right) L_4 \right] + s^2 \left[\left(-c_{66} - \frac{\partial c_{26}}{\partial \theta} + c_{22} \frac{\partial^2}{\partial \theta^2} \right) + \left(\frac{\partial c_{22}}{\partial \theta} \right) \frac{\partial}{\partial \theta} \right] \right. \\
& \left. - \omega^2 \rho^* \right\} u_\theta + \left\{ (c_{56} L_1 + c_{34} L_3 + (c_{36} + c_{45}) L_5) + s \left[\left(2c_{56} + \frac{\partial c_{25}}{\partial \theta} + (c_{25} + c_{46}) \frac{\partial}{\partial \theta} \right) \right. \right. \\
& \left. \left. \times L_2 + \left(2c_{36} + \frac{\partial c_{23}}{\partial \theta} + (c_{23} + c_{44}) \frac{\partial}{\partial \theta} \right) L_4 \right] + s^2 \left[\left(c_{24} \frac{\partial^2}{\partial \theta^2} \right) + \left(c_{46} + \frac{\partial c_{24}}{\partial \theta} \right) \frac{\partial}{\partial \theta} \right] \right\} u_z \\
& + \left\{ (e_{16} L_1 + e_{34} L_3 + (e_{14} + e_{36}) L_5) + s \left[\left(2e_{16} + \frac{\partial e_{12}}{\partial \theta} + (e_{12} + e_{26}) \frac{\partial}{\partial \theta} \right) L_2 + \left(2e_{36} \right. \right. \right. \\
& \left. \left. + \frac{\partial e_{32}}{\partial \theta} + (e_{24} + e_{32}) \frac{\partial}{\partial \theta} \right) L_4 \right] + s^2 \left[\left(e_{22} \frac{\partial^2}{\partial \theta^2} \right) + \left(e_{26} + \frac{\partial e_{22}}{\partial \theta} \right) \frac{\partial}{\partial \theta} \right] \right\} \phi + \left\{ (d_{16} L_1 \right. \\
& \left. + d_{34} L_3 + (d_{14} + d_{36}) L_5) + s \left[\left(2d_{16} + \frac{\partial d_{12}}{\partial \theta} + (d_{12} + d_{26}) \frac{\partial}{\partial \theta} \right) L_2 + \left(2d_{36} + \frac{\partial d_{32}}{\partial \theta} \right. \right. \\
& \left. \left. + (d_{24} + d_{32}) \frac{\partial}{\partial \theta} \right) L_4 \right] + s^2 \left[\left(d_{22} \frac{\partial^2}{\partial \theta^2} \right) + \left(d_{26} + \frac{\partial d_{22}}{\partial \theta} \right) \frac{\partial}{\partial \theta} \right] \right\} \psi = 0, \tag{2.8b}
\end{aligned}$$

$$\left\{ (c_{15} L_1 + c_{35} L_3 + (c_{13} + c_{55}) L_5) + s \left[\left(c_{15} + c_{25} + \frac{\partial c_{14}}{\partial \theta} + (c_{14} + c_{56}) \frac{\partial}{\partial \theta} \right) L_2 + \left(c_{23} + c_{55} \right. \right. \right.$$

$$\begin{aligned}
& + \frac{\partial c_{45}}{\partial \theta} + (c_{36} + c_{45}) \frac{\partial}{\partial \theta} \Big) L_4 \Big] + s^2 \left[\left(\frac{\partial c_{24}}{\partial \theta} + c_{46} \frac{\partial^2}{\partial \theta^2} \right) + \left(c_{24} + \frac{\partial c_{46}}{\partial \theta} \right) \frac{\partial}{\partial \theta} \right] \Big\} u_r \\
& + \left\{ (c_{56} L_1 + c_{34} L_3 + (c_{36} + c_{45}) L_5) + s \left[\left(\frac{\partial c_{46}}{\partial \theta} + (c_{25} + c_{46}) \frac{\partial}{\partial \theta} \right) L_2 + \left(-c_{36} + c_{45} \right. \right. \right. \\
& \left. \left. \left. + \frac{\partial c_{44}}{\partial \theta} + (c_{23} + c_{44}) \frac{\partial}{\partial \theta} \right) L_4 \right] + s^2 \left[\left(-\frac{\partial c_{46}}{\partial \theta} + c_{24} \frac{\partial^2}{\partial \theta^2} \right) + \left(-c_{46} + \frac{\partial c_{24}}{\partial \theta} \right) \frac{\partial}{\partial \theta} \right] \right\} u_\theta \\
& + s \left[\left(c_{55} + \frac{\partial c_{45}}{\partial \theta} + 2c_{45} \frac{\partial}{\partial \theta} \right) L_2 + \left(c_{35} + \frac{\partial c_{34}}{\partial \theta} + 2c_{34} \frac{\partial}{\partial \theta} \right) L_4 \right] + s^2 \left[\left(c_{44} \frac{\partial^2}{\partial \theta^2} \right) \right. \\
& \left. + \left(\frac{\partial c_{44}}{\partial \theta} \right) \frac{\partial}{\partial \theta} \right] - \omega^2 \rho^* \Big\} u_z + \left\{ (e_{15} L_1 + e_{33} L_3 + (e_{13} + e_{35}) L_5) + s \left[\left(e_{15} + \frac{\partial e_{14}}{\partial \theta} \right. \right. \right. \\
& \left. \left. \left. + (e_{14} + e_{25}) \frac{\partial}{\partial \theta} \right) L_2 + \left(e_{35} + \frac{\partial e_{34}}{\partial \theta} + (e_{23} + e_{34}) \frac{\partial}{\partial \theta} \right) L_4 \right] + s^2 \left[\left(e_{24} \frac{\partial^2}{\partial \theta^2} \right) + \left(\frac{\partial e_{24}}{\partial \theta} \right) \right. \right. \\
& \left. \left. \times \frac{\partial}{\partial \theta} \right] \right\} \phi + \left\{ (d_{15} L_1 + d_{33} L_3 + (d_{13} + d_{35}) L_5) + s \left[\left(d_{15} + \frac{\partial d_{14}}{\partial \theta} + (d_{14} + d_{25}) \frac{\partial}{\partial \theta} \right) L_2 \right. \right. \\
& \left. \left. + \left(d_{35} + \frac{\partial d_{34}}{\partial \theta} + (d_{23} + d_{34}) \frac{\partial}{\partial \theta} \right) L_4 \right] + s^2 \left[\left(d_{24} \frac{\partial^2}{\partial \theta^2} \right) + \left(\frac{\partial d_{24}}{\partial \theta} \right) \frac{\partial}{\partial \theta} \right] \right\} \psi = 0, \quad (2.8c)
\end{aligned}$$

$$\begin{aligned}
& \left\{ (e_{11} L_1 + e_{35} L_3 + (e_{15} + e_{31}) L_5) + s \left[\left(e_{11} + e_{12} + \frac{\partial e_{21}}{\partial \theta} + (e_{16} + e_{21}) \frac{\partial}{\partial \theta} \right) L_2 + \left(e_{15} + e_{32} \right. \right. \right. \\
& \left. \left. \left. + \frac{\partial e_{25}}{\partial \theta} + (e_{25} + e_{36}) \frac{\partial}{\partial \theta} \right) L_4 \right] + s^2 \left[\left(\frac{\partial e_{22}}{\partial \theta} + e_{26} \frac{\partial^2}{\partial \theta^2} \right) + \left(e_{22} + \frac{\partial e_{26}}{\partial \theta} \right) \frac{\partial}{\partial \theta} \right] \right\} u_r \\
& + \left\{ (e_{16} L_1 + e_{34} L_3 + (e_{14} + e_{36}) L_5) + s \left[\left(\frac{\partial e_{26}}{\partial \theta} + (e_{12} + e_{26}) \frac{\partial}{\partial \theta} \right) L_2 + \left(e_{14} - e_{36} \right. \right. \right. \\
& \left. \left. \left. + \frac{\partial e_{24}}{\partial \theta} + (e_{24} + e_{32}) \frac{\partial}{\partial \theta} \right) L_4 \right] + s^2 \left[\left(-\frac{\partial e_{26}}{\partial \theta} + e_{22} \frac{\partial^2}{\partial \theta^2} \right) + \left(-e_{26} + \frac{\partial e_{22}}{\partial \theta} \right) \frac{\partial}{\partial \theta} \right] \right\} u_\theta \\
& + \left\{ (e_{15} L_1 + e_{33} L_3 + (e_{13} + e_{35}) L_5) + s \left[\left(e_{15} + \frac{\partial e_{25}}{\partial \theta} + (e_{14} + e_{25}) \frac{\partial}{\partial \theta} \right) L_2 + \left(e_{13} + \frac{\partial e_{23}}{\partial \theta} \right. \right. \right. \\
& \left. \left. \left. + (e_{14} + e_{25}) \frac{\partial}{\partial \theta} \right) L_2 + \left(e_{13} + \frac{\partial e_{23}}{\partial \theta} + (e_{23} + e_{34}) \frac{\partial}{\partial \theta} \right) L_4 \right] + s^2 \left[\left(e_{24} \frac{\partial^2}{\partial \theta^2} \right) + \left(\frac{\partial e_{24}}{\partial \theta} \right) \right. \right. \\
& \left. \left. \times \frac{\partial}{\partial \theta} \right] \right\} u_z - \left\{ (\eta_{11} L_1 + \eta_{33} L_3 + 2\eta_{13} L_5) + s \left[\left(\eta_{11} + \frac{\partial \eta_{12}}{\partial \theta} + 2\eta_{12} \frac{\partial}{\partial \theta} \right) L_2 + \left(\eta_{13} \right. \right. \right. \\
& \left. \left. \left. + \frac{\partial \eta_{23}}{\partial \theta} + 2\eta_{23} \frac{\partial}{\partial \theta} \right) L_4 \right] + s^2 \left[\left(\eta_{22} \frac{\partial^2}{\partial \theta^2} \right) + \left(\frac{\partial \eta_{22}}{\partial \theta} \right) \frac{\partial}{\partial \theta} \right] \right\} \phi - \{ (g_{11} L_1 + g_{33} L_3 \\
& + 2g_{13} L_5) + s \left[\left(g_{11} + \frac{\partial g_{12}}{\partial \theta} + 2g_{12} \frac{\partial}{\partial \theta} \right) L_2 + \left(g_{13} + \frac{\partial g_{23}}{\partial \theta} + 2g_{23} \frac{\partial}{\partial \theta} \right) L_4 \right] \\
& + s^2 \left[\left(g_{22} \frac{\partial^2}{\partial \theta^2} \right) + \left(\frac{\partial g_{22}}{\partial \theta} \right) \frac{\partial}{\partial \theta} \right] \Big\} \psi = 0, \quad (2.8d)
\end{aligned}$$

$$\begin{aligned}
& \left\{ (d_{11} L_1 + d_{35} L_3 + (d_{15} + d_{31}) L_5) + s \left[\left(d_{11} + d_{12} + \frac{\partial d_{21}}{\partial \theta} + (d_{16} + d_{21}) \frac{\partial}{\partial \theta} \right) L_2 + \left(d_{15} + d_{32} \right. \right. \right. \\
& \left. \left. \left. + \frac{\partial d_{25}}{\partial \theta} + (d_{25} + d_{36}) \frac{\partial}{\partial \theta} \right) L_4 \right] + s^2 \left[\left(\frac{\partial d_{22}}{\partial \theta} + d_{26} \frac{\partial^2}{\partial \theta^2} \right) + \left(d_{22} + \frac{\partial d_{26}}{\partial \theta} \right) \frac{\partial}{\partial \theta} \right] \right\} u_r
\end{aligned}$$

$$\begin{aligned}
& + \left\{ (d_{16}L_1 + d_{34}L_3 + (d_{14} + d_{36})L_5) + s \left[\left(\frac{\partial d_{26}}{\partial \theta} + (d_{12} + d_{26}) \frac{\partial}{\partial \theta} \right) L_2 + \left(d_{14} - d_{36} \right. \right. \right. \\
& \left. \left. \left. + \frac{\partial d_{24}}{\partial \theta} + (d_{24} + d_{32}) \frac{\partial}{\partial \theta} \right) L_4 \right] + s^2 \left[\left(-\frac{\partial d_{26}}{\partial \theta} + d_{22} \frac{\partial^2}{\partial \theta^2} \right) + \left(-d_{26} + \frac{\partial d_{22}}{\partial \theta} \right) \frac{\partial}{\partial \theta} \right] \right\} u_\theta \\
& + \left\{ (d_{15}L_1 + d_{33}L_3 + (d_{13} + d_{35})L_5) + s \left[\left(d_{15} + \frac{\partial d_{25}}{\partial \theta} + (d_{14} + d_{25}) \frac{\partial}{\partial \theta} \right) L_2 + \left(d_{13} + \frac{\partial d_{23}}{\partial \theta} \right. \right. \right. \\
& \left. \left. \left. + (d_{14} + d_{25}) \frac{\partial}{\partial \theta} \right) L_2 + \left(d_{13} + \frac{\partial d_{23}}{\partial \theta} + (d_{23} + d_{34}) \frac{\partial}{\partial \theta} \right) L_4 \right] + s^2 \left[\left(d_{24} \frac{\partial^2}{\partial \theta^2} \right) + \left(\frac{\partial d_{24}}{\partial \theta} \right) \right. \right. \\
& \left. \left. \times \frac{\partial}{\partial \theta} \right] \right\} u_z - \left\{ (g_{11}L_1 + g_{33}L_3 + 2g_{13}L_5) + s \left[\left(g_{11} + \frac{\partial g_{12}}{\partial \theta} + 2g_{12} \frac{\partial}{\partial \theta} \right) L_2 + \left(g_{13} \right. \right. \right. \\
& \left. \left. \left. + \frac{\partial g_{23}}{\partial \theta} + 2g_{23} \frac{\partial}{\partial \theta} \right) L_4 \right] + s^2 \left[\left(g_{22} \frac{\partial^2}{\partial \theta^2} \right) + \left(\frac{\partial g_{22}}{\partial \theta} \right) \frac{\partial}{\partial \theta} \right] \right\} \phi - \{ (\mu_{11}L_1 + \mu_{33}L_3 \\
& + 2\mu_{13}L_5) + s \left[\left(\mu_{11} + \frac{\partial \mu_{12}}{\partial \theta} + 2\mu_{12} \frac{\partial}{\partial \theta} \right) L_2 + \left(\mu_{13} + \frac{\partial \mu_{23}}{\partial \theta} + 2\mu_{23} \frac{\partial}{\partial \theta} \right) L_4 \right] \\
& + s^2 \left[\left(\mu_{22} \frac{\partial^2}{\partial \theta^2} \right) + \left(\frac{\partial \mu_{22}}{\partial \theta} \right) \frac{\partial}{\partial \theta} \right] \} \psi = 0, \tag{2.8e}
\end{aligned}$$

其中

$$s = \frac{1}{\rho \cos \xi + R},$$

$$L_1 = \cos^2 \xi \frac{\partial^2}{\partial \rho^2} + \frac{\sin^2 \xi}{\rho} \frac{\partial}{\partial \rho} - \frac{2 \sin \xi \cos \xi}{\rho} \frac{\partial^2}{\partial \rho \partial \xi} + \frac{2 \sin \xi \cos \xi}{\rho^2} \frac{\partial}{\partial \xi} + \frac{\sin^2 \xi}{\rho^2} \frac{\partial^2}{\partial \xi^2},$$

$$L_2 = \cos \xi \frac{\partial}{\partial \rho} - \frac{\sin \xi}{\rho} \frac{\partial}{\partial \xi},$$

$$L_3 = \sin^2 \xi \frac{\partial^2}{\partial \rho^2} + \frac{\cos^2 \xi}{\rho} \frac{\partial}{\partial \rho} + \frac{2 \sin \xi \cos \xi}{\rho} \frac{\partial^2}{\partial \rho \partial \xi} - \frac{2 \sin \xi \cos \xi}{\rho^2} \frac{\partial}{\partial \xi} + \frac{\cos^2 \xi}{\rho^2} \frac{\partial^2}{\partial \xi^2},$$

$$L_4 = -\sin \xi \frac{\partial}{\partial \rho} - \frac{\cos \xi}{\rho} \frac{\partial}{\partial \xi},$$

$$L_5 = -\sin \xi \cos \xi \frac{\partial^2}{\partial \rho^2} + \frac{\sin \xi \cos \xi}{\rho} \frac{\partial}{\partial \rho} - \frac{\cos 2\xi}{\rho} \frac{\partial^2}{\partial \rho \partial \xi} + \frac{\cos 2\xi}{\rho^2} \frac{\partial}{\partial \xi} + \frac{\sin \xi \cos \xi}{\rho^2} \frac{\partial^2}{\partial \xi^2}$$

根據 Hartranft 與 Sih[7] 對於彈性楔形體分析所採用之特徵函數展開法，上式中的位移

分量、電勢與磁勢之漸近解可表示成

$$u_r(\rho, \theta, \xi) = \sum_{m=1}^{\infty} \sum_{n=0}^{\infty} \rho^{\lambda_m+n} \hat{U}_n^{(i)}(\theta, \xi) \tag{2.9a}$$

$$u_\theta(\rho, \theta, \xi) = \sum_{m=1}^{\infty} \sum_{n=0}^{\infty} \rho^{\lambda_m+n} \hat{V}_n^{(i)}(\theta, \xi) \tag{2.9b}$$

$$u_z(\rho, \theta, \xi) = \sum_{m=1}^{\infty} \sum_{n=0}^{\infty} \rho^{\lambda_m+n} \hat{W}_n^{(i)}(\theta, \xi) \tag{2.9c}$$

$$\phi(\rho, \theta, \xi) = \sum_{m=1}^{\infty} \sum_{n=0}^{\infty} \rho^{\lambda_m+n} \hat{\Phi}_n^{(i)}(\theta, \xi) \quad (2.9d)$$

$$\psi(\rho, \theta, \xi) = \sum_{m=1}^{\infty} \sum_{n=0}^{\infty} \rho^{\lambda_m+n} \hat{\Psi}_n^{(i)}(\theta, \xi) \quad (2.9e)$$

其中 λ_m 可以為一複數 (complex number)，但實數部分必須為正值，以確保在尖角處 ($\rho = 0$) 的位移、電勢與磁勢為有限值。接著將式 (2.9) 代入式 (2.8) 中，由於考慮 $\rho \rightarrow 0$ 的情況，所以僅取 ρ 的最低次項，整理可得

$$\begin{aligned} \frac{\partial^2 \hat{U}_0^{(i)}}{\partial \xi^2} + \frac{1}{\Delta_1} \left\{ (\lambda_m - 1) [(c_{35} - c_{11}) \sin 2\xi - 2c_{15} \cos 2\xi] \frac{\partial \hat{U}_0^{(i)}}{\partial \xi} + [\lambda_m ((\lambda_m - 1) c_{11} + c_{55}) \right. \\ \times \cos^2 \xi - \lambda_m (\lambda_m - 2) c_{15} \sin 2\xi + \lambda_m ((\lambda_m - 1) c_{55} + c_{11}) \sin^2 \xi] \hat{U}_0^{(i)} + \left[c_{45} \cos^2 \xi \right. \\ \left. + c_{16} \sin^2 \xi + \frac{(c_{14} + c_{56})}{2} \sin 2\xi \right] \frac{\partial^2 \hat{V}_0^{(i)}}{\partial \xi^2} + (\lambda_m - 1) [(c_{45} - c_{16}) \sin 2\xi - (c_{14} + c_{56}) \\ \times \cos 2\xi] \frac{\partial \hat{V}_0^{(i)}}{\partial \xi} + \left[\lambda_m ((\lambda_m - 1) c_{16} + c_{45}) \cos^2 \xi - \lambda_m (\lambda_m - 2) \frac{(c_{14} + c_{56})}{2} \sin 2\xi \right. \\ \left. + \lambda_m ((\lambda_m - 1) c_{45} + c_{16}) \sin^2 \xi \right] \hat{V}_0^{(i)} + \left[c_{35} \cos^2 \xi + c_{15} \sin^2 \xi + \frac{(c_{13} + c_{55})}{2} \sin 2\xi \right] \\ \times \frac{\partial^2 \hat{W}_0^{(i)}}{\partial \xi^2} + (\lambda_m - 1) [(c_{35} - c_{15}) \sin 2\xi - (c_{13} + c_{55}) \cos 2\xi] \frac{\partial \hat{W}_0^{(i)}}{\partial \xi} + \left[\lambda_m ((\lambda_m - 1) \right. \\ \times c_{15} + c_{35}) \cos^2 \xi - \lambda_m (\lambda_m - 2) \frac{(c_{13} + c_{55})}{2} \sin 2\xi + \lambda_m ((\lambda_m - 1) c_{35} + c_{15}) \sin^2 \xi \\ \times W_0^{(i)} + \left[e_{35} \cos^2 \xi + e_{11} \sin^2 \xi + \frac{(e_{15} + e_{31})}{2} \sin 2\xi \right] \frac{\partial^2 \hat{\Phi}_0^{(i)}}{\partial \xi^2} + (\lambda_m - 1) [(e_{35} - e_{11}) \\ \times \sin 2\xi - (e_{15} + e_{31}) \cos 2\xi] \frac{\partial \hat{\Phi}_0^{(i)}}{\partial \xi} + [\lambda_m ((\lambda_m - 1) e_{11} + e_{35}) \cos^2 \xi - \lambda_m (\lambda_m - 2) \\ \times \frac{(e_{15} + e_{31})}{2} \sin 2\xi + \lambda_m ((\lambda_m - 1) e_{35} + e_{11}) \sin^2 \xi] \hat{\Phi}_0^{(i)} + [d_{35} \cos^2 \xi + d_{11} \sin^2 \xi \\ \left. + \frac{(d_{15} + d_{31})}{2} \sin 2\xi \right] \frac{\partial^2 \hat{\Psi}_0^{(i)}}{\partial \xi^2} + (\lambda_m - 1) [(d_{35} - d_{11}) \sin 2\xi - (d_{15} + d_{31}) \cos 2\xi] \\ \times \frac{\partial \hat{\Psi}_0^{(i)}}{\partial \xi} + \left[\lambda_m ((\lambda_m - 1) d_{11} + d_{35}) \cos^2 \xi - \lambda_m (\lambda_m - 2) \frac{(d_{15} + d_{31})}{2} \sin 2\xi + \lambda_m \right. \\ \left. \times ((\lambda_m - 1) d_{35} + d_{11}) \sin^2 \xi \right] \hat{\Psi}_0^{(i)} \left. \right\} = 0, \quad (2.10a) \end{aligned}$$

$$\begin{aligned} \frac{\partial^2 \hat{V}_0^{(i)}}{\partial \xi^2} + \frac{1}{\Delta_2} \left\{ (\lambda_m - 1) [(c_{44} - c_{66}) \sin 2\xi - 2c_{46} \cos 2\xi] \frac{\partial \hat{V}_0^{(i)}}{\partial \xi} + [\lambda_m ((\lambda_m - 1) c_{66} + c_{44}) \right. \\ \times \cos^2 \xi - \lambda_m (\lambda_m - 2) c_{46} \sin 2\xi + \lambda_m ((\lambda_m - 1) c_{44} + c_{66}) \sin^2 \xi] \hat{V}_0^{(i)} + \left[c_{45} \cos^2 \xi \right. \end{aligned}$$

$$\begin{aligned}
& +c_{16}\sin^2\xi + \frac{(c_{14} + c_{56})}{2} \sin 2\xi \left] \frac{\partial^2 \hat{U}_0^{(i)}}{\partial \xi^2} + (\lambda_m - 1) [(c_{45} - c_{16}) \sin 2\xi - (c_{14} + c_{56}) \right. \\
& \times \cos 2\xi] \frac{\partial \hat{U}_0^{(i)}}{\partial \xi} + \left[\lambda_m ((\lambda_m - 1) c_{16} + c_{45}) \cos^2 \xi - \lambda_m (\lambda_m - 2) \frac{(c_{14} + c_{56})}{2} \sin 2\xi \right. \\
& + \lambda_m ((\lambda_m - 1) c_{45} + c_{16}) \sin^2 \xi] \hat{U}_0^{(i)} + \left[c_{34} \cos^2 \xi + c_{56} \sin^2 \xi + \frac{(c_{36} + c_{45})}{2} \sin 2\xi \right] \\
& \times \frac{\partial^2 \hat{W}_0^{(i)}}{\partial \xi^2} + (\lambda_m - 1) [(c_{34} - c_{56}) \sin 2\xi - (c_{36} + c_{45}) \cos 2\xi] \frac{\partial \hat{W}_0^{(i)}}{\partial \xi} + \left[\lambda_m ((\lambda_m - 1) \right. \\
& \times c_{56} + c_{34}) \cos^2 \xi - \lambda_m (\lambda_m - 2) \frac{(c_{36} + c_{45})}{2} \sin 2\xi + \lambda_m ((\lambda_m - 1) c_{34} + c_{56}) \sin^2 \xi \left. \right] \\
& \times W_0^{(i)} + \left[e_{34} \cos^2 \xi + e_{16} \sin^2 \xi + \frac{(e_{14} + e_{36})}{2} \sin 2\xi \right] \frac{\partial^2 \hat{\Phi}_0^{(i)}}{\partial \xi^2} + (\lambda_m - 1) [(e_{34} - e_{16}) \\
& \times \sin 2\xi - (e_{14} + e_{36}) \cos 2\xi] \frac{\partial \hat{\Phi}_0^{(i)}}{\partial \xi} + \left[\lambda_m ((\lambda_m - 1) e_{16} + e_{34}) \cos^2 \xi + \lambda_m (\lambda_m - 2) \right. \\
& \times \frac{(e_{14} + e_{36})}{2} \sin 2\xi + \lambda_m ((\lambda_m - 1) e_{34} + e_{16}) \sin^2 \xi \left. \right] \hat{\Phi}_0^{(i)} + \left[d_{34} \cos^2 \xi + d_{16} \sin^2 \xi \right. \\
& + \frac{(d_{14} + d_{36})}{2} \sin 2\xi \left. \right] \frac{\partial^2 \hat{\Psi}_0^{(i)}}{\partial \xi^2} + (\lambda_m - 1) [(d_{34} - d_{16}) \sin 2\xi - (d_{14} + d_{36}) \cos 2\xi] \\
& \times \frac{\partial \hat{\Psi}_0^{(i)}}{\partial \xi} + \left[\lambda_m ((\lambda_m - 1) d_{16} + d_{34}) \cos^2 \xi - \lambda_m (\lambda_m - 2) \frac{(d_{14} + d_{36})}{2} \sin 2\xi + \lambda_m \right. \\
& \times ((\lambda_m - 1) d_{34} + d_{16}) \sin^2 \xi \left. \right] \hat{\Psi}_0^{(i)} \left. \right\} = 0, \tag{2.10b}
\end{aligned}$$

$$\begin{aligned}
& \frac{\partial^2 \hat{W}_0^{(i)}}{\partial \xi^2} + \frac{1}{\Delta_3} \left\{ (\lambda_m - 1) [(c_{33} - c_{55}) \sin 2\xi - 2c_{35} \cos 2\xi] \frac{\partial \hat{W}_0^{(i)}}{\partial \xi} + [\lambda_m ((\lambda_m - 1) c_{55} + c_{33}) \right. \\
& \times \cos^2 \xi - \lambda_m (\lambda_m - 2) c_{35} \sin 2\xi + \lambda_m ((\lambda_m - 1) c_{33} + c_{55}) \sin^2 \xi] \hat{W}_0^{(i)} + \left[c_{35} \cos^2 \xi \right. \\
& + c_{15} \sin^2 \xi + \frac{(c_{13} + c_{55})}{2} \sin 2\xi \left. \right] \frac{\partial^2 \hat{U}_0^{(i)}}{\partial \xi^2} + (\lambda_m - 1) [(c_{45} - c_{16}) \sin 2\xi - (c_{14} + c_{56}) \\
& \times \cos 2\xi] \frac{\partial \hat{U}_0^{(i)}}{\partial \xi} + \left[\lambda_m ((\lambda_m - 1) c_{15} + c_{35}) \cos^2 \xi - \lambda_m (\lambda_m - 2) \frac{(c_{13} + c_{55})}{2} \sin 2\xi \right. \\
& + \lambda_m ((\lambda_m - 1) c_{35} + c_{15}) \sin^2 \xi \left. \right] \hat{U}_0^{(i)} + \left[c_{34} \cos^2 \xi + c_{56} \sin^2 \xi + \frac{(c_{36} + c_{45})}{2} \sin 2\xi \right] \\
& \times \frac{\partial^2 \hat{V}_0^{(i)}}{\partial \xi^2} + (\lambda_m - 1) [(c_{34} - c_{56}) \sin 2\xi - (c_{36} + c_{45}) \cos 2\xi] \frac{\partial \hat{V}_0^{(i)}}{\partial \xi} + \left[\lambda_m ((\lambda_m - 1) c_{56} \right. \\
& + c_{34}) \cos^2 \xi - \lambda_m (\lambda_m - 2) \frac{(c_{36} + c_{45})}{2} \sin 2\xi + \lambda_m ((\lambda_m - 1) c_{34} + c_{56}) \sin^2 \xi \left. \right] \hat{V}_0^{(i)} \\
& + \left[e_{33} \cos^2 \xi + e_{15} \sin^2 \xi + \frac{(e_{13} + e_{35})}{2} \sin 2\xi \right] \frac{\partial^2 \hat{\Phi}_0^{(i)}}{\partial \xi^2} + (\lambda_m - 1) [(e_{33} - e_{15}) \sin 2\xi \\
& - (e_{13} + e_{35}) \cos 2\xi] \frac{\partial \hat{\Phi}_0^{(i)}}{\partial \xi} + \left[\lambda_m ((\lambda_m - 1) e_{15} + e_{33}) \cos^2 \xi - \lambda_m (\lambda_m - 2) \frac{(e_{13} + e_{35})}{2} \right.
\end{aligned}$$

$$\begin{aligned}
& \times \sin 2\xi + \lambda_m ((\lambda_m - 1) e_{33} + e_{15}) \sin^2 \xi \left] \hat{\Phi}_0^{(i)} + \left[d_{33} \cos^2 \xi + d_{15} \sin^2 \xi + \frac{(d_{13} + d_{35})}{2} \right. \right. \\
& \times \sin 2\xi \left. \left. \frac{\partial^2 \hat{\Psi}_0^{(i)}}{\partial \xi^2} + (\lambda_m - 1) [(d_{33} - d_{15}) \sin 2\xi - (d_{13} + d_{35}) \cos 2\xi] \frac{\partial \hat{\Psi}_0^{(i)}}{\partial \xi} + \left[\lambda_m \right. \right. \right. \\
& \times ((\lambda_m - 1) d_{15} + d_{33}) \cos^2 \xi - \lambda_m (\lambda_m - 2) \frac{(d_{13} + d_{35})}{2} \sin 2\xi + \lambda_m ((\lambda_m - 1) d_{33} + d_{15}) \\
& \left. \left. \left. \times \sin^2 \xi \right] \Psi_0^{(i)} \right\} = 0, \tag{2.10c}
\end{aligned}$$

$$\begin{aligned}
& \frac{\partial^2 \hat{\Phi}_0^{(i)}}{\partial \xi^2} + \frac{1}{\Delta_4} \left\{ (\lambda_m - 1) [(\eta_{33} - \eta_{11}) \sin 2\xi - 2\eta_{13} \cos 2\xi] \frac{\partial \hat{\Phi}_0^{(i)}}{\partial \xi} + [\lambda_m ((\lambda_m - 1) \eta_{11} + \eta_{33}) \right. \\
& \times \cos^2 \xi - \lambda_m (\lambda_m - 2) \eta_{13} \sin 2\xi + \lambda_m ((\lambda_m - 1) \eta_{33} + \eta_{11}) \sin^2 \xi] \hat{\Phi}_0^{(i)} - \left[e_{35} \cos^2 \xi \right. \\
& \left. + e_{11} \sin^2 \xi + \frac{(e_{15} + e_{31})}{2} \sin 2\xi \right] \frac{\partial^2 \hat{U}_0^{(i)}}{\partial \xi^2} - (\lambda_m - 1) [(e_{35} - e_{11}) \sin 2\xi - (e_{15} + e_{31}) \\
& \times \cos 2\xi] \frac{\partial \hat{U}_0^{(i)}}{\partial \xi} - \left[\lambda_m ((\lambda_m - 1) e_{11} + e_{35}) \cos^2 \xi - \lambda_m (\lambda_m - 2) \frac{(e_{15} + e_{31})}{2} \sin 2\xi + \lambda_m \right. \\
& \times ((\lambda_m - 1) e_{35} + e_{11}) \sin^2 \xi \left. \right] \hat{U}_0^{(i)} - \left[e_{34} \cos^2 \xi + e_{16} \sin^2 \xi + \frac{(e_{14} + e_{36})}{2} \sin 2\xi \right] \frac{\partial^2 \hat{V}_0^{(i)}}{\partial \xi^2} \\
& - [(e_{34} - e_{16}) \sin 2\xi - (e_{14} + e_{36}) \cos 2\xi] \frac{\partial \hat{V}_0^{(i)}}{\partial \xi} - \left[\lambda_m ((\lambda_m - 1) e_{16} + e_{34}) \cos^2 \xi - \lambda_m \right. \\
& \times (\lambda_m - 2) \frac{(e_{14} + e_{36})}{2} \sin 2\xi + \lambda_m ((\lambda_m - 1) e_{34} + e_{16}) \sin^2 \xi \left. \right] \hat{V}_0^{(i)} - \left[e_{33} \cos^2 \xi + e_{15} \sin^2 \xi \right. \\
& \left. + \frac{(e_{13} + e_{35})}{2} \sin 2\xi \right] \frac{\partial^2 \hat{W}_0^{(i)}}{\partial \xi^2} - (\lambda_m - 1) [(e_{33} - e_{15}) \sin 2\xi - (e_{13} + e_{35}) \cos 2\xi] \frac{\partial \hat{W}_0^{(i)}}{\partial \xi} \\
& - \left[\lambda_m ((\lambda_m - 1) e_{15} + e_{33}) \cos^2 \xi - \lambda_m (\lambda_m - 2) \frac{(e_{13} + e_{35})}{2} \sin 2\xi + \lambda_m ((\lambda_m - 1) e_{33} + e_{15}) \right. \\
& \times \sin^2 \xi \left. \right] \hat{W}_0^{(i)} + [g_{33} \cos^2 \xi + g_{11} \sin^2 \xi + g_{13} \sin 2\xi] \frac{\partial^2 \hat{\Psi}_0^{(i)}}{\partial \xi^2} + (\lambda_m - 1) [(g_{33} - g_{11}) \\
& \times \sin 2\xi - 2g_{13} \cos 2\xi] \frac{\partial \hat{\Psi}_0^{(i)}}{\partial \xi} + [\lambda_m ((\lambda_m - 1) g_{11} + g_{33}) \cos^2 \xi - \lambda_m (\lambda_m - 2) g_{13} \sin 2\xi \\
& \left. + \lambda_m ((\lambda_m - 1) g_{33} + g_{11}) \sin^2 \xi \right] \hat{\Psi}_0^{(i)} \left. \right\} = 0, \tag{2.10d}
\end{aligned}$$

$$\begin{aligned}
& \frac{\partial^2 \hat{\Psi}_0^{(i)}}{\partial \xi^2} + \frac{1}{\Delta_5} \left\{ (\lambda_m - 1) [(\mu_{33} - \mu_{11}) \sin 2\xi - 2\mu_{13} \cos 2\xi] \frac{\partial \hat{\Psi}_0^{(i)}}{\partial \xi} + [\lambda_m ((\lambda_m - 1) \mu_{11} + \mu_{33}) \right. \\
& \times \cos^2 \xi - \lambda_m (\lambda_m - 2) \mu_{13} \sin 2\xi + \lambda_m ((\lambda_m - 1) \mu_{33} + \mu_{11}) \sin^2 \xi] \hat{\Psi}_0^{(i)} - \left[d_{35} \cos^2 \xi \right. \\
& \left. + d_{11} \sin^2 \xi + \frac{(d_{15} + d_{31})}{2} \sin 2\xi \right] \frac{\partial^2 \hat{U}_0^{(i)}}{\partial \xi^2} - (\lambda_m - 1) [(d_{35} - e_{11}) \sin 2\xi - (d_{15} + d_{31}) \\
& \times \cos 2\xi] \frac{\partial \hat{U}_0^{(i)}}{\partial \xi} - \left[\lambda_m ((\lambda_m - 1) d_{11} + d_{35}) \cos^2 \xi - \lambda_m (\lambda_m - 2) \frac{(d_{15} + d_{31})}{2} \sin 2\xi + \lambda_m \right.
\end{aligned}$$

$$\begin{aligned}
& \times ((\lambda_m - 1) d_{35} + d_{11}) \sin^2 \xi \left] \hat{U}_0^{(i)} - \left[d_{34} \cos^2 \xi + d_{16} \sin^2 \xi + \frac{(d_{14} + d_{36})}{2} \sin 2\xi \right] \frac{\partial^2 \hat{V}_0^{(i)}}{\partial \xi^2} \\
& - [(d_{34} - d_{16}) \sin 2\xi - (d_{14} + d_{36}) \cos 2\xi] \frac{\partial \hat{V}_0^{(i)}}{\partial \xi} - \left[\lambda_m ((\lambda_m - 1) d_{16} + d_{34}) \cos^2 \xi - \lambda_m \right. \\
& \times (\lambda_m - 2) \frac{(d_{14} + d_{36})}{2} \sin 2\xi + \lambda_m ((\lambda_m - 1) d_{34} + d_{16}) \sin^2 \xi \left. \right] \hat{V}_0^{(i)} - \left[d_{33} \cos^2 \xi + d_{15} \sin^2 \xi \right. \\
& \left. + \frac{(d_{13} + d_{35})}{2} \sin 2\xi \right] \frac{\partial^2 \hat{W}_0^{(i)}}{\partial \xi^2} - (\lambda_m - 1) [(d_{33} - d_{15}) \sin 2\xi - (d_{13} + d_{35}) \cos 2\xi] \frac{\partial \hat{W}_0^{(i)}}{\partial \xi} \\
& - \left[\lambda_m ((\lambda_m - 1) d_{15} + d_{33}) \cos^2 \xi - \lambda_m (\lambda_m - 2) \frac{(d_{13} + d_{35})}{2} \sin 2\xi + \lambda_m ((\lambda_m - 1) d_{33} + d_{15}) \right. \\
& \left. \times \sin^2 \xi \right] \hat{W}_0^{(i)} + [g_{33} \cos^2 \xi + g_{11} \sin^2 \xi + g_{13} \sin 2\xi] \frac{\partial^2 \hat{\Phi}_0^{(i)}}{\partial \xi^2} + (\lambda_m - 1) [(g_{33} - g_{11}) \\
& \times \sin 2\xi - 2g_{13} \cos 2\xi] \frac{\partial \hat{\Phi}_0^{(i)}}{\partial \xi} + [\lambda_m ((\lambda_m - 1) g_{11} + g_{33}) \cos^2 \xi - \lambda_m (\lambda_m - 2) g_{13} \sin 2\xi \\
& \left. + \lambda_m ((\lambda_m - 1) g_{33} + g_{11}) \sin^2 \xi] \hat{\Phi}_0^{(i)} \right\} = 0, \tag{2.10e}
\end{aligned}$$

其中

$$\Delta_1 = c_{11} \sin^2 \xi + c_{55} \cos^2 \xi + c_{15} \sin 2\xi$$

$$\Delta_2 = c_{66} \sin^2 \xi + c_{44} \cos^2 \xi + c_{46} \sin 2\xi$$

$$\Delta_3 = c_{55} \sin^2 \xi + c_{33} \cos^2 \xi + c_{35} \sin 2\xi$$

$$\Delta_4 = \eta_{11} \sin^2 \xi + \eta_{33} \cos^2 \xi + \eta_{13} \sin 2\xi$$

$$\Delta_5 = \mu_{11} \sin^2 \xi + \mu_{33} \cos^2 \xi + \mu_{13} \sin 2\xi$$

由於之前提到將座標系統 (r, Z) 轉換至 (ρ, ξ) 系統的緣故，使得式 (2.10) 中各項之係數均為 ξ ， θ 與 γ 之函數導致無法直接求取式 (2.10) 之閉合解 (close-form solution)，因此使用級數法 (power series method) 以解決因變異係數所造成偏微分方程式求解之不便。為得到較精確的解，須採用較高階的項次，但這常會造成數值較算上的困難，於是我們將分析模型切割為數個子域 (sub-domain)，並在各子域中建立式 (2.10) 之級數解；另外，各子域間必須藉由連續條件 (continuity condition) 以互相聯結。如此，集合各子域的級數解便可建立全域 ξ 之通解 (general solution)。

利用泰勒展開式 (Taylor's expansion series) 描述於各子域中式 (2.10) 的變異係數

如下

$$\begin{aligned} \frac{\sin 2\xi}{\Delta_l} &= \sum_{k=0}^K a_{lk}^{(i)} (\xi - \bar{\xi}_i)^k, \quad \frac{\cos^2 \xi}{\Delta_l} = \sum_{k=0}^K b_{lk}^{(i)} (\xi - \bar{\xi}_i)^k, \quad \frac{\sin^2 \xi}{\Delta_l} = \sum_{k=0}^K c_{lk}^{(i)} (\xi - \bar{\xi}_i)^k, \\ \frac{\cos 2\xi}{\Delta_l} &= \sum_{k=0}^K d_{lk}^{(i)} (\xi - \bar{\xi}_i)^k, \quad l = 1 \sim 5 \end{aligned} \quad (2.11)$$

其中 $\bar{\xi}_i$ 為 i 子域的中點。因此，式 (2.9) 於各子域下的解可以假設為

$$\begin{aligned} \hat{U}_0^{(i)} &= \sum_{j=0}^J \hat{A}_j^{(i)} (\xi - \bar{\xi}_i)^j, \quad \hat{V}_0^{(i)} = \sum_{j=0}^J \hat{B}_j^{(i)} (\xi - \bar{\xi}_i)^j, \quad \hat{W}_0^{(i)} = \sum_{j=0}^J \hat{C}_j^{(i)} (\xi - \bar{\xi}_i)^j, \\ \hat{\Phi}_0^{(i)} &= \sum_{j=0}^J \hat{D}_j^{(i)} (\xi - \bar{\xi}_i)^j, \quad \hat{\Psi}_0^{(i)} = \sum_{j=0}^J \hat{E}_j^{(i)} (\xi - \bar{\xi}_i)^j \end{aligned} \quad (2.12)$$

將方程式 (2.11) 與 (2.12) 代入式 (2.10) 中，可得式 (2.12) 中各係數間之遞迴方程式

$$\begin{aligned} &\hat{A}_{j+2}^{(i)} + \left(c_{45} b_{10}^{(i)} + c_{16} c_{10}^{(i)} + \frac{(c_{14} + c_{56})}{2} a_{10}^{(i)} \right) \hat{B}_{j+2}^{(i)} + \left(c_{35} b_{10}^{(i)} + c_{15} c_{10}^{(i)} + \frac{(c_{13} + c_{55})}{2} a_{10}^{(i)} \right) \hat{C}_{j+2}^{(i)} \\ &\quad + \left(e_{35} b_{10}^{(i)} + e_{11} c_{10}^{(i)} + \frac{(e_{15} + e_{31})}{2} a_{10}^{(i)} \right) \hat{D}_{j+2}^{(i)} + \left(d_{35} b_{10}^{(i)} + d_{11} c_{10}^{(i)} + \frac{(d_{15} + d_{31})}{2} a_{10}^{(i)} \right) \hat{E}_{j+2}^{(i)} \\ &= \frac{-1}{(j+2)(j+1)} \left\{ \sum_{k=0}^{j-1} (k+2)(k+1) \left[\left(c_{45} b_{1j-k}^{(i)} + c_{16} c_{1j-k}^{(i)} + \frac{(c_{14} + c_{56})}{2} a_{1j-k}^{(i)} \right) \hat{B}_{k+2}^{(i)} \right. \right. \\ &\quad + \left(c_{35} b_{1j-k}^{(i)} + c_{15} c_{1j-k}^{(i)} + \frac{(c_{13} + c_{55})}{2} a_{1j-k}^{(i)} \right) \hat{C}_{k+2}^{(i)} + \left(e_{35} b_{1j-k}^{(i)} + e_{11} c_{1j-k}^{(i)} + \frac{(e_{15} + e_{31})}{2} a_{1j-k}^{(i)} \right) \hat{D}_{k+2}^{(i)} \\ &\quad \left. \left. + \left(d_{35} b_{1j-k}^{(i)} + d_{11} c_{1j-k}^{(i)} + \frac{(d_{13} + d_{31})}{2} a_{1j-k}^{(i)} \right) \hat{E}_{k+2}^{(i)} \right] \right. \\ &\quad + \sum_{k=0}^j (k+1)(\lambda_m - 1) \left[((c_{55} - c_{11}) a_{1j-k}^{(i)} - 2c_{15} d_{1j-k}^{(i)}) \hat{A}_{k+1}^{(i)} \right. \\ &\quad + ((c_{45} - c_{16}) a_{1j-k}^{(i)} - (c_{14} + c_{56}) d_{1j-k}^{(i)}) \hat{B}_{k+1}^{(i)} + ((c_{35} - c_{15}) a_{1j-k}^{(i)} - (c_{13} + c_{55}) d_{1j-k}^{(i)}) \hat{C}_{k+1}^{(i)} \\ &\quad + ((e_{35} - e_{11}) a_{1j-k}^{(i)} - (e_{15} + e_{31}) d_{1j-k}^{(i)}) \hat{D}_{k+1}^{(i)} + ((d_{35} - d_{11}) a_{1j-k}^{(i)} - (d_{15} + d_{31}) d_{1j-k}^{(i)}) \hat{E}_{k+1}^{(i)} \\ &\quad + [\lambda_m ((\lambda_m - 1) c_{11} + c_{55}) b_{1j-k}^{(i)} - \lambda_m (\lambda_m - 2) c_{15} a_{1j-k}^{(i)} + \lambda_m ((\lambda_m - 1) c_{55} + c_{11}) c_{1j-k}^{(i)}] \hat{A}_k^{(i)} \\ &\quad + \left[\lambda_m ((\lambda_m - 1) c_{16} + c_{45}) b_{1j-k}^{(i)} - \lambda_m (\lambda_m - 2) \frac{(c_{14} + c_{56})}{2} a_{1j-k}^{(i)} + \lambda_m ((\lambda_m - 1) c_{45} + c_{16}) c_{1j-k}^{(i)} \right] \hat{B}_k^{(i)} \\ &\quad + \left[\lambda_m ((\lambda_m - 1) c_{15} + c_{35}) b_{1j-k}^{(i)} - \lambda_m (\lambda_m - 2) \frac{(c_{13} + c_{55})}{2} a_{1j-k}^{(i)} + \lambda_m ((\lambda_m - 1) c_{35} + c_{15}) c_{1j-k}^{(i)} \right] \hat{C}_k^{(i)} \\ &\quad + \left[\lambda_m ((\lambda_m - 1) e_{11} + e_{35}) b_{1j-k}^{(i)} - \lambda_m (\lambda_m - 2) \frac{(e_{15} + e_{31})}{2} a_{1j-k}^{(i)} + \lambda_m ((\lambda_m - 1) e_{35} + e_{11}) c_{1j-k}^{(i)} \right] \hat{D}_k^{(i)} \\ &\quad \left. \left. + \left[\lambda_m ((\lambda_m - 1) d_{11} + d_{35}) b_{1j-k}^{(i)} - \lambda_m (\lambda_m - 2) \frac{(d_{15} + d_{31})}{2} a_{1j-k}^{(i)} + \lambda_m ((\lambda_m - 1) d_{35} + d_{11}) c_{1j-k}^{(i)} \right] \hat{E}_k^{(i)} \right] \right\} \end{aligned} \quad (2.13a)$$

$$\begin{aligned}
& \hat{B}_{j+2}^{(i)} + \left(c_{45} b_{20}^{(i)} + c_{16} c_{20}^{(i)} + \frac{(c_{14} + c_{56})}{2} a_{20}^{(i)} \right) \hat{A}_{j+2}^{(i)} + \left(c_{34} b_{20}^{(i)} + c_{56} c_{20}^{(i)} + \frac{(c_{36} + c_{45})}{2} a_{20}^{(i)} \right) \hat{C}_{j+2}^{(i)} \\
& + \left(e_{34} b_{20}^{(i)} + e_{16} c_{20}^{(i)} + \frac{(e_{14} + e_{36})}{2} a_{20}^{(i)} \right) \hat{D}_{j+2}^{(i)} + \left(d_{34} b_{20}^{(i)} + d_{16} c_{20}^{(i)} + \frac{(d_{14} + d_{36})}{2} a_{20}^{(i)} \right) \hat{E}_{j+2}^{(i)} \\
& = \frac{-1}{(j+2)(j+1)} \left\{ \sum_{k=0}^{j-1} (k+2)(k+1) \left[\left(c_{45} b_{2j-k}^{(i)} + c_{16} c_{2j-k}^{(i)} + \frac{(c_{14} + c_{56})}{2} a_{2j-k}^{(i)} \right) \hat{A}_{k+2}^{(i)} \right. \right. \\
& + \left(c_{34} b_{2j-k}^{(i)} + c_{56} c_{2j-k}^{(i)} + \frac{(c_{36} + c_{45})}{2} a_{2j-k}^{(i)} \right) \hat{C}_{k+2}^{(i)} + \left(e_{34} b_{2j-k}^{(i)} + e_{16} c_{2j-k}^{(i)} + \frac{(e_{14} + e_{36})}{2} a_{2j-k}^{(i)} \right) \hat{D}_{k+2}^{(i)} \\
& + \left. \left(d_{34} b_{2j-k}^{(i)} + d_{16} c_{2j-k}^{(i)} + \frac{(d_{14} + d_{36})}{2} a_{2j-k}^{(i)} \right) \hat{E}_{k+2}^{(i)} \right] \\
& + \sum_{k=0}^j (k+1)(\lambda_m - 1) \left[[(c_{45} - c_{16})(a_2)_{j-k} - (c_{14} + c_{56})(d_2)_{j-k}] \hat{A}_{k+1}^{(i)} \right. \\
& + [(c_{44} - c_{56}) a_{2j-k}^{(i)} - 2c_{46} d_{2j-k}^{(i)}] \hat{B}_{k+1}^{(i)} + [(c_{34} - c_{56}) a_{2j-k}^{(i)} - (c_{36} + c_{45}) d_{2j-k}^{(i)}] \hat{C}_{k+1}^{(i)} \\
& + [(e_{34} - e_{16}) a_{2j-k}^{(i)} - (e_{14} + e_{36}) d_{2j-k}^{(i)}] \hat{D}_{k+1}^{(i)} + [(d_{34} - d_{16}) a_{2j-k}^{(i)} - (d_{14} + d_{36}) d_{2j-k}^{(i)}] \hat{E}_{k+1}^{(i)} \\
& + \left[\lambda_m ((\lambda_m - 1) c_{16} + c_{45}) b_{2j-k}^{(i)} - \lambda_m (\lambda_m - 2) \frac{(c_{14} + c_{56})}{2} a_{2j-k}^{(i)} + \lambda_m ((\lambda_m - 1) c_{45} + c_{16}) c_{2j-k}^{(i)} \right] \hat{A}_k^{(i)} \\
& + \left[\lambda_m ((\lambda_m - 1) c_{66} + c_{44}) b_{2j-k}^{(i)} - \lambda_m (\lambda_m - 2) c_{46} a_{2j-k}^{(i)} + \lambda_m ((\lambda_m - 1) c_{44} + c_{66}) c_{2j-k}^{(i)} \right] \hat{B}_k^{(i)} \\
& + \left[\lambda_m ((\lambda_m - 1) c_{56} + c_{34}) b_{2j-k}^{(i)} - \lambda_m (\lambda_m - 2) \frac{(c_{36} + c_{45})}{2} a_{2j-k}^{(i)} + \lambda_m ((\lambda_m - 1) c_{34} + c_{56}) c_{2j-k}^{(i)} \right] \hat{C}_k^{(i)} \\
& + \left[\lambda_m ((\lambda_m - 1) e_{16} + e_{34}) b_{2j-k}^{(i)} - \lambda_m (\lambda_m - 2) \frac{(e_{14} + e_{36})}{2} a_{2j-k}^{(i)} + \lambda_m ((\lambda_m - 1) e_{34} + e_{16}) c_{2j-k}^{(i)} \right] \hat{D}_k^{(i)} \\
& + \left. \left[\lambda_m ((\lambda_m - 1) d_{16} + d_{34}) b_{2j-k}^{(i)} - \lambda_m (\lambda_m - 2) \frac{(d_{14} + d_{36})}{2} a_{2j-k}^{(i)} + \lambda_m ((\lambda_m - 1) d_{34} + d_{16}) c_{2j-k}^{(i)} \right] \hat{E}_k^{(i)} \right\} \\
& \tag{2.13b}
\end{aligned}$$

$$\begin{aligned}
& \hat{C}_{j+2}^{(i)} + \left(c_{35} b_{30}^{(i)} + c_{15} c_{30}^{(i)} + \frac{(c_{13} + c_{55})}{2} a_{30}^{(i)} \right) \hat{A}_{j+2}^{(i)} + \left(c_{34} b_{30}^{(i)} + c_{56} c_{30}^{(i)} + \frac{(c_{36} + c_{45})}{2} a_{30}^{(i)} \right) \hat{B}_{j+2}^{(i)} \\
& + \left(e_{33} b_{30}^{(i)} + e_{15} c_{30}^{(i)} + \frac{(e_{13} + e_{35})}{2} a_{30}^{(i)} \right) \hat{D}_{j+2}^{(i)} + \left(d_{33} b_{30}^{(i)} + d_{15} c_{30}^{(i)} + \frac{(d_{13} + d_{35})}{2} a_{30}^{(i)} \right) \hat{E}_{j+2}^{(i)} \\
& = \frac{-1}{(j+2)(j+1)} \left\{ \sum_{k=0}^{j-1} (k+2)(k+1) \left[\left(c_{35} b_{3j-k}^{(i)} + c_{15} c_{3j-k}^{(i)} + \frac{(c_{13} + c_{55})}{2} a_{3j-k}^{(i)} \right) \hat{A}_{k+2}^{(i)} \right. \right. \\
& + \left(c_{34} b_{3j-k}^{(i)} + c_{56} c_{3j-k}^{(i)} + \frac{(c_{36} + c_{45})}{2} a_{3j-k}^{(i)} \right) \hat{B}_{k+2}^{(i)} + \left(e_{33} b_{3j-k}^{(i)} + e_{15} c_{3j-k}^{(i)} + \frac{(e_{13} + e_{35})}{2} a_{3j-k}^{(i)} \right) \hat{D}_{k+2}^{(i)} \\
& + \left. \left(d_{33} b_{3j-k}^{(i)} + d_{15} c_{3j-k}^{(i)} + \frac{(d_{13} + d_{35})}{2} a_{3j-k}^{(i)} \right) \hat{E}_{k+2}^{(i)} \right] \\
& \left. \right\}
\end{aligned}$$

$$\begin{aligned}
& + \sum_{k=0}^j (k+1) (\lambda_m - 1) \left[[(c_{35} - c_{15}) a_{3j-k}^{(i)} - (c_{13} + c_{55}) d_{3j-k}^{(i)}] \hat{A}_{k+1} \right. \\
& + [(c_{34} - c_{56}) a_{3j-k}^{(i)} - (c_{36} + c_{45}) d_{3j-k}^{(i)}] \hat{B}_{k+1} + [(c_{33} - c_{55}) a_{3j-k}^{(i)} - 2c_{35} d_{3j-k}^{(i)}] \hat{C}_{k+1} \\
& + [(e_{33} - e_{15}) a_{3j-k}^{(i)} - (e_{13} + e_{35}) d_{3j-k}^{(i)}] \hat{D}_{k+1} + [(d_{33} - d_{15}) a_{3j-k}^{(i)} - (d_{13} + d_{35}) d_{3j-k}^{(i)}] \hat{E}_{k+1} \\
& + \left[\lambda_m ((\lambda_m - 1) c_{15} + c_{35}) b_{3j-k}^{(i)} - \lambda_m (\lambda_m - 2) \frac{(c_{13} + c_{55})}{2} a_{3j-k}^{(i)} + \lambda_m ((\lambda_m - 1) c_{35} + c_{15}) c_{3j-k}^{(i)} \right] \hat{A}_k \\
& + \left[\lambda_m ((\lambda_m - 1) c_{56} + c_{34}) b_{3j-k}^{(i)} - \lambda_m (\lambda_m - 2) \frac{(c_{36} + c_{45})}{2} a_{3j-k}^{(i)} + \lambda_m ((\lambda_m - 1) c_{34} + c_{56}) c_{3j-k}^{(i)} \right] \hat{B}_k \\
& + \left[\lambda_m ((\lambda_m - 1) c_{55} + c_{33}) b_{3j-k}^{(i)} - \lambda_m (\lambda_m - 2) c_{35} a_{3j-k}^{(i)} + \lambda_m ((\lambda_m - 1) c_{33} + c_{55}) c_{3j-k}^{(i)} \right] \hat{C}_k \\
& + \left[\lambda_m ((\lambda_m - 1) e_{15} + e_{33}) b_{3j-k}^{(i)} - \lambda_m (\lambda_m - 2) \frac{(e_{13} + e_{35})}{2} a_{3j-k}^{(i)} + \lambda_m ((\lambda_m - 1) e_{33} + e_{15}) c_{3j-k}^{(i)} \right] \hat{D}_k \\
& + \left. \left[\lambda_m ((\lambda_m - 1) d_{15} + d_{33}) b_{3j-k}^{(i)} - \lambda_m (\lambda_m - 2) \frac{(d_{13} + d_{35})}{2} a_{3j-k}^{(i)} + \lambda_m ((\lambda_m - 1) d_{33} + d_{15}) c_{3j-k}^{(i)} \right] \hat{E}_k \right\} \\
\end{aligned} \tag{2.13c}$$

$$\begin{aligned}
& \hat{D}_{j+2}^{(i)} - \left(e_{35} b_{40}^{(i)} + e_{11} c_{40}^{(i)} + \frac{(e_{15} + e_{31})}{2} a_{40}^{(i)} \right) \hat{A}_{j+2}^{(i)} - \left(e_{34} b_{40}^{(i)} + e_{16} c_{40}^{(i)} + \frac{(e_{14} + e_{36})}{2} a_{40}^{(i)} \right) \hat{B}_{j+2}^{(i)} \\
& - \left(e_{33} b_{40}^{(i)} + e_{15} c_{40}^{(i)} + \frac{(e_{13} + e_{35})}{2} a_{40}^{(i)} \right) \hat{C}_{j+2}^{(i)} + \left(g_{33} b_{40}^{(i)} + g_{11} c_{40}^{(i)} + g_{13} a_{40}^{(i)} \right) \hat{E}_{j+2}^{(i)} \\
& = \frac{1}{(j+2)(j+1)} \left\{ \sum_{k=0}^{j-1} (k+2)(k+1) \left[\left(e_{35} b_{4j-k}^{(i)} + e_{11} c_{4j-k}^{(i)} + \frac{(e_{15} + e_{31})}{2} a_{4j-k}^{(i)} \right) \hat{A}_{k+2}^{(i)} \right. \right. \\
& + \left(e_{34} b_{4j-k}^{(i)} + e_{16} c_{4j-k}^{(i)} + \frac{(e_{14} + e_{36})}{2} a_{4j-k}^{(i)} \right) \hat{B}_{k+2} + \left(e_{33} b_{4j-k}^{(i)} + e_{15} c_{4j-k}^{(i)} + \frac{(e_{13} + e_{35})}{2} a_{4j-k}^{(i)} \right) \hat{C}_{k+2} \\
& \left. \left. - \left(g_{33} b_{4j-k}^{(i)} + g_{11} c_{4j-k}^{(i)} + g_{13} a_{4j-k}^{(i)} \right) \hat{E}_{j+2} \right] \right\} \\
& + \sum_{k=0}^j (k+1) (\lambda_m - 1) \left[[(e_{35} - e_{11}) a_{4j-k}^{(i)} - (e_{15} + e_{31}) d_{4j-k}^{(i)}] \hat{A}_{k+1} \right. \\
& + [(e_{34} - e_{16}) a_{4j-k}^{(i)} - (e_{14} + e_{36}) d_{4j-k}^{(i)}] \hat{B}_{k+1} + [(e_{33} - e_{15}) a_{4j-k}^{(i)} - (e_{13} + e_{35}) d_{4j-k}^{(i)}] \hat{C}_{k+1} \\
& - [(\eta_{33} - \eta_{11}) a_{4j-k}^{(i)} - 2\eta_{13} d_{4j-k}^{(i)}] \hat{D}_{k+1} - [(g_{33} - g_{11}) a_{4j-k}^{(i)} - 2g_{13} d_{4j-k}^{(i)}] \hat{E}_{k+1} \\
& + \left[\lambda_m ((\lambda_m - 1) e_{11} + e_{35}) b_{4j-k}^{(i)} - \lambda_m (\lambda_m - 2) \frac{(e_{15} + e_{31})}{2} a_{4j-k}^{(i)} + \lambda_m ((\lambda_m - 1) e_{35} + e_{11}) c_{4j-k}^{(i)} \right] \hat{A}_k \\
& + \left[\lambda_m ((\lambda_m - 1) e_{16} + e_{34}) b_{4j-k}^{(i)} - \lambda_m (\lambda_m - 2) \frac{(e_{14} + e_{36})}{2} a_{4j-k}^{(i)} + \lambda_m ((\lambda_m - 1) e_{34} + e_{16}) c_{4j-k}^{(i)} \right] \hat{B}_k \\
& + \left[\lambda_m ((\lambda_m - 1) e_{15} + e_{33}) b_{4j-k}^{(i)} - \lambda_m (\lambda_m - 2) \frac{(e_{13} + e_{35})}{2} a_{4j-k}^{(i)} + \lambda_m ((\lambda_m - 1) e_{33} + e_{15}) c_{4j-k}^{(i)} \right] \hat{C}_k
\end{aligned}$$

$$\begin{aligned}
& - \left[\lambda_m ((\lambda_m - 1) \eta_{11} + \eta_{33}) b_{4j-k}^{(i)} - \lambda_m (\lambda_m - 2) \eta_{13} a_{4j-k}^{(i)} + \lambda_m ((\lambda_m - 1) \eta_{33} + \eta_{11}) c_{4j-k}^{(i)} \right] \hat{D}_k \\
& - \left[\lambda_m ((\lambda_m - 1) g_{11} + g_{33}) b_{4j-k}^{(i)} - \lambda_m (\lambda_m - 2) g_{13} a_{4j-k}^{(i)} + \lambda_m ((\lambda_m - 1) g_{33} + g_{11}) c_{4j-k}^{(i)} \right] \hat{E}_k \Bigg\} \\
& \hspace{20em} (2.13d)
\end{aligned}$$

$$\begin{aligned}
& \hat{E}_{j+2}^{(i)} - \left(d_{35} b_{50}^{(i)} + d_{11} c_{50}^{(i)} + \frac{(d_{15} + d_{31})}{2} a_{50}^{(i)} \right) \hat{A}_{j+2}^{(i)} - \left(d_{34} b_{50}^{(i)} + d_{16} c_{50}^{(i)} + \frac{(d_{14} + d_{36})}{2} a_{50}^{(i)} \right) \hat{B}_{j+2}^{(i)} \\
& - \left(d_{33} b_{50}^{(i)} + d_{15} c_{50}^{(i)} + \frac{(d_{13} + d_{35})}{2} a_{50}^{(i)} \right) \hat{C}_{j+2}^{(i)} + (\mu_{33} b_{50}^{(i)} + \mu_{11} c_{50}^{(i)} + \mu_{13} a_{50}^{(i)}) \hat{D}_{j+2}^{(i)} \\
& = \frac{1}{(j+2)(j+1)} \left\{ \sum_{k=0}^{j-1} (k+2)(k+1) \left[\left(d_{35} b_{5j-k}^{(i)} + d_{11} c_{5j-k}^{(i)} + \frac{(d_{15} + d_{31})}{2} a_{5j-k}^{(i)} \right) \hat{A}_{k+2}^{(i)} \right. \right. \\
& + \left(d_{34} b_{5j-k}^{(i)} + d_{16} c_{5j-k}^{(i)} + \frac{(d_{14} + d_{36})}{2} a_{5j-k}^{(i)} \right) \hat{B}_{k+2}^{(i)} + \left(d_{33} b_{5j-k}^{(i)} + d_{15} c_{5j-k}^{(i)} + \frac{(d_{13} + d_{35})}{2} a_{5j-k}^{(i)} \right) \hat{C}_{k+2}^{(i)} \\
& \left. \left. - (g_{33} b_{5j-k}^{(i)} + g_{11} c_{5j-k}^{(i)} + g_{13} a_{5j-k}^{(i)}) \hat{D}_{k+2} \right] \right. \\
& + \sum_{k=0}^j \left[(k+1)(\lambda_m - 1) \left[(d_{35} - d_{11}) a_{5j-k}^{(i)} - (d_{15} + d_{31}) d_{5j-k}^{(i)} \right] \hat{A}_{k+1}^{(i)} \right. \\
& + \left[(d_{34} - d_{16}) a_{5j-k}^{(i)} - (d_{14} + d_{36}) d_{5j-k}^{(i)} \right] \hat{B}_{k+1}^{(i)} + \left[(d_{33} - d_{15}) a_{5j-k}^{(i)} - (d_{13} + d_{35}) d_{5j-k}^{(i)} \right] \hat{C}_{k+1}^{(i)} \\
& \left. - [(g_{33} - g_{11}) a_{5j-k}^{(i)} - 2g_{13} d_{5j-k}^{(i)}] \hat{D}_{k+1} - [(\mu_{33} - \mu_{11}) a_{5j-k}^{(i)} - 2\mu_{13} d_{5j-k}^{(i)}] \hat{E}_{k+1} \right. \\
& + \left[\lambda_m ((\lambda_m - 1) d_{11} + d_{35}) b_{5j-k}^{(i)} - \lambda_m (\lambda_m - 2) \frac{(d_{15} + d_{31})}{2} a_{5j-k}^{(i)} + \lambda_m ((\lambda_m - 1) d_{35} + d_{11}) c_{5j-k}^{(i)} \right] \hat{A}_k^{(i)} \\
& + \left[\lambda_m ((\lambda_m - 1) d_{16} + d_{34}) b_{5j-k}^{(i)} - \lambda_m (\lambda_m - 2) \frac{(d_{14} + d_{36})}{2} a_{5j-k}^{(i)} + \lambda_m ((\lambda_m - 1) d_{34} + d_{16}) c_{5j-k}^{(i)} \right] \hat{B}_k^{(i)} \\
& + \left[\lambda_m ((\lambda_m - 1) d_{15} + d_{33}) b_{5j-k}^{(i)} - \lambda_m (\lambda_m - 2) \frac{(d_{13} + d_{35})}{2} a_{5j-k}^{(i)} + \lambda_m ((\lambda_m - 1) d_{15} + d_{33}) c_{5j-k}^{(i)} \right] \hat{C}_k^{(i)} \\
& + \left[\lambda_m ((\lambda_m - 1) g_{11} + g_{33}) b_{5j-k}^{(i)} - \lambda_m (\lambda_m - 2) g_{13} a_{5j-k}^{(i)} + \lambda_m ((\lambda_m - 1) g_{33} + g_{11}) c_{5j-k}^{(i)} \right] \hat{D}_k \\
& \left. + \left[\lambda_m ((\lambda_m - 1) \mu_{11} + \mu_{33}) b_{5j-k}^{(i)} - \lambda_m (\lambda_m - 2) \mu_{13} a_{5j-k}^{(i)} + \lambda_m ((\lambda_m - 1) \mu_{33} + \mu_{11}) c_{5j-k}^{(i)} \right] \hat{E}_k \right\} \\
& \hspace{20em} (2.13e)
\end{aligned}$$

聯立式 (2.13) 可解得 $\hat{A}_{j+2}^{(i)}$ 、 $\hat{B}_{j+2}^{(i)}$ 、 $\hat{C}_{j+2}^{(i)}$ 、 $\hat{D}_{j+2}^{(i)}$ 與 $\hat{E}_{j+2}^{(i)}$ ，再根據遞迴關係所有 $j \geq 0$ 的項次均可由 $\hat{A}_0^{(i)}$ 、 $\hat{A}_1^{(i)}$ 、 $\hat{B}_0^{(i)}$ 、 $\hat{B}_1^{(i)}$ 、 $\hat{C}_0^{(i)}$ 、 $\hat{C}_1^{(i)}$ 、 $\hat{D}_0^{(i)}$ 、 $\hat{D}_1^{(i)}$ 、 $\hat{E}_0^{(i)}$ 與 $\hat{E}_1^{(i)}$ 來表示，故式 (2.9) 子域 i 的解可簡單表示為

$$\hat{U}_0^{(i)}(\theta, \xi) = \hat{A}_0^{(i)} \hat{U}_{00}^{(i)}(\theta, \xi) + \hat{A}_1^{(i)} \hat{U}_{01}^{(i)}(\theta, \xi) + \hat{B}_0^{(i)} \hat{U}_{02}^{(i)}(\theta, \xi) + \hat{B}_1^{(i)} \hat{U}_{03}^{(i)}(\theta, \xi) + \hat{C}_0^{(i)} \hat{U}_{04}^{(i)}(\theta, \xi)$$

$$+ \hat{C}_1^{(i)} \hat{U}_{05}^{(i)}(\theta, \xi) + \hat{D}_0^{(i)} \hat{U}_{06}^{(i)}(\theta, \xi) + \hat{D}_1^{(i)} \hat{U}_{07}^{(i)}(\theta, \xi) + \hat{E}_0^{(i)} \hat{U}_{08}^{(i)}(\theta, \xi) + \hat{E}_1^{(i)} \hat{U}_{09}^{(i)}(\theta, \xi) \quad (2.14a)$$

$$\begin{aligned} \hat{V}_0^{(i)}(\theta, \xi) &= \hat{A}_0^{(i)} \hat{V}_{00}^{(i)}(\theta, \xi) + \hat{A}_1^{(i)} \hat{V}_{01}^{(i)}(\theta, \xi) + \hat{B}_0^{(i)} \hat{V}_{02}^{(i)}(\theta, \xi) + \hat{B}_1^{(i)} \hat{V}_{03}^{(i)}(\theta, \xi) + \hat{C}_0^{(i)} \hat{V}_{04}^{(i)}(\theta, \xi) \\ &+ \hat{C}_1^{(i)} \hat{V}_{05}^{(i)}(\theta, \xi) + \hat{D}_0^{(i)} \hat{V}_{06}^{(i)}(\theta, \xi) + \hat{D}_1^{(i)} \hat{V}_{07}^{(i)}(\theta, \xi) + \hat{E}_0^{(i)} \hat{V}_{08}^{(i)}(\theta, \xi) + \hat{E}_1^{(i)} \hat{V}_{09}^{(i)}(\theta, \xi) \end{aligned} \quad (2.14b)$$

$$\begin{aligned} \hat{W}_0^{(i)}(\theta, \xi) &= \hat{A}_0^{(i)} \hat{W}_{00}^{(i)}(\theta, \xi) + \hat{A}_1^{(i)} \hat{W}_{01}^{(i)}(\theta, \xi) + \hat{B}_0^{(i)} \hat{W}_{02}^{(i)}(\theta, \xi) + \hat{B}_1^{(i)} \hat{W}_{03}^{(i)}(\theta, \xi) + \hat{C}_0^{(i)} \hat{W}_{04}^{(i)}(\theta, \xi) \\ &+ \hat{C}_1^{(i)} \hat{W}_{05}^{(i)}(\theta, \xi) + \hat{D}_0^{(i)} \hat{W}_{06}^{(i)}(\theta, \xi) + \hat{D}_1^{(i)} \hat{W}_{07}^{(i)}(\theta, \xi) + \hat{E}_0^{(i)} \hat{W}_{08}^{(i)}(\theta, \xi) + \hat{E}_1^{(i)} \hat{W}_{09}^{(i)}(\theta, \xi) \end{aligned} \quad (2.14c)$$

$$\begin{aligned} \hat{\Phi}_0^{(i)}(\theta, \xi) &= \hat{A}_0^{(i)} \hat{\Phi}_{00}^{(i)}(\theta, \xi) + \hat{A}_1^{(i)} \hat{\Phi}_{01}^{(i)}(\theta, \xi) + \hat{B}_0^{(i)} \hat{\Phi}_{02}^{(i)}(\theta, \xi) + \hat{B}_1^{(i)} \hat{\Phi}_{03}^{(i)}(\theta, \xi) + \hat{C}_0^{(i)} \hat{\Phi}_{04}^{(i)}(\theta, \xi) \\ &+ \hat{C}_1^{(i)} \hat{\Phi}_{05}^{(i)}(\theta, \xi) + \hat{D}_0^{(i)} \hat{\Phi}_{06}^{(i)}(\theta, \xi) + \hat{D}_1^{(i)} \hat{\Phi}_{07}^{(i)}(\theta, \xi) + \hat{E}_0^{(i)} \hat{\Phi}_{08}^{(i)}(\theta, \xi) + \hat{E}_1^{(i)} \hat{\Phi}_{09}^{(i)}(\theta, \xi) \end{aligned} \quad (2.14d)$$

$$\begin{aligned} \hat{\Psi}_0^{(i)}(\theta, \xi) &= \hat{A}_0^{(i)} \hat{\Psi}_{00}^{(i)}(\theta, \xi) + \hat{A}_1^{(i)} \hat{\Psi}_{01}^{(i)}(\theta, \xi) + \hat{B}_0^{(i)} \hat{\Psi}_{02}^{(i)}(\theta, \xi) + \hat{B}_1^{(i)} \hat{\Psi}_{03}^{(i)}(\theta, \xi) + \hat{C}_0^{(i)} \hat{\Psi}_{04}^{(i)}(\theta, \xi) \\ &+ \hat{C}_1^{(i)} \hat{\Psi}_{05}^{(i)}(\theta, \xi) + \hat{D}_0^{(i)} \hat{\Psi}_{06}^{(i)}(\theta, \xi) + \hat{D}_1^{(i)} \hat{\Psi}_{07}^{(i)}(\theta, \xi) + \hat{E}_0^{(i)} \hat{\Psi}_{08}^{(i)}(\theta, \xi) + \hat{E}_1^{(i)} \hat{\Psi}_{09}^{(i)}(\theta, \xi) \end{aligned} \quad (2.14e)$$

2.4 電磁彈性迴轉體之邊界條件與連續條件

如圖 2.4 中將全域 ξ 切割為 n 個子域，子域 i 之解含待定係數 $\hat{A}_0^{(i)}$ 、 $\hat{A}_1^{(i)}$ 、 $\hat{B}_0^{(i)}$ 、 $\hat{B}_1^{(i)}$ 、 $\hat{C}_0^{(i)}$ 、 $\hat{C}_1^{(i)}$ 、 $\hat{D}_0^{(i)}$ 、 $\hat{D}_1^{(i)}$ 、 $\hat{E}_0^{(i)}$ 與 $\hat{E}_1^{(i)}$ ；因此， n 個子域將會產生 $10n$ 個待定之係數。相鄰子域間須滿足下列連續條件

$$\sigma_{rr}^{(i)}(\rho, \theta, \xi_i) \sin \xi_i + \sigma_{rz}^{(i)}(\rho, \theta, \xi_i) \cos \xi_i = \sigma_{rr}^{(i+1)}(\rho, \theta, \xi_i) \sin \xi_i + \sigma_{rz}^{(i+1)}(\rho, \theta, \xi_i) \cos \xi_i \quad (2.15a)$$

$$\sigma_{rz}^{(i)}(\rho, \theta, \xi_i) \sin \xi_i + \sigma_{zz}^{(i)}(\rho, \theta, \xi_i) \cos \xi_i = \sigma_{rz}^{(i+1)}(\rho, \theta, \xi_i) \sin \xi_i + \sigma_{zz}^{(i+1)}(\rho, \theta, \xi_i) \cos \xi_i \quad (2.15b)$$

$$\sigma_{\theta r}^{(i)}(\rho, \theta, \xi_i) \sin \xi_i + \sigma_{\theta z}^{(i)}(\rho, \theta, \xi_i) \cos \xi_i = \sigma_{\theta r}^{(i+1)}(\rho, \theta, \xi_i) \sin \xi_i + \sigma_{\theta z}^{(i+1)}(\rho, \theta, \xi_i) \cos \xi_i \quad (2.15c)$$

$$D_r^{(i)}(\rho, \theta, \xi_i) \sin \xi_i + D_z^{(i)}(\rho, \theta, \xi_i) \cos \xi_i = D_r^{(i+1)}(\rho, \theta, \xi_i) \sin \xi_i + D_z^{(i+1)}(\rho, \theta, \xi_i) \cos \xi_i \quad (2.15d)$$

$$B_r^{(i)}(\rho, \theta, \xi_i) \sin \xi_i + B_z^{(i)}(\rho, \theta, \xi_i) \cos \xi_i = B_r^{(i+1)}(\rho, \theta, \xi_i) \sin \xi_i + B_z^{(i+1)}(\rho, \theta, \xi_i) \cos \xi_i \quad (2.15e)$$

$$u_r^{(i)}(\rho, \theta, \xi_i) = u_r^{(i+1)}(\rho, \theta, \xi_i) \quad (2.15f)$$

$$u_\theta^{(i)}(\rho, \theta, \xi_i) = u_\theta^{(i+1)}(\rho, \theta, \xi_i) \quad (2.15g)$$

$$u_z^{(i)}(\rho, \theta, \xi_i) = u_z^{(i+1)}(\rho, \theta, \xi_i) \quad (2.15h)$$

$$\phi^{(i)}(\rho, \theta, \xi_i) = \phi^{(i+1)}(\rho, \theta, \xi_i) \quad (2.15i)$$

$$\psi^{(i)}(\rho, \theta, \xi_i) = \psi^{(i+1)}(\rho, \theta, \xi_i) \quad (2.15j)$$

上式中上標 i 表示於子域 i 中之物理量， $i = 1, 2, \dots, n-1$ 。因此，式 (2.15) 總共可組成 $10(n-1)$ 條方程式，尚需 10 條方程式，則由於 $\xi = \xi_0$ 與 $\xi = \xi_n$ 之邊界條件所構成。不同邊界條件可表示如下：

自由端 (traction free conditions)

$$\begin{aligned} \sigma_{rr}^{(k)} \sin \xi + \sigma_{rz}^{(k)} \cos \xi &= 0 \\ \sigma_{rz}^{(k)} \sin \xi + \sigma_{zz}^{(k)} \cos \xi &= 0 \\ \sigma_{\theta r}^{(k)} \sin \xi + \sigma_{\theta z}^{(k)} \cos \xi &= 0 \end{aligned} \quad (2.16a)$$

固定端 (clamped conditions)

$$u_r^{(k)} = u_z^{(k)} = u_\theta^{(k)} = 0 \quad (2.16b)$$

電磁開路 (electrically and magnetically open conditions)

$$\begin{aligned} D_r^{(k)} \sin \xi + D_z^{(k)} \cos \xi &= 0 \\ B_r^{(k)} \sin \xi + B_z^{(k)} \cos \xi &= 0 \end{aligned} \quad (2.16c)$$

電磁閉路 (electrically and magnetically closed conditions)

$$\begin{aligned} \phi^{(k)} &= 0 \\ \psi^{(k)} &= 0 \end{aligned} \quad (2.16d)$$

其中 $k=1$ 與 $k=n$ 分別代表於 $\xi = \xi_0$ 及 $\xi = \xi_n$ 之邊界條件。

由邊界條件及連續條件所組成的 $10n$ 條齊性方程式含 $10n$ 個待定係數。此些線性代數方程式之以知係數所構成之 $10n \times 10n$ 行列式須為零，則此方程式有非零解 (nontrivial solution)。此行列式中之元素均為 λ_m 之函數，透過 Müller[50] 所提供之數值方法，尋找當行列式為零時 λ_m 之根。將此根依其實數由小至大排列 $\lambda_i (i=1, 2, \dots)$ ，當 λ_1 的實數部分 ($\text{Re}[\lambda_1]$) 小於 1.0，應力、電位移與磁通量之奇異性階數為 $\text{Re}[\lambda_1]-1$ 。

2.5 壓電迴轉體於尖角處之漸近解

倘若欲分析的問題為壓電迴轉體，此時僅需將式 (2.1) 中有關於磁性相關之材料性質省略即可，即忽略壓磁係數 $[\bar{d}]$ 、電磁耦合係數 $[\bar{g}]$ 與磁導係數 $[\bar{\mu}]$ ，經過同樣的推導流程，可推得類似於式 (2.10) 之四條變係數常微分方程式

$$\begin{aligned}
& \frac{\partial^2 \hat{U}_0^{(i)}}{\partial \xi^2} + \frac{1}{\Delta_1} \left\{ (\lambda_m - 1) [(c_{55} - c_{11}) \sin 2\xi - 2c_{15} \cos 2\xi] \frac{\partial \hat{U}_0^{(i)}}{\partial \xi} + [\lambda_m ((\lambda_m - 1) c_{11} + c_{55}) \right. \\
& \quad \times \cos^2 \xi - \lambda_m (\lambda_m - 2) c_{15} \sin 2\xi + \lambda_m ((\lambda_m - 1) c_{55} + c_{11}) \sin^2 \xi] \hat{U}_0^{(i)} + \left[c_{45} \cos^2 \xi \right. \\
& \quad \left. + c_{16} \sin^2 \xi + \frac{(c_{14} + c_{56})}{2} \sin 2\xi \right] \frac{\partial^2 \hat{V}_0^{(i)}}{\partial \xi^2} + (\lambda_m - 1) [(c_{45} - c_{16}) \sin 2\xi - (c_{14} + c_{56}) \\
& \quad \times \cos 2\xi] \frac{\partial \hat{V}_0^{(i)}}{\partial \xi} + \left[\lambda_m ((\lambda_m - 1) c_{16} + c_{45}) \cos^2 \xi - \lambda_m (\lambda_m - 2) \frac{(c_{14} + c_{56})}{2} \sin 2\xi \right. \\
& \quad \left. + \lambda_m ((\lambda_m - 1) c_{45} + c_{16}) \sin^2 \xi \right] \hat{V}_0^{(i)} + \left[c_{35} \cos^2 \xi + c_{15} \sin^2 \xi + \frac{(c_{13} + c_{55})}{2} \sin 2\xi \right] \\
& \quad \times \frac{\partial^2 \hat{W}_0^{(i)}}{\partial \xi^2} + (\lambda_m - 1) [(c_{35} - c_{15}) \sin 2\xi - (c_{13} + c_{55}) \cos 2\xi] \frac{\partial \hat{W}_0^{(i)}}{\partial \xi} + \left[\lambda_m ((\lambda_m - 1) \right. \\
& \quad \times c_{15} + c_{35}) \cos^2 \xi - \lambda_m (\lambda_m - 2) \frac{(c_{13} + c_{55})}{2} \sin 2\xi + \lambda_m ((\lambda_m - 1) c_{35} + c_{15}) \sin^2 \xi \left. \right] \\
& \quad \times W_0^{(i)} + \left[e_{35} \cos^2 \xi + e_{11} \sin^2 \xi + \frac{(e_{15} + e_{31})}{2} \sin 2\xi \right] \frac{\partial^2 \hat{\Phi}_0^{(i)}}{\partial \xi^2} + (\lambda_m - 1) [(e_{35} - e_{11}) \\
& \quad \times \sin 2\xi - (e_{15} + e_{31}) \cos 2\xi] \frac{\partial \hat{\Phi}_0^{(i)}}{\partial \xi} + [\lambda_m ((\lambda_m - 1) e_{11} + e_{35}) \cos^2 \xi - \lambda_m (\lambda_m - 2) \\
& \quad \times \frac{(e_{15} + e_{31})}{2} \sin 2\xi + \lambda_m ((\lambda_m - 1) e_{35} + e_{11}) \sin^2 \xi] \hat{\Phi}_0^{(i)} \left. \right\} = 0, \tag{2.17a}
\end{aligned}$$

$$\begin{aligned}
& \frac{\partial^2 \hat{V}_0^{(i)}}{\partial \xi^2} + \frac{1}{\Delta_2} \left\{ (\lambda_m - 1) [(c_{44} - c_{66}) \sin 2\xi - 2c_{46} \cos 2\xi] \frac{\partial \hat{V}_0^{(i)}}{\partial \xi} + [\lambda_m ((\lambda_m - 1) c_{66} + c_{44}) \right. \\
& \quad \times \cos^2 \xi - \lambda_m (\lambda_m - 2) c_{46} \sin 2\xi + \lambda_m ((\lambda_m - 1) c_{44} + c_{66}) \sin^2 \xi] \hat{V}_0^{(i)} + \left[c_{45} \cos^2 \xi \right. \\
& \quad \left. + c_{16} \sin^2 \xi + \frac{(c_{14} + c_{56})}{2} \sin 2\xi \right] \frac{\partial^2 \hat{U}_0^{(i)}}{\partial \xi^2} + (\lambda_m - 1) [(c_{45} - c_{16}) \sin 2\xi - (c_{14} + c_{56}) \\
& \quad \times \cos 2\xi] \frac{\partial \hat{U}_0^{(i)}}{\partial \xi} + \left[\lambda_m ((\lambda_m - 1) c_{16} + c_{45}) \cos^2 \xi - \lambda_m (\lambda_m - 2) \frac{(c_{14} + c_{56})}{2} \sin 2\xi \right. \\
& \quad \left. + \lambda_m ((\lambda_m - 1) c_{45} + c_{16}) \sin^2 \xi \right] \hat{U}_0^{(i)} + \left[c_{34} \cos^2 \xi + c_{56} \sin^2 \xi + \frac{(c_{36} + c_{45})}{2} \sin 2\xi \right] \\
& \quad \times \frac{\partial^2 \hat{W}_0^{(i)}}{\partial \xi^2} + (\lambda_m - 1) [(c_{34} - c_{56}) \sin 2\xi - (c_{36} + c_{45}) \cos 2\xi] \frac{\partial \hat{W}_0^{(i)}}{\partial \xi} + \left[\lambda_m ((\lambda_m - 1) \right.
\end{aligned}$$

$$\begin{aligned}
& \times c_{56} + c_{34}) \cos^2 \xi - \lambda_m (\lambda_m - 2) \frac{(c_{36} + c_{45})}{2} \sin 2\xi + \lambda_m ((\lambda_m - 1) c_{34} + c_{56}) \sin^2 \xi \Big] \\
& \times W_0^{(i)} + \left[e_{34} \cos^2 \xi + e_{16} \sin^2 \xi + \frac{(e_{14} + e_{36})}{2} \sin 2\xi \right] \frac{\partial^2 \hat{\Phi}_0^{(i)}}{\partial \xi^2} + (\lambda_m - 1) [(e_{34} - e_{16}) \\
& \times \sin 2\xi - (e_{14} + e_{36}) \cos 2\xi] \frac{\partial \hat{\Phi}_0^{(i)}}{\partial \xi} + \left[\lambda_m ((\lambda_m - 1) e_{16} + e_{34}) \cos^2 \xi + \lambda_m (\lambda_m - 2) \right. \\
& \left. \times \frac{(e_{14} + e_{36})}{2} \sin 2\xi + \lambda_m ((\lambda_m - 1) e_{34} + e_{16}) \sin^2 \xi \right] \hat{\Phi}_0^{(i)} \Big\} = 0, \tag{2.17b}
\end{aligned}$$

$$\begin{aligned}
& \frac{\partial^2 \hat{W}_0^{(i)}}{\partial \xi^2} + \frac{1}{\Delta_3} \left\{ (\lambda_m - 1) [(c_{33} - c_{55}) \sin 2\xi - 2c_{35} \cos 2\xi] \frac{\partial \hat{W}_0^{(i)}}{\partial \xi} + [\lambda_m ((\lambda_m - 1) c_{55} + c_{33}) \right. \\
& \times \cos^2 \xi - \lambda_m (\lambda_m - 2) c_{35} \sin 2\xi + \lambda_m ((\lambda_m - 1) c_{33} + c_{55}) \sin^2 \xi] \hat{W}_0^{(i)} + \left[c_{35} \cos^2 \xi \right. \\
& \left. + c_{15} \sin^2 \xi + \frac{(c_{13} + c_{55})}{2} \sin 2\xi \right] \frac{\partial^2 \hat{U}_0^{(i)}}{\partial \xi^2} + (\lambda_m - 1) [(c_{45} - c_{16}) \sin 2\xi - (c_{14} + c_{56}) \\
& \times \cos 2\xi] \frac{\partial \hat{U}_0^{(i)}}{\partial \xi} + \left[\lambda_m ((\lambda_m - 1) c_{15} + c_{35}) \cos^2 \xi - \lambda_m (\lambda_m - 2) \frac{(c_{13} + c_{55})}{2} \sin 2\xi \right. \\
& \left. + \lambda_m ((\lambda_m - 1) c_{35} + c_{15}) \sin^2 \xi \right] \hat{U}_0^{(i)} + \left[c_{34} \cos^2 \xi + c_{56} \sin^2 \xi + \frac{(c_{36} + c_{45})}{2} \sin 2\xi \right] \\
& \times \frac{\partial^2 \hat{V}_0^{(i)}}{\partial \xi^2} + (\lambda_m - 1) [(c_{34} - c_{56}) \sin 2\xi - (c_{36} + c_{45}) \cos 2\xi] \frac{\partial \hat{V}_0^{(i)}}{\partial \xi} + \left[\lambda_m ((\lambda_m - 1) c_{56} \right. \\
& \left. + c_{34}) \cos^2 \xi - \lambda_m (\lambda_m - 2) \frac{(c_{36} + c_{45})}{2} \sin 2\xi + \lambda_m ((\lambda_m - 1) c_{34} + c_{56}) \sin^2 \xi \right] \hat{V}_0^{(i)} \\
& + \left[e_{33} \cos^2 \xi + e_{15} \sin^2 \xi + \frac{(e_{13} + e_{35})}{2} \sin 2\xi \right] \frac{\partial^2 \hat{\Phi}_0^{(i)}}{\partial \xi^2} + (\lambda_m - 1) [(e_{33} - e_{15}) \sin 2\xi \\
& - (e_{13} + e_{35}) \cos 2\xi] \frac{\partial \hat{\Phi}_0^{(i)}}{\partial \xi} + \left[\lambda_m ((\lambda_m - 1) e_{15} + e_{33}) \cos^2 \xi - \lambda_m (\lambda_m - 2) \frac{(e_{13} + e_{35})}{2} \right. \\
& \left. \times \sin 2\xi + \lambda_m ((\lambda_m - 1) e_{33} + e_{15}) \sin^2 \xi \right] \hat{\Phi}_0^{(i)} \Big\} = 0, \tag{2.17c}
\end{aligned}$$

$$\begin{aligned}
& \frac{\partial^2 \hat{\Phi}_0^{(i)}}{\partial \xi^2} + \frac{1}{\Delta_4} \left\{ (\lambda_m - 1) [(\eta_{33} - \eta_{11}) \sin 2\xi - 2\eta_{13} \cos 2\xi] \frac{\partial \hat{\Phi}_0^{(i)}}{\partial \xi} + [\lambda_m ((\lambda_m - 1) \eta_{11} + \eta_{33}) \right. \\
& \times \cos^2 \xi - \lambda_m (\lambda_m - 2) \eta_{13} \sin 2\xi + \lambda_m ((\lambda_m - 1) \eta_{33} + \eta_{11}) \sin^2 \xi] \hat{\Phi}_0^{(i)} - \left[e_{35} \cos^2 \xi \right. \\
& \left. + e_{11} \sin^2 \xi + \frac{(e_{15} + e_{31})}{2} \sin 2\xi \right] \frac{\partial^2 \hat{U}_0^{(i)}}{\partial \xi^2} - (\lambda_m - 1) [(e_{35} - e_{11}) \sin 2\xi - (e_{15} + e_{31}) \\
& \times \cos 2\xi] \frac{\partial \hat{U}_0^{(i)}}{\partial \xi} - \left[\lambda_m ((\lambda_m - 1) e_{11} + e_{35}) \cos^2 \xi - \lambda_m (\lambda_m - 2) \frac{(e_{15} + e_{31})}{2} \sin 2\xi + \lambda_m \right. \\
& \left. \times ((\lambda_m - 1) e_{35} + e_{11}) \sin^2 \xi \right] \hat{U}_0^{(i)} - \left[e_{34} \cos^2 \xi + e_{16} \sin^2 \xi + \frac{(e_{14} + e_{36})}{2} \sin 2\xi \right] \frac{\partial^2 \hat{V}_0^{(i)}}{\partial \xi^2} \\
& - [(e_{34} - e_{16}) \sin 2\xi - (e_{14} + e_{36}) \cos 2\xi] \frac{\partial \hat{V}_0^{(i)}}{\partial \xi} - \left[\lambda_m ((\lambda_m - 1) e_{16} + e_{34}) \cos^2 \xi - \lambda_m \right.
\end{aligned}$$

$$\begin{aligned}
& \times (\lambda_m - 2) \frac{(e_{14} + e_{36})}{2} \sin 2\xi + \lambda_m ((\lambda_m - 1) e_{34} + e_{16}) \sin^2 \xi \Big] \hat{V}_0^{(i)} - \left[e_{33} \cos^2 \xi + e_{15} \sin^2 \xi \right. \\
& \left. + \frac{(e_{13} + e_{35})}{2} \sin 2\xi \right] \frac{\partial^2 \hat{W}_0^{(i)}}{\partial \xi^2} - (\lambda_m - 1) [(e_{33} - e_{15}) \sin 2\xi - (e_{13} + e_{35}) \cos 2\xi] \frac{\partial \hat{W}_0^{(i)}}{\partial \xi} \\
& - \left[\lambda_m ((\lambda_m - 1) e_{15} + e_{33}) \cos^2 \xi - \lambda_m (\lambda_m - 2) \frac{(e_{13} + e_{35})}{2} \sin 2\xi + \lambda_m ((\lambda_m - 1) e_{33} + e_{15}) \right. \\
& \left. \times \sin^2 \xi \right] \hat{W}_0^{(i)} \Big\} = 0, \tag{2.17d}
\end{aligned}$$

如同式 (2.11) 及 (2.12) 之級數展開，可得係數間之遞迴關係如下

$$\begin{aligned}
& \hat{A}_{j+2}^{(i)} + \left(c_{45} b_{10}^{(i)} + c_{16} c_{10}^{(i)} + \frac{(c_{14} + c_{56})}{2} a_{10}^{(i)} \right) \hat{B}_{j+2}^{(i)} + \left(c_{35} b_{10}^{(i)} + c_{15} c_{10}^{(i)} + \frac{(c_{13} + c_{55})}{2} a_{10}^{(i)} \right) \hat{C}_{j+2}^{(i)} \\
& + \left(e_{35} b_{10}^{(i)} + e_{11} c_{10}^{(i)} + \frac{(e_{15} + e_{31})}{2} a_{10}^{(i)} \right) \hat{D}_{j+2}^{(i)} \\
& = \frac{-1}{(j+2)(j+1)} \left\{ \sum_{k=0}^{j-1} (k+2)(k+1) \left[\left(c_{45} b_{1j-k}^{(i)} + c_{16} c_{1j-k}^{(i)} + \frac{(c_{14} + c_{56})}{2} a_{1j-k}^{(i)} \right) \hat{B}_{k+2}^{(i)} \right. \right. \\
& \left. \left. + \left(c_{35} b_{1j-k}^{(i)} + c_{15} c_{1j-k}^{(i)} + \frac{(c_{13} + c_{55})}{2} a_{1j-k}^{(i)} \right) \hat{C}_{k+2}^{(i)} + \left(e_{35} b_{1j-k}^{(i)} + e_{11} c_{1j-k}^{(i)} + \frac{(e_{15} + e_{31})}{2} a_{1j-k}^{(i)} \right) \hat{D}_{k+2}^{(i)} \right] \right. \\
& \left. + \sum_{k=0}^j (k+1)(\lambda_m - 1) \left[((c_{55} - c_{11}) a_{1j-k}^{(i)} - 2c_{15} d_{1j-k}^{(i)}) \hat{A}_{k+1}^{(i)} \right. \right. \\
& \left. \left. + ((c_{45} - c_{16}) a_{1j-k}^{(i)} - (c_{14} + c_{56}) d_{1j-k}^{(i)}) \hat{B}_{k+1}^{(i)} + ((c_{35} - c_{15}) a_{1j-k}^{(i)} - (c_{13} + c_{55}) d_{1j-k}^{(i)}) \hat{C}_{k+1}^{(i)} \right. \right. \\
& \left. \left. + ((e_{35} - e_{11}) a_{1j-k}^{(i)} - (e_{15} + e_{31}) d_{1j-k}^{(i)}) \hat{D}_{k+1}^{(i)} \right. \right. \\
& \left. \left. + [\lambda_m ((\lambda_m - 1) c_{11} + c_{55}) b_{1j-k}^{(i)} - \lambda_m (\lambda_m - 2) e_{15} a_{1j-k}^{(i)} + \lambda_m ((\lambda_m - 1) c_{55} + c_{11}) c_{1j-k}^{(i)}] \hat{A}_k^{(i)} \right. \right. \\
& \left. \left. + \left[\lambda_m ((\lambda_m - 1) c_{16} + c_{45}) b_{1j-k}^{(i)} - \lambda_m (\lambda_m - 2) \frac{(c_{14} + c_{56})}{2} a_{1j-k}^{(i)} + \lambda_m ((\lambda_m - 1) c_{45} + c_{16}) c_{1j-k}^{(i)} \right] \hat{B}_k^{(i)} \right. \right. \\
& \left. \left. + \left[\lambda_m ((\lambda_m - 1) c_{15} + c_{35}) b_{1j-k}^{(i)} - \lambda_m (\lambda_m - 2) \frac{(c_{13} + c_{55})}{2} a_{1j-k}^{(i)} + \lambda_m ((\lambda_m - 1) c_{35} + c_{15}) c_{1j-k}^{(i)} \right] \hat{C}_k^{(i)} \right. \right. \\
& \left. \left. + \left[\lambda_m ((\lambda_m - 1) e_{11} + e_{35}) b_{1j-k}^{(i)} - \lambda_m (\lambda_m - 2) \frac{(e_{15} + e_{31})}{2} a_{1j-k}^{(i)} + \lambda_m ((\lambda_m - 1) e_{35} + e_{11}) c_{1j-k}^{(i)} \right] \hat{D}_k^{(i)} \right] \right\}, \tag{2.18a}
\end{aligned}$$

$$\begin{aligned}
& \hat{B}_{j+2}^{(i)} + \left(c_{45} b_{20}^{(i)} + c_{16} c_{20}^{(i)} + \frac{(c_{14} + c_{56})}{2} a_{20}^{(i)} \right) \hat{A}_{j+2}^{(i)} + \left(c_{34} b_{20}^{(i)} + c_{56} c_{20}^{(i)} + \frac{(c_{36} + c_{45})}{2} a_{20}^{(i)} \right) \hat{C}_{j+2}^{(i)} \\
& + \left(e_{34} b_{20}^{(i)} + e_{16} c_{20}^{(i)} + \frac{(e_{14} + e_{36})}{2} a_{20}^{(i)} \right) \hat{D}_{j+2}^{(i)} \\
& = \frac{-1}{(j+2)(j+1)} \left\{ \sum_{k=0}^{j-1} (k+2)(k+1) \left[\left(c_{45} b_{2j-k}^{(i)} + c_{16} c_{2j-k}^{(i)} + \frac{(c_{14} + c_{56})}{2} a_{2j-k}^{(i)} \right) \hat{A}_{k+2}^{(i)} \right. \right.
\end{aligned}$$

$$\begin{aligned}
& + \left(c_{34} b_{2j-k}^{(i)} + c_{56} c_{2j-k}^{(i)} + \frac{(c_{36} + c_{45})}{2} a_{2j-k}^{(i)} \right) \hat{C}_{k+2} + \left(e_{34} b_{2j-k}^{(i)} + c_{16} c_{2j-k}^{(i)} + \frac{(e_{14} + e_{36})}{2} a_{2j-k}^{(i)} \right) \hat{D}_{k+2} \Big] \\
& + \sum_{k=0}^j (k+1) (\lambda_m - 1) \left[[(c_{45} - c_{16}) (a_2)_{j-k} - (c_{14} + c_{56}) (d_2)_{j-k}] \hat{A}_{k+1} \right. \\
& + [(c_{44} - c_{56}) a_{2j-k}^{(i)} - 2c_{46} d_{2j-k}^{(i)}] \hat{B}_{k+1} + [(c_{34} - c_{56}) a_{2j-k}^{(i)} - (c_{36} + c_{45}) d_{2j-k}^{(i)}] \hat{C}_{k+1} \\
& + [(e_{34} - e_{16}) a_{2j-k}^{(i)} - (e_{14} + e_{36}) d_{2j-k}^{(i)}] \hat{D}_{k+1} \\
& + \left[\lambda_m ((\lambda_m - 1) c_{16} + c_{45}) b_{2j-k}^{(i)} - \lambda_m (\lambda_m - 2) \frac{(c_{14} + c_{56})}{2} a_{2j-k}^{(i)} + \lambda_m ((\lambda_m - 1) c_{45} + c_{16}) c_{2j-k}^{(i)} \right] \hat{A}_k \\
& + \left[\lambda_m ((\lambda_m - 1) c_{66} + c_{44}) b_{2j-k}^{(i)} - \lambda_m (\lambda_m - 2) c_{46} a_{2j-k}^{(i)} + \lambda_m ((\lambda_m - 1) c_{44} + c_{66}) c_{2j-k}^{(i)} \right] \hat{B}_k \\
& + \left[\lambda_m ((\lambda_m - 1) c_{56} + c_{34}) b_{2j-k}^{(i)} - \lambda_m (\lambda_m - 2) \frac{(c_{36} + c_{45})}{2} a_{2j-k}^{(i)} + \lambda_m ((\lambda_m - 1) c_{34} + c_{56}) c_{2j-k}^{(i)} \right] \hat{C}_k \\
& + \left. \left[\lambda_m ((\lambda_m - 1) e_{16} + e_{34}) b_{2j-k}^{(i)} - \lambda_m (\lambda_m - 2) \frac{(e_{14} + e_{36})}{2} a_{2j-k}^{(i)} + \lambda_m ((\lambda_m - 1) e_{34} + e_{16}) c_{2j-k}^{(i)} \right] \hat{D}_k \right] \Big\}, \tag{2.18b}
\end{aligned}$$

$$\begin{aligned}
& \hat{C}_{j+2}^{(i)} + \left(c_{35} b_{30}^{(i)} + c_{15} c_{30}^{(i)} + \frac{(c_{13} + c_{55})}{2} a_{30}^{(i)} \right) \hat{A}_{j+2} + \left(c_{34} b_{30}^{(i)} + c_{56} c_{30}^{(i)} + \frac{(c_{36} + c_{45})}{2} a_{30}^{(i)} \right) \hat{B}_{j+2} \\
& + \left(e_{33} b_{30}^{(i)} + e_{15} c_{30}^{(i)} + \frac{(e_{13} + e_{35})}{2} a_{30}^{(i)} \right) \hat{D}_{j+2} \\
& = \frac{-1}{(j+2)(j+1)} \left\{ \sum_{k=0}^{j-1} (k+2)(k+1) \left[\left(c_{35} b_{3j-k}^{(i)} + c_{15} c_{3j-k}^{(i)} + \frac{(c_{13} + c_{55})}{2} a_{3j-k}^{(i)} \right) \hat{A}_{k+2} \right. \right. \\
& + \left(c_{34} b_{3j-k}^{(i)} + c_{56} c_{3j-k}^{(i)} + \frac{(c_{36} + c_{45})}{2} a_{3j-k}^{(i)} \right) \hat{B}_{k+2} + \left(e_{33} b_{3j-k}^{(i)} + e_{15} c_{3j-k}^{(i)} + \frac{(e_{13} + e_{35})}{2} a_{3j-k}^{(i)} \right) \hat{C}_{k+2} \Big] \\
& + \sum_{k=0}^j (k+1) (\lambda_m - 1) \left[[(c_{35} - c_{15}) a_{3j-k}^{(i)} - (c_{13} + c_{55}) d_{3j-k}^{(i)}] \hat{A}_{k+1} \right. \\
& + [(c_{34} - c_{56}) a_{3j-k}^{(i)} - (c_{36} + c_{45}) d_{3j-k}^{(i)}] \hat{B}_{k+1} + [(c_{33} - c_{55}) a_{3j-k}^{(i)} - 2c_{35} d_{3j-k}^{(i)}] \hat{C}_{k+1} \\
& + [(e_{33} - e_{15}) a_{3j-k}^{(i)} - (e_{13} + e_{35}) d_{3j-k}^{(i)}] \hat{D}_{k+1} \\
& + \left[\lambda_m ((\lambda_m - 1) c_{15} + c_{35}) b_{3j-k}^{(i)} - \lambda_m (\lambda_m - 2) \frac{(c_{13} + c_{55})}{2} a_{3j-k}^{(i)} + \lambda_m ((\lambda_m - 1) c_{35} + c_{15}) c_{3j-k}^{(i)} \right] \hat{A}_k \\
& + \left[\lambda_m ((\lambda_m - 1) c_{56} + c_{34}) b_{3j-k}^{(i)} - \lambda_m (\lambda_m - 2) \frac{(c_{36} + c_{45})}{2} a_{3j-k}^{(i)} + \lambda_m ((\lambda_m - 1) c_{34} + c_{56}) c_{3j-k}^{(i)} \right] \hat{B}_k \\
& + \left. \left[\lambda_m ((\lambda_m - 1) c_{55} + c_{33}) b_{3j-k}^{(i)} - \lambda_m (\lambda_m - 2) c_{35} a_{3j-k}^{(i)} + \lambda_m ((\lambda_m - 1) c_{33} + c_{55}) c_{3j-k}^{(i)} \right] \hat{C}_k \right\}
\end{aligned}$$

$$+ \left[\lambda_m ((\lambda_m - 1) e_{15} + e_{33}) b_{3j-k}^{(i)} - \lambda_m (\lambda_m - 2) \frac{(e_{13} + e_{35})}{2} a_{3j-k}^{(i)} + \lambda_m ((\lambda_m - 1) e_{33} + e_{15}) c_{3j-k}^{(i)} \hat{D}_k \right] \hat{D}_k \Bigg\}, \quad (2.18c)$$

$$\begin{aligned} & \hat{D}_{j+2}^{(i)} - \left(e_{35} b_{40}^{(i)} + e_{11} c_{40}^{(i)} + \frac{(e_{15} + e_{31})}{2} a_{40}^{(i)} \right) \hat{A}_{j+2}^{(i)} - \left(e_{34} b_{40}^{(i)} + e_{16} c_{40}^{(i)} + \frac{(e_{14} + e_{36})}{2} a_{40}^{(i)} \right) \hat{B}_{j+2}^{(i)} \\ & - \left(e_{33} b_{40}^{(i)} + e_{15} c_{40}^{(i)} + \frac{(e_{13} + e_{35})}{2} a_{40}^{(i)} \right) \hat{C}_{j+2}^{(i)} \\ & = \frac{1}{(j+2)(j+1)} \left\{ \sum_{k=0}^{j-1} (k+2)(k+1) \left[\left(e_{35} b_{4j-k}^{(i)} + e_{11} c_{4j-k}^{(i)} + \frac{(e_{15} + e_{31})}{2} a_{4j-k}^{(i)} \right) \hat{A}_{k+2}^{(i)} \right. \right. \\ & + \left. \left(e_{34} b_{4j-k}^{(i)} + e_{16} c_{4j-k}^{(i)} + \frac{(e_{14} + e_{36})}{2} a_{4j-k}^{(i)} \right) \hat{B}_{k+2}^{(i)} + \left(e_{33} b_{4j-k}^{(i)} + e_{15} c_{4j-k}^{(i)} + \frac{(e_{13} + e_{35})}{2} a_{4j-k}^{(i)} \right) \hat{C}_{k+2}^{(i)} \right] \\ & + \sum_{k=0}^j (k+1) (\lambda_m - 1) \left[[(e_{35} - e_{11}) a_{4j-k}^{(i)} - (e_{15} + e_{31}) d_{4j-k}^{(i)}] \hat{A}_{k+1}^{(i)} \right. \\ & + [(e_{34} - e_{16}) a_{4j-k}^{(i)} - (e_{14} + e_{36}) d_{4j-k}^{(i)}] \hat{B}_{k+1}^{(i)} + [(e_{33} - e_{15}) a_{4j-k}^{(i)} - (e_{13} + e_{35}) d_{4j-k}^{(i)}] \hat{C}_{k+1}^{(i)} \\ & - [(\eta_{33} - \eta_{11}) a_{4j-k}^{(i)} - 2\eta_{13} d_{4j-k}^{(i)}] \hat{D}_{k+1}^{(i)} \\ & + \left. \left[\lambda_m ((\lambda_m - 1) e_{11} + e_{35}) b_{4j-k}^{(i)} - \lambda_m (\lambda_m - 2) \frac{(e_{15} + e_{31})}{2} a_{4j-k}^{(i)} + \lambda_m ((\lambda_m - 1) e_{35} + e_{11}) c_{4j-k}^{(i)} \right] \hat{A}_k^{(i)} \right. \\ & + \left. \left[\lambda_m ((\lambda_m - 1) e_{16} + e_{34}) b_{4j-k}^{(i)} - \lambda_m (\lambda_m - 2) \frac{(e_{14} + e_{36})}{2} a_{4j-k}^{(i)} + \lambda_m ((\lambda_m - 1) e_{34} + e_{16}) c_{4j-k}^{(i)} \right] \hat{B}_k^{(i)} \right. \\ & + \left. \left[\lambda_m ((\lambda_m - 1) e_{15} + e_{33}) b_{4j-k}^{(i)} - \lambda_m (\lambda_m - 2) \frac{(e_{13} + e_{35})}{2} a_{4j-k}^{(i)} + \lambda_m ((\lambda_m - 1) e_{33} + e_{15}) c_{4j-k}^{(i)} \right] \hat{C}_k^{(i)} \right. \\ & \left. - \left[\lambda_m ((\lambda_m - 1) \eta_{11} + \eta_{33}) b_{4j-k}^{(i)} - \lambda_m (\lambda_m - 2) \eta_{13} a_{4j-k}^{(i)} + \lambda_m ((\lambda_m - 1) \eta_{33} + \eta_{11}) c_{4j-k}^{(i)} \right] \hat{D}_k \right] \Bigg\}, \quad (2.18d) \end{aligned}$$

子域 i 漸近解可簡單表示為

$$\begin{aligned} \hat{U}_{0i}^{(i)}(\theta, \xi) &= \hat{A}_0^{(i)} \hat{U}_{00}^{(i)}(\theta, \xi) + \hat{A}_1^{(i)} \hat{U}_{01}^{(i)}(\theta, \xi) + \hat{B}_0^{(i)} \hat{U}_{02}^{(i)}(\theta, \xi) + \hat{B}_1^{(i)} \hat{U}_{03}^{(i)}(\theta, \xi) + \hat{C}_0^{(i)} \hat{U}_{04}^{(i)}(\theta, \xi) \\ &+ \hat{C}_1^{(i)} \hat{U}_{05}^{(i)}(\theta, \xi) + \hat{D}_0^{(i)} \hat{U}_{06}^{(i)}(\theta, \xi) + \hat{D}_1^{(i)} \hat{U}_{07}^{(i)}(\theta, \xi) \end{aligned} \quad (2.19a)$$

$$\begin{aligned} \hat{V}_{0i}^{(i)}(\theta, \xi) &= \hat{A}_0^{(i)} \hat{V}_{00}^{(i)}(\theta, \xi) + \hat{A}_1^{(i)} \hat{V}_{01}^{(i)}(\theta, \xi) + \hat{B}_0^{(i)} \hat{V}_{02}^{(i)}(\theta, \xi) + \hat{B}_1^{(i)} \hat{V}_{03}^{(i)}(\theta, \xi) + \hat{C}_0^{(i)} \hat{V}_{04}^{(i)}(\theta, \xi) \\ &+ \hat{C}_1^{(i)} \hat{V}_{05}^{(i)}(\theta, \xi) + \hat{D}_0^{(i)} \hat{V}_{06}^{(i)}(\theta, \xi) + \hat{D}_1^{(i)} \hat{V}_{07}^{(i)}(\theta, \xi) \end{aligned} \quad (2.19b)$$

$$\begin{aligned} \hat{W}_{0i}^{(i)}(\theta, \xi) &= \hat{A}_0^{(i)} \hat{W}_{00}^{(i)}(\theta, \xi) + \hat{A}_1^{(i)} \hat{W}_{01}^{(i)}(\theta, \xi) + \hat{B}_0^{(i)} \hat{W}_{02}^{(i)}(\theta, \xi) + \hat{B}_1^{(i)} \hat{W}_{03}^{(i)}(\theta, \xi) + \hat{C}_0^{(i)} \hat{W}_{04}^{(i)}(\theta, \xi) \\ &+ \hat{C}_1^{(i)} \hat{W}_{05}^{(i)}(\theta, \xi) + \hat{D}_0^{(i)} \hat{W}_{06}^{(i)}(\theta, \xi) + \hat{D}_1^{(i)} \hat{W}_{07}^{(i)}(\theta, \xi) \end{aligned} \quad (2.19c)$$

$$\begin{aligned} \hat{\Phi}_{0i}^{(i)}(\theta, \xi) = & \hat{A}_0^{(i)} \hat{\Phi}_{00}^{(i)}(\theta, \xi) + \hat{A}_1^{(i)} \hat{\Phi}_{01}^{(i)}(\theta, \xi) + \hat{B}_0^{(i)} \hat{\Phi}_{02}^{(i)}(\theta, \xi) + \hat{B}_1^{(i)} \hat{\Phi}_{03}^{(i)}(\theta, \xi) + \hat{C}_0^{(i)} \hat{\Phi}_{04}^{(i)}(\theta, \xi) \\ & + \hat{C}_1^{(i)} \hat{\Phi}_{05}^{(i)}(\theta, \xi) + \hat{D}_0^{(i)} \hat{\Phi}_{06}^{(i)}(\theta, \xi) + \hat{D}_1^{(i)} \hat{\Phi}_{07}^{(i)}(\theta, \xi) \end{aligned} \quad (2.19d)$$

2.6 壓電迴轉體之邊界條件與連續條件

此處同 2.4 節，在分析壓電迴轉體亦將全域 ξ 切割為 n 個子域，如此會產生 $8n$ 個待定係數。由各子域間之連續條件可得 $8(n-1)$ 條方程式，其連續條件同於式 (2.15) 但不考慮有關於磁性之部分如式 (2.15e) 與式 (2.15j)。尚需 8 條方程式則由 $\xi = \xi_0$ 與 $\xi = \xi_n$ 處之邊界條件構成。同樣地，邊界條件可參考式 (2.16)，但於式 (2.16c) 與式 (2.16d) 中省略磁性相關的部分。如此 $8n$ 個待定係數可透過由連續條件與邊界條件所提供的 $8n$ 條齊次方程式決定之。可由建立 $8n \times 8n$ 矩陣，並令其行列式值為零以求得 λ_m ，如同前節所述應力與電位移之奇異性階數為 $\text{Re}[\lambda_1]-1$ 。



第三章 電磁彈性迴轉體奇異性之結果與討論

已發表文獻中尚未有關於電磁彈性迴轉體奇異性之研究結果，所以僅就過往文獻中壓電迴轉體所得之電彈奇異性階數作為比較之對象。可於第二章之公式推導過程中令磁性相關之材料係數為零並且不考慮磁性之邊界條件及連續條件，即為忽略磁性之效應，相關細節可參考前章 2.5 及 2.6 節。因此電磁彈性相關方程式可以輕易地簡化為僅考量壓電效應。將全域 ξ 切割為數個相等大小之子域，配合每個子域利用不同項數之級數解所得之最小奇異性階數實數部 $\text{Re}[\lambda_1]$ 與文獻之結果相比較。

邊界條件則以四個英文字母命名之，前兩個字母為表示於 $\xi = \xi_0$ 之邊界條件；後兩個字母為表示於 $\xi = \xi_n$ 之邊界條件。其中第一與第三個字母表示力學邊界條件，C 為固定端 (clamped)；F 為自由端 (free)。另外第二與第四個字母則表示電磁邊界條件，C 為 electrically closed；O 為 electrically open。本論文中若有關於邊界條件之論述均遵守此規則。本研究分析所採用之材料參數均列於表 3.1。

3.1 迴轉體奇異性漸近解之驗證

透過對於雙材料迴轉體最小奇異性階數實數部 $\text{Re}[\lambda_1]$ 之收斂性分析以及與已發表的論文 [52, 53] 相比較，驗證於前章節所推導出漸近解之正確性與準確性。考量的迴轉體之幾何形狀為圖 2.2 中 $\beta = 90^\circ$ 與 $\beta_1 = 90^\circ$ 以及 $\beta = 90^\circ$ 與 $\beta_1 = 180^\circ$ 。所考慮之雙材料迴轉體含 CdSe/PZT-5H、CdSe/PZT-6B、CdSe/BaTiO₃ 與 PZT-6B/PZT-6B(Im.)。壓電材料之極化方向與迴轉體之旋轉軸 Z 軸平行 ($\gamma = 0^\circ$)；兩材料之交界面為 $X - Y$ 平面。所有材料之性質均列於表 3.1；其中 PZT-6B(Im.) 為一虛擬材料，相關性質常數參考於 Xu 與 Mutoh[53]，其材料之彈性係數同於 PZT-6B 但壓電常數與介電常數均大於實際材料 PZT-6B。

表 3.2 顯示數值結果會隨著子域數或級數解項數增加而上下振盪，最終趨於定值而達收斂 (convergence)。本研究所得之結果與 Li 等人 [52] 結果相當一致，可達四位有效位數。再利用本研究推導出之漸近解分析 PZT-6B/PZT-6B(Im.) 壓電材料迴轉體並與 Xu 與 Mutoh[53] 採用 Ting 等人 [49] 之軸對稱假設下所得之結果比較，其精確性可達五位有效，因此可證明本方法之正確性及有效性，並且顯示由本研究推得之漸近解亦能有效應用於壓電材料。

3.2 壓電迴轉體奇異性結果與討論

根據前章所推導出之漸近解型態，可知道電彈奇異性為實數部之 $(\lambda_m - 1)$ 所控制， $\text{Re}[\lambda_m]$ 越小表示奇異性強度越強。所以，我們最感興趣的部分為 $\text{Re}[\lambda_m]$ 之最小根 (即為 $\text{Re}[\lambda_1]$)，當在 0 與 1 之間即代表電彈奇異性之存在。因此，在後續討論的圖表均繪出 $\text{Re}[\lambda_1]$ 之數值曲線。於本節中將探討單一材料或雙材料壓電迴轉體因材料性質、邊界條件、極化方向與幾何形狀對 $\text{Re}[\lambda_1]$ 的影響，其中考慮的材料有壓電材料 PZT-4 與 PZT-6B 以及彈性材料 Si，材料性質均列於表 3.1。本節所得之數值結果，均基於將全域 ξ 分割為 8 個等份子域，每個子域之級數解均採 12 項。

3.2.1 單一壓電材料迴轉體

圖 3.1 與圖 3.2 為討論單壓電迴轉體於不同極化方向與邊界條件下 λ_1 隨 θ 變化之行為，迴轉體幾何形狀為 270° ($\beta = 90^\circ$, $\beta_1 = 180^\circ$ ，如圖 2.2)。

圖 3.1(a) 與圖 3.2(a) 考慮單壓電迴轉體於 FOFO 與 COCO 邊界條件下 $\gamma = 0^\circ$ 、 45° 與 90° 時 λ_1 隨 θ 變化情形。從圖 3.1(a) 與圖 3.2(a) 中發現於不同極化方向 γ 值下，當力學邊界條件為 free-free 時會擁有較強之電彈奇異性。圖 3.1(a) 中較為特別的是當 $\gamma = 0^\circ$ 與 90° 時，其 λ_1 曲線幾乎完全重合；而圖 3.2(a) 中所示為 PZT-6B 迴轉體並未有此現象。圖 3.1(a) 之 COCO 邊界條件且 $\gamma = 45^\circ$ 時 λ_1 曲線有較大之變化，其最大的變化幅度約 6.31%。

圖 3.1(b) 與圖 3.2(b) 為 $\gamma = 45^\circ$ 之 270° ($\beta = 90^\circ, \beta_1 = 180^\circ$) 單一壓電迴轉體於不同邊界條件時 λ_1 隨 θ 變化之情況，圖 3.1(b) 與圖 3.2(b) 中 PZT-4 與 PZT-6B 迴轉體於改變邊界條件時有類似的行為發生，例如：FOFO 與 FCFC 邊界條件之 λ_1 曲線幾近完全重合，表示當力學邊界條件為 free-free 時，電學邊界條件的改變對於電彈奇異性幾乎沒有影響；當力學邊界條件為 clamped-clamped 時，電學邊界條件的改變似乎對於奇異性之影響也不明顯，僅在 PZT-4 迴轉體 (圖 3.1(b)) 且 $\theta = 0^\circ$ 時，COCO 與 CCCC 邊界條件之 λ_1 曲線最大差異為 0.52%。觀察圖 3.1(b) 與圖 3.2(b)，當 $\gamma = 45^\circ$ 時，PZT-4 迴轉體之 θ 趨近於 180° 時，於任意邊界條件下電彈奇異性均漸趨轉弱；而 PZT-6B 迴轉體於 $\theta = 100^\circ$ 附近有最弱之電彈奇異性，當 θ 趨近於 0° 或 180° 時電彈奇異性反而增強，至於為何產生如此之現象或許只能歸咎於材料本身之性質。另外，從圖 3.1(b) 與圖 3.2(b) 中可見當 $\gamma = 45^\circ$ 且不同邊界條件下，於 $\theta = 0^\circ$ 處有最強之電彈奇異性。

圖 3.3 與圖 3.4 為單一壓電材料 PZT-4 與 PZT-6B 迴轉體於 $\gamma = 0^\circ$ 與 45° 且不同邊界條件下 λ_1 隨 β 變化之情形。圖中顯示力學邊界條件為 free-free 時較 clamped-clamped 之電彈奇異性強烈。另外，可從圖中發現單純改變電學邊界條件並不會對電彈奇異性造成明顯之影響，甚至在 free-free 力學邊界條件時， λ_1 曲線幾乎完全重合。觀察圖 3.4(b)，在 free-free 或 clamped-clamped 力學邊界條件下且 $\gamma = 0^\circ$ 時，於 $30^\circ < \beta < 120^\circ$ 之範圍中 λ_1 曲線成向上凹的走勢；而 $\gamma = 45^\circ$ 則呈現向下凹的現象。在圖 3.3(b) 中並未發現 λ_1 曲線有如圖 3.4(b) 之變化，因此可說明極化方向的改變是否對於奇異性行為造成明顯的影響，是依據各種材料本身之性質而定，並非壓電材料均有固定之變化行為。

3.2.2 雙壓電材料迴轉體

圖 3.5 為討論雙壓電迴轉體於不同極化方向與邊界條件下 $\text{Re}[\lambda_1]$ 隨 θ 變化之行為，壓電迴轉體組合為壓電材料 1/壓電材料 2，其中壓電材料 1 之 $\beta = 90^\circ$ ；壓電材料 2 之 $\beta_1 = 180^\circ$ ，如圖 2.2。圖 3.5(a) 與 (b) 中，壓電材料 1 為 PZT-4，壓電材料 2 為

PZT-6B；圖 3.5(c) 與 (d) 中，壓電材料 1 為 PZT-6B，壓電材料 2 為 PZT-4。

觀察圖 3.5(a) 與 (c) 發現於不同之邊界條件下 θ 改變時，兩圖之 $\text{Re}[\lambda_1]$ 曲線變化趨勢明顯不同，例如當 $\gamma = 90^\circ$ 時，圖 3.5(c) 中的 PZT-6B/PZT-4 壓電迴轉體於 $\theta = 90^\circ$ 總有最強烈之奇異性；而圖 3.5(a) 中 PZT-4/PZT-6B 壓電迴轉體卻總為最弱。另外，當 $\gamma = 45^\circ$ 時，圖 3.5(a) 中 $\theta = 180^\circ$ 之電彈奇異性強度總較 $\theta = 0^\circ$ 時弱；而圖 3.5(c) 中 $\theta = 0^\circ$ 與 $\theta = 180^\circ$ 電彈奇異性強度卻相當，故極化方向的改變對於雙壓電迴轉體有明顯之影響。觀察圖 3.5(b) 與 (d)，發現圖 3.5(b) 中在不同邊界條件下，當 θ 趨近於 180° 時奇異性強度會大幅度的減弱，其中又以 FCFC 邊界條件的變化幅度最大約達 17.12%。而圖 3.5(d) 中，當電學邊界條件為 closed-closed 時，會有類似圖 3.5(b) 中當 θ 趨近於 180° 時奇異性強度減弱行為，其中 CCCC 邊界條件曲線擁有最大的減弱幅度為約 9.43%。若電學邊界條件為 open-open 時 $\theta = 0^\circ$ 與 180° 之奇異性強度相當；於 $\theta = 90^\circ$ 附近時之奇異性強度最弱。

圖 3.6 為雙壓電材料複合迴轉體於 $\gamma = 0^\circ$ 與 45° 且不同邊界條件下 $\text{Re}[\lambda_1]$ 隨 β 變化之情形。圖 3.6(a) 與 (b) 為 PZT-4/PZT-6B 迴轉體，以 PZT-4 之幾何形狀為 β ，PZT-6B 保持 $\beta_1 = 180^\circ$ ；圖 3.6(c) 與 (d) 為 PZT-6B/PZT-4 迴轉體，以 PZT-6B 之幾何形狀為 β ，PZT-4 保持 $\beta_1 = 180^\circ$ 。從圖 3.6(a) 與 (c) 中，發現於圖 3.6(c) 中 COCO 邊界條件之奇異性強度一直保持為最弱；而在圖 3.6(a) 中並未有如此之現象。此外，CCCC 邊界條件於 $\beta = 180^\circ$ (裂縫之狀態) 時有相當強烈之奇異性，其 $\text{Re}[\lambda_1] = 0.432$ 相較於一般彈性材料裂縫狀態時奇異性為 0.500 更加強烈。

觀察圖 3.6(b) 與 (d) 於 FOFO 邊界條件時，發現圖 3.6(b) 中 λ_1 曲線對於極化方向 γ 變化較為敏感，因為於圖 3.6(d) 中 $\gamma = 0^\circ$ 與 $\gamma = 90^\circ$ 之 $\text{Re}[\lambda_1]$ 曲線幾乎重合，而 $\gamma = 45^\circ$ 時之曲線也僅有在 $0^\circ < \beta < 98^\circ$ 之範圍中有稍微較明顯之變化。另外，COCO 邊界條件下極化方向的改變對圖 3.6(b) 之 λ_1 曲線影響較為顯著，因為於圖 3.6(d) 中 $\gamma = 0^\circ$ 與 $\gamma = 90^\circ$ 曲線亦有許多範圍相重合。

3.2.3 壓電/彈性材料 Si 迴轉體

圖 3.7 為探討 PZT-4/Si 與 PZT-6B/Si 迴轉體於不同極化方向與邊界條件下 λ_1 隨 θ 變化之行為，其中 PZT-4 與 PZT-6B 之 $\beta = 90^\circ$ ；Si 之 $\beta_1 = 180^\circ$ ，如圖 2.2。

觀察圖 3.7(a) 與 (c)，當 $\gamma = 0^\circ$ 且 FOF- 邊界條件時，兩圖之 λ_1 值約為 0.552，因假設壓電材料為橫向等向性材料之緣故，所以 λ_1 值不隨 θ 變化；而邊界條件為 COC- 時，圖 3.7(a) 之 λ_1 值顯示有較為強烈之電彈奇異性，較圖 3.7(c) 之奇異性強約 3.05%。圖 3.7(c) 中，COC- 邊界條件之 λ_1 曲線隨 θ 變化時相較於 FOF- 邊界條件者有較大幅度之變化，約達 5.26%。

圖 3.7(b) 與 (d) 分別為 PZT-4/Si 與 PZT-6B/Si 迴轉體，其 $\gamma = 45^\circ$ 於不同邊界條件時 $\text{Re}[\lambda_1]$ 隨 θ 變化之情形。圖 3.7(b) 中發現電學邊界條件為 closed 時奇異性變化相當劇烈，其中 CCC- 邊界條件下 λ_1 值最大與最小之差異約達 20.00%；而 FCF- 邊界條件時差異甚至達約 32.72%。又 FCF- 邊界條件於 $\theta = 180^\circ$ 時 λ_1 為 0.733，顯示奇異性強度相當弱。圖 3.7(d) 中於 $0^\circ < \theta < 70^\circ$ 範圍中 FOF- 與 FCF- 邊界條件有相近的奇異性；於 $105^\circ < \theta < 180^\circ$ 範圍中 COC- 與 CCC- 之 λ_1 曲線幾乎重合。

圖 3.8 為 PZT-4/Si 或 PZT-6B/Si 迴轉體於 $\gamma = 0^\circ$ 與 45° 且不同邊界條件下 λ_1 隨 β 變化之情形。以 PZT-4 與 PZT-6B 之幾何形狀為 β ，PZT-6B 保持 $\beta_1 = 180^\circ$ ；如圖 3.8(a) 與 (c)，其中 CCC- 邊界條件且 $\beta = 180^\circ$ 時，總有相當強烈之奇異性，圖 3.8(a) 中 λ_1 為 0.382；圖 3.8(c) 中 λ_1 為 0.448。因此於設計或製造時須特別留意該狀態，否則可能會引致強烈之奇異性而導致元件提早破壞。圖 3.8(b) 與 (d) 為 FOF- 與 COC- 邊界條件於不同極化方向 γ 時奇異性的變化情形，觀察兩圖發現 γ 值的改變對 PZT-4/Si 迴轉體之 FOF- 邊界條件影響較大；而對 PZT-6B/Si 迴轉體時，則對於 COC- 邊界條件影響較大。圖 3.8(d) 中較為特別的是當 COC- 邊界條件且 $\gamma = 90^\circ$ 時之曲線幾乎與 FOF- 邊界條件之 $\gamma = 0^\circ$ 與 90° 之曲線完全重合。

3.3 電磁彈迴轉體奇異性結果與討論

本節中將探討單一材料或雙材料電磁彈迴轉體因為材料性質、邊界條件、極化方向與幾何形狀對於 $\text{Re}[\lambda_1]$ 的影響。考慮的材料有電磁彈性材料 $\text{BaTiO}_3\text{-CoFe}_2\text{O}_4$ 、壓電材料 PZT-4 與 PZT-6B 以及彈性材料 Si，材料性質列於表 3.1。本研究中所考量之電磁彈性材料為壓電材料 BaTiO_3 與壓磁材料 CoFe_2O_4 之複合物，其中 BaTiO_3 為填充物 (inclusion)； CoFe_2O_4 為基質 (matrix)。其材料性質與 BaTiO_3 及 CoFe_2O_4 之混合體積比例有關 [51]，成一線性關係 $\bar{\kappa}_{ij} = \bar{\kappa}_{ij}^B V_I + \bar{\kappa}_{ij}^F (1 - V_I)$ ，其中 $\bar{\kappa}_{ij}^B$ 與 $\bar{\kappa}_{ij}^F$ 為材料 BaTiO_3 與 CoFe_2O_4 的材料性質 (如表 3.1)； V_I 為內含物 BaTiO_3 之體積比例 (volume fraction)。本節所得之數值結果，均基於將全域 ξ 分割為 8 個等份子域，每個子域之級數解均採 12 項。

3.3.1 單一電磁彈性材料迴轉體

圖 3.9 為討論單一電磁彈材料迴轉體於不同極化方向與邊界條件下 λ_1 隨 θ 變化之行為。迴轉體幾何形狀為 270° ($\beta = 90^\circ$, $\beta_1 = 180^\circ$ ，如圖 2.2)。

由於假設 $\text{BaTiO}_3\text{-CoFe}_2\text{O}_4$ 為橫向等向性材料，其極化方向平行於 \bar{Z} 軸，故當極化方向 $\gamma = 0^\circ$ 時，可知於 $X-Y$ 平面上材料性質完全一致，由於 θ 為 X 與 Y 之函數，因此可以預期到 λ_1 的變化與 θ 值完全無關，所以於圖 3.9(a) 中 λ_1 曲線成一水平直線；當 γ 由 0° 變化至 90° ，以 $\gamma = 45^\circ$ 時 λ_1 值稍有較大之變化，其中又以力學邊界條件為 clamped-clamped 較明顯，但該變化之最大差異於 $\theta = 0^\circ$ 也僅限於 2.00% 以下。根據圖 3.9(b) 當 $\gamma = 45^\circ$ 且 θ 改變時，於各邊界條件下 λ_1 曲線均顯示於 $\theta = 0^\circ$ 有最強之奇異性。另外，力學邊界條件對於 λ_1 之影響遠大於電磁邊界條件，因為力學邊界條件為 free-free 時之奇異性較 clamped-clamped 時強，改變邊界條件僅造成 clamped-clamped 兩條 λ_1 產生些微差異，該最大差異為 0.34% 發生於 $\theta = 0^\circ$ 。

根據圖 3.9(c) 與 (d) 分別為 FOFO 與 COCO 邊界條件下， $V_I=20\%$ 、 50% 與 100%

之 270° ($\beta = 90^\circ$, $\beta_1 = 180^\circ$) 單一電磁彈性材料迴轉體 λ_1 變化曲線。其中 $V_I=100\%$ 時為忽略電磁彈性材料之磁性效應。觀察圖 3.9(c) 與 (d)，發現圖 3.9(c) 之 λ_1 值多分布於 0.541 至 0.548 之間，最大差異僅在 1.30% 以內；而圖 3.9(d) 中 λ_1 值分布範圍較廣於 0.572 至 0.598 間，最大差異約達 4.52%，因此可知改變單一電磁彈性材料之 V_I 值對 COCO 邊界條件影響較劇。另外，比較有趣的是圖 3.9(d) 中可分成 $\gamma = 0^\circ$ 與 45° 兩組，其共同之趨勢為 V_I 越小則對應之奇異性越強，而圖 3.9(c) 邊界條件為 FOFO 則無該特性。

圖 3.10 為 $V_I=50\%$ 之 $\text{BaTiO}_3\text{-CoFe}_2\text{O}_4$ 迴轉體於 $\gamma = 0^\circ$ 與 45° 且不同邊界條件下 $\text{Re}[\lambda_1]$ 隨 β 變化之情形。從過去彈性或壓電材料迴轉體相關文獻中可知應力或電彈奇異性會隨著 β 增加而愈趨強烈，圖中亦顯示電磁彈奇異性亦有相同之趨勢。當 $\beta = 180^\circ$ 時為模擬裂縫之狀態，此時無論邊界條件或極化方向如何變化，均為電磁彈奇異性最強之時刻，其 $\lambda_1 \leq 0.5$ 。根據圖 3.10 可再次發現力學邊界條件為 free-free 時奇異性強度較 clamped-clamped 時強之現象，至於電磁邊界條件 closed 與 open 的變換僅對奇異性強度造成些微的影響。圖 3.10(b) 顯示當極化方向由 $\gamma = 0^\circ$ 轉至 45° 亦僅造成奇異性強度些微的變化，其中可發現力學邊界條件為 clamped-clamped 較 free-free 明顯。

透過圖 3.10(c) 比較 $\text{BaTiO}_3\text{-CoFe}_2\text{O}_4$ 之 $V_I=20\%$ 、 50% 與 80% 於 $\gamma = 45^\circ$ 且 $\theta = 0^\circ$ 時 λ_1 的差異，圖中可以明顯看到 FOFO 邊界條件的三線幾近重合；而 COCO 邊界條件 $V_I=20\%$ 與 $V_I=50\%$ 之 λ_1 曲線最大差異為 0.32%，於是說明改變單一電磁彈性材料之 V_I 值對於造成 λ_1 值的變化影響可說是微乎其微。

3.3.2 雙電磁彈性材料迴轉體

圖 3.11 為討論雙電磁彈迴轉體於不同極化方向與邊界條件下 λ_1 隨 θ 變化之行為。透過改變材料 V_I 值以達到改變電磁彈性材料性質之目的。電磁彈迴轉體組合為電磁彈材料 1/電磁彈材料 2，其中電磁彈材料 1 之 $\beta = 90^\circ$ ，材料為 $V_I^{(1)}$ 之 $\text{BaTiO}_3\text{-CoFe}_2\text{O}_4$ ；電磁彈材料 2 之 $\beta_1 = 180^\circ$ ，材料為 $V_I^{(2)}$ 之 $\text{BaTiO}_3\text{-CoFe}_2\text{O}_4$ ，如圖 2.2。圖 3.11(a)、(b)

與 (d) 中，電磁彈材料 1 之 $V_I^{(1)} = 50\%$ ；電磁彈材料 2 之 $V_I^{(1)} = 50\%$ 。而圖 3.11(c) 中， $V_I^{(2)} = 20\%$ 、 40% 、 60% 與 80% 。

根據圖 3.11(a) 可發現控制 λ_1 值大小的主要因素仍為邊界條件，力學邊界條件為 clamped-clamped 之電磁彈奇異性仍然較 free-free 弱。無論邊界條件為 FOFO 或 COCO，當 $\gamma = 45^\circ$ 時仍然造成奇異性有較大幅度的變化，其中又以力學邊界條件為 clamped-clamped 時較為明顯。另外，COCO 邊界條件下 $\gamma = 45^\circ$ ，於 $\theta = 140^\circ$ 時曲線產生一折角，該點表示 λ_1 值實數與複數之轉換處；以本曲線為例，當 $\theta \geq 140^\circ$ 時 λ_1 則從實數轉變至複數。其餘各條件之 λ_1 仍保持實數。圖 3.11(b) 顯示電磁邊界條件依然不是影響奇異性變化之主因，如力學邊界為 free-free 之情況下，即便電磁邊界條件 closed 與 open 的改變，FOFO 與 FCFC 邊界條件之 λ_1 曲線顯示幾乎重疊，其中僅有極些微之改變。

圖 3.11(c) 為 FOFO 邊界條件下電磁彈材料 2 之 V_I 改變時， λ_1 隨 θ 變化之情形。其中 λ_1 的範圍多集中於 0.536 至 0.560 之間，圖中顯示 λ_1 有隨 $V_I^{(2)}$ 值上升而下降趨勢（表示奇異性越強），其與圖 3.9(d) 中單電磁彈性材料迴轉體之 λ_1 曲線趨勢相反。圖 3.11(c) 顯示當 $V_I^{(2)}=20\%$ 時 λ_1 隨 θ 之變化最為明顯，但最大差異也僅 1.82%。圖 3.11(d) 中 COCO 邊界條件時似乎沒有如圖 3.11(c) 中 FOFO 邊界條件之 λ_1 曲線有序的隨 $V_I^{(2)}$ 變化。圖 3.11(d) 中以 $V_I^{(2)}=80\%$ 之數據曲線較為特別，在 $\theta < 53^\circ$ 擁有最強之奇異性，而當 $\theta > 80^\circ$ 之奇異性又轉為最弱，表示 λ_1 於 $0^\circ < \theta < 90^\circ$ 之範圍中有快速上升的情況。另外，當 θ 越接近 180° 時， λ_1 越趨於集中，其範圍約在 0.584 至 0.589 之間。

圖 3.12 為雙電磁彈迴轉體迴轉體於 $\gamma = 0^\circ$ 與 45° 且不同邊界條件下 $\text{Re}[\lambda_1]$ 隨 β 變化之情形。其中電磁彈材料 1 之幾何形狀為 β ，材料為 $V_I^{(1)}$ 之 $\text{BaTiO}_3\text{-CoFe}_2\text{O}_4$ ；電磁彈材料 2 之 $\beta_1 = 180^\circ$ ，材料為 $V_I^{(2)}$ 之 $\text{BaTiO}_3\text{-CoFe}_2\text{O}_4$ 。

圖 3.12(a) 與 (b) 中，當極化方向 $\gamma = 0^\circ$ 與 45° 且於不同邊界條件時，當 $\gamma = 0^\circ$ 可發現約在 $\beta > 20^\circ$ 之各邊界條件之 $\text{Re}[\lambda_1]$ 值開始有較大的差異（圖 3.12(a)）；當 $\gamma = 45^\circ$

時約在 $55^\circ < \beta < 110^\circ$ 之範圍內電磁邊界條件的改變似乎對奇異性僅有些微之影響 (圖 3.12(b))，因為圖 3.12(b) 顯示 FOFO 與 FCFC 邊界條件之曲線以及 COCO 與 CCCC 邊界條件之曲線於該範圍內相互重合。另外各曲線均出現折角的情況，如前述折角處為表示實數與複數的交界點，舉例來說 FOFO 邊界條件下於 $66^\circ < \beta < 173^\circ$ 為實數，該曲線其餘各點為複數。各曲線均有其特殊之形態，因此邊界條件於固定極化方向 γ 值時為控制 λ_1 變化的主要因素。於 CCCC 邊界條件且 $\beta = 180^\circ$ 時為模擬裂縫之狀態，此時不論 $\gamma = 0^\circ$ 或 45° 之 $\text{Re}[\lambda_1]$ 值均低於其餘邊界條件之值，表示奇異性於此情況下最為強烈，較容易成為材料破壞之起始點。

圖 3.12(c) 為 FOFO 與 COCO 邊界條件下，觀察 $\gamma = 0^\circ$ 、 45° 與 90° ， $V_I^{(2)} = 20\%$ 之 $\text{BaTiO}_3\text{-CoFe}_2\text{O}_4$ 之 $\beta_1 = 180^\circ$ ， $V_I^{(1)} = 50\%$ 之 $\text{BaTiO}_3\text{-CoFe}_2\text{O}_4$ 之 β 變化時， λ_1 變化的情況。基本上 γ 的變化並不會使曲線之趨勢有特殊的變化，但可以發現因 γ 值所造成較為明顯之影響多集中於部分範圍，例如 FOFO 邊界條件時 $52^\circ < \beta < 102^\circ$ ；COCO 時 $29^\circ < \beta < 140^\circ$ 。圖 3.12(d) 為 FOFO 與 COCO 邊界條件下雙電磁彈與單電磁彈迴轉體之比較。圖中顯示 FOFO 邊界條件之單一或雙電磁彈性材料之 λ_1 值極為相近，該數值所顯示之結果與一般因雙材料之材料性質不連續而產生較為強烈之電磁彈奇異性之想法及經驗相左，但在 COCO 邊界條件時圖中數據卻與該概念相符合，因此電磁彈性材料間複雜的行為模式仍有許多探討之空間。

3.3.3 電磁彈性/彈性材料 Si 迴轉體

圖 3.13 為討論 $\text{BaTiO}_3\text{-CoFe}_2\text{O}_4/\text{Si}$ 迴轉體於不同極化方向與邊界條件下 λ_1 隨 θ 變化之行為。其中 $\text{BaTiO}_3\text{-CoFe}_2\text{O}_4$ 之 $\beta = 90^\circ$ ；Si 之 $\beta_1 = 180^\circ$ ，如圖 2.2。

圖 3.13(a) 與 (c) 為 FOF- 與 COC- 邊界條件且 $\gamma = 0^\circ$ 、 45° 與 90° 時， $V_I = 50\%$ 與 20% 之 $\text{BaTiO}_3\text{-CoFe}_2\text{O}_4/\text{Si}$ 迴轉體，其 λ_1 值隨 θ 變化之情形。從圖 3.13(a) 與 (c) 中可發現在各 γ 值以及 FOF- 與 COC- 邊界條件下奇異性的變化均不明顯， λ_1 值變化約在 0.500% 以內，其中又以圖 3.13(c) 之 λ_1 曲線變化幅度較圖 3.13(a) 明顯。圖 3.13(b) 與

(d) 為 $\gamma = 45^\circ$ 時於不同邊界條件下 λ_1 隨 θ 變化之情形。當電磁邊界條件為 closed 的情況下，圖 3.13(b) 中 λ_1 最大與最小的差異約達 7.00% 較圖 3.13(d) 中僅有 1.33% 明顯。因此電磁邊界條件的改變對於 BaTiO₃-CoFe₂O₄/Si 複合迴轉體之 λ_1 值有顯著之影響。概觀圖 3.13，發現力學邊界條件 free-free 總有較 clamped-clamped 強之奇異性。

圖 3.14 為 BaTiO₃-CoFe₂O₄/Si 迴轉體於 $\gamma = 0^\circ$ 與 45° 且不同邊界條件下 $\text{Re}[\lambda_1]$ 隨 β 變化之情形，其中 BaTiO₃-CoFe₂O₄ 之幾何形狀為 β 。圖 3.14(a) 中 $\gamma = 45^\circ$ 時，發現 CCC- 邊界條件於 $\beta = 180^\circ$ 時 $\lambda_1 = 0.449$ ，相較於一般彈性材料於裂縫狀態時，擁有更加強烈之奇異性。另外，而 FOF- 與 FCF- 邊界條件之 λ_1 曲線有極為類似之行為。圖 3.14(c) 為 $V_I = 50\%$ 與 20% 之 BaTiO₃-CoFe₂O₄/Si 迴轉體於 FOF- 與 CCC- 邊界條件下之電磁彈奇異性隨 β 值變化情形。其中可發現 CCC- 邊界條件下 $V_I = 50\%$ 之 BaTiO₃-CoFe₂O₄/Si 迴轉體會擁有較強之奇異性，最大差異發生於 $\beta = 180^\circ$ 時約 5.56%。另外，圖中可見 FOF- 邊界條件時 $V_I = 20\%$ 與 50% 之 BaTiO₃-CoFe₂O₄/Si 迴轉體有極為類似之行為，兩 λ_1 曲線於大部分區域幾乎重合，其中當 $V_I = 20\%$ 時 $\beta > 167^\circ$ 為複數；而當 $V_I = 50\%$ 時 $\beta > 171^\circ$ 為複數。圖 3.14(b) 與 (d) 分別為 $V_I = 50\%$ 與 20% 之 BaTiO₃-CoFe₂O₄/Si 迴轉體之奇異性隨 β 值變化之情形。圖 3.14(b) 中很明顯可發現在邊界條件 FOF- 與 COC- 之情況下，改變電磁彈性材料之極化方向 γ ，似乎對於奇異性的影響微乎其微，圖中可見各 γ 值之 λ_1 曲線多相互重合。

3.3.4 電磁彈性/壓電材料迴轉體

圖 3.15 與圖 3.16 為討論 $V_I = 50\%$ 之 BaTiO₃-CoFe₂O₄/PZT-4 與 BaTiO₃-CoFe₂O₄/PZT-6B 迴轉體於不同極化方向與邊界條件下 λ_1 隨 θ 變化之行為。其中 BaTiO₃-CoFe₂O₄ 之 $\beta = 90^\circ$ ；壓電材料之 $\beta_1 = 180^\circ$ ，如圖 2.2。由兩圖可觀察到相較於雙壓電迴轉體 $\text{Re}[\lambda_1]$ 之變化更為明顯，推測原因為電磁彈性與壓電材料間的材料性質差異較雙壓電材料大，故可能產生的奇異性行為也較複雜多變化。

圖 3.15(a) 中因為壓電材料 PZT-4 亦假設為橫向等向性材料，故當 $\gamma = 0^\circ$ 時， θ 值

無論如何變化 λ_1 均維持定值。當 FOFO 邊界條件時，極化方向的改變並未使 λ_1 有劇烈之變化。而 COCO 邊界條件時 $\text{Re}[\lambda_1]$ 曲線出現折角 (如 $\gamma = 45^\circ$ 時，於 $\theta = 118^\circ$)，如此乃因實數與複數根之轉換，如 $\gamma = 45^\circ$ 時 $\theta < 117^\circ$ 與 $\gamma = 90^\circ$ 時 $19^\circ < \theta < 161^\circ$ 其 λ_1 為實數。觀察圖 3.15(a) 與 (c)，發現 $\text{BaTiO}_3\text{-CoFe}_2\text{O}_4$ 由 $V_I=50\%$ 轉變成 20% 時，COCO 邊界條件之奇異性隨 θ 變化之 λ_1 值在邊界條件為 COCO 時之奇異性整體有增強之趨勢，但隨 θ 之變化幅度並不如 $V_I=50\%$ 明顯；而 FOFO 邊界條件時奇異性整體亦有稍增強之現象但不明顯。觀察圖 3.15(b) 與 (d)，其中兩圖間以 COCO 與 CCCC 之 λ_1 曲線差異較大，在 $V_I = 20\%$ 之 COCO 曲線中並未產生如 $V_I=50\%$ 曲線中有折角之現象；而邊界條件為 CCCC 時，於 $V_I=50\%$ 時 λ_1 曲線變化幅度約有 7.42% ，而當 $V_I=20\%$ 時則成長至 11.8% 。

圖 3.15(a) 與圖 3.16(a) 中發現 FOFO 邊界條件下於不同之極化方向 γ 值下 λ 曲線有著相似的趨勢，但以圖 3.16(a) 中 λ_1 分布之範圍較為集中；而圖 3.16(a) 中 COCO 邊界條件之 $\text{Re}[\lambda_1]$ 曲線相較於圖 3.15(a) 變化幅度較小。圖 3.15(b) 與 3.16(b) 於不同邊界條件且 $\gamma = 45^\circ$ 時，兩圖有著明顯差異。圖 3.16(b) 中 FOFO 與 FCFC 邊界條件之 $\text{Re}[\lambda_1]$ 曲線幾乎完全重合，表示僅改變電磁彈與電學邊界條件，不會對奇異性強度造成顯著的影響，另外對於 COCO 與 CCCC 邊界條件的影響亦有限，不如圖 3.15(b) 中當改變電磁彈與電學邊界條件時造成各 $\text{Re}[\lambda_1]$ 曲線有明顯之差異。圖 3.16(c) 將 $\text{BaTiO}_3\text{-CoFe}_2\text{O}_4$ 之 V_I 降為 20% ，FOFO 邊界條件時 λ_1 變化與圖 3.16(a) 之 FOFO 邊界條件 λ_1 曲線有類似之趨勢，但奇異性強度稍為增強約 0.95% 。綜合圖 3.15(b) 與 (d) 以及圖 3.16(b) 與 (d) 可觀察到當 $\text{BaTiO}_3\text{-CoFe}_2\text{O}_4$ 之 V_I 由 50% 轉為 20% 時，CCCC 邊界條件之奇異性均有變強之現象，其中又以 $\text{BaTiO}_3\text{-CoFe}_2\text{O}_4/\text{PZT-4}$ 迴轉體改變幅度較大。

圖 3.17 為 $\text{BaTiO}_3\text{-CoFe}_2\text{O}_4/\text{PZT-4}$ 迴轉體於 $\gamma = 0^\circ$ 與 45° 且不同邊界條件下 $\text{Re}[\lambda_1]$ 隨 β 變化之情形，其中 $\text{BaTiO}_3\text{-CoFe}_2\text{O}_4$ 之幾何形狀為 β ；PZT-4 之 $\beta_1 = 180^\circ$ 。

根據彈性材料相關文獻中所得之經驗，力學邊界條件為 free-free 應較 clamped-

clamped 擁有較強之奇異性，但於圖 3.17(a) 中，當 $\beta > 147^\circ$ 時 CCCC 邊界條件卻擁有最小之 λ_1 值，當 $\beta = 180^\circ$ 時之奇異性較一般彈性材料於裂縫情況下所得之 λ_1 值為 0.500 更為強烈，此處 FOFO 邊界條件之 $\lambda_1 = 0.476$ ；而 CCCC 邊界條件之 $\lambda_1 = 0.453$ ，表示因為 $\text{BaTiO}_3\text{-CoFe}_2\text{O}_4$ 與 PZT-4 間材料性質的差異與邊界條件的改變造成於裂縫尖端點之奇異性更加強烈，使得破壞之可能性提升。比較將 $\text{BaTiO}_3\text{-CoFe}_2\text{O}_4$ 之 V_I 改為 20%(圖 3.17(c))，變化最明顯的為 CCCC 邊界條件於 $\beta = 180^\circ$ 時其 λ_1 降至 0.419，奇異性變為更加強烈；而 FOFO 於 $\beta = 180^\circ$ 之 λ_1 反升至 0.500。另外，FCFC 邊界條件在各 β 下奇異性總為最弱。

圖 3.17(b) 與 (d) 為 $V_I=50\%$ 與 20% 之 $\text{BaTiO}_3\text{-CoFe}_2\text{O}_4/\text{PZT-4}$ 迴轉體於 FOFO 與 COCO 邊界條件且不同 γ 值時奇異性隨 β 值變化之情況。由圖 3.17(b) 觀察改變 γ 值所造成 λ_1 的改變，發現 γ 值的變化對於 COCO 邊界條件有較為明顯之影響；在 FOFO 的情況下僅有在 $\beta > 150^\circ$ 時之範圍內發現曲線產生折角之現象，其餘各 γ 值之 λ_1 曲線均有極為類似的走勢。另外在 $\beta = 180^\circ$ 時，於 FOFO 與 COCO 邊界條件下 γ 值的改變不會造成 λ_1 明顯的變化，因此可推論邊界條件與幾何形狀為影響奇異性之主要因素。圖 3.17(d) 中，當 $\text{BaTiO}_3\text{-CoFe}_2\text{O}_4$ 之 V_I 降為 20% 時，基本上 λ_1 之變化趨勢類似於圖 3.17(b)，但如同於圖 3.17(c) 中所提到 FOFO 邊界條件於 $\beta = 180^\circ$ 時 λ_1 會回升至 0.500，而且於 γ 值均有相同之現象。此外，在 COCO 邊界條件且 $\gamma = 90^\circ$ 時 λ_1 均為實數，不同於圖 3.17(b) 中 V_I 為 50% 時於 $22^\circ < \beta < 98^\circ$ 的範圍中 λ_1 為複數。

圖 3.18 為 $\text{BaTiO}_3\text{-CoFe}_2\text{O}_4/\text{PZT-6B}$ 迴轉體於 $\gamma = 0^\circ$ 與 45° 且不同邊界條件下 $\text{Re}[\lambda_1]$ 隨 β 變化之情形，其中 $\text{BaTiO}_3\text{-CoFe}_2\text{O}_4$ 之幾何形狀為 β ；PZT-6B 之 $\beta_1 = 180^\circ$ 。

圖 3.18(a) 與 (c) 為 $V_I=50\%$ 與 20% 之 $\text{BaTiO}_3\text{-CoFe}_2\text{O}_4/\text{PZT-6B}$ 迴轉體之 $\text{Re}[\lambda_1]$ 曲線，其中顯示僅改變電磁邊界條件與電學邊界條件對於力學邊界條件為 free-free 之 $\text{Re}[\lambda_1]$ 值影響相當有限，僅有在 $140^\circ < \beta < 180^\circ$ 的範圍中有些微之改變。觀察圖 3.18(a) 與 (c) 中之 CCCC 邊界條件當 $\beta = 180^\circ$ 時 λ_1 值稍小於 0.500，該情況與 $\text{BaTiO}_3\text{-CoFe}_2\text{O}_4/\text{PZT-4}$ 迴轉體所顯示的現象類似，但奇異性強度卻不如其強烈。整體

而言，電磁邊界條件與電學邊界條件的改變對於 $\text{BaTiO}_3\text{-CoFe}_2\text{O}_4/\text{PZT-4}$ 迴轉體之影響程度似乎更勝於 $\text{BaTiO}_3\text{-CoFe}_2\text{O}_4/\text{PZT-6B}$ 迴轉體。圖 3.18(b) 與 (d) 為極化方向改變對於 $\text{BaTiO}_3\text{-CoFe}_2\text{O}_4/\text{PZT-6B}$ 迴轉體之奇異性所造成之影響，發現極化方向 γ 值的改變對於奇異性影響甚微，相較於圖 3.17(b) 與 (d)， $\text{BaTiO}_3\text{-CoFe}_2\text{O}_4/\text{PZT-4}$ 迴轉體則受到極化方向改變較大的影響。比較圖 3.18(b) 與 (d) 其中各 $\text{Re}[\lambda_1]$ 均有類似的變化，其中較大的差異也僅有 $\gamma = 0^\circ$ 的 COCO 邊界條件之 $\text{Re}[\lambda_1]$ 曲線，當 $\text{BaTiO}_3\text{-CoFe}_2\text{O}_4$ 的 V_I 為 50% 時其曲線折角發生於 $\beta = 130^\circ$ ，而 $\text{BaTiO}_3\text{-CoFe}_2\text{O}_4$ 的 V_I 為 20% 時則發生於 $\beta = 160^\circ$ 。



第四章 三維電磁彈性楔形體之奇異性

4.1 電磁彈楔形體於尖角處之漸近解

本節考慮電磁彈楔形體，以 (r, θ, Z) 座標系統可以很方便描述該幾何形狀；假設此楔形體之材料性質以 $(\bar{X}, \bar{Y}, \bar{Z})$ 座標系統描述。在以下求解過程中，將 $(\bar{X}, \bar{Y}, \bar{Z})$ 座標系統所描述之材料性質轉換至 (r, θ, Z) 座標系統，如此可以便利於分析。該轉換如同第二章所敘述者（公式可參考附錄 A）。

如同 2.2 節所敘述，根據式 (2.4) 之關係，可將應力 σ_{ij} 、電位移 D_{ij} 及磁感應強度 B_{ij} ，分別以位移分量 u_i^* 、電勢 ϕ_i^* 與磁勢 ψ_i^* 表示，整理於附錄 B。於是三維力平衡方程式及馬克斯威爾方程式亦可以 u_i^* 、 ϕ_i^* 與 ψ_i^* 表示（見式 (2.5)）。在解決楔形體的問題時，可直接在 (r, θ, Z) 進行作業（參考圖 4.2），故毋須將座標轉換至 (ρ, θ, ξ) 系統，因此可假設式 (2.5) 的解為

$$u_r^*(r, \theta, Z, t) = \sum_{m=1}^{\infty} \sum_{n=0}^{\infty} r^{\lambda_m+n} \hat{U}_n^{(i)}(\theta, Z) e^{i\omega t} \quad (4.1a)$$

$$u_\theta^*(r, \theta, Z, t) = \sum_{m=1}^{\infty} \sum_{n=0}^{\infty} r^{\lambda_m+n} \hat{V}_n^{(i)}(\theta, Z) e^{i\omega t} \quad (4.1b)$$

$$u_Z^*(r, \theta, Z, t) = \sum_{m=1}^{\infty} \sum_{n=0}^{\infty} r^{\lambda_m+n} \hat{W}_n^{(i)}(\theta, Z) e^{i\omega t} \quad (4.1c)$$

$$\phi^*(r, \theta, Z, t) = \sum_{m=1}^{\infty} \sum_{n=0}^{\infty} r^{\lambda_m+n} \hat{\Phi}_n^{(i)}(\theta, Z) e^{i\omega t} \quad (4.1d)$$

$$\psi^*(r, \theta, Z, t) = \sum_{m=1}^{\infty} \sum_{n=0}^{\infty} r^{\lambda_m+n} \hat{\Psi}_n^{(i)}(\theta, Z) e^{i\omega t} \quad (4.1e)$$

類似於 2.3 節的做法將式 (4.1) 與 (2.4) 代入式 (2.3)

$$\begin{aligned} \sum_{m=1}^{\infty} \sum_{n=0}^{\infty} \left\{ r^{\lambda_m+n-2} \left[\left(-c_{22} + \lambda_m \left(\lambda_m c_{11} + \frac{\partial c_{16}}{\partial \theta} \right) + \frac{\partial c_{26}}{\partial \theta} \right) \hat{U}_n^{(i)} + \left(2\lambda_m c_{16} + \frac{\partial c_{66}}{\partial \theta} \right) \frac{\partial \hat{U}_n^{(i)}}{\partial \theta} \right. \right. \\ \left. \left. + c_{66} \frac{\partial^2 \hat{U}_n^{(i)}}{\partial \theta^2} + (\lambda_m - 1) \left(\lambda_m c_{16} - c_{26} + \frac{\partial c_{66}}{\partial \theta} \right) \hat{V}_n^{(i)} + \left(\lambda_m c_{12} - c_{22} + (\lambda_m - 1) c_{66} \right) \right. \right. \end{aligned}$$

$$\begin{aligned}
& + \frac{\partial c_{26}}{\partial \theta} \left) \frac{\partial \hat{V}_n^{(i)}}{\partial \theta} + c_{26} \frac{\partial^2 \hat{V}_n^{(i)}}{\partial \theta^2} + \lambda_m \left(\lambda_m c_{15} - c_{25} + \frac{\partial c_{56}}{\partial \theta} \right) \hat{W}_n^{(i)} + \left(\lambda_m (c_{14} + c_{56}) - c_{24} \right. \\
& + \frac{\partial c_{46}}{\partial \theta} \left) \frac{\partial \hat{W}_n^{(i)}}{\partial \theta} + c_{46} \frac{\partial^2 \hat{W}_n^{(i)}}{\partial \theta^2} + \lambda_m \left(\lambda_m e_{11} - e_{12} + \frac{\partial e_{16}}{\partial \theta} \right) \hat{\Phi}_n^{(i)} + \left(\lambda_m (e_{16} + e_{21}) - e_{22} \right. \\
& + \frac{\partial e_{26}}{\partial \theta} \left) \frac{\partial \hat{\Phi}_n^{(i)}}{\partial \theta} + e_{26} \frac{\partial^2 \hat{\Phi}_n^{(i)}}{\partial \theta^2} + \lambda_m \left(\lambda_m d_{11} - d_{12} + \frac{\partial d_{16}}{\partial \theta} \right) \hat{\Psi}_n^{(i)} + \left(\lambda_m (d_{16} + d_{21}) - d_{22} \right. \\
& + \frac{\partial d_{26}}{\partial \theta} \left) \frac{\partial \hat{\Psi}_n^{(i)}}{\partial \theta} + d_{26} \frac{\partial^2 \hat{\Psi}_n^{(i)}}{\partial \theta^2} \left. \right] + r^{\lambda_m + n - 1} \left[2c_{56} \frac{\partial^2 \hat{U}_n^{(i)}}{\partial \theta \partial z} + \left((2\lambda_m + 1) c_{15} + \frac{\partial c_{56}}{\partial \theta} \right) \frac{\partial \hat{U}_n^{(i)}}{\partial z} \right. \\
& + (c_{25} + c_{46}) \frac{\partial^2 \hat{V}_n^{(i)}}{\partial \theta \partial z} + \left((\lambda_m + 1) c_{14} - c_{24} + (\lambda_m - 1) c_{56} - \frac{\partial c_{46}}{\partial \theta} \right) \frac{\partial \hat{V}_n^{(i)}}{\partial z} + (c_{36} + c_{45}) \\
& \times \frac{\partial^2 \hat{W}_n^{(i)}}{\partial \theta \partial z} + \left((\lambda_m + 1) c_{13} - c_{23} + \lambda_m c_{55} + \frac{\partial c_{36}}{\partial \theta} \right) \frac{\partial \hat{W}_n^{(i)}}{\partial z} + (e_{25} + e_{36}) \frac{\partial^2 \hat{\Phi}_n^{(i)}}{\partial \theta \partial z} + \left(e_{31} \right. \\
& + \lambda_m (e_{15} + e_{31}) - e_{32} + \frac{\partial e_{36}}{\partial \theta} \left) \frac{\partial \hat{\Phi}_n^{(i)}}{\partial z} + (d_{25} + d_{36}) \frac{\partial^2 \hat{\Psi}_n^{(i)}}{\partial \theta \partial z} + \left(d_{31} + \lambda_m (d_{15} + d_{31}) - d_{32} \right. \\
& + \frac{\partial d_{36}}{\partial \theta} \left) \frac{\partial \hat{\Psi}_n^{(i)}}{\partial z} \left. \right] + r^{\lambda_m + n} \left(c_{55} \frac{\partial^2 \hat{U}_n^{(i)}}{\partial z^2} + c_{45} \frac{\partial^2 \hat{V}_n^{(i)}}{\partial z^2} + c_{35} \frac{\partial^2 \hat{W}_n^{(i)}}{\partial z^2} + e_{35} \frac{\partial^2 \hat{\Phi}_n^{(i)}}{\partial z^2} \right. \\
& \left. + d_{35} \frac{\partial^2 \hat{\Psi}_n^{(i)}}{\partial z^2} + m_s \omega^2 \hat{U}_n^{(i)} \right) \left. \right\} = 0, \tag{4.2a}
\end{aligned}$$

$$\begin{aligned}
& \sum_{m=1}^{\infty} \sum_{n=0}^{\infty} \left\{ r^{\lambda_m + n - 2} \left[\left(c_{26} + \lambda_m \left((\lambda_m + 1) c_{16} + c_{26} + \frac{\partial c_{12}}{\partial \theta} \right) + \frac{\partial c_{22}}{\partial \theta} \right) \hat{U}_n^{(i)} + \left(c_{22} + c_{66} \right. \right. \right. \\
& + \lambda_m (c_{12} + c_{66}) + \frac{\partial c_{26}}{\partial \theta} \left) \frac{\partial \hat{U}_n^{(i)}}{\partial \theta} + c_{26} \frac{\partial^2 \hat{U}_n^{(i)}}{\partial \theta^2} + (\lambda_m - 1) \left((\lambda_m + 1) c_{66} + \frac{\partial c_{26}}{\partial \theta} \right) \hat{V}_n^{(i)} \right. \\
& + \left(2\lambda_m c_{26} + \frac{\partial c_{22}}{\partial \theta} \right) \frac{\partial \hat{V}_n^{(i)}}{\partial \theta} + c_{22} \frac{\partial^2 \hat{V}_n^{(i)}}{\partial \theta^2} + \lambda_m \left((\lambda_m + 1) c_{56} + \frac{\partial c_{25}}{\partial \theta} \right) \hat{W}_n^{(i)} + \left(\lambda_m \right. \\
& \times (c_{25} + c_{46}) + c_{46} + \frac{\partial c_{24}}{\partial \theta} \left) \frac{\partial \hat{W}_n^{(i)}}{\partial \theta} + c_{24} \frac{\partial^2 \hat{W}_n^{(i)}}{\partial \theta^2} + \lambda_m \left((\lambda_m + 1) e_{16} + \frac{\partial e_{12}}{\partial \theta} \right) \hat{\Phi}_n^{(i)} \right. \\
& + \left(\lambda_m (e_{12} + e_{26}) + e_{26} + \frac{\partial e_{22}}{\partial \theta} \right) \frac{\partial \hat{\Phi}_n^{(i)}}{\partial \theta} + e_{22} \frac{\partial^2 \hat{\Phi}_n^{(i)}}{\partial \theta^2} + \lambda_m \left((\lambda_m + 1) d_{16} + \frac{\partial d_{12}}{\partial \theta} \right) \hat{\Psi}_n^{(i)} \\
& + \left(\lambda_m (d_{12} + d_{26}) + d_{26} + \frac{\partial d_{22}}{\partial \theta} \right) \frac{\partial \hat{\Psi}_n^{(i)}}{\partial \theta} + d_{22} \frac{\partial^2 \hat{\Psi}_n^{(i)}}{\partial \theta^2} \left. \right] + r^{\lambda_m + n - 1} \left[(c_{25} + c_{46}) \frac{\partial^2 \hat{U}_n^{(i)}}{\partial \theta \partial z} \right. \\
& + \left(\lambda_m c_{14} + c_{24} + (\lambda_m + 2) c_{56} + \frac{\partial c_{25}}{\partial \theta} \right) \frac{\partial \hat{U}_n^{(i)}}{\partial z} + 2c_{24} \frac{\partial^2 \hat{V}_n^{(i)}}{\partial \theta \partial z} + \left(c_{46} + 2\lambda_m c_{46} + \frac{\partial c_{24}}{\partial \theta} \right) \\
& \times \frac{\partial \hat{V}_n^{(i)}}{\partial z} + (c_{23} + c_{44}) \frac{\partial^2 \hat{W}_n^{(i)}}{\partial \theta \partial z} + \left((\lambda_m + 2) c_{36} + \lambda_m c_{45} + \frac{\partial c_{23}}{\partial \theta} \right) \frac{\partial \hat{W}_n^{(i)}}{\partial z} + (e_{24} + e_{32}) \\
& \times \frac{\partial^2 \hat{\Phi}_n^{(i)}}{\partial \theta \partial z} + \left(\lambda_m e_{14} + (\lambda_m + 2) e_{36} + \frac{\partial e_{32}}{\partial \theta} \right) \frac{\partial \hat{\Phi}_n^{(i)}}{\partial z} + (d_{24} + d_{32}) \frac{\partial^2 \hat{\Psi}_n^{(i)}}{\partial \theta \partial z} + (\lambda_m d_{14} \\
& + (\lambda_m + 2) d_{36} + \frac{\partial d_{32}}{\partial \theta} \left) \frac{\partial \hat{\Psi}_n^{(i)}}{\partial z} \left. \right] + r^{\lambda_m + n} \left(c_{45} \frac{\partial^2 \hat{U}_n^{(i)}}{\partial z^2} + c_{44} \frac{\partial^2 \hat{V}_n^{(i)}}{\partial z^2} + c_{34} \frac{\partial^2 \hat{W}_n^{(i)}}{\partial z^2} \right. \\
& \left. + e_{34} \frac{\partial^2 \hat{\Phi}_n^{(i)}}{\partial z^2} + d_{34} \frac{\partial^2 \hat{\Psi}_n^{(i)}}{\partial z^2} + m_s \omega^2 \hat{V}_n^{(i)} \right) \left. \right\} = 0, \tag{4.2b}
\end{aligned}$$

$$\begin{aligned}
& \sum_{m=1}^{\infty} \sum_{n=0}^{\infty} \left\{ r^{\lambda_m+n-2} \left[\left(\lambda_m \left(\lambda_m c_{15} + c_{25} + \frac{\partial c_{14}}{\partial \theta} \right) + \frac{\partial c_{24}}{\partial \theta} \right) \hat{U}_n^{(i)} + \left(c_{24} + \lambda_m (c_{14} + c_{56}) + \frac{\partial c_{46}}{\partial \theta} \right) \right. \right. \\
& \quad \times \frac{\partial \hat{U}_n^{(i)}}{\partial \theta} + c_{46} \frac{\partial^2 \hat{U}_n^{(i)}}{\partial \theta^2} + (\lambda_m - 1) \left(\lambda_m c_{56} + \frac{\partial c_{46}}{\partial \theta} \right) \hat{V}_n^{(i)} + \left(\lambda_m c_{25} + (\lambda_m - 1) c_{46} + \frac{\partial c_{24}}{\partial \theta} \right) \\
& \quad \times \frac{\partial \hat{V}_n^{(i)}}{\partial \theta} + c_{24} \frac{\partial^2 \hat{V}_n^{(i)}}{\partial \theta^2} + \lambda_m \left(\lambda_m c_{55} + \frac{\partial c_{45}}{\partial \theta} \right) \hat{W}_n^{(i)} + \left(2\lambda_m c_{45} + \frac{\partial c_{44}}{\partial \theta} \right) \frac{\partial \hat{W}_n^{(i)}}{\partial \theta} + c_{44} \\
& \quad \times \frac{\partial^2 \hat{W}_n^{(i)}}{\partial \theta^2} + \lambda_m \left(\lambda_m e_{15} + \frac{\partial e_{14}}{\partial \theta} \right) \hat{\Phi}_n^{(i)} + \left(\lambda_m (e_{14} + e_{25}) + \frac{\partial e_{24}}{\partial \theta} \right) \frac{\partial \hat{\Phi}_n^{(i)}}{\partial \theta} + e_{24} \frac{\partial^2 \hat{\Phi}_n^{(i)}}{\partial \theta^2} \\
& \quad + \lambda_m \left(\lambda_m d_{15} + \frac{\partial d_{14}}{\partial \theta} \right) + \lambda_m \left(\lambda_m d_{15} + \frac{\partial d_{14}}{\partial \theta} \right) \hat{\Psi}_n^{(i)} + \left(\lambda_m (d_{14} + d_{25}) + \frac{\partial d_{24}}{\partial \theta} \right) \frac{\partial \hat{\Psi}_n^{(i)}}{\partial \theta} \\
& \quad \left. + d_{24} \frac{\partial^2 \hat{\Psi}_n^{(i)}}{\partial \theta^2} \right] + r^{\lambda_m+n-1} \left[(c_{36} + c_{45}) \frac{\partial^2 \hat{U}_n^{(i)}}{\partial \theta \partial z} + \left(c_{23} + c_{55} + \lambda_m (c_{13} + c_{55}) + \frac{\partial c_{45}}{\partial \theta} \right) \frac{\partial \hat{U}_n^{(i)}}{\partial z} \right. \\
& \quad + (c_{23} + c_{44}) \frac{\partial^2 \hat{V}_n^{(i)}}{\partial \theta \partial z} + \left((\lambda_m - 1) c_{36} + (\lambda_m + 1) c_{45} + \frac{\partial c_{44}}{\partial \theta} \right) \frac{\partial \hat{V}_n^{(i)}}{\partial z} + 2c_{34} \frac{\partial^2 \hat{W}_n^{(i)}}{\partial \theta \partial z} \\
& \quad + \left((2\lambda_m + 1) c_{35} + \frac{\partial c_{34}}{\partial \theta} \right) \frac{\partial \hat{W}_n^{(i)}}{\partial z} + (e_{23} + e_{34}) \frac{\partial^2 \hat{\Phi}_n^{(i)}}{\partial \theta \partial z} + \left(e_{35} + \lambda_m (e_{13} + e_{35}) + \frac{\partial e_{34}}{\partial \theta} \right) \\
& \quad \times \frac{\partial \hat{\Phi}_n^{(i)}}{\partial z} + (e_{23} + e_{34}) \frac{\partial^2 \hat{\Psi}_n^{(i)}}{\partial \theta \partial z} + \left(d_{35} + \lambda_m (d_{13} + d_{35}) + \frac{\partial d_{34}}{\partial \theta} \right) \frac{\partial \hat{\Psi}_n^{(i)}}{\partial z} \left. \right] + r^{\lambda_m+n} \left(c_{35} \frac{\partial^2 \hat{U}_n^{(i)}}{\partial z^2} \right. \\
& \quad \left. + c_{34} \frac{\partial^2 \hat{V}_n^{(i)}}{\partial z^2} + c_{33} \frac{\partial^2 \hat{W}_n^{(i)}}{\partial z^2} + e_{33} \frac{\partial^2 \hat{\Phi}_n^{(i)}}{\partial z^2} + d_{33} \frac{\partial^2 \hat{\Psi}_n^{(i)}}{\partial z^2} + m_s \omega^2 \hat{W}_n^{(i)} \right) \left. \right\} = 0, \tag{4.2c}
\end{aligned}$$

$$\begin{aligned}
& \sum_{m=1}^{\infty} \sum_{n=0}^{\infty} \left\{ r^{\lambda_m+n-2} \left[\left(\lambda_m \left(\lambda_m e_{11} + e_{12} + \frac{\partial e_{21}}{\partial \theta} \right) + \frac{\partial e_{22}}{\partial \theta} \right) \hat{U}_n^{(i)} + \left(e_{22} + \lambda_m (e_{16} + e_{21}) + \frac{\partial e_{26}}{\partial \theta} \right) \right. \right. \\
& \quad \times \frac{\partial \hat{U}_n^{(i)}}{\partial \theta} + e_{26} \frac{\partial^2 \hat{U}_n^{(i)}}{\partial \theta^2} + (\lambda_m - 1) \left(\lambda_m e_{16} + \frac{\partial e_{26}}{\partial \theta} \right) \hat{V}_n^{(i)} + \left(\lambda_m e_{12} + (\lambda_m - 1) e_{26} + \frac{\partial e_{22}}{\partial \theta} \right) \\
& \quad \times \frac{\partial \hat{V}_n^{(i)}}{\partial \theta} + e_{22} \frac{\partial^2 \hat{V}_n^{(i)}}{\partial \theta^2} + \lambda_m \left(\lambda_m e_{15} + \frac{\partial e_{25}}{\partial \theta} \right) \hat{W}_n^{(i)} + \left(\lambda_m (e_{14} + e_{25}) + \frac{\partial e_{24}}{\partial \theta} \right) \frac{\partial \hat{W}_n^{(i)}}{\partial \theta} + e_{24} \\
& \quad \times \frac{\partial^2 \hat{W}_n^{(i)}}{\partial \theta^2} - \lambda_m \left(\lambda_m \eta_{11} + \frac{\partial \eta_{12}}{\partial \theta} \right) \hat{\Phi}_n^{(i)} - \left(2\lambda_m \eta_{12} + \frac{\partial \eta_{22}}{\partial \theta} \right) \frac{\partial \hat{\Phi}_n^{(i)}}{\partial \theta} - \eta_{22} \frac{\partial^2 \hat{\Phi}_n^{(i)}}{\partial \theta^2} - \lambda_m \\
& \quad \times \left(\lambda_m g_{11} + \frac{\partial g_{12}}{\partial \theta} \right) \hat{\Psi}_n^{(i)} - \left(2\lambda_m g_{12} + \frac{\partial g_{22}}{\partial \theta} \right) \frac{\partial \hat{\Psi}_n^{(i)}}{\partial \theta} - g_{22} \frac{\partial^2 \hat{\Psi}_n^{(i)}}{\partial \theta^2} \left. \right] + r^{\lambda_m+n-1} \left[\left(e_{25} + e_{36} \right) \right. \\
& \quad \times \frac{\partial^2 \hat{U}_n^{(i)}}{\partial \theta \partial z} + \left((\lambda_m + 1) e_{15} + \lambda_m e_{31} + e_{32} + \frac{\partial e_{25}}{\partial \theta} \right) \frac{\partial \hat{U}_n^{(i)}}{\partial z} + (e_{24} + e_{32}) \frac{\partial^2 \hat{V}_n^{(i)}}{\partial \theta \partial z} + \left((\lambda_m - 1) \right. \\
& \quad \times e_{36} + (\lambda_m + 1) e_{14} + \frac{\partial e_{24}}{\partial \theta} \left. \right) \frac{\partial \hat{V}_n^{(i)}}{\partial z} + (e_{23} + e_{34}) \frac{\partial^2 \hat{W}_n^{(i)}}{\partial \theta \partial z} + \left((\lambda_m + 1) e_{13} + \lambda_m e_{35} + \frac{\partial e_{23}}{\partial \theta} \right) \\
& \quad \times \frac{\partial \hat{W}_n^{(i)}}{\partial z} - 2\eta_{23} \frac{\partial^2 \hat{\Phi}_n^{(i)}}{\partial \theta \partial z} - \left((2\lambda_m + 1) \eta_{13} + \frac{\partial \eta_{23}}{\partial \theta} \right) \frac{\partial \hat{\Phi}_n^{(i)}}{\partial z} - 2g_{23} \frac{\partial^2 \hat{\Psi}_n^{(i)}}{\partial \theta \partial z} - \left((2\lambda_m + 1) \right. \\
& \quad \times g_{13} + \frac{\partial g_{23}}{\partial \theta} \left. \right) \frac{\partial \hat{\Psi}_n^{(i)}}{\partial z} \left. \right] + r^{\lambda_m+n} \left(e_{35} \frac{\partial^2 \hat{U}_n^{(i)}}{\partial z^2} + e_{34} \frac{\partial^2 \hat{V}_n^{(i)}}{\partial z^2} + e_{33} \frac{\partial^2 \hat{W}_n^{(i)}}{\partial z^2} - \eta_{33} \frac{\partial^2 \hat{\Phi}_n^{(i)}}{\partial z^2} \right. \\
& \quad \left. - g_{33} \frac{\partial^2 \hat{\Psi}_n^{(i)}}{\partial z^2} \right) \left. \right\} = 0, \tag{4.2d}
\end{aligned}$$

$$\begin{aligned}
& \sum_{m=1}^{\infty} \sum_{n=0}^{\infty} \left\{ r^{\lambda_m+n-2} \left[\left(\lambda_m \left(\lambda_m d_{11} + d_{12} + \frac{\partial d_{21}}{\partial \theta} \right) + \frac{\partial d_{22}}{\partial \theta} \right) \hat{U}_n^{(i)} + \left(d_{22} + \lambda_m (d_{16} + d_{21}) + \frac{\partial d_{26}}{\partial \theta} \right) \right. \right. \\
& \quad \times \frac{\partial \hat{U}_n^{(i)}}{\partial \theta} + d_{26} \frac{\partial^2 \hat{U}_n^{(i)}}{\partial \theta^2} + (\lambda_m - 1) \left(\lambda_m d_{16} + \frac{\partial d_{26}}{\partial \theta} \right) \hat{V}_n^{(i)} + \left(\lambda_m d_{12} + (\lambda_m - 1) d_{26} + \frac{\partial d_{22}}{\partial \theta} \right) \\
& \quad \times \frac{\partial \hat{V}_n^{(i)}}{\partial \theta} + d_{22} \frac{\partial^2 \hat{V}_n^{(i)}}{\partial \theta^2} + \lambda_m \left(\lambda_m d_{15} + \frac{\partial d_{25}}{\partial \theta} \right) \hat{W}_n^{(i)} + \left(\lambda_m (d_{14} + d_{25}) + \frac{\partial d_{24}}{\partial \theta} \right) \frac{\partial \hat{W}_n^{(i)}}{\partial \theta} + d_{24} \\
& \quad \times \frac{\partial^2 \hat{W}_n^{(i)}}{\partial \theta^2} - \lambda_m \left(\lambda_m g_{11} + \frac{\partial g_{12}}{\partial \theta} \right) \hat{\Phi}_n^{(i)} - \left(2\lambda_m g_{12} + \frac{\partial g_{22}}{\partial \theta} \right) \frac{\partial \hat{\Phi}_n^{(i)}}{\partial \theta} - g_{22} \frac{\partial^2 \hat{\Phi}_n^{(i)}}{\partial \theta^2} - \lambda_m \\
& \quad \times \left(\lambda_m \mu_{11} + \frac{\partial \mu_{12}}{\partial \theta} \right) \hat{\Psi}_n^{(i)} - \left(2\lambda_m \mu_{12} + \frac{\partial \mu_{22}}{\partial \theta} \right) \frac{\partial \hat{\Psi}_n^{(i)}}{\partial \theta} - \mu_{22} \frac{\partial^2 \hat{\Psi}_n^{(i)}}{\partial \theta^2} \left. \right] + r^{\lambda_m+n-1} \left[\left(d_{25} + d_{36} \right) \right. \\
& \quad \times \frac{\partial^2 \hat{U}_n^{(i)}}{\partial \theta \partial z} + \left((\lambda_m + 1) d_{15} + \lambda_m d_{31} + d_{32} + \frac{\partial d_{25}}{\partial \theta} \right) \frac{\partial \hat{U}_n^{(i)}}{\partial z} + (d_{24} + d_{32}) \frac{\partial^2 \hat{V}_n^{(i)}}{\partial \theta \partial z} + \left((\lambda_m - 1) \right. \\
& \quad \times d_{36} + (\lambda_m + 1) d_{14} + \frac{\partial d_{24}}{\partial \theta} \left. \right) \frac{\partial \hat{V}_n^{(i)}}{\partial z} + (d_{23} + d_{34}) \frac{\partial^2 \hat{W}_n^{(i)}}{\partial \theta \partial z} + \left((\lambda_m + 1) d_{13} + \lambda_m d_{35} + \frac{\partial d_{23}}{\partial \theta} \right) \\
& \quad \times \frac{\partial \hat{W}_n^{(i)}}{\partial z} - 2g_{23} \frac{\partial^2 \hat{\Phi}_n^{(i)}}{\partial \theta \partial z} - \left((2\lambda_m + 1) g_{13} + \frac{\partial g_{23}}{\partial \theta} \right) \frac{\partial \hat{\Phi}_n^{(i)}}{\partial z} - 2\mu_{23} \frac{\partial^2 \hat{\Psi}_n^{(i)}}{\partial \theta \partial z} - \left((2\lambda_m + 1) \right. \\
& \quad \times \mu_{13} + \frac{\partial \mu_{23}}{\partial \theta} \left. \right) \frac{\partial \hat{\Psi}_n^{(i)}}{\partial z} \left. \right] + r^{\lambda_m+n} \left(d_{35} \frac{\partial^2 \hat{U}_n^{(i)}}{\partial z^2} + d_{34} \frac{\partial^2 \hat{V}_n^{(i)}}{\partial z^2} + d_{33} \frac{\partial^2 \hat{W}_n^{(i)}}{\partial z^2} - g_{33} \frac{\partial^2 \hat{\Phi}_n^{(i)}}{\partial z^2} \right. \\
& \quad \left. - \mu_{33} \frac{\partial^2 \hat{\Psi}_n^{(i)}}{\partial z^2} \right) \left. \right\} = 0 \tag{4.2e}
\end{aligned}$$

為了探討於 $r \rightarrow 0$ 附近的行為，我們僅需考慮式 (4.2) 中 $n=0$ 且 r 為最低階次之項，因此可以重新把式 (4.2) 整理為

$$\begin{aligned}
& \frac{\partial^2 \hat{U}_0^{(i)}}{\partial \theta^2} + p_1(\theta) \frac{\partial \hat{U}_0^{(i)}}{\partial \theta} + p_2(\theta) \hat{U}_0^{(i)} + p_3(\theta) \frac{\partial^2 \hat{V}_0^{(i)}}{\partial \theta^2} + p_4(\theta) \frac{\partial \hat{V}_0^{(i)}}{\partial \theta} + p_5(\theta) \hat{V}_0^{(i)} + p_6(\theta) \frac{\partial^2 \hat{W}_0^{(i)}}{\partial \theta^2} \\
& + p_7(\theta) \frac{\partial \hat{W}_0^{(i)}}{\partial \theta} + p_8(\theta) \hat{W}_0^{(i)} + p_9(\theta) \frac{\partial^2 \hat{\Phi}_0^{(i)}}{\partial \theta^2} + p_{10}(\theta) \frac{\partial \hat{\Phi}_0^{(i)}}{\partial \theta} + p_{11}(\theta) \hat{\Phi}_0^{(i)} + p_{12}(\theta) \frac{\partial^2 \hat{\Psi}_0^{(i)}}{\partial \theta^2} \\
& + p_{13}(\theta) \frac{\partial \hat{\Psi}_0^{(i)}}{\partial \theta} + p_{14}(\theta) \hat{\Psi}_0^{(i)} = 0, \tag{4.3a}
\end{aligned}$$

$$\begin{aligned}
& \frac{\partial^2 \hat{V}_0^{(i)}}{\partial \theta^2} + q_1(\theta) \frac{\partial \hat{V}_0^{(i)}}{\partial \theta} + q_2(\theta) \hat{V}_0^{(i)} + q_3(\theta) \frac{\partial^2 \hat{U}_0^{(i)}}{\partial \theta^2} + q_4(\theta) \frac{\partial \hat{U}_0^{(i)}}{\partial \theta} + q_5(\theta) \hat{U}_0^{(i)} + q_6(\theta) \frac{\partial^2 \hat{W}_0^{(i)}}{\partial \theta^2} \\
& + q_7(\theta) \frac{\partial \hat{W}_0^{(i)}}{\partial \theta} + q_8(\theta) \hat{W}_0^{(i)} + q_9(\theta) \frac{\partial^2 \hat{\Phi}_0^{(i)}}{\partial \theta^2} + q_{10}(\theta) \frac{\partial \hat{\Phi}_0^{(i)}}{\partial \theta} + q_{11}(\theta) \hat{\Phi}_0^{(i)} + q_{12}(\theta) \frac{\partial^2 \hat{\Psi}_0^{(i)}}{\partial \theta^2} \\
& + q_{13}(\theta) \frac{\partial \hat{\Psi}_0^{(i)}}{\partial \theta} + q_{14}(\theta) \hat{\Psi}_0^{(i)} = 0, \tag{4.3b}
\end{aligned}$$

$$\begin{aligned}
& \frac{\partial^2 \hat{W}_0^{(i)}}{\partial \theta^2} + r_1(\theta) \frac{\partial \hat{W}_0^{(i)}}{\partial \theta} + r_2(\theta) \hat{W}_0^{(i)} + r_3(\theta) \frac{\partial^2 \hat{U}_0^{(i)}}{\partial \theta^2} + r_4(\theta) \frac{\partial \hat{U}_0^{(i)}}{\partial \theta} + r_5(\theta) \hat{U}_0^{(i)} + r_6(\theta) \frac{\partial^2 \hat{V}_0^{(i)}}{\partial \theta^2} \\
& + r_7(\theta) \frac{\partial \hat{V}_0^{(i)}}{\partial \theta} + r_8(\theta) \hat{V}_0^{(i)} + r_9(\theta) \frac{\partial^2 \hat{\Phi}_0^{(i)}}{\partial \theta^2} + r_{10}(\theta) \frac{\partial \hat{\Phi}_0^{(i)}}{\partial \theta} + r_{11}(\theta) \hat{\Phi}_0^{(i)} + r_{12}(\theta) \frac{\partial^2 \hat{\Psi}_0^{(i)}}{\partial \theta^2}
\end{aligned}$$

$$+ r_{13}(\theta) \frac{\partial \hat{\Psi}_0^{(i)}}{\partial \theta} + r_{14}(\theta) \hat{\Psi}_0^{(i)} = 0, \quad (4.3c)$$

$$\begin{aligned} & \frac{\partial^2 \hat{\Phi}_0^{(i)}}{\partial \theta^2} + s_1(\theta) \frac{\partial \hat{\Phi}_0^{(i)}}{\partial \theta} + s_2(\theta) \hat{\Phi}_0^{(i)} + s_3(\theta) \frac{\partial^2 \hat{U}_0^{(i)}}{\partial \theta^2} + s_4(\theta) \frac{\partial \hat{U}_0^{(i)}}{\partial \theta} + s_5(\theta) \hat{U}_0^{(i)} + s_6(\theta) \frac{\partial^2 \hat{V}_0^{(i)}}{\partial \theta^2} \\ & + s_7(\theta) \frac{\partial \hat{V}_0^{(i)}}{\partial \theta} + s_8(\theta) \hat{V}_0^{(i)} + s_9(\theta) \frac{\partial^2 \hat{W}_0^{(i)}}{\partial \theta^2} + s_{10}(\theta) \frac{\partial \hat{W}_0^{(i)}}{\partial \theta} + s_{11}(\theta) \hat{W}_0^{(i)} + s_{12}(\theta) \frac{\partial^2 \hat{\Psi}_0^{(i)}}{\partial \theta^2} \\ & + s_{13}(\theta) \frac{\partial \hat{\Psi}_0^{(i)}}{\partial \theta} + s_{14}(\theta) \hat{\Psi}_0^{(i)} = 0, \end{aligned} \quad (4.3d)$$

$$\begin{aligned} & \frac{\partial^2 \hat{\Psi}_0^{(i)}}{\partial \theta^2} + t_1(\theta) \frac{\partial \hat{\Psi}_0^{(i)}}{\partial \theta} + t_2(\theta) \hat{\Psi}_0^{(i)} + t_3(\theta) \frac{\partial^2 \hat{U}_0^{(i)}}{\partial \theta^2} + t_4(\theta) \frac{\partial \hat{U}_0^{(i)}}{\partial \theta} + t_5(\theta) \hat{U}_0^{(i)} + t_6(\theta) \frac{\partial^2 \hat{V}_0^{(i)}}{\partial \theta^2} \\ & + t_7(\theta) \frac{\partial \hat{V}_0^{(i)}}{\partial \theta} + t_8(\theta) \hat{V}_0^{(i)} + t_9(\theta) \frac{\partial^2 \hat{W}_0^{(i)}}{\partial \theta^2} + t_{10}(\theta) \frac{\partial \hat{W}_0^{(i)}}{\partial \theta} + t_{11}(\theta) \hat{W}_0^{(i)} + t_{12}(\theta) \frac{\partial^2 \hat{\Phi}_0^{(i)}}{\partial \theta^2} \\ & + t_{13}(\theta) \frac{\partial \hat{\Phi}_0^{(i)}}{\partial \theta} + t_{14}(\theta) \hat{\Phi}_0^{(i)} = 0, \end{aligned} \quad (4.3e)$$

式 (4.3) 中係數 p_j 、 q_j 、 r_j 、 s_j 與 t_j 詳列於附錄 C。

式 (4.3) 為變係數常微分方程式，該變係數僅與 θ 相關。若欲直接求取式 (4.3) 之閉合解是不可行的。相同於我們對旋轉體分析時的做法，使用級數法以解決因變係數所造成求解之困擾，並且將全域 θ 分割為數個子域，以克服在求取較高精度之解時，對級數法取較多項次而造成數值計算上的困難。

於圖 4.3 中可見全域 θ 已被分割為數個子域，可透過級數法建立每個子域中式 (4.3) 之解，接著利用連續條件串連相鄰子域之解，則可建構全域之通解。當分析問題為多材料之楔形體時，根據此模型建立的規則，只需要將圖 4.4 中 β 與 β_1 範圍內子域之材料係數進行變換，並且配合適當的連續條件即可。因此，於分析多材料楔形體時，此架構為一相當便利之工具。令子域 i 中式 (4.3) 之變係數之泰勒級數展開為

$$\begin{aligned} p_j(\theta) &= \sum_{k=0}^K (\zeta_j)_k^{(i)} (\theta - \bar{\theta}_i)^k, & q_j(\theta) &= \sum_{k=0}^K (\vartheta_j)_k^{(i)} (\theta - \bar{\theta}_i)^k, & r_j(\theta) &= \sum_{k=0}^K (\varsigma_j)_k^{(i)} (\theta - \bar{\theta}_i)^k, \\ s_j(\theta) &= \sum_{k=0}^K (\varphi_j)_k^{(i)} (\theta - \bar{\theta}_i)^k, & t_j(\theta) &= \sum_{k=0}^K (\chi_j)_k^{(i)} (\theta - \bar{\theta}_i)^k, & j &= 1, 2, \dots, 14 \end{aligned} \quad (4.4)$$

此時可將式 (4.3) 之解亦假設為級數之形式

$$\hat{U}_0^{(i)} = \sum_{j=0}^J \hat{A}_j^{(i)} (\theta - \bar{\theta}_i)^j, \quad (4.5a)$$

$$\hat{V}_0^{(i)} = \sum_{j=0}^J \hat{B}_j^{(i)} (\theta - \bar{\theta}_i)^j, \quad (4.5b)$$

$$\hat{W}_0^{(i)} = \sum_{j=0}^J \hat{C}_j^{(i)} (\theta - \bar{\theta}_i)^j, \quad (4.5c)$$

$$\hat{\Phi}_0^{(i)} = \sum_{j=0}^J \hat{D}_j^{(i)} (\theta - \bar{\theta}_i)^j, \quad (4.5d)$$

$$\hat{\Psi}_0^{(i)} = \sum_{j=0}^J \hat{E}_j^{(i)} (\theta - \bar{\theta}_i)^j, \quad (4.5e)$$

接著將式 (4.4) 與 (4.5) 代入式 (4.3) 中，即可得式 (4.5) 中各係數間之遞迴關係式

$$\begin{aligned} & \hat{A}_{j+2}^{(i)} + (\zeta_3)_0^{(i)} \hat{B}_{j+2}^{(i)} + (\zeta_6)_0^{(i)} \hat{C}_{j+2}^{(i)} + (\zeta_9)_0^{(i)} \hat{D}_{j+2}^{(i)} + (\zeta_{12})_0^{(i)} \hat{E}_{j+2}^{(i)} \\ &= \frac{-1}{(j+2)(j+1)} \left\{ \sum_{k=0}^{j-1} \left[(k+2)(k+1) \left((\zeta_3)_{j-k}^{(i)} \hat{B}_{k+2}^{(i)} + (\zeta_6)_{j-k}^{(i)} \hat{C}_{k+2}^{(i)} + (\zeta_9)_{j-k}^{(i)} \hat{D}_{k+2}^{(i)} \right. \right. \right. \\ & \quad \left. \left. \left. + (\zeta_{12})_{j-k}^{(i)} \hat{E}_{k+2}^{(i)} \right) \right] + \sum_{k=0}^j \left[(k+1) \left((\zeta_1)_{j-k}^{(i)} \hat{A}_{k+1}^{(i)} + (\zeta_4)_{j-k}^{(i)} \hat{B}_{k+1}^{(i)} + (\zeta_7)_{j-k}^{(i)} \hat{C}_{k+1}^{(i)} \right. \right. \right. \\ & \quad \left. \left. \left. + (\zeta_{10})_{j-k}^{(i)} \hat{D}_{k+1}^{(i)} + (\zeta_{13})_{j-k}^{(i)} \hat{E}_{k+1}^{(i)} \right) \right] + \left((\zeta_2)_{j-k}^{(i)} \hat{A}_k^{(i)} + (\zeta_5)_{j-k}^{(i)} \hat{B}_k^{(i)} + (\zeta_8)_{j-k}^{(i)} \hat{C}_k^{(i)} \right. \right. \\ & \quad \left. \left. + (\zeta_{11})_{j-k}^{(i)} \hat{D}_k^{(i)} + (\zeta_{14})_{j-k}^{(i)} \hat{E}_k^{(i)} \right) \right] \left. \right\} \quad (4.6a) \end{aligned}$$

$$\begin{aligned} & \hat{B}_{j+2}^{(i)} + (\vartheta_3)_0^{(i)} \hat{A}_{j+2}^{(i)} + (\vartheta_6)_0^{(i)} \hat{C}_{j+2}^{(i)} + (\vartheta_9)_0^{(i)} \hat{D}_{j+2}^{(i)} + (\vartheta_{12})_0^{(i)} \hat{E}_{j+2}^{(i)} \\ &= \frac{-1}{(j+2)(j+1)} \left\{ \sum_{k=0}^{j-1} \left[(k+2)(k+1) \left((\vartheta_3)_{j-k}^{(i)} \hat{A}_{k+2}^{(i)} + (\vartheta_6)_{j-k}^{(i)} \hat{C}_{k+2}^{(i)} + (\vartheta_9)_{j-k}^{(i)} \hat{D}_{k+2}^{(i)} \right. \right. \right. \\ & \quad \left. \left. \left. + (\vartheta_{12})_{j-k}^{(i)} \hat{E}_{k+2}^{(i)} \right) \right] + \sum_{k=0}^j \left[(k+1) \left((\vartheta_1)_{j-k}^{(i)} \hat{B}_{k+1}^{(i)} + (\vartheta_4)_{j-k}^{(i)} \hat{A}_{k+1}^{(i)} + (\vartheta_7)_{j-k}^{(i)} \hat{C}_{k+1}^{(i)} \right. \right. \right. \\ & \quad \left. \left. \left. + (\vartheta_{10})_{j-k}^{(i)} \hat{D}_{k+1}^{(i)} + (\vartheta_{13})_{j-k}^{(i)} \hat{E}_{k+1}^{(i)} \right) \right] + \left((\vartheta_2)_{j-k}^{(i)} \hat{B}_k^{(i)} + (\vartheta_5)_{j-k}^{(i)} \hat{A}_k^{(i)} + (\vartheta_8)_{j-k}^{(i)} \hat{C}_k^{(i)} \right. \right. \\ & \quad \left. \left. + (\vartheta_{11})_{j-k}^{(i)} \hat{D}_k^{(i)} + (\vartheta_{14})_{j-k}^{(i)} \hat{E}_k^{(i)} \right) \right] \left. \right\} \quad (4.6b) \end{aligned}$$

$$\begin{aligned} & \hat{C}_{j+2}^{(i)} + (\varsigma_3)_0^{(i)} \hat{A}_{j+2}^{(i)} + (\varsigma_6)_0^{(i)} \hat{B}_{j+2}^{(i)} + (\varsigma_9)_0^{(i)} \hat{D}_{j+2}^{(i)} + (\varsigma_{12})_0^{(i)} \hat{E}_{j+2}^{(i)} \\ &= \frac{-1}{(j+2)(j+1)} \left\{ \sum_{k=0}^{j-1} \left[(k+2)(k+1) \left((\varsigma_3)_{j-k}^{(i)} \hat{A}_{k+2}^{(i)} + (\varsigma_6)_{j-k}^{(i)} \hat{B}_{k+2}^{(i)} + (\varsigma_9)_{j-k}^{(i)} \hat{D}_{k+2}^{(i)} \right. \right. \right. \\ & \quad \left. \left. \left. + (\varsigma_{12})_{j-k}^{(i)} \hat{E}_{k+2}^{(i)} \right) \right] + \sum_{k=0}^j \left[(k+1) \left((\varsigma_1)_{j-k}^{(i)} \hat{C}_{k+1}^{(i)} + (\varsigma_4)_{j-k}^{(i)} \hat{A}_{k+1}^{(i)} + (\varsigma_7)_{j-k}^{(i)} \hat{B}_{k+1}^{(i)} \right. \right. \right. \\ & \quad \left. \left. \left. + (\varsigma_{10})_{j-k}^{(i)} \hat{D}_{k+1}^{(i)} + (\varsigma_{13})_{j-k}^{(i)} \hat{E}_{k+1}^{(i)} \right) \right] + \left((\varsigma_2)_{j-k}^{(i)} \hat{C}_k^{(i)} + (\varsigma_5)_{j-k}^{(i)} \hat{A}_k^{(i)} + (\varsigma_8)_{j-k}^{(i)} \hat{B}_k^{(i)} \right) \right] \left. \right\} \end{aligned}$$

$$+ (\varsigma_{11})_{j-k}^{(i)} \hat{D}_k^{(i)} + (\varsigma_{14})_{j-k}^{(i)} \hat{E}_k^{(i)} \Big] \Big\} \quad (4.6c)$$

$$\begin{aligned} & \hat{D}_{j+2}^{(i)} + (\varphi_3)_0^{(i)} \hat{A}_{j+2}^{(i)} + (\varphi_6)_0^{(i)} \hat{B}_{j+2}^{(i)} + (\varphi_9)_0^{(i)} \hat{C}_{j+2}^{(i)} + (\varphi_{12})_0^{(i)} \hat{E}_{j+2}^{(i)} \\ &= \frac{-1}{(j+2)(j+1)} \left\{ \sum_{k=0}^{j-1} \left[(k+2)(k+1) \left((\varphi_3)_{j-k}^{(i)} \hat{A}_{k+2}^{(i)} + (\varphi_6)_{j-k}^{(i)} \hat{B}_{k+2}^{(i)} + (\varphi_9)_{j-k}^{(i)} \hat{C}_{k+2}^{(i)} \right. \right. \right. \\ & \quad \left. \left. + (\varphi_{12})_{j-k}^{(i)} \hat{E}_{k+2}^{(i)} \right) \right] + \sum_{k=0}^j \left[(k+1) \left((\varphi_1)_{j-k}^{(i)} \hat{D}_{k+1}^{(i)} + (\varphi_4)_{j-k}^{(i)} \hat{A}_{k+1}^{(i)} + (\varphi_7)_{j-k}^{(i)} \hat{B}_{k+1}^{(i)} \right. \right. \\ & \quad \left. \left. + (\varphi_{10})_{j-k}^{(i)} \hat{C}_{k+1}^{(i)} + (\varphi_{13})_{j-k}^{(i)} \hat{E}_{k+1}^{(i)} \right) \right] + \left((\varphi_2)_{j-k}^{(i)} \hat{D}_k^{(i)} + (\varphi_5)_{j-k}^{(i)} \hat{A}_k^{(i)} + (\varphi_8)_{j-k}^{(i)} \hat{B}_k^{(i)} \right. \\ & \quad \left. + (\varphi_{11})_{j-k}^{(i)} \hat{C}_k^{(i)} + (\varphi_{14})_{j-k}^{(i)} \hat{E}_k^{(i)} \right) \Big\} \quad (4.6d) \end{aligned}$$

$$\begin{aligned} & \hat{E}_{j+2}^{(i)} + (\chi_3)_0^{(i)} \hat{A}_{j+2}^{(i)} + (\chi_6)_0^{(i)} \hat{B}_{j+2}^{(i)} + (\chi_9)_0^{(i)} \hat{C}_{j+2}^{(i)} + (\chi_{12})_0^{(i)} \hat{D}_{j+2}^{(i)} \\ &= \frac{-1}{(j+2)(j+1)} \left\{ \sum_{k=0}^{j-1} \left[(k+2)(k+1) \left((\chi_3)_{j-k}^{(i)} \hat{A}_{k+2}^{(i)} + (\chi_6)_{j-k}^{(i)} \hat{B}_{k+2}^{(i)} + (\chi_9)_{j-k}^{(i)} \hat{C}_{k+2}^{(i)} \right. \right. \right. \\ & \quad \left. \left. + (\chi_{12})_{j-k}^{(i)} \hat{D}_{k+2}^{(i)} \right) \right] + \sum_{k=0}^j \left[(k+1) \left((\chi_1)_{j-k}^{(i)} \hat{E}_{k+1}^{(i)} + (\chi_4)_{j-k}^{(i)} \hat{A}_{k+1}^{(i)} + (\chi_7)_{j-k}^{(i)} \hat{B}_{k+1}^{(i)} \right. \right. \\ & \quad \left. \left. + (\chi_{10})_{j-k}^{(i)} \hat{C}_{k+1}^{(i)} + (\chi_{13})_{j-k}^{(i)} \hat{D}_{k+1}^{(i)} \right) \right] + \left((\chi_2)_{j-k}^{(i)} \hat{E}_k^{(i)} + (\chi_5)_{j-k}^{(i)} \hat{A}_k^{(i)} + (\chi_8)_{j-k}^{(i)} \hat{B}_k^{(i)} \right. \\ & \quad \left. + (\chi_{11})_{j-k}^{(i)} \hat{C}_k^{(i)} + (\chi_{14})_{j-k}^{(i)} \hat{D}_k^{(i)} \right) \Big\} \quad (4.6e) \end{aligned}$$

因此子域 i 之漸近解可簡單表示為

$$\begin{aligned} \hat{U}_0^{(i)}(\theta) &= \hat{A}_0^{(i)} \hat{U}_{00}^{(i)}(\theta) + \hat{A}_1^{(i)} \hat{U}_{01}^{(i)}(\theta) + \hat{B}_0^{(i)} \hat{U}_{02}^{(i)}(\theta) + \hat{B}_1^{(i)} \hat{U}_{03}^{(i)}(\theta) + \hat{C}_0^{(i)} \hat{U}_{04}^{(i)}(\theta) + \hat{C}_1^{(i)} \hat{U}_{05}^{(i)}(\theta) \\ & \quad + \hat{D}_0^{(i)} \hat{U}_{06}^{(i)}(\theta) + \hat{D}_1^{(i)} \hat{U}_{07}^{(i)}(\theta) + \hat{E}_0^{(i)} \hat{U}_{08}^{(i)}(\theta) + \hat{E}_1^{(i)} \hat{U}_{09}^{(i)}(\theta) \quad (4.7a) \end{aligned}$$

$$\begin{aligned} \hat{V}_0^{(i)}(\theta) &= \hat{A}_0^{(i)} \hat{V}_{00}^{(i)}(\theta) + \hat{A}_1^{(i)} \hat{V}_{01}^{(i)}(\theta) + \hat{B}_0^{(i)} \hat{V}_{02}^{(i)}(\theta) + \hat{B}_1^{(i)} \hat{V}_{03}^{(i)}(\theta) + \hat{C}_0^{(i)} \hat{V}_{04}^{(i)}(\theta) + \hat{C}_1^{(i)} \hat{V}_{05}^{(i)}(\theta) \\ & \quad + \hat{D}_0^{(i)} \hat{V}_{06}^{(i)}(\theta) + \hat{D}_1^{(i)} \hat{V}_{07}^{(i)}(\theta) + \hat{E}_0^{(i)} \hat{V}_{08}^{(i)}(\theta) + \hat{E}_1^{(i)} \hat{V}_{09}^{(i)}(\theta) \quad (4.7b) \end{aligned}$$

$$\begin{aligned} \hat{W}_0^{(i)}(\theta) &= \hat{A}_0^{(i)} \hat{W}_{00}^{(i)}(\theta) + \hat{A}_1^{(i)} \hat{W}_{01}^{(i)}(\theta) + \hat{B}_0^{(i)} \hat{W}_{02}^{(i)}(\theta) + \hat{B}_1^{(i)} \hat{W}_{03}^{(i)}(\theta) + \hat{C}_0^{(i)} \hat{W}_{04}^{(i)}(\theta) + \hat{C}_1^{(i)} \hat{W}_{05}^{(i)}(\theta) \\ & \quad + \hat{D}_0^{(i)} \hat{W}_{06}^{(i)}(\theta) + \hat{D}_1^{(i)} \hat{W}_{07}^{(i)}(\theta) + \hat{E}_0^{(i)} \hat{W}_{08}^{(i)}(\theta) + \hat{E}_1^{(i)} \hat{W}_{09}^{(i)}(\theta) \quad (4.7c) \end{aligned}$$

$$\begin{aligned} \hat{\Phi}_0^{(i)}(\theta) &= \hat{A}_0^{(i)} \hat{\Phi}_{00}^{(i)}(\theta) + \hat{A}_1^{(i)} \hat{\Phi}_{01}^{(i)}(\theta) + \hat{B}_0^{(i)} \hat{\Phi}_{02}^{(i)}(\theta) + \hat{B}_1^{(i)} \hat{\Phi}_{03}^{(i)}(\theta) + \hat{C}_0^{(i)} \hat{\Phi}_{04}^{(i)}(\theta) + \hat{C}_1^{(i)} \hat{\Phi}_{05}^{(i)}(\theta) \\ & \quad + \hat{D}_0^{(i)} \hat{\Phi}_{06}^{(i)}(\theta) + \hat{D}_1^{(i)} \hat{\Phi}_{07}^{(i)}(\theta) + \hat{E}_0^{(i)} \hat{\Phi}_{08}^{(i)}(\theta) + \hat{E}_1^{(i)} \hat{\Phi}_{09}^{(i)}(\theta) \quad (4.7d) \end{aligned}$$

$$\begin{aligned}\hat{\Psi}_0^{(i)}(\theta) = & \hat{A}_0^{(i)}\hat{\Psi}_{00}^{(i)}(\theta) + \hat{A}_1^{(i)}\hat{\Psi}_{01}^{(i)}(\theta) + \hat{B}_0^{(i)}\hat{\Psi}_{02}^{(i)}(\theta) + \hat{B}_1^{(i)}\hat{\Psi}_{03}^{(i)}(\theta) + \hat{C}_0^{(i)}\hat{\Psi}_{04}^{(i)}(\theta) + \hat{C}_1^{(i)}\hat{\Psi}_{05}^{(i)}(\theta) \\ & + \hat{D}_0^{(i)}\hat{\Psi}_{06}^{(i)}(\theta) + \hat{D}_1^{(i)}\hat{\Psi}_{07}^{(i)}(\theta) + \hat{E}_0^{(i)}\hat{\Psi}_{08}^{(i)}(\theta) + \hat{E}_1^{(i)}\hat{\Psi}_{09}^{(i)}(\theta)\end{aligned}\quad (4.7e)$$

4.2 電磁彈性楔形體之邊界條件與連續條件

為了便於數值上的計算，如圖 4.3 將楔形體全域 θ 分割為 n 個子域，子域 i 中分別產生係數 $\hat{A}_0^{(i)}$ 、 $\hat{A}_1^{(i)}$ 、 $\hat{B}_0^{(i)}$ 、 $\hat{B}_1^{(i)}$ 、 $\hat{C}_0^{(i)}$ 、 $\hat{C}_1^{(i)}$ 、 $\hat{D}_0^{(i)}$ 、 $\hat{D}_1^{(i)}$ 、 $\hat{E}_0^{(i)}$ 與 $\hat{E}_1^{(i)}$ ，因此全域共有 $10n$ 個待定之係數。而相鄰子域間須透過以下之連續條件相互連結

$$\sigma_{\theta\theta}^{(i)}(r, \theta_i, Z) = \sigma_{\theta\theta}^{(i+1)}(r, \theta_i, Z), \quad (4.8a)$$

$$\sigma_{z\theta}^{(i)}(r, \theta_i, Z) = \sigma_{z\theta}^{(i+1)}(r, \theta_i, Z), \quad (4.8b)$$

$$\sigma_{r\theta}^{(i)}(r, \theta_i, Z) = \sigma_{r\theta}^{(i+1)}(r, \theta_i, Z), \quad (4.8c)$$

$$D_\theta^{(i)}(r, \theta_i, Z) = D_\theta^{(i+1)}(r, \theta_i, Z), \quad (4.8d)$$

$$B_\theta^{(i)}(r, \theta_i, Z) = B_\theta^{(i+1)}(r, \theta_i, Z), \quad (4.8e)$$

$$u_r^{(i)}(r, \theta_i, Z) = u_r^{(i+1)}(r, \theta_i, Z), \quad (4.8f)$$

$$u_\theta^{(i)}(r, \theta_i, Z) = u_\theta^{(i+1)}(r, \theta_i, Z), \quad (4.8g)$$

$$u_z^{(i)}(r, \theta_i, Z) = u_z^{(i+1)}(r, \theta_i, Z), \quad (4.8h)$$

$$\phi^{(i)}(r, \theta_i, Z) = \phi^{(i+1)}(r, \theta_i, Z), \quad (4.8i)$$

$$\psi^{(i)}(r, \theta_i, Z) = \psi^{(i+1)}(r, \theta_i, Z), \quad (4.8j)$$

上式中上標 i 表示於子域 i 中之物理量， $i = 1, 2, \dots, n-1$ ，因此式 (4.8) 總共有 $10(n-1)$ 條方程式。另外，還需滿足於 $\theta = \theta_0$ 與 $\theta = \theta_n$ 之電磁彈邊界條件，共有 10 條方程式。邊界條件可表示如下：

自由端 (traction free conditions)

$$\sigma_{\theta\theta}^{(k)} = \sigma_{z\theta}^{(k)} = \sigma_{r\theta}^{(k)} = 0, \quad (4.9a)$$

固定端 (clamped conditions)

$$u_r^{(k)} = u_z^{(k)} = u_\theta^{(k)} = 0 \quad (4.9b)$$

電磁開路 (electrically and magnetically open conditions)

$$\begin{aligned} D_\theta^{(k)} &= 0 \\ B_\theta^{(k)} &= 0 \end{aligned} \quad (4.9c)$$

電磁閉路 (electrically and magnetically closed conditions)

$$\begin{aligned} \phi^{(k)} &= 0 \\ \psi^{(k)} &= 0 \end{aligned} \quad (4.9d)$$

當 $k=1$ 與 n 時為分別考慮為邊界 $\theta=\theta_0$ 及 $\theta=\theta_n$ 之邊界條件。

因此前述的 $10n$ 個待定之係數可透過由邊界條件及連續條件所組成的 $10n$ 條齊性方程式來決定。同第二章對旋轉體問題的處理，可透過建立 $10n \times 10n$ 矩陣，使矩陣行列式值為零以求其非零解 (nontrivial solution)。

4.3 壓電楔形體於尖角處之漸近解

此節討論的問題為壓電楔形體，如同 2.5 節做法將式 (2.1) 中有關於磁性相關之材料性質省略進行分析即可，省略的材料係數為壓磁係數 $[d]$ 、電磁耦合係數 $[g]$ 與磁導係數 $[\mu]$ 。同樣的推導方式，可得四條類似於式 (4.3) 之變係數常微分方程式

$$\begin{aligned} \frac{\partial^2 \hat{U}_0^{(i)}}{\partial \theta^2} + p_1(\theta) \frac{\partial \hat{U}_0^{(i)}}{\partial \theta} + p_2(\theta) \hat{U}_0^{(i)} + p_3(\theta) \frac{\partial^2 \hat{V}_0^{(i)}}{\partial \theta^2} + p_4(\theta) \frac{\partial \hat{V}_0^{(i)}}{\partial \theta} + p_5(\theta) \hat{V}_0^{(i)} + p_6(\theta) \frac{\partial^2 \hat{W}_0^{(i)}}{\partial \theta^2} \\ + p_7(\theta) \frac{\partial \hat{W}_0^{(i)}}{\partial \theta} + p_8(\theta) \hat{W}_0^{(i)} + p_9(\theta) \frac{\partial^2 \hat{\Phi}_0^{(i)}}{\partial \theta^2} + p_{10}(\theta) \frac{\partial \hat{\Phi}_0^{(i)}}{\partial \theta} + p_{11}(\theta) \hat{\Phi}_0^{(i)} = 0, \end{aligned} \quad (4.10a)$$

$$\begin{aligned} \frac{\partial^2 \hat{V}_0^{(i)}}{\partial \theta^2} + q_1(\theta) \frac{\partial \hat{V}_0^{(i)}}{\partial \theta} + q_2(\theta) \hat{V}_0^{(i)} + q_3(\theta) \frac{\partial^2 \hat{U}_0^{(i)}}{\partial \theta^2} + q_4(\theta) \frac{\partial \hat{U}_0^{(i)}}{\partial \theta} + q_5(\theta) \hat{U}_0^{(i)} + q_6(\theta) \frac{\partial^2 \hat{W}_0^{(i)}}{\partial \theta^2} \\ + q_7(\theta) \frac{\partial \hat{W}_0^{(i)}}{\partial \theta} + q_8(\theta) \hat{W}_0^{(i)} + q_9(\theta) \frac{\partial^2 \hat{\Phi}_0^{(i)}}{\partial \theta^2} + q_{10}(\theta) \frac{\partial \hat{\Phi}_0^{(i)}}{\partial \theta} + q_{11}(\theta) \hat{\Phi}_0^{(i)} = 0, \end{aligned} \quad (4.10b)$$

$$\frac{\partial^2 \hat{W}_0^{(i)}}{\partial \theta^2} + r_1(\theta) \frac{\partial \hat{W}_0^{(i)}}{\partial \theta} + r_2(\theta) \hat{W}_0^{(i)} + r_3(\theta) \frac{\partial^2 \hat{U}_0^{(i)}}{\partial \theta^2} + r_4(\theta) \frac{\partial \hat{U}_0^{(i)}}{\partial \theta} + r_5(\theta) \hat{U}_0^{(i)} + r_6(\theta) \frac{\partial^2 \hat{V}_0^{(i)}}{\partial \theta^2}$$

$$+ r_7(\theta) \frac{\partial \hat{V}_0^{(i)}}{\partial \theta} + r_8(\theta) \hat{V}_0^{(i)} + r_9(\theta) \frac{\partial^2 \hat{\Phi}_0^{(i)}}{\partial \theta^2} + r_{10}(\theta) \frac{\partial \hat{\Phi}_0^{(i)}}{\partial \theta} + r_{11}(\theta) \hat{\Phi}_0^{(i)} = 0, \quad (4.10c)$$

$$\begin{aligned} & \frac{\partial^2 \hat{\Phi}_0^{(i)}}{\partial \theta^2} + s_1(\theta) \frac{\partial \hat{\Phi}_0^{(i)}}{\partial \theta} + s_2(\theta) \hat{\Phi}_0^{(i)} + s_3(\theta) \frac{\partial^2 \hat{U}_0^{(i)}}{\partial \theta^2} + s_4(\theta) \frac{\partial \hat{U}_0^{(i)}}{\partial \theta} + s_5(\theta) \hat{U}_0^{(i)} + s_6(\theta) \frac{\partial^2 \hat{V}_0^{(i)}}{\partial \theta^2} \\ & + s_7(\theta) \frac{\partial \hat{V}_0^{(i)}}{\partial \theta} + s_8(\theta) \hat{V}_0^{(i)} + s_9(\theta) \frac{\partial^2 \hat{W}_0^{(i)}}{\partial \theta^2} + s_{10}(\theta) \frac{\partial \hat{W}_0^{(i)}}{\partial \theta} + s_{11}(\theta) \hat{W}_0^{(i)} = 0 \end{aligned} \quad (4.10d)$$

如同式 (4.4) 及 (4.5) 之級數展開，可得係數間之遞迴關係如下

$$\begin{aligned} & \hat{A}_{j+2}^{(i)} + (\zeta_3)_0^{(i)} \hat{B}_{j+2}^{(i)} + (\zeta_6)_0^{(i)} \hat{C}_{j+2}^{(i)} + (\zeta_9)_0^{(i)} \hat{D}_{j+2}^{(i)} \\ & = \frac{-1}{(j+2)(j+1)} \left\{ \sum_{k=0}^{j-1} \left[(k+2)(k+1) \left((\zeta_3)_{j-k}^{(i)} \hat{B}_{k+2}^{(i)} + (\zeta_6)_{j-k}^{(i)} \hat{C}_{k+2}^{(i)} + (\zeta_9)_{j-k}^{(i)} \hat{D}_{k+2}^{(i)} \right) \right] \right. \\ & + \sum_{k=0}^j \left[(k+1) \left((\zeta_1)_{j-k}^{(i)} \hat{A}_{k+1}^{(i)} + (\zeta_4)_{j-k}^{(i)} \hat{B}_{k+1}^{(i)} + (\zeta_7)_{j-k}^{(i)} \hat{C}_{k+1}^{(i)} + (\zeta_{10})_{j-k}^{(i)} \hat{D}_{k+1}^{(i)} \right) \right. \\ & \left. \left. + (\zeta_2)_{j-k}^{(i)} \hat{A}_k^{(i)} + (\zeta_5)_{j-k}^{(i)} \hat{B}_k^{(i)} + (\zeta_8)_{j-k}^{(i)} \hat{C}_k^{(i)} + (\zeta_{11})_{j-k}^{(i)} \hat{D}_k^{(i)} \right] \right\} \end{aligned} \quad (4.11a)$$

$$\begin{aligned} & \hat{B}_{j+2}^{(i)} + (\vartheta_3)_0^{(i)} \hat{A}_{j+2}^{(i)} + (\vartheta_6)_0^{(i)} \hat{C}_{j+2}^{(i)} + (\vartheta_9)_0^{(i)} \hat{D}_{j+2}^{(i)} \\ & = \frac{-1}{(j+2)(j+1)} \left\{ \sum_{k=0}^{j-1} \left[(k+2)(k+1) \left((\vartheta_3)_{j-k}^{(i)} \hat{A}_{k+2}^{(i)} + (\vartheta_6)_{j-k}^{(i)} \hat{C}_{k+2}^{(i)} + (\vartheta_9)_{j-k}^{(i)} \hat{D}_{k+2}^{(i)} \right) \right] \right. \\ & + \sum_{k=0}^j \left[(k+1) \left((\vartheta_1)_{j-k}^{(i)} \hat{B}_{k+1}^{(i)} + (\vartheta_4)_{j-k}^{(i)} \hat{A}_{k+1}^{(i)} + (\vartheta_7)_{j-k}^{(i)} \hat{C}_{k+1}^{(i)} + (\vartheta_{10})_{j-k}^{(i)} \hat{D}_{k+1}^{(i)} \right) \right. \\ & \left. \left. + (\vartheta_2)_{j-k}^{(i)} \hat{B}_k^{(i)} + (\vartheta_5)_{j-k}^{(i)} \hat{A}_k^{(i)} + (\vartheta_8)_{j-k}^{(i)} \hat{C}_k^{(i)} + (\vartheta_{11})_{j-k}^{(i)} \hat{D}_k^{(i)} \right] \right\} \end{aligned} \quad (4.11b)$$

$$\begin{aligned} & \hat{C}_{j+2}^{(i)} + (\varsigma_3)_0^{(i)} \hat{A}_{j+2}^{(i)} + (\varsigma_6)_0^{(i)} \hat{B}_{j+2}^{(i)} + (\varsigma_9)_0^{(i)} \hat{D}_{j+2}^{(i)} \\ & = \frac{-1}{(j+2)(j+1)} \left\{ \sum_{k=0}^{j-1} \left[(k+2)(k+1) \left((\varsigma_3)_{j-k}^{(i)} \hat{A}_{k+2}^{(i)} + (\varsigma_6)_{j-k}^{(i)} \hat{B}_{k+2}^{(i)} + (\varsigma_9)_{j-k}^{(i)} \hat{D}_{k+2}^{(i)} \right) \right] \right. \\ & + \sum_{k=0}^j \left[(k+1) \left((\varsigma_1)_{j-k}^{(i)} \hat{C}_{k+1}^{(i)} + (\varsigma_4)_{j-k}^{(i)} \hat{A}_{k+1}^{(i)} + (\varsigma_7)_{j-k}^{(i)} \hat{B}_{k+1}^{(i)} + (\varsigma_{10})_{j-k}^{(i)} \hat{D}_{k+1}^{(i)} \right) \right. \\ & \left. \left. + (\varsigma_2)_{j-k}^{(i)} \hat{C}_k^{(i)} + (\varsigma_5)_{j-k}^{(i)} \hat{A}_k^{(i)} + (\varsigma_8)_{j-k}^{(i)} \hat{B}_k^{(i)} + (\varsigma_{11})_{j-k}^{(i)} \hat{D}_k^{(i)} \right] \right\} \end{aligned} \quad (4.11c)$$

$$\begin{aligned} & \hat{D}_{j+2}^{(i)} + (\varphi_3)_0^{(i)} \hat{A}_{j+2}^{(i)} + (\varphi_6)_0^{(i)} \hat{B}_{j+2}^{(i)} + (\varphi_9)_0^{(i)} \hat{C}_{j+2}^{(i)} \\ & = \frac{-1}{(j+2)(j+1)} \left\{ \sum_{k=0}^{j-1} \left[(k+2)(k+1) \left((\varphi_3)_{j-k}^{(i)} \hat{A}_{k+2}^{(i)} + (\varphi_6)_{j-k}^{(i)} \hat{B}_{k+2}^{(i)} + (\varphi_9)_{j-k}^{(i)} \hat{C}_{k+2}^{(i)} \right) \right] \right\} \end{aligned}$$

$$\begin{aligned}
& + \sum_{k=0}^j \left[(k+1) \left((\varphi_1)_{j-k}^{(i)} \hat{D}_{k+1}^{(i)} + (\varphi_4)_{j-k}^{(i)} \hat{A}_{k+1}^{(i)} + (\varphi_7)_{j-k}^{(i)} \hat{B}_{k+1}^{(i)} + (\varphi_{10})_{j-k}^{(i)} \hat{C}_{k+1}^{(i)} \right) \right. \\
& \left. + (\varphi_2)_{j-k}^{(i)} \hat{D}_k^{(i)} + (\varphi_5)_{j-k}^{(i)} \hat{A}_k^{(i)} + (\varphi_8)_{j-k}^{(i)} \hat{B}_k^{(i)} + (\varphi_{11})_{j-k}^{(i)} \hat{C}_k^{(i)} \right] \} \quad (4.11d)
\end{aligned}$$

子域 i 之漸近解可簡單表示為

$$\begin{aligned}
\hat{U}_0^{(i)}(\theta) &= \hat{A}_0^{(i)} \hat{U}_{00}^{(i)}(\theta) + \hat{A}_1^{(i)} \hat{U}_{01}^{(i)}(\theta) + \hat{B}_0^{(i)} \hat{U}_{02}^{(i)}(\theta) + \hat{B}_1^{(i)} \hat{U}_{03}^{(i)}(\theta) + \hat{C}_0^{(i)} \hat{U}_{04}^{(i)}(\theta) + \hat{C}_1^{(i)} \hat{U}_{05}^{(i)}(\theta) \\
&+ \hat{D}_0^{(i)} \hat{U}_{06}^{(i)}(\theta) + \hat{D}_1^{(i)} \hat{U}_{07}^{(i)}(\theta) \quad (4.12a)
\end{aligned}$$

$$\begin{aligned}
\hat{V}_0^{(i)}(\theta) &= \hat{A}_0^{(i)} \hat{V}_{00}^{(i)}(\theta) + \hat{A}_1^{(i)} \hat{V}_{01}^{(i)}(\theta) + \hat{B}_0^{(i)} \hat{V}_{02}^{(i)}(\theta) + \hat{B}_1^{(i)} \hat{V}_{03}^{(i)}(\theta) + \hat{C}_0^{(i)} \hat{V}_{04}^{(i)}(\theta) + \hat{C}_1^{(i)} \hat{V}_{05}^{(i)}(\theta) \\
&+ \hat{D}_0^{(i)} \hat{V}_{06}^{(i)}(\theta) + \hat{D}_1^{(i)} \hat{V}_{07}^{(i)}(\theta) \quad (4.12b)
\end{aligned}$$

$$\begin{aligned}
\hat{W}_0^{(i)}(\theta) &= \hat{A}_0^{(i)} \hat{W}_{00}^{(i)}(\theta) + \hat{A}_1^{(i)} \hat{W}_{01}^{(i)}(\theta) + \hat{B}_0^{(i)} \hat{W}_{02}^{(i)}(\theta) + \hat{B}_1^{(i)} \hat{W}_{03}^{(i)}(\theta) + \hat{C}_0^{(i)} \hat{W}_{04}^{(i)}(\theta) + \hat{C}_1^{(i)} \hat{W}_{05}^{(i)}(\theta) \\
&+ \hat{D}_0^{(i)} \hat{W}_{06}^{(i)}(\theta) + \hat{D}_1^{(i)} \hat{W}_{07}^{(i)}(\theta) \quad (4.12c)
\end{aligned}$$

$$\begin{aligned}
\hat{\Phi}_0^{(i)}(\theta) &= \hat{A}_0^{(i)} \hat{\Phi}_{00}^{(i)}(\theta) + \hat{A}_1^{(i)} \hat{\Phi}_{01}^{(i)}(\theta) + \hat{B}_0^{(i)} \hat{\Phi}_{02}^{(i)}(\theta) + \hat{B}_1^{(i)} \hat{\Phi}_{03}^{(i)}(\theta) + \hat{C}_0^{(i)} \hat{\Phi}_{04}^{(i)}(\theta) + \hat{C}_1^{(i)} \hat{\Phi}_{05}^{(i)}(\theta) \\
&+ \hat{D}_0^{(i)} \hat{\Phi}_{06}^{(i)}(\theta) + \hat{D}_1^{(i)} \hat{\Phi}_{07}^{(i)}(\theta) \quad (4.12d)
\end{aligned}$$

4.4 壓電楔形體之邊界條件與連續條件

同 4.2 節的方式，將壓電楔形體全域 θ 切割為 n 個子域，參考式 (4.12) 如此會產生 $8n$ 個待定係數。各子域之間以連續條件相連接可得 $8(n-1)$ 條方程式，其連續條件同於式 (4.8)，由於不考量磁性的部分，因此式 (4.8e) 與式 (4.8j) 可被忽略。尚需 8 條方程式則由 $\theta = \theta_0$ 與 $\theta = \theta_n$ 處之邊界條件構成，可參考式 (4.9) 但同樣省略式 (4.9c) 與 (4.9d) 中有關於磁性的部分。則 $8n$ 個待定係數可透過由連續條件與邊界條件所提供的 $8n$ 條方程式決定之。類似於特徵值得分析，可由 $8n \times 8n$ 矩陣令其行列式值為零以求得 λ_m ，同迴轉體與電磁彈性楔形體之分析，應力與電位移之奇異性階數為 $\text{Re}[\lambda_1]-1$ 。

第五章 電磁彈楔形體奇異性之結果與討論

同第三章為驗證根據前章節所推導之漸近解的正確性及準確性，透過增加子域數或每個子域中級數解之項數以進行最小之電磁彈性奇異性階數之實數部 ($\text{Re}[\lambda_1]$) 的收斂性分析，並與已發表之文獻結果進行比較。考量單一 PZT-4 壓電材料楔形體，並令 PZT-4 擁有側向等向性的特性，其材料性質列於表 3.1 中。

5.1 楔形體奇異性漸近解之驗證

表 5.1 中包含三案例。第一個案例為一裂縫 (參考圖 4.4, $\beta = 90^\circ$ 與 $\beta_1 = 90^\circ$) 之問題，材料之極化方向為 Z 軸 ($\gamma = 0^\circ$, 如圖 4.1)，裂縫表面為 traction free 與 charge free ($\sigma_{\theta\theta} = \sigma_{\theta r} = \sigma_{\theta z} = D_\theta = 0$)。與 Sosa 與 Pak [35] 透過特徵函數展開法分析三維壓電材料裂縫問題所得之結果進行比較，其分析的案例為極化方向為平行 Z 軸之壓電材料之裂縫問題，故於文獻中可推得 λ_m 的閉合解 (closed-form solution)。由本研究所得之數據與其相同至小數點下第四位，如此表示本研究提出之方法的正確性及準確性均可被採信。

另外兩個案例為 180° ($\beta = 90^\circ$ 與 $\beta_1 = 90^\circ$) 與 360° ($\beta = 180^\circ$ 與 $\beta_1 = 180^\circ$) 之楔形體 (幾何形狀參考圖 4.4)，極化方向為平行 $X - Y$ 平面且 $\theta = 180^\circ$ 與 270° ，邊界條件均為 FOCC。表 5.1 中 Hwu 與 Ikeda [33] 的分析結果為基於 $X - Y$ 平面上之廣義平面應變與 short circuit 假設之二維解，其文中令 $\varepsilon_{zz} = 0$ 與 $E_z = 0$ ，藉此忽略 Z 方向分量對於分析中之影響，於是可直接消除材料常數有關於 c_{ij} (i 或 $j = 3$)、 e_{k6} 與 η_{k3} 的項。根據 Hwu 與 Ikeda [33] 的假設所得到的 λ_m 與利用前章推導得之完全一致。透過上述的驗證，可發現於推導初期式 (4.2) 雖均包含對於 Z 的偏微分項，但當進行下一步驟取 r 的最低階次項時關於 Z 的偏微分項全被消除，於是式 (4.3) 與 Z 無關。再者觀察式 (4.3)

的係數 (參考附錄 3) 亦均不見材料 c_{ij} (i 或 $j = 3$)、 e_{k6} 與 η_{k3} 係數。表 5.1 顯示透過增加子域數或增加子域中級數解項數可驅使解收斂，在選取子域數或及數項數時必須仔細拿捏。

5.2 壓電楔形體奇異性結果與討論

以第四章所推導出之漸近解形態，可得電彈性奇異性階數為實數部之 $(\lambda_m - 1)$ 所控制，其中 $\text{Re}[\lambda_m]$ 越小表示奇異性強度越強，因此將針對 $\text{Re}[\lambda_m]$ 之最小根 ($\text{Re}[\lambda_1]$)，當值為 0 與 1 之間時表示奇異性的存在。於本節中將討論於單一材料或雙材料壓電楔形體因材料性質、邊界條件、極化方向與幾何形狀對 $\text{Re}[\lambda_1]$ 的影響。其中考慮的材料有壓電材料 PZT-4 與 PZT-6B 以及彈性材料 Si，材料性質均列於表 3.1。本節所得之數值結果，均基於將全域 θ 分割為 8 個等份子域，每個子域之級數解均採 12 項。

5.2.1 單一壓電材料楔形體

圖 5.1 為單一壓電材料 PZT-4 與 PZT-6B 楔形體，其極化方向 $\gamma = 0^\circ$ 且 $\theta = 0^\circ$ 時，於不同邊界條件之 λ_1 隨楔形體幾何變化之情形。從圖中可發現改變電學邊界條件時，對電彈奇異性僅造成非常微小之影響。觀察圖 5.1(a) 與 (b)，當力學邊界條件為 free-free 時，PZT-6B 楔形體之電彈奇異性較強；當力學邊界條件為 clamped-clamped 時，則為 PZT-4 楔形體導致之電彈奇異性較 PZT-6B 者強。回顧單一壓電材料迴轉體之電彈奇異性隨幾何變化之情形，電學邊界條件的改變亦似乎對電彈奇異性沒有產生任何之影響，因此不論單一壓電材料迴轉體或楔形體，似乎仍以力學邊界條件為控制 λ_1 值主要之關鍵。

圖 5.2 為 $360^\circ (\beta = \beta_1 = 180^\circ)$ 與 $270^\circ (\beta = 90^\circ, \beta_1 = 180^\circ)$ 單一壓電材料楔形體於 $\theta = 0^\circ$ 且不同邊界條件時， λ_1 隨 γ 變化之情形，幾何形狀可參考圖 4.4。很明顯可以發現圖 5.2(a) 與 (c) 中，當 $\beta = 180^\circ$ 時 PZT-4 與 PZT-6B 楔形體之 λ_1 曲線變化形態有很大的不同，例如在圖 5.2(a) 中 PZT-4 楔形體於四種邊界條件下且 $\gamma = 90^\circ$ 時，電彈奇異

性均為最弱；而圖 5.2(c) 為 PZT-6B 楔形體時，除了 FCFC 邊界條件以外，其餘邊界條件下當 $\gamma = 90^\circ$ 時均有最強之電彈奇異性。圖 5.2 (b) 與 (d) 中，當 $\beta = 90^\circ$ 時 λ_1 曲線亦有很不一樣的變化，但基本上類似於圖 5.2 (a) 與 (c) 中 $\gamma = 90^\circ$ 之行為，PZT-6B 楔形體於 $\gamma = 90^\circ$ 時擁有最強之電彈奇異性；PZT-4 楔形體於 $\gamma = 90^\circ$ 之電彈奇異性則為最弱。PZT-6B 楔形體邊界條件為 FOFO 與 CCCC 時之 λ_1 值甚至低於 0.500，表示比一般彈性材料於裂縫的狀態下更加容易產生破壞。另外，圖 5.2 (b) 與 (d) 中發現，FCFC 與 COCO 邊界條件之 λ_1 有類似行為；而 FOFO 與 CCCC 邊界條件較為類似。

圖 5.3 為單一 270° 壓電材料 PZT-4 與 PZT-6B 楔形體 ($\beta = 90^\circ$, $\beta_1 = 180^\circ$) 於不同極化方向且邊界條件為 FOFO 與 COCO 時， $\text{Re}[\lambda_1]$ 隨 θ 變化之情況。觀察圖 5.3(a) 與 (b)，不意外的當 $\gamma = 0^\circ$ 時 $\text{Re}[\lambda_1]$ 曲線為一水平直線，原因為壓電材料之性質被假設為側向等向性材料。另外，從圖 5.3(a) 與 (b) 中可發現當 PZT-4 楔形體且邊界條件為 COCO 時，於 $0^\circ < \theta < 180^\circ$ 範圍中均以 $\gamma = 0^\circ$ 時之奇異性為最強，而 PZT-6B 楔形體則無此現象。於 FOFO 與 COCO 邊界條件下並考量不同之 γ 值均以 $\theta = 90^\circ$ 時擁有最強之奇異性。圖 5.3(a) 與 (b) 中顯示當邊界條件為 FOFO 時，極化方向為 $\gamma = 90^\circ$ (平行於 $X - Y$ 平面) 內且 $\theta = 90^\circ$ 時 (平行於 Y 軸)，擁有最強之電彈奇異性，其中 PZT-4 楔形體之 $\text{Re}[\lambda_1]$ 甚至達 0.384，奇異性之強烈程度更勝於裂縫狀態下之彈性材料 ($\lambda_1 = 0.500$)，為極有可能產生破壞之形態。

5.2.2 雙壓電材料楔形體

圖 5.4 為 PZT-4/PZT-6B 與 PZT-6B/PZT-4 雙壓電楔形體，其極化方向 $\gamma = 0^\circ$ 且於不同邊界條件時之 $\text{Re}[\lambda_1]$ 隨楔形體幾何變化之情形。圖 5.4(a) 中 PZT-4 之 $\beta = 90^\circ$ ，PZT-6B 之 $\beta_1 = 180^\circ$ ；圖 5.4(b) 中 PZT-6B 之 $\beta = 90^\circ$ ，PZT-4 之 $\beta_1 = 180^\circ$ 。觀察圖 5.4(a) 與 (b) 中發現改變電學邊界條件對於雙壓電複合楔形體 $\text{Re}[\lambda_1]$ 曲線變化之影響較單一壓電材料楔形體明顯，如圖 5.4(b) 中，COCO 與 CCCC 邊界條件兩 λ_1 曲線於 $\beta = 64^\circ$ 時有最大差異 3.52%，雖說電學邊界條件之影響稍較單一壓電材料楔形體時

顯著，但該影響仍相當有限。圖 5.4(a) 中 PZT-4 材料之 β 值改變時，於 $\beta < 63^\circ$ 的範圍內且力學邊界條件 clamped-clamped 之電彈奇異性強度大於當力學邊界條件 free-free 時；而圖 5.4(b) 中 PZT-6B 材料之 β 值改變時，其 $\text{Re}[\lambda_1]$ 曲線變化的行為則類似過去經驗中力學邊界條件為 free-free 時有較強之電彈奇異性。

圖 5.5 為雙壓電材料楔形體於 $\theta = 0^\circ$ 且不同邊界條件時， λ_1 隨 γ 變化之情形。圖 5.5(a) 為模擬裂縫狀態， $\beta = \beta_1 = 180^\circ$ ；圖 5.5(b) 為 $\beta = 90^\circ$ 之 PZT-4， $\beta_1 = 180^\circ$ 之 PZT-6B；圖 5.5(c) 為 $\beta = 90^\circ$ 之 PZT-6B， $\beta_1 = 180^\circ$ 之 PZT-4。觀察三圖似乎沒有共同的變化規則，或許是因為極化方向的改變，造成楔形體電彈之耦合效應，使得電彈奇異性產生複雜的變化。圖 5.5(a)、(b) 與 (c) 中 FCFC 邊界條件之 $\text{Re}[\lambda_1]$ 曲線約在 $\gamma = 70^\circ$ 與 114° 附近，產生該邊界條件下較弱之電彈奇異性，於該極化方向時較不易產生破壞。另外，在圖 5.2(b) 之 FCFC 邊界條件與圖 5.2(c) 之 COCO 邊界條件 $\text{Re}[\lambda_1]$ 值均出現約達 0.700，該電彈奇異性強度較弱，因此在精密元件設計上為可考量之範圍。

圖 5.6 為雙壓電材料楔形體於不同極化方向且邊界條件為 FOFO 與 COCO 時， $\text{Re}[\lambda_1]$ 隨 θ 變化之情況。圖 5.6(a) 中 PZT-4 之 $\beta = 90^\circ$ ，PZT-6B 之 $\beta_1 = 180^\circ$ ；圖 5.6(b) 中 PZT-6B 之 $\beta = 90^\circ$ ，PZT-4 之 $\beta_1 = 180^\circ$ 。觀察圖 5.6(a) 與 (b) 中邊界條件為 FOFO 時，兩圖之 $\text{Re}[\lambda_1]$ 隨 θ 變化的行為相類似。當 $\gamma = 0^\circ$ 時，圖 5.6(b) 中 PZT-6B/PZT-4 楔形體擁有較強之電彈奇異性。另外，於 $\gamma = 45^\circ$ 與 90° 之情況下，圖 5.6(a) 中之 $\text{Re}[\lambda_1]$ 曲線變化幅度相較圖 5.6(b) 者大；而當邊界條件為 COCO 時，圖 5.6(a) 中三 γ 值之 $\text{Re}[\lambda_1]$ 曲線則顯示出較圖 5.6(b) 強烈之電彈奇異性。其餘較為特別的是從圖 5.6(a) 與 (b) 中可發現各曲線中發生最強奇異性的位至發生於 $\beta > 90^\circ$ ，該原因為何目前尚無法明瞭，於此只能推測因兩種不同的壓電材料組合造成複雜的電彈耦合效應以致於電彈奇異性會產生特殊的變化。

5.2.3 壓電/彈性材料 Si 楔形體

圖 5.7 為 PZT-4/Si 與 PZT-6B/Si 楔形體，其極化方向 $\gamma = 0^\circ$ 且 $\theta = 0^\circ$ ，於不同邊界條件之 $\text{Re}[\lambda_1]$ 隨楔形體幾何變化之情形。其中 PZT-4 與 PZT-6B 之幾何形狀為 β ；Si 之 $\beta_1 = 180^\circ$ 。圖 5.7(a) 中 PZT-4/Si 楔形體之 β 改變時，其結果不如以往經驗中力學邊界條件為 free-free 時總擁有較強之電彈奇異性，反而於 $\beta < 63^\circ$ 的範圍內力學邊界條件為 clamped-clamped 較強；另外，在力學邊界條件為 clamped-clamped 之 $\text{Re}[\lambda_1]$ 曲線產生折角於 $\beta = 128^\circ$ ，當 $\beta > 128^\circ$ 時 λ_1 為複數。圖 5.7(b) 之 $\text{Re}[\lambda_1]$ 曲線並無特殊之變化，符合前述當邊界條件為 free-free 時有較強之電彈奇異性之經驗，單純改變電學邊界條件似乎不會影響電彈奇異性。

圖 5.8 為 PZT-4/Si 與 PZT-6B/Si 楔形體於 $\theta = 0^\circ$ 且不同邊界條件時， λ_1 隨 γ 變化之情形。圖 5.8(a) 與 (b) 分別為 PZT-4 之 $\beta = 180^\circ$ 與 $\beta = 90^\circ$ ；圖 5.8(c) 與 (d) 分別為 PZT-6B 之 $\beta = 180^\circ$ 與 $\beta = 90^\circ$ ；而 Si 均保持 $\beta_1 = 180^\circ$ 。觀察圖 5.8(a) 與 (b) 以及 (c) 與 (d)，發現於大部分 γ 值下 PZT-4/Si 複合楔形體擁有較弱之電彈奇異性。從四圖中可見 γ 值遠離 0° 與 180° 時，PZT-6B/Si 楔形體之電彈奇異性會增強；而 PZT-4/Si 楔形體時反倒有減弱之趨勢，甚至於圖 5.8(b) 中 PZT-4/Si 楔形體於 $\beta = 90^\circ$ 且 FCFC 邊界條件時，其 $\lambda_1 = 0.747$ 為相當弱之電彈奇異性，因此於該狀態下複合楔形體破壞之可能性相對低。

圖 5.9 為 PZT-4/Si 與 PZT-6B/Si 楔形體於不同極化方向且邊界條件為 FOF- 與 COC- 時， $\text{Re}[\lambda_1]$ 隨 θ 變化之情況。圖 5.9(a) 中 PZT-4 之 $\beta = 90^\circ$ ，Si 之 $\beta_1 = 180^\circ$ ；圖 5.9(b) 中 PZT-6B 之 $\beta = 90^\circ$ ，Si 之 $\beta_1 = 180^\circ$ 。觀察圖 5.9(a) 與 (b) 發現於不同極化方向 γ 值下且 θ 改變時，其 $\text{Re}[\lambda_1]$ 有完全不一樣之趨勢，但可明顯看出圖 5.9(b) 中 PZT-6B/Si 複合楔形體當 $\gamma \neq 0$ 時， $\text{Re}[\lambda_1]$ 隨 θ 變化幅度平均約 18% 較圖 5.9(a) 之 PZT-4/Si 複合楔形體約 4% 劇烈。另外，圖 5.9(b) 中 $\gamma = 45^\circ$ 與 90° 於 FOF- 以及 COC- 邊界條件下 $\theta = 0^\circ$ 與 180° 擁有最強之電彈奇異性，但圖 5.9(a) 中 PZT-4/Si 之複

合楔形體卻不然。圖 5.9(b) 中當 θ 接近 90° 亦擁有強烈的電彈奇異性產生；但圖 5.9(a) 卻顯示 θ 接近 90° 反而造成電彈奇異性漸弱。

5.3 電磁彈楔形體奇異性結果與討論

本節中將探討單一材料或雙材料電磁彈楔形體因為材料性質、邊界條件、極化方向與幾何形狀對 $\text{Re}[\lambda_1]$ 的影響。考慮的材料有電磁彈性材料 $\text{BaTiO}_3\text{-CoFe}_2\text{O}_4$ ($V_I=20\%$ 與 50%)、壓電材料 PZT-4 與 PZT-6B 以及彈性材料 Si，材料性質列於表 3.1。本研究中所考量之電磁彈性材料為壓電材料 BaTiO_3 與壓磁材料 CoFe_2O_4 之複合物，其材料性質如同 3.3 節所提及的與 BaTiO_3 及 CoFe_2O_4 之混合體積比例有關 [51]，其成一線性關係 $\bar{K}_{ij} = \bar{K}_{ij}^B V_I + \bar{K}_{ij}^F (1 - V_I)$ ，相關性質可參考表 3.1。本節所得之數值結果，均基於將全域 θ 分割為 8 個等份子域，每個子域之級數解均採 12 項。

5.3.1 單一電磁彈性材料楔形體

圖 5.10 為 $V_I = 50\%$ 與 20% 單一電磁彈材料楔形體，其極化方向 $\gamma = 0^\circ$ 且 $\theta = 0^\circ$ 時，於不同邊界條件之 λ_1 隨楔形體幾何變化之情形。觀察圖 5.10(a) 與 (b) 可發現其行為如同單一壓電或電磁彈材料迴轉體中所提到的力學邊界條件為 free-free 時電磁彈奇異性較力學邊界條為 clamped-clamped 時強。另外，當改變電磁邊界條件時，對電磁彈奇異性行為僅造成非常些微的影響。基本上當 $\beta = 0^\circ$ 時 $\lambda_1=0.500$ ，而 $\beta = 180^\circ$ 時 $\lambda_1=1.0$ ，即代表沒有任何奇異性。從圖 5.10(a) 與 (b) 中顯示在 $V_I=50\%$ 與 20% 之 $\text{BaTiO}_3\text{-CoFe}_2\text{O}_4$ 單一電磁彈性材料楔形體有極度相似的奇異性行為，整體而言 $V_I=20\%$ 之 $\text{BaTiO}_3\text{-CoFe}_2\text{O}_4$ 楔形體較 $V_I=50\%$ 者之電磁彈奇異性強約 1.5% 以內，如此表示 V_I 值並非影響單一電磁彈性楔形體之電磁彈奇異性的主要因素。

圖 5.11 為 $V_I = 50\%$ 與 20% 之 $\text{BaTiO}_3\text{-CoFe}_2\text{O}_4$ 楔形體於 $\theta = 0^\circ$ 且不同邊界條件時， λ_1 隨 γ 變化之情形。圖 5.11(a) 與 (c) 中 $\beta = 180^\circ$ ， $\beta_1 = 180^\circ$ ；圖 5.11(b) 與 (d) 中 $\beta = 90^\circ$ ， $\beta_1 = 180^\circ$ 。觀察圖 5.11(a) 與 (c) 發現在不同邊界條件下 $\gamma = 90^\circ$ 時總擁有較

強之電磁彈奇異性，其中又 $V_I=50\%$ 較 $V_I=20\%$ 強，其中圖 5.11(c) 中 FCFC 邊界條件在 $\gamma = 34^\circ$ 及 $\gamma = 147^\circ$ 均擁有較 $\gamma = 90^\circ$ 強之奇異性。圖 5.11(b) 與 (d) 則為 $\beta = 90^\circ$ 時 $\text{Re}[\lambda_1]$ 變化之情形，觀察後發現 FOFO 與 CCCC 邊界條件之 $\text{Re}[\lambda_1]$ 變化形態相似，而 FCFC 與 COCO 邊界條件較為相似。FOFO 與 CCCC 邊界條件之 $\text{Re}[\lambda_1]$ 曲線與圖 5.11(a)、(c) 中敘述一致當 $\gamma = 90^\circ$ 時擁有較強之電磁彈奇異性；而 FCFC 與 COCO 邊界條件時則為 $\gamma = 0^\circ$ 與 180° 時為最強。以整體來說四種邊界條件下均以 $V_I=20\%$ 擁有稍強之電磁彈奇異性，例如以 FOFO 邊界條件於 $\gamma = 90^\circ$ 之電磁彈奇異性強度作為比較， $V_I = 20\%$ 之 $\text{BaTiO}_3\text{-CoFe}_2\text{O}_4$ 楔形體之奇異性約強於 $V_I = 50\%$ 者 1.50% 以內。

圖 5.12(a) 與 (b) 為 $V_I=50\%$ 與 $V_I=20\%$ 的 270° 單一電磁彈性材料楔形體，其 $\beta = 90^\circ$ 與 $\beta_1 = 180^\circ$ ，當極化方向沿著 θ 方向變化時 $\text{Re}[\lambda_1]$ 變化之情形。從兩圖可以觀察到當 $\gamma = 0^\circ$ 時，其 $\text{Re}[\lambda_1]$ 曲線為一水平線，因為一般假設 $\text{BaTiO}_3\text{-CoFe}_2\text{O}_4$ 為側向等向性材料，故當極化方向為垂直 $X-Y$ 平面時，對於電磁彈奇異性是不會產生影響的。於圖 5.12(a) 與 (b) 中 $\theta = 90^\circ$ 時，邊界條件為 FOFO 或 COCO 均有較強烈之奇異性，甚至當 $\gamma = 90^\circ$ (極化方向為 $X-Y$ 平面內) 時其 $\text{Re}[\lambda_1]$ 值約達 0.350 左右，其中又以 $\text{BaTiO}_3\text{-CoFe}_2\text{O}_4$ 之 $V_I=20\%$ 時，邊界條件 FOFO 之 $\text{Re}[\lambda_1]$ 達 0.347 為最強烈，亦為最容易造成破壞之狀態。

5.3.2 雙電磁彈性材料楔形體

圖 5.13 為雙電磁彈材料楔形體，其極化方向 $\gamma = 0^\circ$ 且於不同邊界條件時之 $\text{Re}[\lambda_1]$ 隨楔形體幾何變化之情形。電磁彈楔形體組合為電磁彈材料 1/電磁彈材料 2，其中電磁彈材料 1 之幾何形狀為 β ，材料為 $V_I^{(1)}$ 之 $\text{BaTiO}_3\text{-CoFe}_2\text{O}_4$ ；電磁彈材料 2 之 $\beta_1 = 180^\circ$ ，材料為 $V_I^{(2)}$ 之 $\text{BaTiO}_3\text{-CoFe}_2\text{O}_4$ ，圖 5.13(a) 中 $V_I^{(1)}=50\%$ ， $V_I^{(2)}=20\%$ ；圖 5.13(b) 則為 $V_I^{(1)}=20\%$ ， $V_I^{(2)}=50\%$ 。

觀察圖 5.13 中發現與之前曾提到對單一電磁彈性材料之楔形體若單單改變電磁邊界條件時對奇異性僅會產生非常些微之影響的說法於此處並不成立，因為於

圖 5.13(a) 中 FOFO 邊界條件且 $\beta < 42^\circ$ 時並未與 FCFC 之 $\text{Re}[\lambda_1]$ 曲線相貼近；COCO 邊界條件且 $\beta < 63^\circ$ 時亦有同樣之現象發生，反而在 $\beta < 42^\circ$ 之範圍中 FOFO 與 COCO 邊界條件之 $\text{Re}[\lambda_1]$ 曲線相互貼近。表示電磁邊界條件的改變對於雙電磁彈複合楔形體之電磁彈奇異性會造成某種程度上的影響，但該影響並不強烈，其中 COCO 與 CCCC 邊界條件之 $\text{Re}[\lambda_1]$ 曲線的最大差異也僅在 2.50% 以內。圖 5.13(b) 中也有類似的現象產生，當 $\beta < 80^\circ$ 時 CCCC 邊界條件之 $\text{Re}[\lambda_1]$ 曲線向 FOFO 與 FCFC 之 $\text{Re}[\lambda_1]$ 曲線貼近。圖 5.13(c) 與 (d) 為雙電磁彈材料複合楔形體於 FOFO 與 COCO 邊界條件時， $\gamma = 0^\circ$ 與 45° 造成之影響，從圖中可發現 $\gamma = 0^\circ$ 與 45° 之曲線僅有些微差異。觀察兩圖，在圖 5.13(c) 中 $\beta < 50^\circ$ 時，四條曲線幾乎完全重合；圖 5.13(d) 中 $\beta < 22^\circ$ 時，四條曲線也可發現幾乎完全重合之現象。

圖 5.14 為雙電磁彈性材料楔形體於 $\theta = 0^\circ$ 且不同邊界條件時， λ_1 隨 γ 變化之情形。圖 5.14(a) 為 $V_I^{(1)} = 50\%$ 與 $V_I^{(2)} = 20\%$ 之 $\text{BaTiO}_3\text{-CoFe}_2\text{O}_4$ 各為 180° ；圖 5.14(b) 為 $V_I^{(1)} = 50\%$ 之 $\text{BaTiO}_3\text{-CoFe}_2\text{O}_4$ 為 $\beta = 90^\circ$ ， $V_I^{(2)} = 20\%$ 之 $\text{BaTiO}_3\text{-CoFe}_2\text{O}_4$ 為 $\beta_1 = 180^\circ$ ，圖 5.14(c) 之材料組合與圖 5.14(b) 相反。圖 5.14(a) 中發現 $\text{Re}[\lambda_1]$ 曲線變化之形態類似於單一電磁彈性材料，當 $\gamma = 90^\circ$ 於不同邊界條件下總有最強之電磁彈奇異性。另外，從圖中可以發現當 $\gamma < 50^\circ$ 範圍內，力學邊界條件 free-free 有較強之奇異性；而當 $\gamma > 130^\circ$ 範圍內，則改為力學邊界條件 clamped-clamped 有較強之電磁彈奇異性。圖 5.14(b) 與 (c) 分別 $V_I^{(1)}/V_I^{(2)}=50\%/20\%$ 與 $V_I^{(1)}/V_I^{(2)}=20\%/50\%$ 其 $\beta = 90^\circ$ 且 $\beta_1 = 180^\circ$ 之雙電磁彈楔形體，其中以 FCFC 與 COCO 邊界條件之 $\text{Re}[\lambda_1]$ 曲線差異較大，於圖 5.14(b) 中 FCFC 邊界條件之 $\text{Re}[\lambda_1]$ 最大至 0.638；而於圖 5.14(c) 中 COCO 邊界條件之 $\text{Re}[\lambda_1]$ 最大至 0.659，其為較弱之電磁彈奇異性，為教不易產生破壞之狀態。

圖 5.15 為雙電磁彈性楔形體於不同極化方向且邊界條件為 FOFO 與 COCO 時， $\text{Re}[\lambda_1]$ 隨 θ 變化之情況。圖 5.15(a) 中 $V_I^{(1)}=50\%$ 之 $\text{BaTiO}_3\text{-CoFe}_2\text{O}_4$ 為 $\beta = 90^\circ$ ， $V_I^{(2)}=20\%$ 之 $\text{BaTiO}_3\text{-CoFe}_2\text{O}_4$ 為 $\beta_1 = 180^\circ$ ；圖 5.15(b) 中 $V_I^{(1)}=20\%$ 之 $\text{BaTiO}_3\text{-CoFe}_2\text{O}_4$ 為 $\beta = 90^\circ$ ， $V_I^{(2)}=50\%$ 之 $\text{BaTiO}_3\text{-CoFe}_2\text{O}_4$ 為 $\beta_1 = 180^\circ$ 。圖 5.15(b) 中 γ 為 45° 或 90°

時，FOFO 或 COCO 邊界條件下其 $\text{Re}[\lambda_1]$ 值隨 θ 變化的幅度較圖 5.15(a) 之 $V_I^{(1)}/V_I^{(2)}=50\%/20\%$ 電磁彈性楔形體明顯，圖 5.15(b) 中 COCO 邊界條件最大與最小的差異達 106.37%。因圖 5.15(a) 中 $V_I^{(1)}/V_I^{(2)}=50\%/20\%$ 楔形體之 $\text{Re}[\lambda]$ 變化曲線較為穩定，因此若實際應用上需要極化方向於 θ 方向作改變時，圖 5.15(a) 中雙電磁彈性材料楔形體會是相對較佳的方案。觀察兩圖，僅單純比較力學邊界條件對於電磁彈奇異性的影響，可發現均以 clamped-clamped 變化較為劇烈。另外亦有類似於前述之經驗，當 $\theta = 90^\circ$ 時擁有最強之電磁彈奇異性，例如圖 5.15(a) 中 $\gamma = 90^\circ$ 時，FOFO 與 COCO 邊界條件其最強奇異性 $\text{Re}[\lambda_1]$ 為 0.372；而圖 5.15(b) 中 $\gamma = 90^\circ$ 時，兩邊界條件其 $\text{Re}[\lambda_1]$ 為 0.332。

5.3.3 電磁彈性/彈性材料 Si 楔形體

圖 5.16 為 $\text{BaTiO}_3\text{-CoFe}_2\text{O}_4/\text{Si}$ 楔形體，其極化方向 $\gamma = 0^\circ$ 且於不同邊界條件時之 $\text{Re}[\lambda_1]$ 隨楔形體幾何變化之情形。其中 $\text{BaTiO}_3\text{-CoFe}_2\text{O}_4$ 之幾何形狀為 β ；Si 之 $\beta_1 = 180^\circ$ 。基本上與前幾小節所討論的結果無異，即僅改變電磁邊界條件僅對於電磁彈奇異性造成些微影響。參考圖 5.16(a) 與 (b)，儘管 $\text{BaTiO}_3\text{-CoFe}_2\text{O}_4$ 之 V_I 改變但曲線均有類似之行為，且在 $\beta = 165^\circ$ 附近有產生折角之現象，當 $\beta > 165^\circ$ 時 λ_1 值為複數。圖 5.16(c) 為比較於 FOF- 與 COC- 邊界條件下改變 $\text{BaTiO}_3\text{-CoFe}_2\text{O}_4$ 之 V_I 值所造成之差異，基本上改變 V_I 值對電磁彈奇異性影響不強烈，該觀察結果在之前文章中亦有提及，在邊界條件為 FOF- 時約在 $\beta > 155^\circ$ 時， $V_I = 50\%$ 之 $\text{BaTiO}_3\text{-CoFe}_2\text{O}_4/\text{Si}$ 楔形體有較強之電磁彈奇異性，而當 $\beta < 120^\circ$ 時則改為 $V_I = 20\%$ 者較強；若 COC- 邊界條件時當 $\beta < 80^\circ$ 時，則 $V_I = 50\%$ 之 $\text{BaTiO}_3\text{-CoFe}_2\text{O}_4/\text{Si}$ 楔形體奇異性強度較 $V_I = 20\%$ 者強烈，即便如此兩者最大差異也未達 1.00%。

圖 5.17 為 $\text{BaTiO}_3\text{-CoFe}_2\text{O}_4/\text{Si}$ 楔形體於 $\theta = 0^\circ$ 且不同邊界條件時， λ_1 隨 γ 變化之情形。圖 5.8(a) 與 (b) 分別為 $V_I = 50\%$ $\text{BaTiO}_3\text{-CoFe}_2\text{O}_4$ 之 $\beta = 180^\circ$ 與 $\beta = 90^\circ$ ；圖 5.8(c) 與 (d) 分別為 $V_I = 20\%$ $\text{BaTiO}_3\text{-CoFe}_2\text{O}_4$ 之 $\beta = 180^\circ$ 與 $\beta = 90^\circ$ 。相較於壓電

材料/Si 組合模式之楔形體，其 $\text{Re}[\lambda_1]$ 曲線變化的行為相對較為單調。單就一般想像，電磁彈性奇異性行為應較電彈性奇異性行為複雜，根據圖中顯示之曲線變化情形似乎該想像之論點無法成立。從圖中可發現於不同邊界條件下最強之電磁彈奇異性均發生於 $V_I = 20\%$ 之 $\text{BaTiO}_3\text{-CoFe}_2\text{O}_4/\text{Si}$ 楔形體。觀察圖 5.17(a) 與 (c)，改變 V_I 值對於 $\text{Re}[\lambda_1]$ 之變化趨勢似乎沒有劇烈之影響；但在圖 5.17(c) 中 $V_I = 20\%$ 之 $\text{BaTiO}_3\text{-CoFe}_2\text{O}_4/\text{Si}$ 楔形體之 $\text{Re}[\lambda_1]$ 曲線有較為明顯起伏，例如圖 5.17(c) 中 COCO 之 $\text{Re}[\lambda_1]$ 曲線中最大與最小差異約為 5.74%；而圖 5.17(c) 中 COCO 邊界條件之 $\text{Re}[\lambda_1]$ 曲線之起伏最大差異為 3.08%。圖 5.17(b) 與 (d) 中 $\text{BaTiO}_3\text{-CoFe}_2\text{O}_4$ 之 $\beta = 90^\circ$ 與 Si 之 $\beta_1 = 180^\circ$ 雙材料楔形體。兩圖中 $\text{Re}[\lambda_1]$ 曲線變化有類似之趨勢。圖 5.17(b) 中 FCFC 邊界條件於 $\gamma = 90^\circ$ 時有最弱之奇異性；但於圖 5.17(d) 反而有稍稍轉強的行為。

圖 5.18 為 $\text{BaTiO}_3\text{-CoFe}_2\text{O}_4/\text{Si}$ 楔形體於不同極化方向且邊界條件為 FOF- 與 COC- 時， $\text{Re}[\lambda_1]$ 隨 θ 變化之情況。圖 5.18(a) 中 $V_I=50\%$ 之 $\text{BaTiO}_3\text{-CoFe}_2\text{O}_4$ 之 $\beta = 90^\circ$ ，Si 之 $\beta_1 = 180^\circ$ ；圖 5.18(b) 中 $V_I=20\%$ 之 $\text{BaTiO}_3\text{-CoFe}_2\text{O}_4$ 之 $\beta = 90^\circ$ ，Si 之 $\beta_1 = 180^\circ$ 。發現圖 5.18(a) 與 (b) 之變化情形很類似，但 $V_I = 20\%$ (CoFe_2O_4 含量較多) 時， λ_1 變化幅度較大，在邊界條件作大 COC-且 $\gamma = 90^\circ$ 時約達 4.32%；而當 $V_I = 50\%$ 時，其餘條件一致時 λ_1 變化僅 1.74%。

5.3.4 電磁彈性/壓電材料楔形體

圖 5.19 為 $\text{BaTiO}_3\text{-CoFe}_2\text{O}_4/\text{PZT-4}$ 楔形體，其極化方向 $\gamma = 0^\circ$ 且於不同邊界條件時之 $\text{Re}[\lambda_1]$ 隨楔形體幾何變化之情形。其中 $\text{BaTiO}_3\text{-CoFe}_2\text{O}_4$ 之幾何形狀為 β ；PZT-4 之 $\beta_1 = 180^\circ$ 。圖 5.19 為 $\text{BaTiO}_3\text{-CoFe}_2\text{O}_4/\text{PZT-4}$ 楔形體，其中 $\text{BaTiO}_3\text{-CoFe}_2\text{O}_4$ 之 β 改變時電磁彈奇異性之變化情形。觀察圖 5.19(a)、(c) 與 (d)，發現當極化方向垂直於 $X - Y$ 平面時，力學條件為 free-free 或 clamped-clamped 時，改變其電磁與電學邊界條件均對奇異性造成極度些微影響，該結果是與單一電磁彈性或壓電材料相同的，圖 5.19(b) 中所顯示之結果卻不盡然如此，在力學條件為 free-free 且

$18^\circ < \beta < 180^\circ$ 以及力學條件為 clamped-clamped 且 $106^\circ < \beta < 180^\circ$ ，電磁與電學邊界條件 open-open 與 closed-closed 之電磁彈奇異性一致，而其餘角度下則以電磁與電學邊界條件為 closed-closed 之電磁彈奇異性較強。圖 5.20 為 $\text{BaTiO}_3\text{-CoFe}_2\text{O}_4/\text{PZT-6B}$ 楔形體，其極化方向 $\gamma = 0^\circ$ 且於不同邊界條件時之 $\text{Re}[\lambda_1]$ 隨楔形體幾何變化之情形。其中 $\text{BaTiO}_3\text{-CoFe}_2\text{O}_4$ 之幾何形狀為 β ；PZT-6B 之 $\beta_1 = 180^\circ$ 。發現力學邊界條件與幾何形狀為控制電磁彈奇異性之主要因素，改變極化方向與電磁與電學邊界條件似乎對 $\text{Re}[\lambda_1]$ 影響並不明顯。

圖 5.21 與圖 5.22 為 $\text{BaTiO}_3\text{-CoFe}_2\text{O}_4/\text{PZT-4}$ 與 $\text{BaTiO}_3\text{-CoFe}_2\text{O}_4/\text{PZT-6B}$ 楔形體於 $\theta = 0^\circ$ 且不同邊界條件時， λ_1 隨 γ 變化之情形。圖 5.21 與圖 5.22 之 (a) 與 (c) 中 $\text{BaTiO}_3\text{-CoFe}_2\text{O}_4$ 之 $\beta = 180^\circ$ ，壓電材料之 $\beta_1 = 180^\circ$ ；圖 5.21 與圖 5.22 之 (b) 與 (d) 中 $\text{BaTiO}_3\text{-CoFe}_2\text{O}_4$ 之 $\beta = 90^\circ$ ，壓電材料之 $\beta_1 = 180^\circ$ ；很明顯從圖中看出相較於單一電磁彈性材料或壓電材料時複雜許多，多數的 $\text{Re}[\lambda_1]$ 曲線均約出現兩次的折角（實數根與複數根之轉換點）。觀察圖 5.21 與圖 5.22， $\text{BaTiO}_3\text{-CoFe}_2\text{O}_4/\text{PZT-6B}$ 楔形體相較於 $\text{BaTiO}_3\text{-CoFe}_2\text{O}_4/\text{PZT-4}$ 楔形體擁有較強之奇異性，該特點與單一壓電材料楔形體之電磁彈奇異性行為類似，當 $\text{BaTiO}_3\text{-CoFe}_2\text{O}_4/\text{PZT-6B}$ 楔形體之 γ 值遠離 0° 與 180° 時奇異性較為強烈；而 $\text{BaTiO}_3\text{-CoFe}_2\text{O}_4/\text{PZT-4}$ 楔形體時則相反，電磁彈奇異性則越趨減弱，意指 $\text{BaTiO}_3\text{-CoFe}_2\text{O}_4/\text{PZT-6B}$ 楔形體在極化方向改變時可能較為容易產生破壞，尤其當極化方向由面外（垂直於 $X-Y$ 平面）方向轉向平面內時。另外，當 $\text{BaTiO}_3\text{-CoFe}_2\text{O}_4$ 之 $V_I=20\%$ 時， $\text{Re}[\lambda_1]$ 曲線似乎有較為明顯的波動，例如圖 5.21(b) 與 (d) 中之 COCO 邊界條件，當 $V_I=50\%$ 者其最大與最小的 $\text{Re}[\lambda_1]$ 值差異約為 12.91%，而 $V_I=20\%$ 則為 19.83%；圖 5.22(a) 與 (c) 中之 FCFC 邊界條件，當 $V_I=50\%$ 者其最大與最小的 $\text{Re}[\lambda_1]$ 值差異約為 18.52%，而 $V_I=20\%$ 則為 20.27%。

圖 5.23 與圖 5.24 分別為 $\text{BaTiO}_3\text{-CoFe}_2\text{O}_4/\text{PZT-4}$ 與 $\text{BaTiO}_3\text{-CoFe}_2\text{O}_4/\text{PZT-6B}$ 楔形體於不同極化方向且邊界條件為 FOF- 與 COC- 時， $\text{Re}[\lambda_1]$ 隨 θ 變化之情況。圖 5.23(a) 與 (b) 分別為 $V_I=50\%$ 與 20% 之 $\text{BaTiO}_3\text{-CoFe}_2\text{O}_4$ 之 $\beta = 90^\circ$ ，PZT-4 之

$\beta_1 = 180^\circ$ ；圖 5.24(a) 與 (b) 分別為 $V_I=50\%$ 與 20% 之 $\text{BaTiO}_3\text{-CoFe}_2\text{O}_4$ 之 $\beta = 90^\circ$ ，PZT-6B 之 $\beta_1 = 180^\circ$ 。從圖中可以清楚看到當 $\gamma = 0^\circ$ 時， $\text{BaTiO}_3\text{-CoFe}_2\text{O}_4$ 改變 V_I 值對於 FOFO 或 COCO 邊界條件之奇異性影響甚微，例如圖 5.23 中邊界條件為 FOFO 時， $V_I = 50\%$ 時 $\text{Re}[\lambda_1]=0.524$ ；而當 $V_I = 20\%$ 時 $\text{Re}[\lambda_1]=0.519$ 。當 $\gamma = 45^\circ$ 或 90° 時，改變電磁彈性材料之 V_I 似乎不會對於 $\text{Re}[\lambda_1]$ 曲線的變化趨勢造成改變，只有當 $V_I = 20\%$ (壓磁材料 CoFe_2O_4 所佔比例為 80%) 時，其 $\text{Re}[\lambda_1]$ 曲線隨 θ 值變化的幅度較大，例如圖 5.23(b) 中 COCO 邊界條件且 $\gamma = 90^\circ$ 時，其最大與最小 $\text{Re}[\lambda_1]$ 差異達 30.62% 。此外，如同前述於 $270^\circ(\beta = 90^\circ, \beta_1 = 180^\circ)$ 之雙材料楔形體之行為， $\theta = 90^\circ$ 時已不再是奇異性最強烈之位置，只能推論因為材料內部分複雜之電磁彈耦合效應造成該現象，但於 $\theta = 90^\circ$ 之附近的點仍有可能產生最強電磁彈奇異性。圖 5.24(a) 與 (b) 為 $\text{BaTiO}_3\text{-CoFe}_2\text{O}_4/\text{PZT-6B}$ 楔形體與圖 5.23(a) 與 (b) 之 $\text{Re}[\lambda_1]$ 有類似的變化曲線，其中力學邊條件為 clamped-clamped 時，以圖 5.24(b) 之變化幅度較大，其中 COCO 邊界條件且 $\gamma = 90^\circ$ 時約達 38.31% ；若力學邊條件為 free-free 時，以圖 5.24(a) 之變化幅度較大，其中 FOFO 邊界條件且 $\gamma = 90^\circ$ 時約達 42.73%

第六章 結論與建議

6.1 結論

本研究根據三維電磁彈性理論，直接求解以位移、電勢與磁勢表示之三維力平衡與馬克斯威爾方程式，以建立電磁彈性迴轉體與楔形體於尖端處之漸近解。推導之過程中，為分析迴轉體 $\rho \rightarrow 0$ 與楔形體 $r \rightarrow 0$ 之奇異性行為，故分別取 ρ 之最低次項（參考式 (2.10)）與 r 之最低次項（參考式 (4.3)）。經整理後，可發現式 (2.10) 與式 (4.3) 均與 Z 無關，表示利用二維之理論亦可推得三維電磁彈性理論之結果。本研究基於三維電磁彈性與壓電材料之材料性質，同時未做任何之假設與簡化，且電磁彈性與壓電材料之極化方向為空間中任意方向，因此相較於從前文獻所提供之二維方法，本研究所建議之方式可解決更加廣泛之奇異性問題。

- (1) 相對於材料組成、極化方向或邊界條件，迴轉體與楔形體的幾何形狀絕對為控制奇異性強度之主要因素，例如裂縫的情況下 ($\beta = 180^\circ$, $\beta_1 = 180^\circ$) 擁有最強烈之奇異性。當固定幾何形狀之情況下，力學邊界條件為 free-free 時之奇異性於大多數情況下多較力學邊界條件為 clamped-clamped 強烈，因此力學邊界條件亦為控制奇異性強度相當重要之因素。
- (2) 單一電磁彈性材料或壓電材料迴轉體，於固定極化方向 γ 值的情況下，單純改變電磁或電學邊界條件對於奇異性的影響非常有限。當電磁彈性材料或壓電材料之極化方向改變所造成奇異性強度之變化，於大部分的圖中發現對於力學邊界條件為 clamped-clamped 之影響較 free-free 明顯。
- (3) 雙材料之複合迴轉體當模擬裂縫 ($\beta = 180^\circ$, $\beta_1 = 180^\circ$) 的狀態時，由於材料彼此間的差異以及電磁彈性或壓電之耦合效應使得破壞的機率增加，往往使得 $\text{Re}[\lambda_1]$

值低於一般彈性材料裂縫之情況下時所得之 $\text{Re}[\lambda_1]$ 值 0.500。

- (4) 當固定楔形體幾何形狀的情況下，在大多數單一或雙材料楔形體之極化方向 $\gamma = 90^\circ$ (極化方向為平行 $X - Y$ 平面) 時，常擁有較強烈之奇異性；但部分情況例如楔形體材料組合中包含壓電材料 PZT-4 時，常造成電磁彈奇異性強度較弱。
- (5) 固定楔形體幾何形狀時，當極化方向 $\gamma = 45^\circ$ 或 90° 且隨 θ 變化時，COCO 邊界條件之 $\text{Re}[\lambda_1]$ 曲線總有較 FOFO 邊界條件大幅度的變化，例如圖 5.15 中雙電磁彈性材料楔形體之 COCO 邊界條件之 $\text{Re}[\lambda_1]$ 曲線變化幅度達 106.37%。

6.2 建議

科技日新月異，材料亦推陳出新，本論文無法涵蓋至大部分之材料，僅提出一種較為廣義的分析方法及模式作為後續研究之參考，因此建議可以對於較新穎且具有實際用途之智能材料進行分析，例如功能梯度性材料 (functionally graded material, FGM)。

根據本研究所得電磁彈奇異性階數之結果，可對於更加複雜之幾何形狀尖端進行應力、電位移與磁通量分析，嘗試推求其強度因子。因本研究中電磁彈性與壓電材料之極化方向毋須平行迴轉體之旋轉軸或垂直於楔形體之中平面，則材料係數經座標轉換後均為 θ 之函數，故求取強度因子之過程中仍可能有許多困難點需克服。

參考文獻

- [1] J. van Suchtelen. Product properties: a new application of composite material. *Phillips Research Reports*, 27:28–37, 1972.
- [2] J. van dan Boomgaard, D.R. Terrell, R.A.J. Born, and F.H.J.I. Giller. An in situ grown eutectic magnetoelectric composite material. part 1: Composition and unidirectional solidification. *Journal of Materials Science*, 9(10):1705–1709, 1974.
- [3] A.M.J.G. van Run, D.R. Terrell, and J.H. Scholing. An in situ grown eutectic magnetoelectric composite material. part 2: Physical properties. *Journal of Materials Science*, 9(10):1710–1714, 1974.
- [4] L. P. M. Bracke and R.G. van Vliet. A broadband magneto-electric transducer using a composite material. *Journal of Intelligent Material Systems and Structures*, 51(3):255–262, 1981.
- [5] M.L. Williams. Stress singularities resulting from various boundary conditions in angular corners of plates under bending. In *Proceeding of 1st U.S. National Congress of Applied Mechanics*, pages 325–329, 1952.
- [6] M.L. Williams. Stress singularities resulting from various boundary conditions in angular corners of plates in extension. *Journal of Applied Mechanics*, 19(4):526–528, 1952.
- [7] R.J. Hartranft and G.C. Sih. The use of eigenfunction expansions in the general solution of three-dimensional crack problems. *Journal of Mathematics and Mechanics*, 19(2):123–138, 1969.

- [8] D.B. Bogy and K.C. Wang. Stress singularities at interface corners in bonded dissimilar isotropic elastic materials. *International Journal of Solids and Structure*, 7(10):993–1005, 1971.
- [9] D.B. Bogy. Two edge-bonded elastic wedges of different material and wedge angles under surface tractions. *ASME Journal of Applied Mechanics*, 28(2):377–386, 1971.
- [10] J.P. Dempsey and G.B. Sinclair. On the stress singular behavior at the vertex of a bi-material wedge. *Journal of Elasticity*, 11(3):317–327, 1981.
- [11] J.P. Dempsey and G.B. Sinclair. On the stress singularities in the plate elasticity of the composite wedge. *Journal of Elasticity*, 9(4):373–391, 1979.
- [12] P.S. Theocaris. The order of singularity at a multi-wedge corner of a composite plate. *International Journal of Engineering Science*, 12(2):107–120, 1974.
- [13] V.L. Hein and F. Erdogan. Stress singularities in a two-material wedge. *International Journal of Fracture Mechanics*, 7(3):317–330, 1971.
- [14] A.K. Rao. Stress concentrations and singularities at interfaces corners. *Zeitschrift für Angewandte Mathematik und Mechanik*, 51(5):395–406, 1971.
- [15] M.C. Kuo and D.B. Bogy. Plane solutions for traction problems on orthotropic unsymmetrical wedges and symmetrically twinned wedges. *ASME Journal of Applied Mechanics*, 41(4):203–208, 1971.
- [16] T.C.T Ting and S.C. Chou. Edge singularities in anisotropic composites. *International Journal of Solids and Structures*, 17(11):1057–1068, 1981.
- [17] M.C. Kuo and D.B. Bogy. Plane solutions for the displacement and traction-

- displacement problems for anisotropic elastic wedges. *Journal of Applied Mechanics*, 41(1):197–202, 1974.
- [18] F. Delale. Stress singularities in bonded anisotropic materials. *International Journal of Solids and Structures*, 20(1):31–40, 1984.
- [19] C. Hwu and T.C.T. Ting. Solutions for the anisotropic elastic wedge at critical wedge angles. *Journal of Elasticity*, 24(1–2):1–20, 1990.
- [20] Y.Y. Lin and J.C. Sung. Stress singularities at the apex of a dissimilar anisotropic wedge. *ASME Journal of Applied Mechanics*, 65(2):454–463, 1998.
- [21] H.P. Chen. Stress singularities in anisotropic multi-material wedges and junctions. *International Journal of Solids and Structures*, 35(11):1057–1073, 1998.
- [22] C.C. Ma and B.L. Hour. Analysis of dissimilar anisotropic wedge subjected to antiplane shear deformation. *International Journal of Solids and Structures*, 25(11):1295–1309, 1989.
- [23] M.H. Kargarnovin, A.R. Shahani, and S.J. Fariborz. Analysis of an isotropic finite wedge under antiplane deformation. *International Journal of Solids and Structures*, 34(1):113–128, 1997.
- [24] A.R. Shahani. Analysis of an anisotropic finite wedge under antiplane deformation. *Journal of Elasticity*, 56(1):17–32, 1999.
- [25] M. Xie and R.A. Chaudhuri. Three-dimensional stress singularity at a bimaterial interface crack front. *Composite Structures*, 40(2):137–142, 1998.
- [26] I.O. Ojikutu, R.O. Low, and R. A. Scott. Stress singularities in laminated composite wedge. *International Journal of Solids and Structures*, 20(8):777–790, 1984.

- [27] W.S. Burton and G.B. Sinclair. On the singularities in reissner's theory for the bending of elastic plates. *Journal of Applied Mechanics*, 53(1):220–222, 1986.
- [28] C.S. Huang. On the singularity induced by boundary conditions in a third-order thick plate theory. *ASME Journal of Applied Mechanics*, 69(6):800–810, 2002.
- [29] C.S. Huang. Stress singularities at angular corners in first-order shear deformation plate theory. *International Journal of Mechanical Sciences*, 45(1):1–20, 2003.
- [30] C.S. Huang and M.J. Chang. Corner stress singularities in a fgm thin plate. *International Journal of Solids and Structures*, 44(9):2802–2819, 2007.
- [31] O.G. McGee, J.W. Kim, and A.W. Leissa. Sharp corner functions for mindlin plates. *ASME Journal of Applied Mechanics*, 72(1):1–9, 2005.
- [32] C.H. Chue and C.I. Liu. A general solution on stress singularities in an anisotropic wedge. *International Journal of Solids and Structures*, 38(38–39):6889–6906, 2001.
- [33] C.H. Chue and C.I. Liu. Disappearance of free-edge stress singularity in composite laminates. *Composite Structures*, 56(1):111–129, 2002.
- [34] C.H. Chue and C.I. Liu. Stress singularities in a bimaterial anisotropic wedge with arbitrary fiber orientation. *Composite Structures*, 58(1):49–56, 2002.
- [35] X.L. Xu and R.K.N.D. Rajapakse. On singularities in composite piezoelectric wedges and junctions. *International Journal of Solids and Structures*, 37(23):3235–3275, 2000.
- [36] M.C. Chen, J.J. Zhu, and K.Y. Sze. Electroelastic singularities in piezoelectric-elastic wedges and junctions. *Engineering Fracture Mechanics*, 73(7):855–868, 2006.

- [37] C. Hwu and T. Ikeda. Eletromechanical fracture analysis for corners and cracks in piezoelectric materials. *International Journal of Solids and Structures*, 45(22–23): 2744–5764, 2008.
- [38] C.H. Chue and C.D. Chen. Decoupled formulation of piezoelectric elasticity under generalized plane deformation and its application to wedge problems. *International Journal of Solids and Structures*, 39(12):3131–3158, 2002.
- [39] H. Sosa and Y. E. Pak. Three-dimensional eigenfunction analysis of a crack in piezoelectric material. *International Journal of Solids and Structures*, 26(1):1–15, 1988.
- [40] C.H. Chue and C.D. Chen. Antiplane stress singularities in a bonded bimaterial piezoelectric wedge. *Archieve of Applied Mechanics*, 72(9):673–685, 2003.
- [41] M. Scherzer and M. Kuna. Combined analytical and numerical solution of 2d interface corner configurations between dissimilar piezoelectric materials. *International Journal of Fracture*, 127(1):61–99, 2004.
- [42] M.C. Chen, J.J. Zhu, and K.Y. Sze. Electroelastic singularities in piezoelectric-elastic wedges and junctions. *Engineering Fracutre Mechanics*, 73(7):855–868, 2006.
- [43] F. Shang and T. Kitamura. On stress singularity at the interface edge between piezoelectric thin film and elastic substrate. *Microsystem Technology*, 11(8–10):1115–1120, 2005.
- [44] Z. Wang and B. Zheng. The general solution of three dimensional problems in piezoelectric media. *International Journal of Solids and Structures*, 32(1):105–115, 1995.
- [45] T.J.C. Liu and C.H. Chue. On the singularities in a bimaterial magneto-electro-elastic composite wedge under antiplane deformation. *Composite Structures*, 72(2): 254–265, 2006.

- [46] W.C. Sue, J.Y. Liou, and J.C. Sung. Investigation of the stress singularity of a magneto-electroelastic bonded antiplane wedge. *Microsystem Technology*, 31(10):2313–2331, 2007.
- [47] T.J.C. Liu. The singularity problem of the magneto-electro-elastic wedge-junction structure with consideration of the air effect. *Archieve of Applied Mechanics*, 79(5):377–393, 2009.
- [48] A.R. Zak. Stresses in the vicinity of boundary discontinuities in bodies of revolution. *ASME Journal of Applied Mechanics*, 31(1):150–152, 1964.
- [49] T.C.T. Ting, Y. Jin, and S.C. Chou. Eigenfuction at a singular point in transversely isotropic materials under axisymmetric deformations. *ASME Journal of Applied Mechanics*, 52(3):565–570, 1985.
- [50] C.S. Huang and A.W. Leissa. Three-dimensional sharp corner displacement functions for bodies of revolution. *ASME Journal of Applied Mechanics*, 74(1):41–46, 2007.
- [51] C.S. Huang and A.W. Leissa. Stress singularities in bimaterial bodies of revolution. *Composite Structures*, 82(4):488–498, 2008.
- [52] Y. Li, Y. Sato, and K. Watanabe. Stress singularity analysis of axisymmetric piezoelectric bonded structure. *JSME International Journal Series A*, 45(3):363–370, 2002.
- [53] J.Q. Xu and Y. Mutoh. Singularity at the interface edge of bonded transversely isotropic piezoelectric dissimilar materials. *JSME International Journal Series A*, 44(4):556–566, 2001.
- [54] Nellya N. Rogacheva. *The Theory of Piezoelectric Shells and Plates*. CRC Press, USA, 1994.

- [55] Y. Ikeda. *Fundamentals of Piezoelectricity*. Oxford University Press, New York, 1996.
- [56] C.W. Nan. Magnetolectric effect in composites of piezoelectric and piezomagnetic phases. *Physical Review B*, 50:6082–6088, 1994.
- [57] Y. Benveniste. Magnetolectric effect in fibrous composites with piezoelectric and piezomagnetic phases. *Physical Review B*, 51:16424–16427, 1995.
- [58] J. Y. Li and M.L. Dunn. Anisotropic coupled-field inclusion and inhomogeneity problems. *Philosophical Magazine A*, 77(5):1341–1350, 1998.
- [59] J. Y. Li and M.L. Dunn. Micromechanics of magnetoelctroelastic composite materials: Average fields and effective behavior. *Journal of Intelligent Material Systems and Structures*, 9(6):404–416, 1998.
- [60] D. E. Müller. A method for solving algebraic equations using an automatic computer. *JSME International Journal Series A*, 10(56):208–215, 1956.
- [61] Z.F. Song and G.C. Sih. Crack initiation behavior in magnetoelctroelastic composite under in-plane deformation. *Theoretical and Applied Fracture Mechanics*, 39(3):189–207, 2003.
- [62] D.H. Chen. A crack normal to and termination at a bimaterial interface. *Engineering Fracture Mechanics*, 49(4):517–532, 1994.
- [63] R.D. Ramón, S. Natarajan, S. Andrés, and G.S. Felipe. Crack analysis in magnetoelctroelastic media using the extended finite element method. In *International Conference on Extended Finite Element Methods – Recent Developments and Applications*, pages 1–5, 2009.

- [64] J.H. Huang and W.S. Kuo. The analysis of piezoelectric piezomagnetic composite materials containing ellipsoidal inclusions. *Journal of Applied Physics*, 81(3):1378–1386, 1997.



表 3.1 材料性質

材料係數		PZT-4 ^a	PZT-5H ^a	PZT-6B ^b	PZT-6B(Im.) ^b	BaTiO ₃ ^c	CoFe ₂ O ₄ ^c	BaTiO ₃ -CoFe ₂ O ₄ ^d (V _I = 0.5)
彈性係數 (GPa)	\bar{c}_{11}	139.0	126.0	168.0	168.0	166.0	286.0	226.0
	\bar{c}_{12}	77.8	55.0	60.0	60.0	77.0	173.0	125.0
	\bar{c}_{13}	74.3	53.0	60.0	60.0	78.0	170.5	124.0
	\bar{c}_{33}	115.0	117.0	163.0	163.0	162.0	269.5	216.0
	\bar{c}_{44}	25.6	35.3	27.1	27.1	43.0	45.3	44.0
壓電係數 (C/m ²)	\bar{e}_{11}	-5.2	17.0	4.6	43.0	11.6	-	5.8
	\bar{e}_{31}	15.1	-6.5	-0.9	-14.0	-4.4	-	-2.2
	\bar{e}_{33}	12.7	23.3	7.1	36.0	18.6	-	9.3
介電係數 $\times 10^{-10}$ (F/m)	$\bar{\eta}_{11}$	64.6	151.0	36.0	200.0	112.0	-	56.4
	$\bar{\eta}_{33}$	56.2	130.0	34.0	247.0	126.0	-	63.5
壓磁係數 (N/Am)	\bar{d}_{11}	-	-	-	-	-	550.0	275.0
	\bar{d}_{33}	-	-	-	-	-	580.3	290.2
	\bar{d}_{33}	-	-	-	-	-	699.7	350.0
磁導係數 $\times 10^{-6}$ (Ns ² /C ²)	$\bar{\mu}_{11}$	-	-	-	-	5.0	590.0	297.0
	$\bar{\mu}_{33}$	-	-	-	-	10.0	157.0	83.5
電磁耦合係數 $\times 10^{-10}$ (Ns/VC)	\bar{g}_{11}	-	-	-	-	0.0	0.0	0.05367
	\bar{g}_{33}	-	-	-	-	0.0	0.0	27.375

^a 為參考 Li 等人 [52]

^b 為參考 Xu 與 Mutoh[53]

^c 為參考 Huang 與 Kuo[64]

^d 為參考 Ramón 等人 [63]

表 3.2 壓電迴轉體之 $\text{Re}[\lambda_1]$ 收斂性分析

幾何形狀	材料 1/材料 2	子域數	級數解項數						文獻		
			5	6	7	9	11	13		15	
$\beta = 90^\circ$	CdSe/ PZT-5H	2	0.9363	0.9348	0.9357	0.9377	0.9387	0.9383	0.9380	0.9381*	
		4	0.9379	0.9381	0.9382	0.9381	0.9381	0.9381	0.9381		
		6	0.9381	0.9381	0.9381	0.9381	0.9381	0.9381	0.9381		
		8	0.9381	0.9381	0.9381	0.9381	0.9381	0.9381	0.9381		
	CdSe/ PZT-6B	2	0.9268	0.9242	0.9308	0.9302	0.9280	0.9272	0.9278	0.9281*	
		4	0.9286	0.9289	0.9279	0.9281	0.9281	0.9281	0.9281		
		6	0.9281	0.9281	0.9281	0.9281	0.9281	0.9281	0.9281		
		8	0.9281	0.9281	0.9281	0.9281	0.9281	0.9281	0.9281		
	$\beta_1 = 90^\circ$	CdSe/ BaTiO ₃	2	0.8949	0.9588	0.9429	0.9172	0.9394	0.9256	0.9284	0.9429*
			4	0.9436	0.9430	0.9430	0.9430	0.9429	0.9429	0.9429	
			6	0.9429	0.9428	0.9428	0.9429	0.9429	0.9429	0.9429	
			8	0.9429	0.9428	0.9429	0.9429	0.9429	0.9429	0.9429	
$\beta_1 = 180^\circ$	PZT-6B/ PZT-6B(Im.)	2	0.98792	0.98475	0.98641	0.98793	0.98713	0.98828	0.98792	0.98724**	
		4	0.98742	0.98732	0.98731	0.98720	0.98613	0.98725	0.98724		
		6	0.98802	0.98764	0.98764	0.98733	0.98724	0.98724	0.98724		
		8	0.98730	0.98724	0.98723	0.98724	0.98724	0.98724	0.98724		
$\beta = 90^\circ$	PZT-6B/ PZT-6B(Im.)	3	0.54766	0.53669	0.52792	0.52053	0.52716	0.52670	0.53197	0.52819**	
		6	0.52694	0.52758	0.52801	0.52836	0.52819	0.52818	0.52820		
		9	0.52803	0.52809	0.52823	0.52820	0.52820	0.52820	0.52820		

註：本表中各分析案例之邊界條件均為 FOFO

* 為 Li 等人 [52] 之結果

** 為 Xu 與 Mutoh[53] 之結果

表 5.1 壓電楔形體之 $\text{Re}[\lambda_1]$ 收斂性分析

幾何形狀	材料一 / 材料二	邊界條件	子域數	級數解項數							文獻	
				6	7	8	9	10	12	14		15
$\beta = 180^\circ$ $\beta_1 = 180^\circ$	PZT-4	FOFO	3	0.4978	0.4916	0.4417	0.4980	0.4998	0.4750	0.5000	0.4999	0.5000 [†]
			4	0.4963	0.4993	0.4999	0.4999	0.4984	0.4999	0.4999	0.4999	
			6	0.4993	0.4999	0.4999	0.5000	0.5000	0.4999	0.5000	0.5000	
			8	0.4999	0.4999	0.4999	0.4999	0.5000	0.5000	0.4999	0.5000	
		FOCC	3	0.1969	0.2052	0.1602	0.1718	0.1965	0.1724	0.1954	0.1895	0.1869 [‡]
			4	0.1895	0.1847	0.1877	0.1879	0.1857	0.1877	0.1865	0.1869	
			6	0.1869	0.1869	0.1869	0.1869	0.1869	0.1869	0.1869	0.1869	
			8	0.1869	0.1869	0.1869	0.1869	0.1869	0.1869	0.1869	0.1869	
$\beta = 90^\circ$ $\beta_1 = 90^\circ$	PZT-4	FOCC	2	0.3751	0.3749	0.3740	0.3736	0.3735	0.3741	0.3737	0.3738	0.3739 [‡]
			3	0.3737	0.3738	0.3739	0.3739	0.3739	0.3739	0.3739	0.3737	
			4	0.3739	0.3739	0.3739	0.3739	0.3739	0.3739	0.3739	0.3739	
			6	0.3739	0.3739	0.3739	0.3739	0.3739	0.3739	0.3739	0.3739	

[†] 為 Sosa 與 Pak[39] 之結果

[‡] 為 Hwu 與 Ikeda[37] 之結果

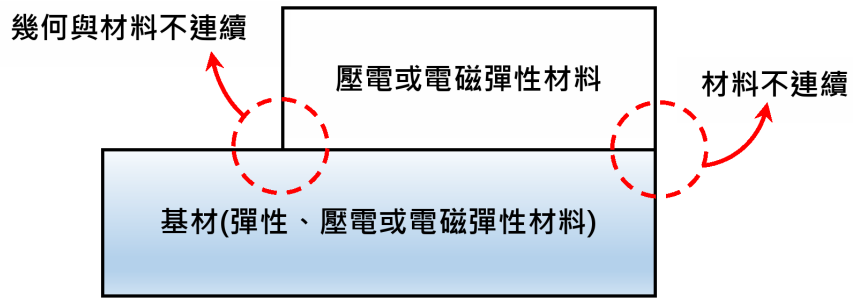


圖 1.1 幾何或材料不連續示意圖

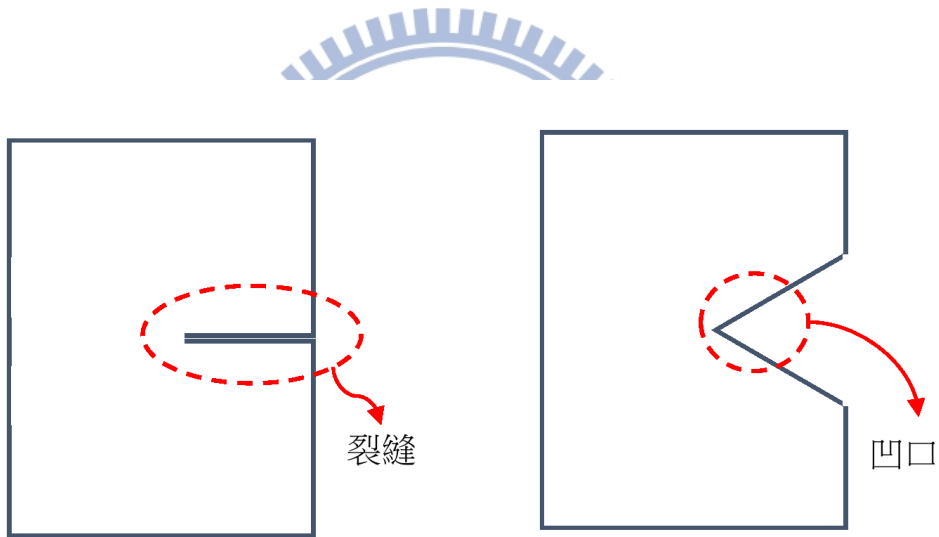


圖 1.2 材料可能缺陷示意圖

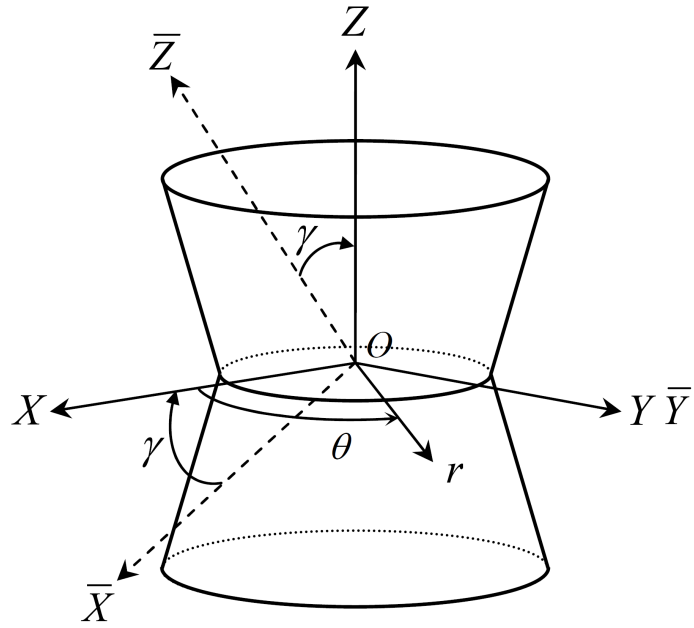


圖 2.1 含尖角之雙材料旋轉體

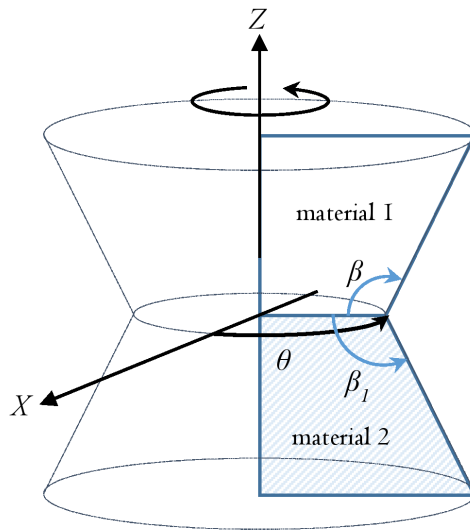


圖 2.2 迴轉體幾何形狀

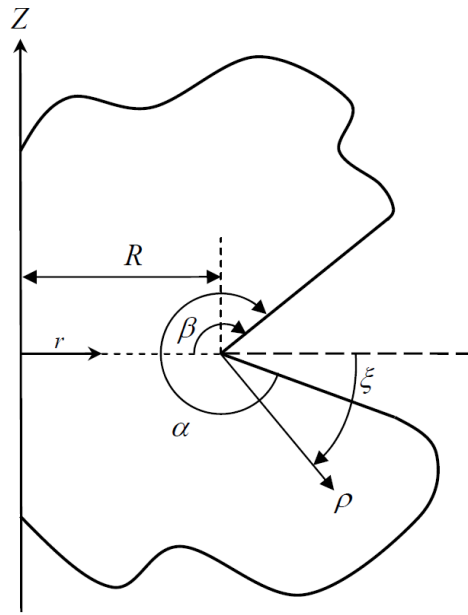


圖 2.3 圓柱 (r, Z) 與尖角 (ρ, ξ) 座標系統

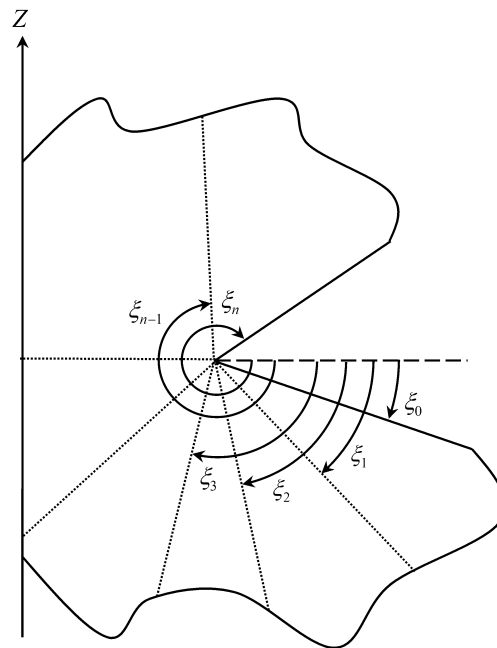
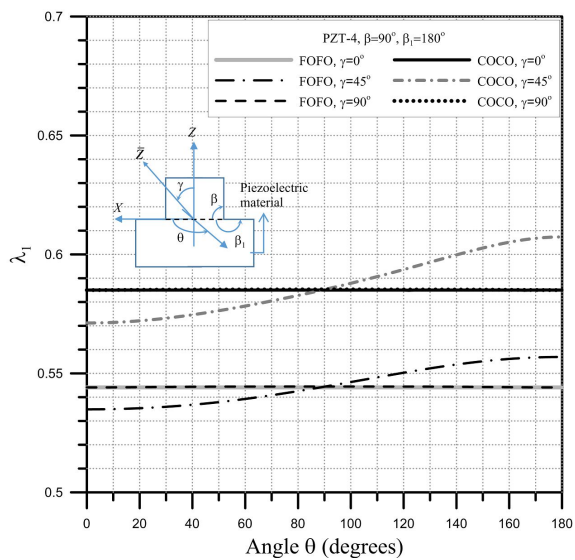
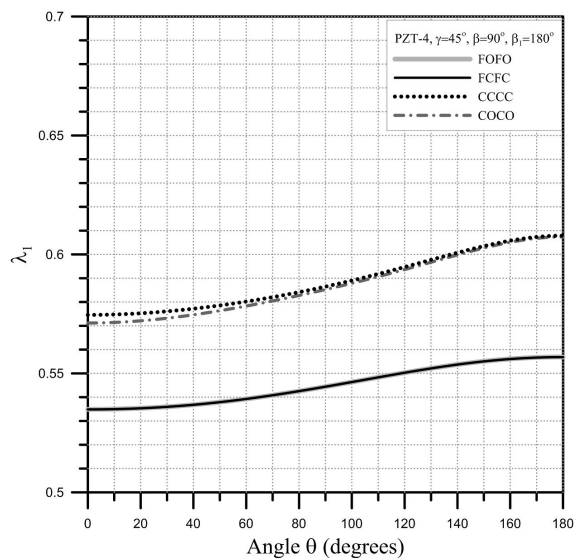


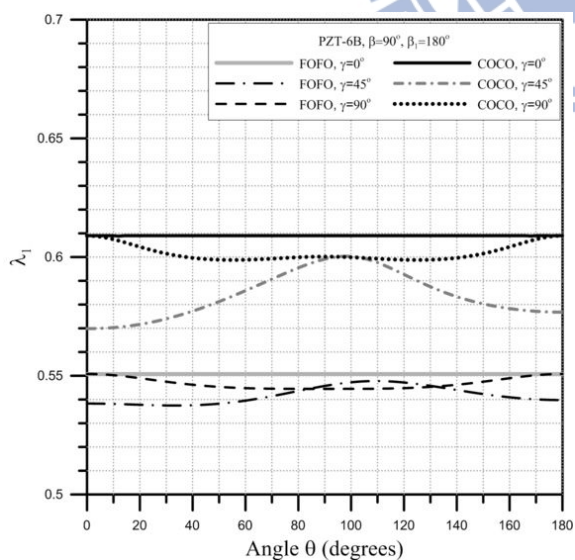
圖 2.4 迴轉體子域 $\xi \in [\xi_0, \xi_n]$



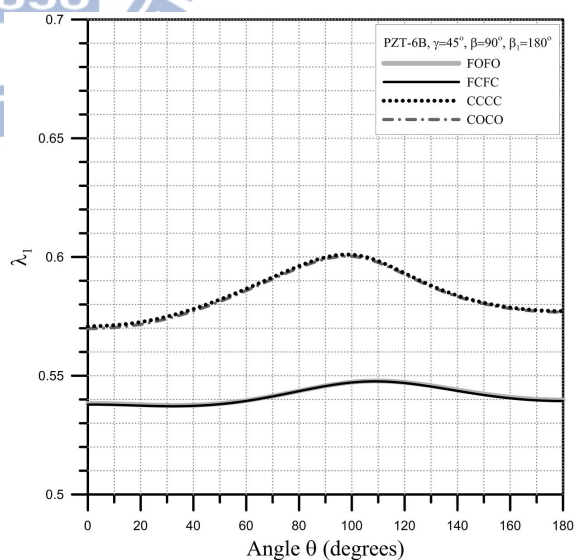
(a)



(b)

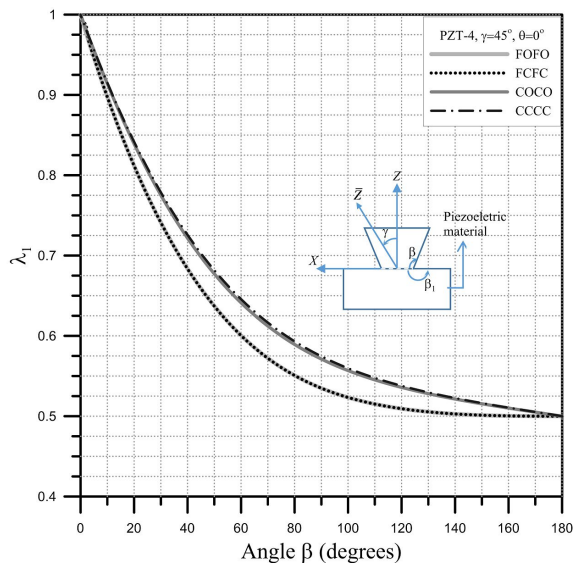
圖 3.1 單 PZT-4 壓電迴轉體 λ_1 隨 θ 之變化

(a)

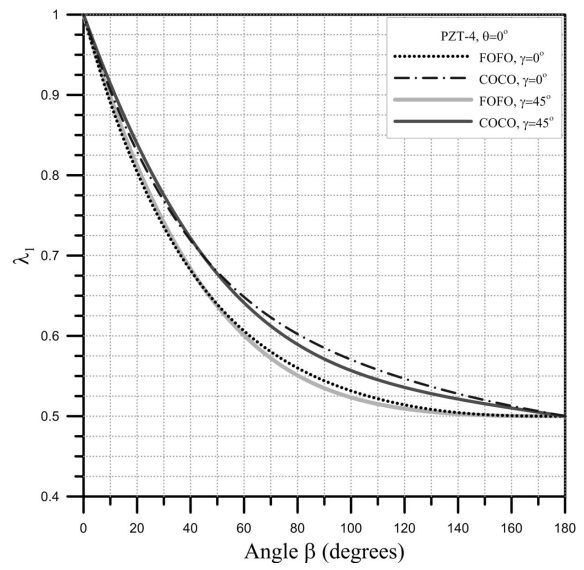


(b)

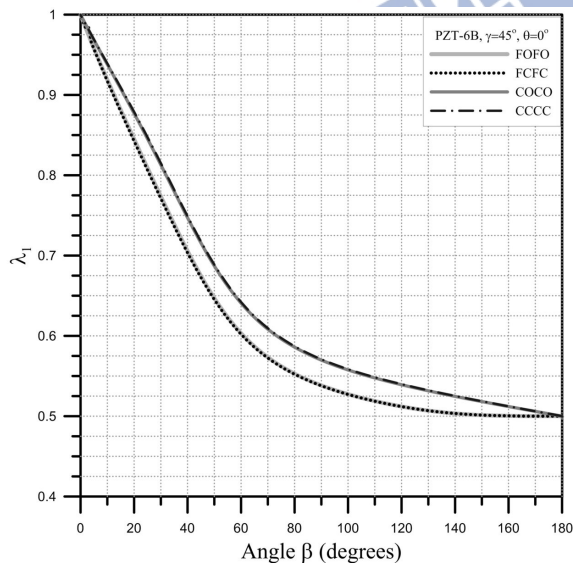
圖 3.2 單 PZT-6B 壓電迴轉體 λ_1 隨 θ 之變化



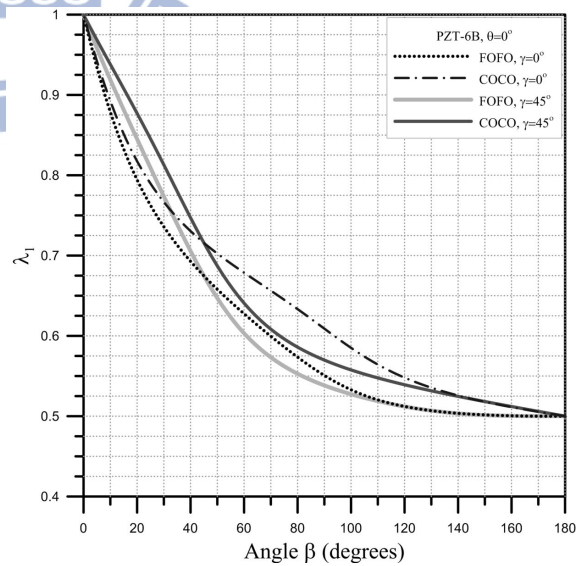
(a)



(b)

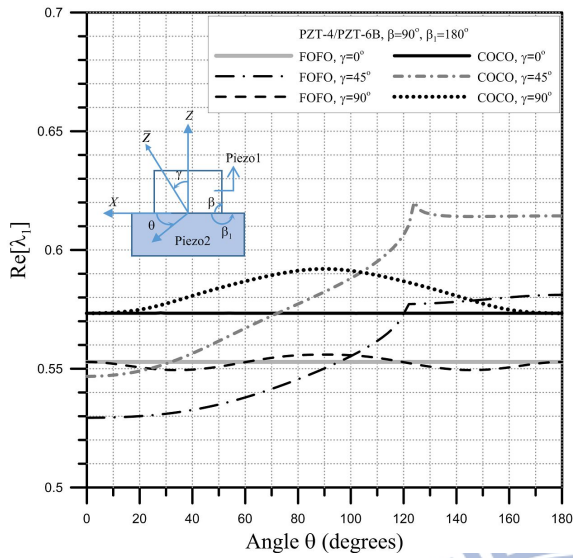
圖 3.3 不同邊界條件下單 PZT-4 迴轉體 λ_1 隨 β 之變化

(a)

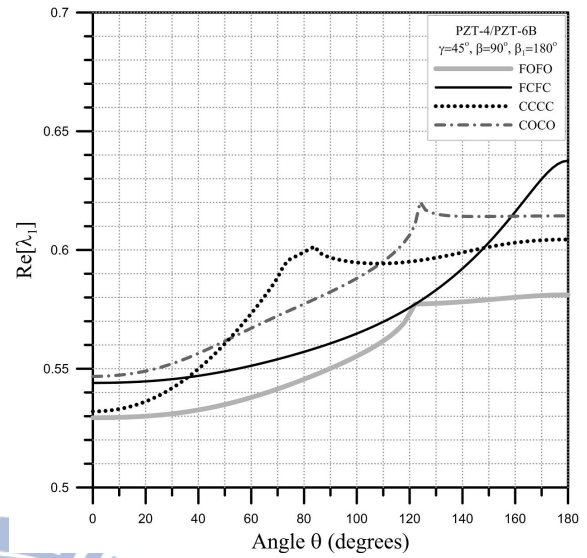


(b)

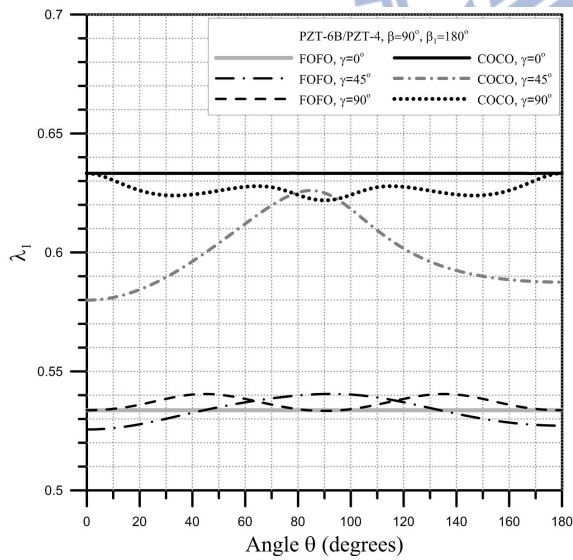
圖 3.4 不同邊界條件下單 PZT-6B 迴轉體 λ_1 隨 β 之變化



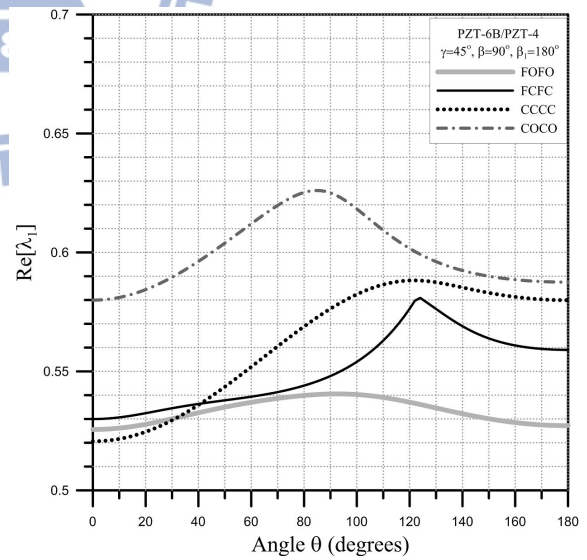
(a)



(b)

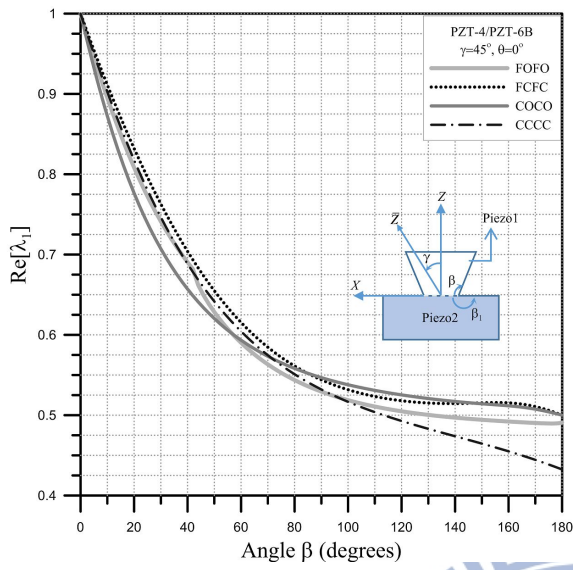


(c)

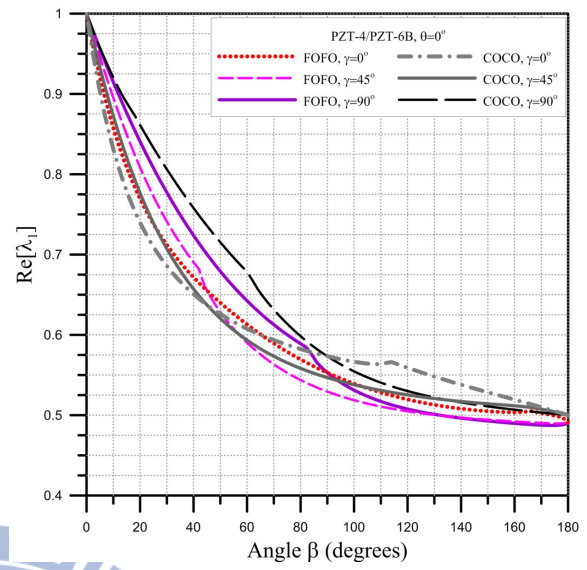


(d)

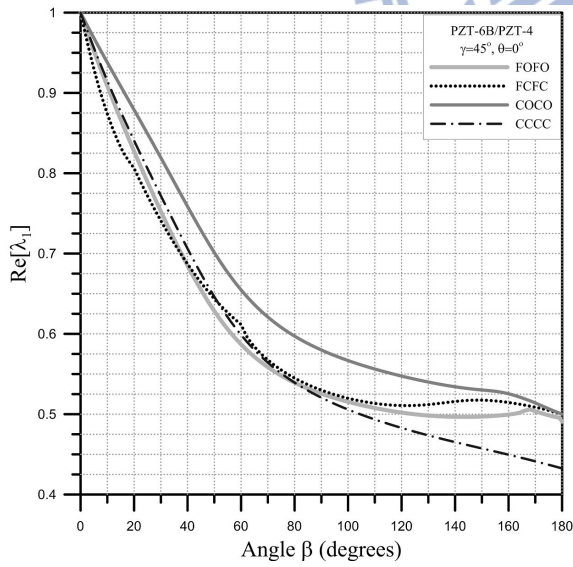
圖 3.5 雙壓電迴轉體 $Re[\lambda_1]$ 隨 θ 之變化



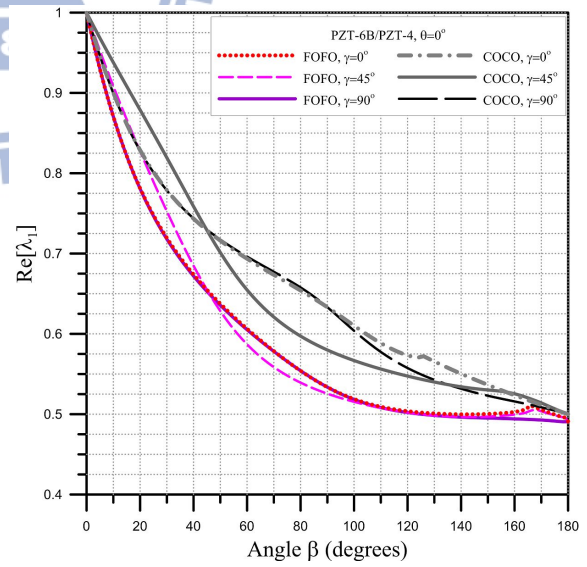
(a)



(b)

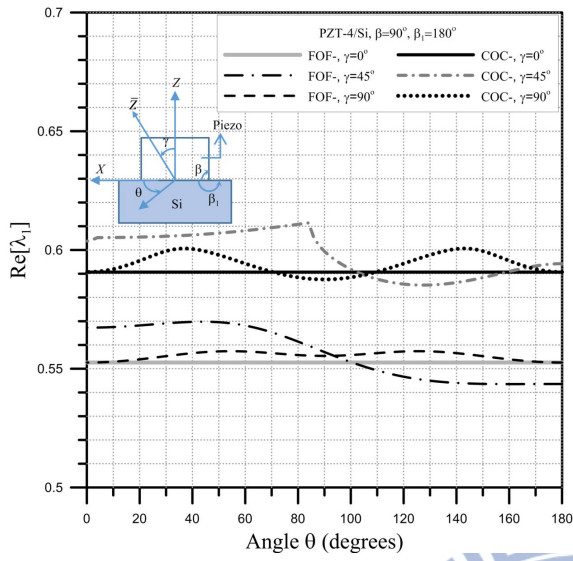


(c)

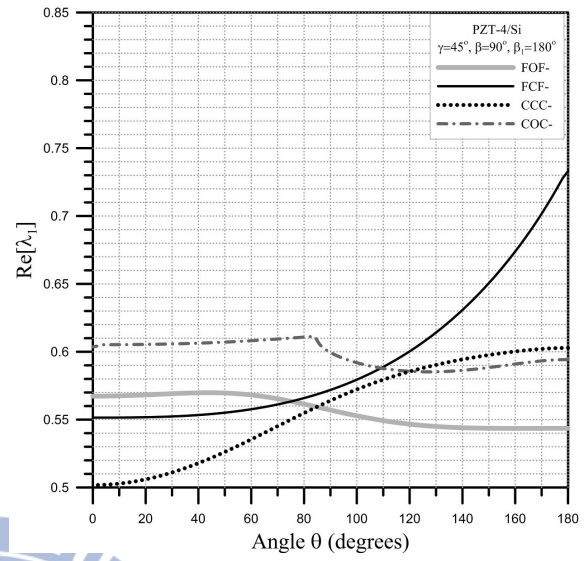


(d)

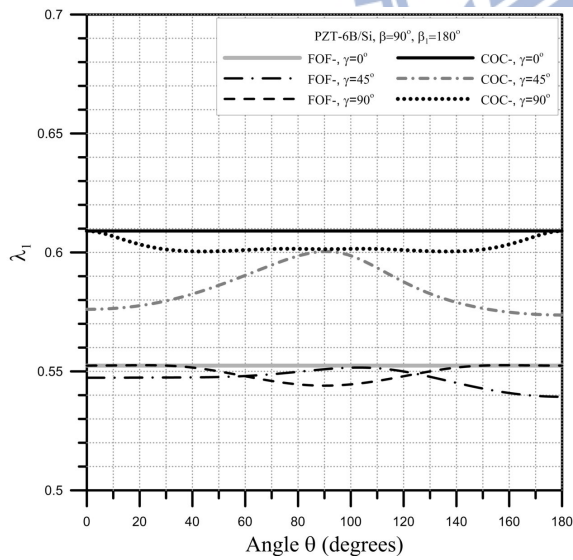
圖 3.6 不同邊界條件下雙壓電迴轉體 $Re[\lambda_1]$ 之變化



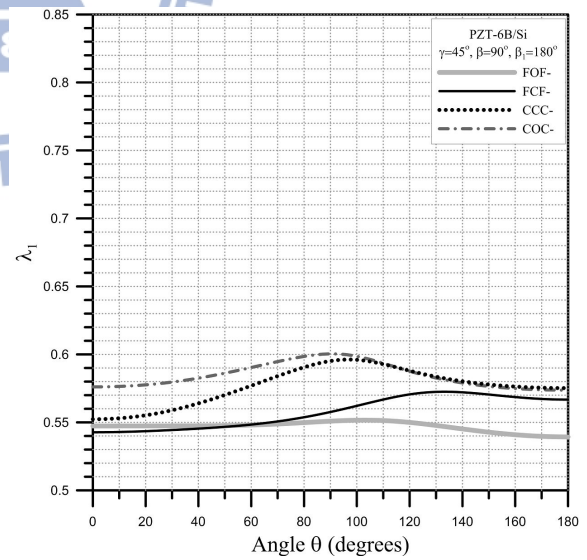
(a)



(b)

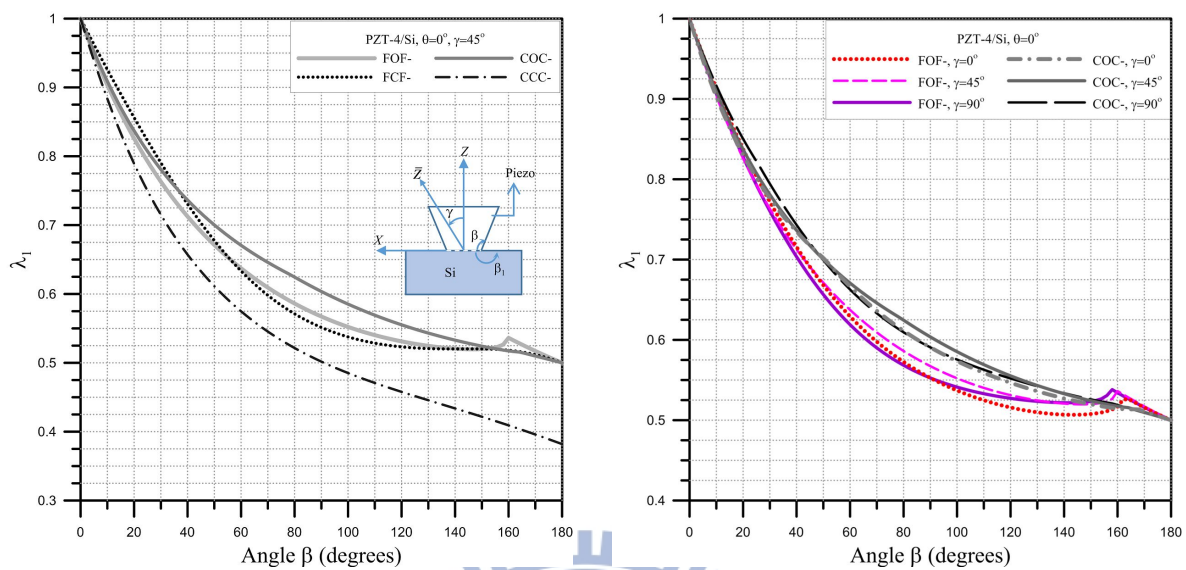


(c)



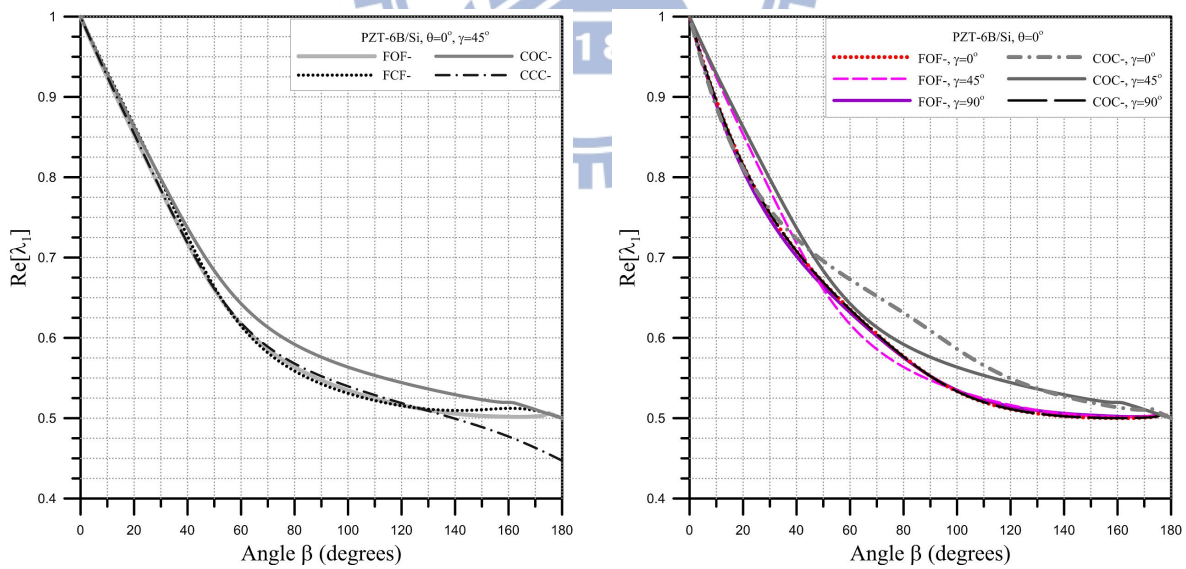
(d)

圖 3.7 壓電材料/Si 迴轉體 $Re[\lambda_1]$ 隨 θ 之變化



(a)

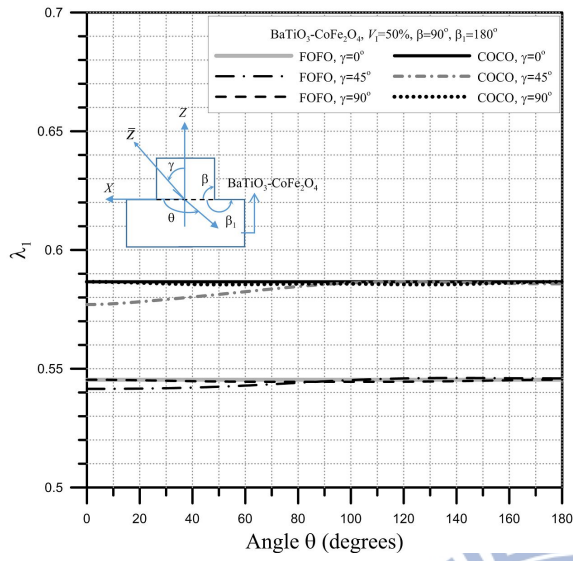
(b)



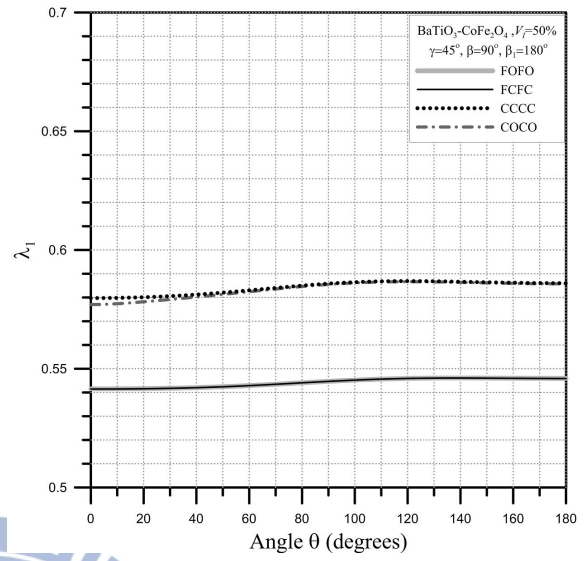
(c)

(d)

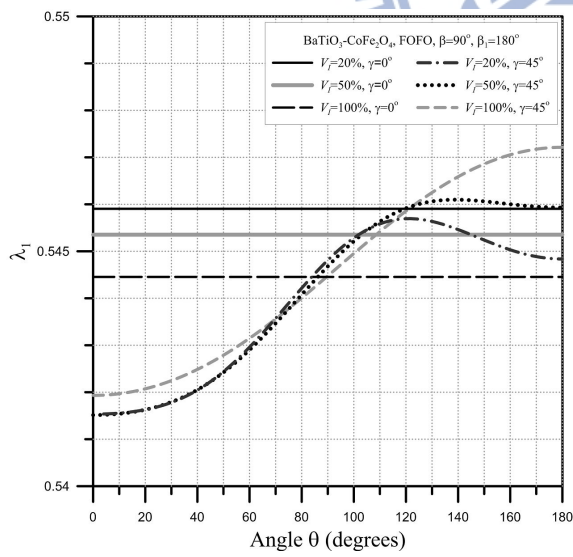
圖 3.8 不同邊界條件下壓電材料/Si 迴轉體 $\text{Re}[\lambda_1]$ 隨 β 之變化



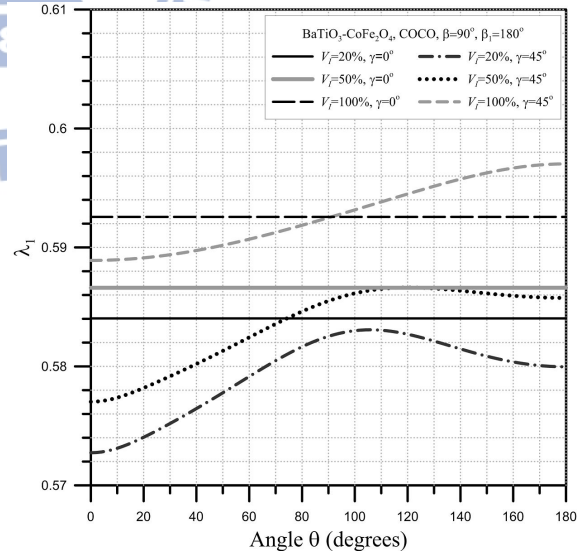
(a)



(b)

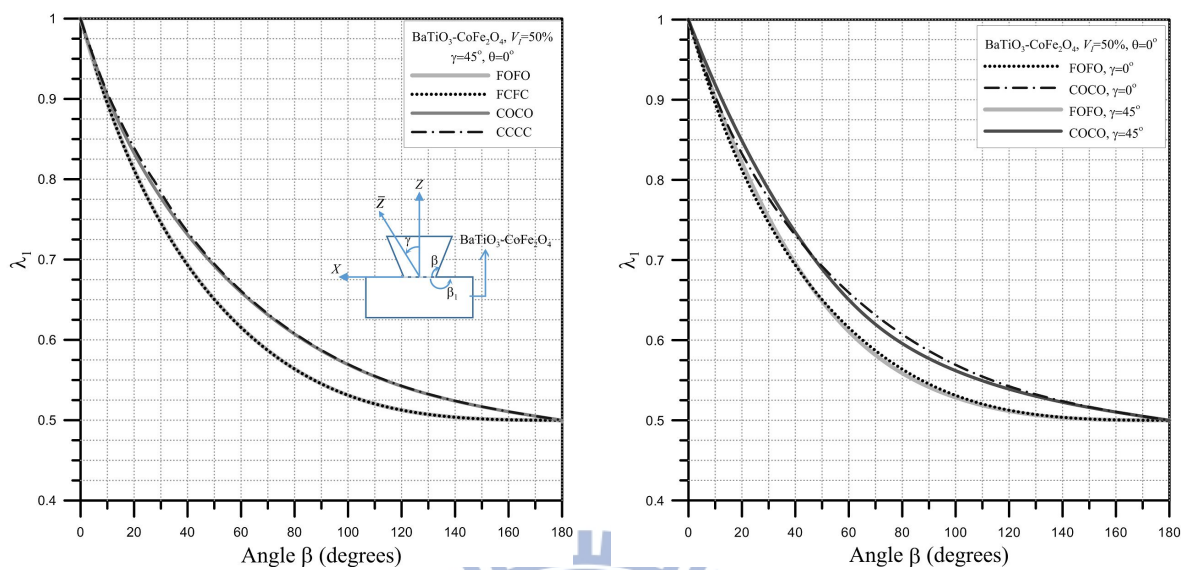


(c)



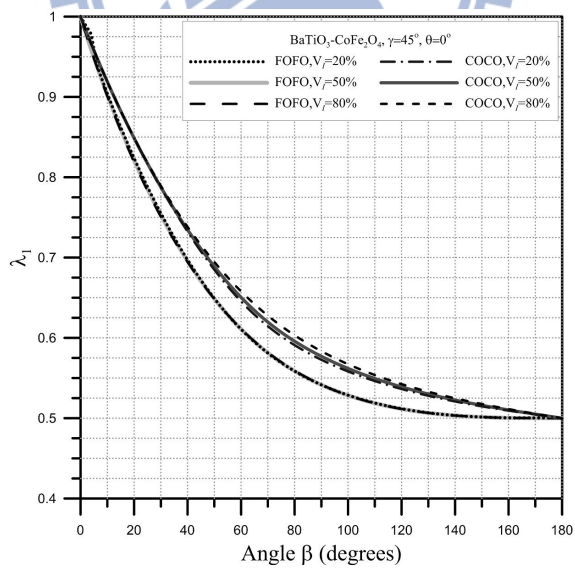
(d)

圖 3.9 單 $\text{BaTiO}_3\text{-CoFe}_2\text{O}_4$ 迴轉體 λ_1 隨 θ 之變化



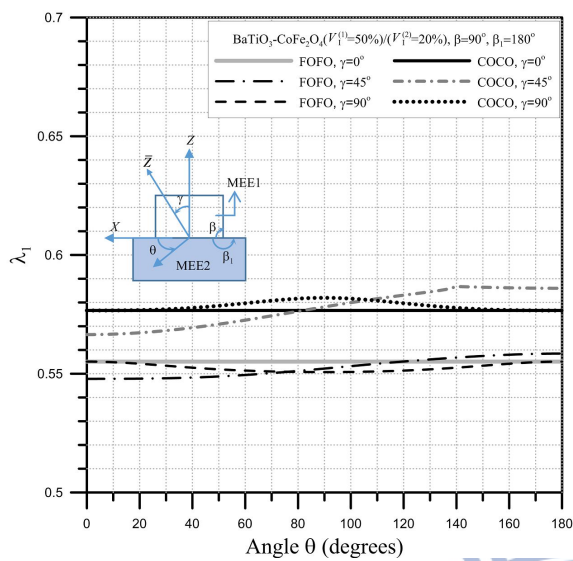
(a)

(b)

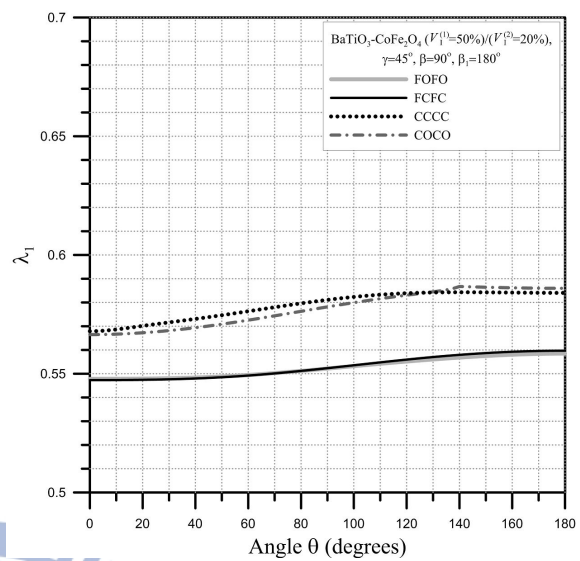


(c)

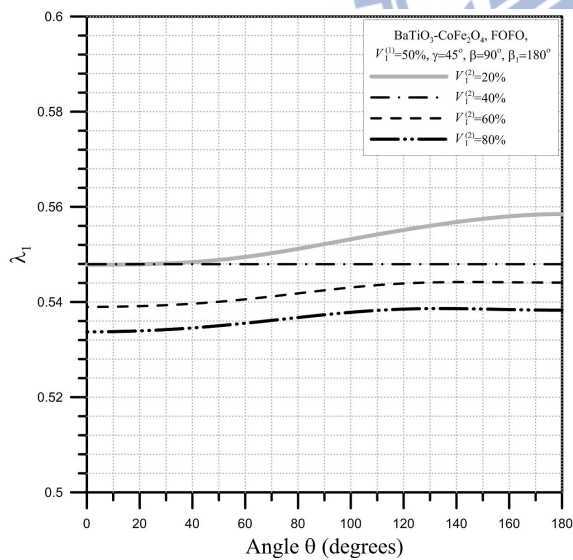
圖 3.10 不同邊界條件下單 $\text{BaTiO}_3\text{-CoFe}_2\text{O}_4$ 迴轉體 λ_1 隨 β 之變化



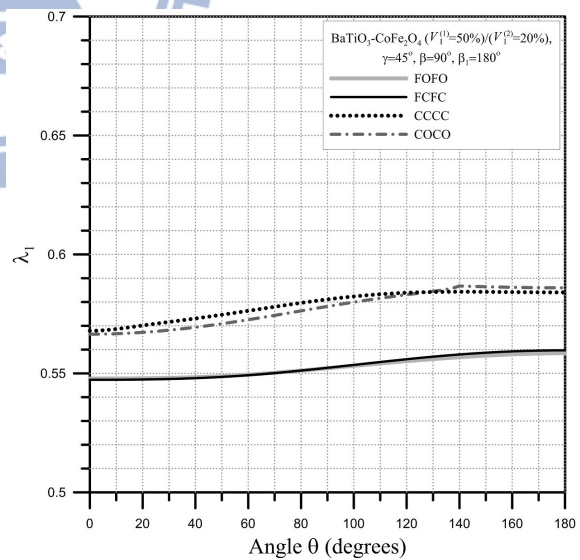
(a)



(b)



(c)



(d)

圖 3.11 雙 $\text{BaTiO}_3\text{-CoFe}_2\text{O}_4$ 迴轉體 λ_1 隨 θ 之變化

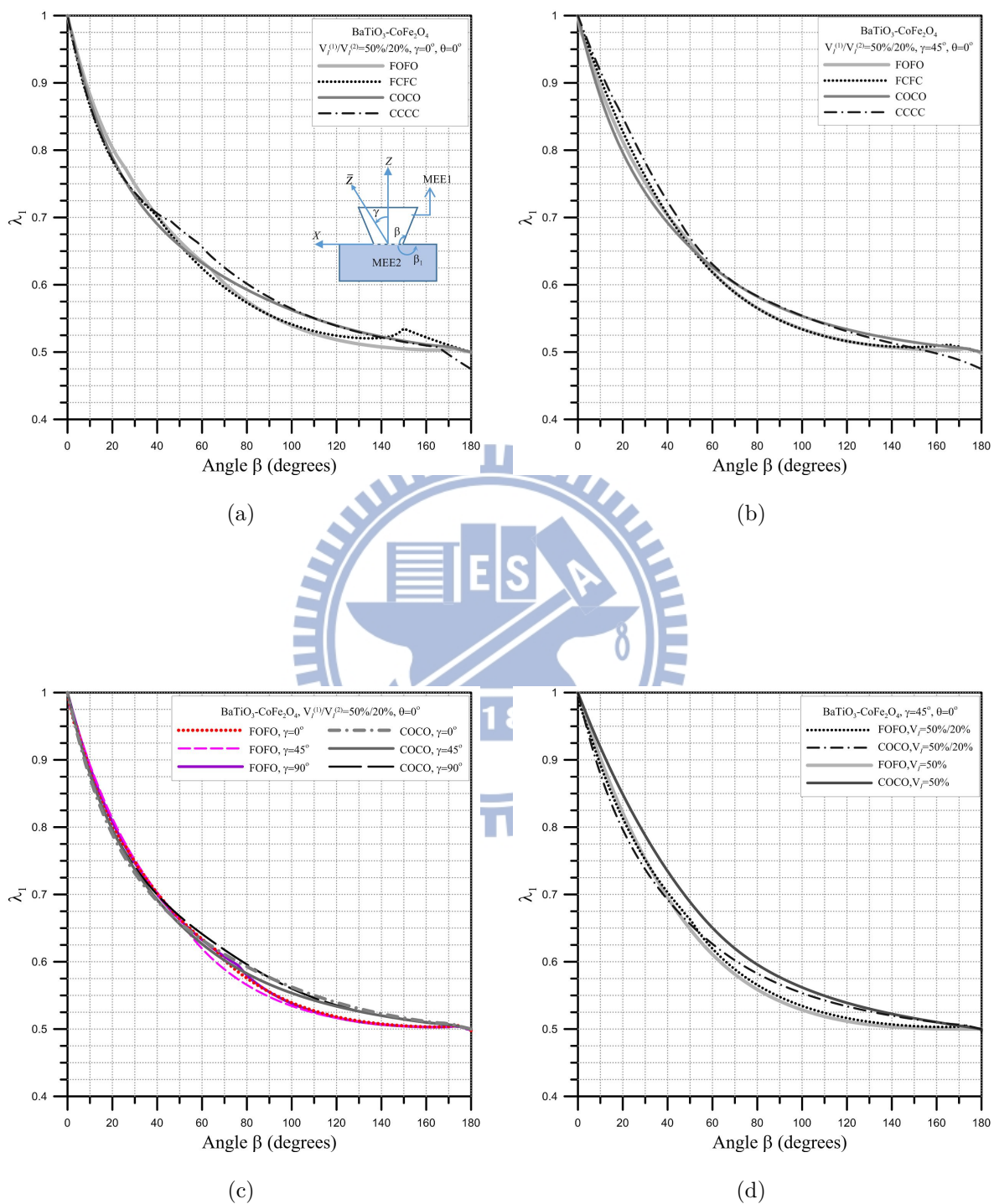
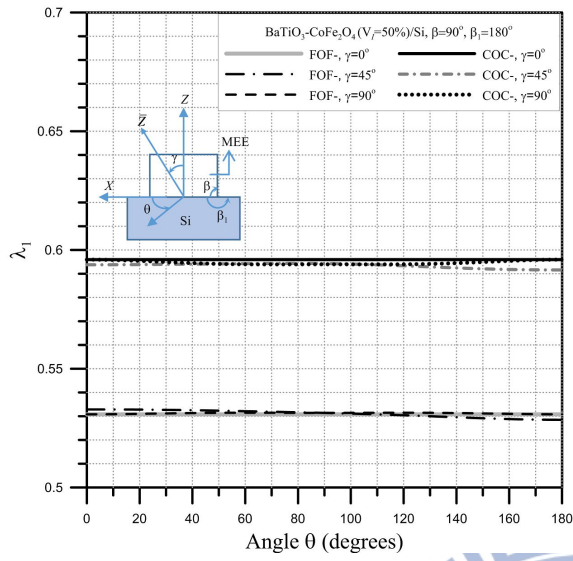
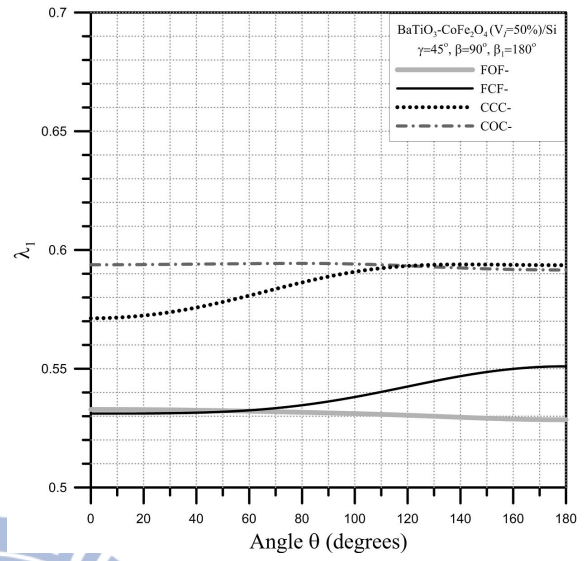


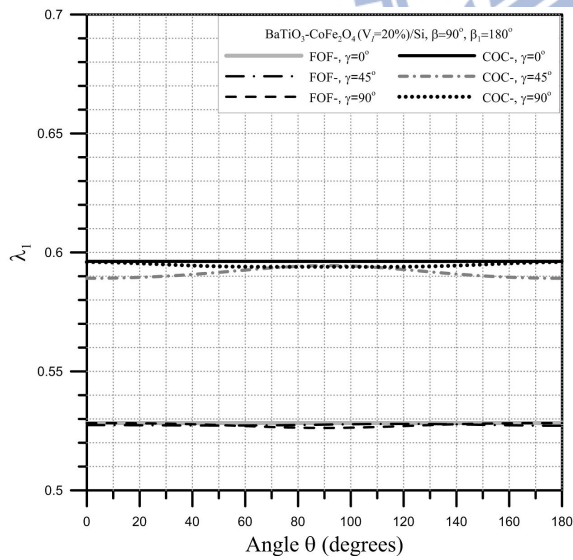
圖 3.12 不同邊界條件下雙 $\text{BaTiO}_3\text{-CoFe}_2\text{O}_4$ 迴轉體 $\text{Re}[\lambda_1]$ 隨 β 之變化



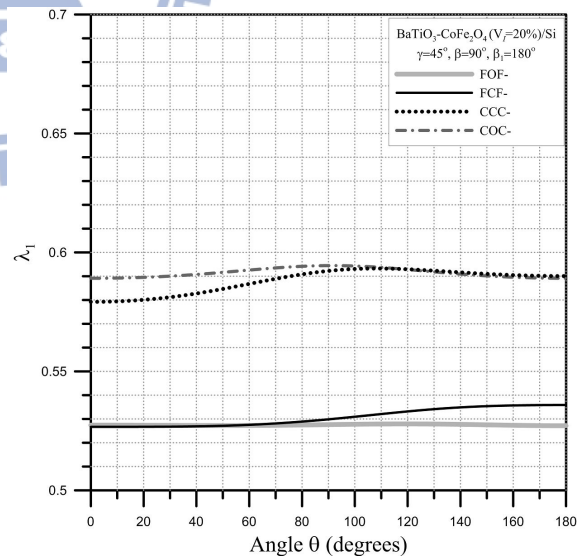
(a)



(b)



(c)



(d)

圖 3.13 $\text{BaTiO}_3\text{-CoFe}_2\text{O}_4$ / Si 迴轉體 λ_1 隨 θ 之變化

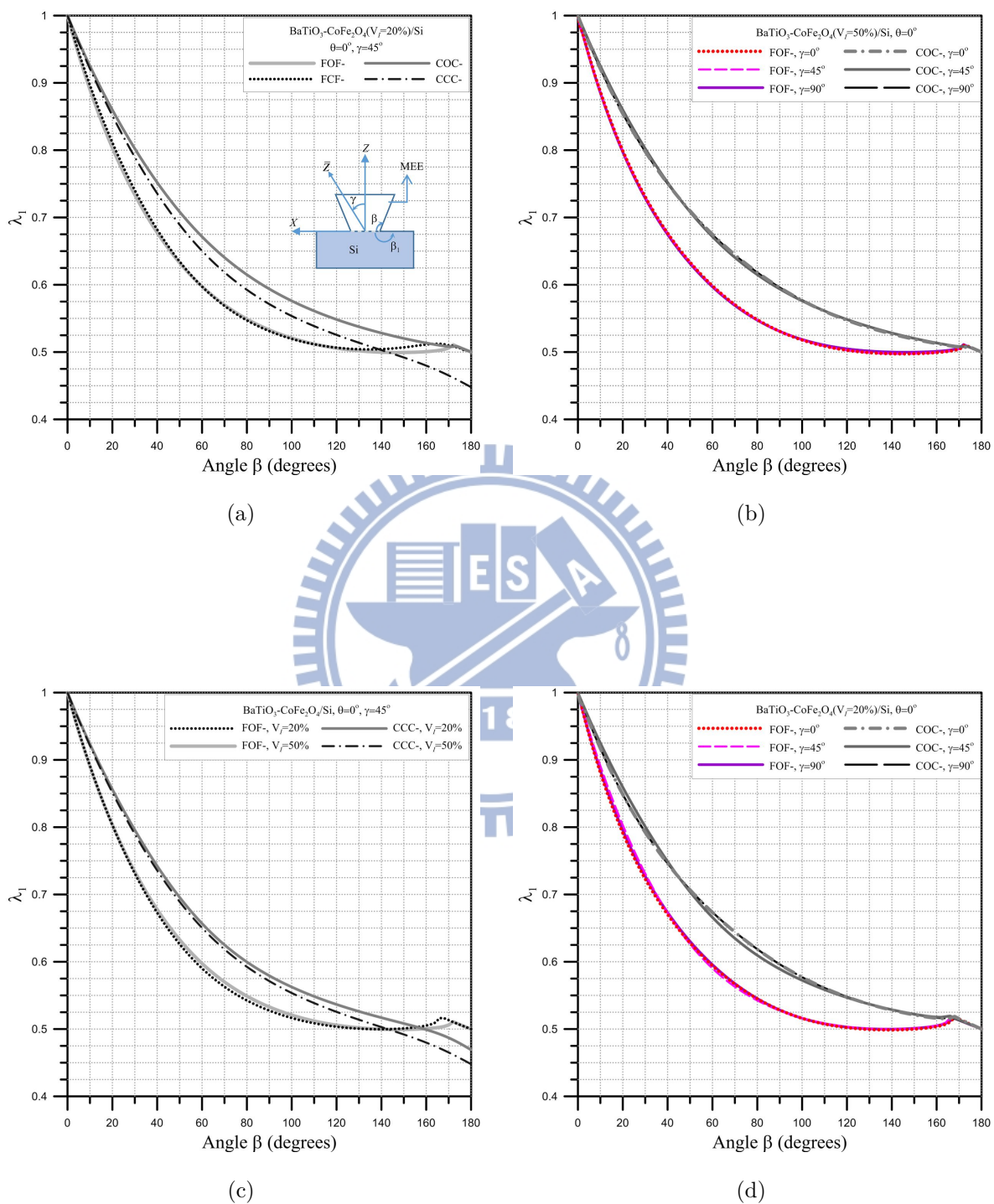
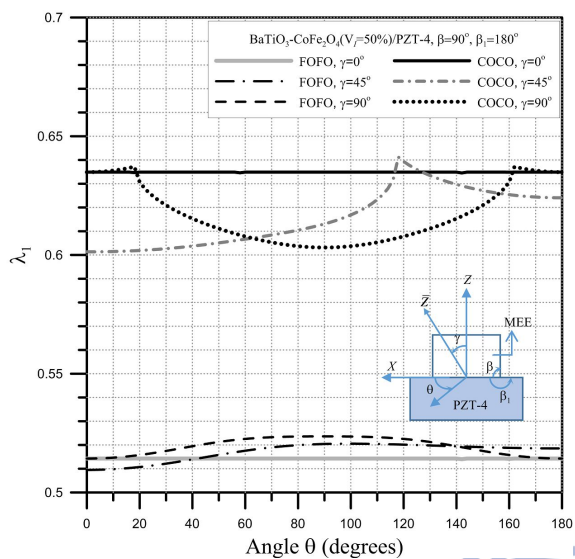
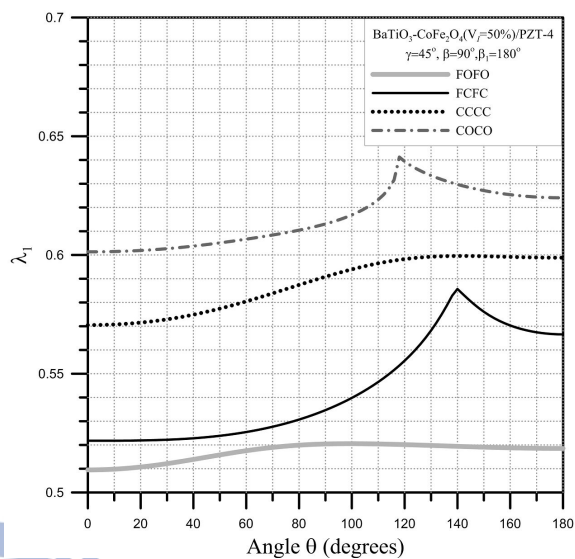


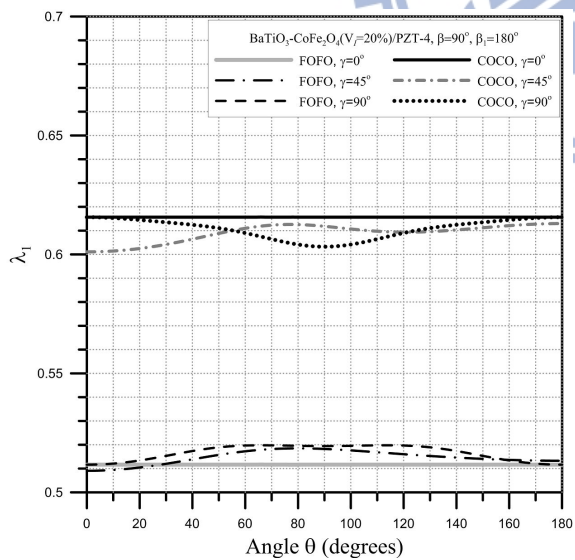
圖 3.14 不同邊界條件下 $\text{BaTiO}_3\text{-CoFe}_2\text{O}_4/\text{Si}$ 迴轉體 $\text{Re}[\lambda_1]$ 隨 β 之變化



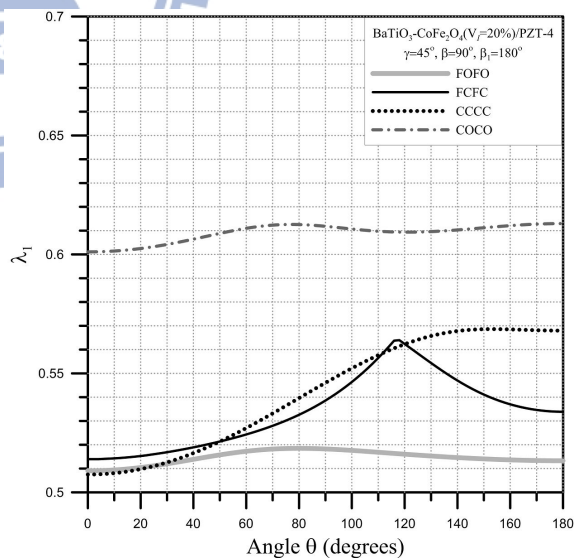
(a)



(b)

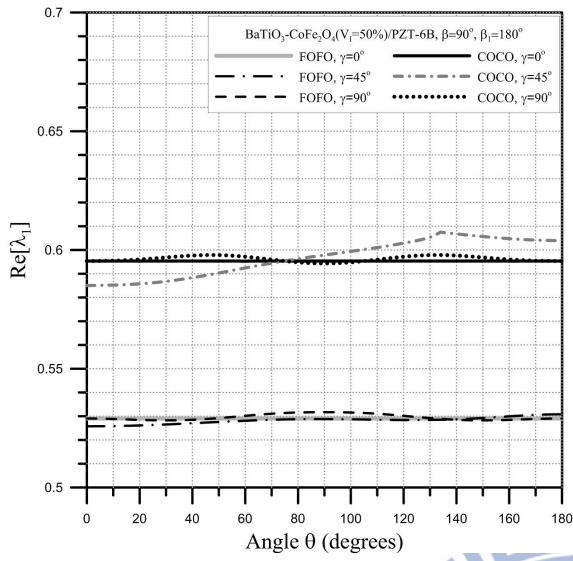


(c)

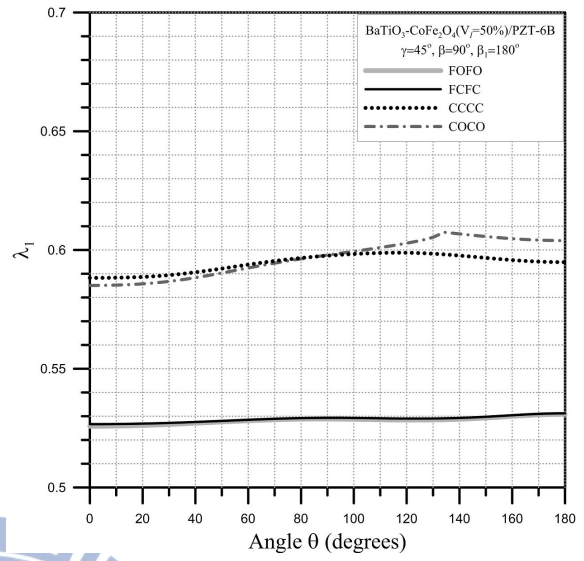


(d)

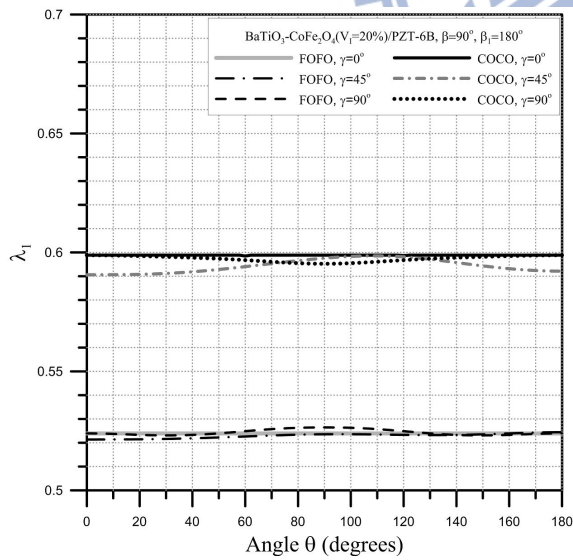
圖 3.15 $\text{BaTiO}_3\text{-CoFe}_2\text{O}_4/\text{PZT-4}$ 迴轉體 $\text{Re}[\lambda_1]$ 隨 θ 之變化



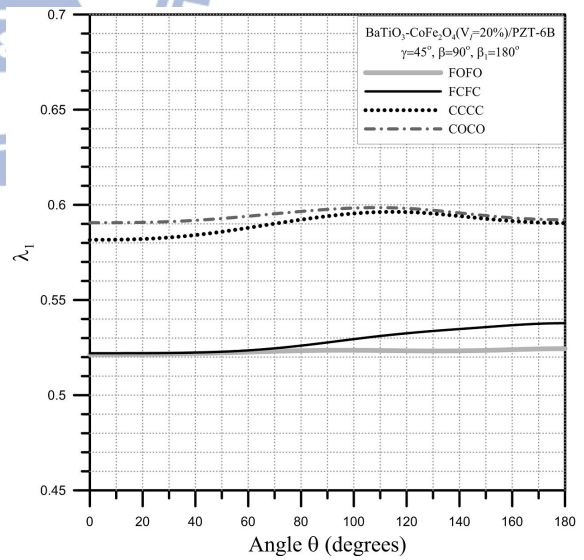
(a)



(b)



(c)



(d)

圖 3.16 $BaTiO_3-CoFe_2O_4/PZT-6B$ 迴轉體 $Re[\lambda_1]$ 隨 θ 之變化

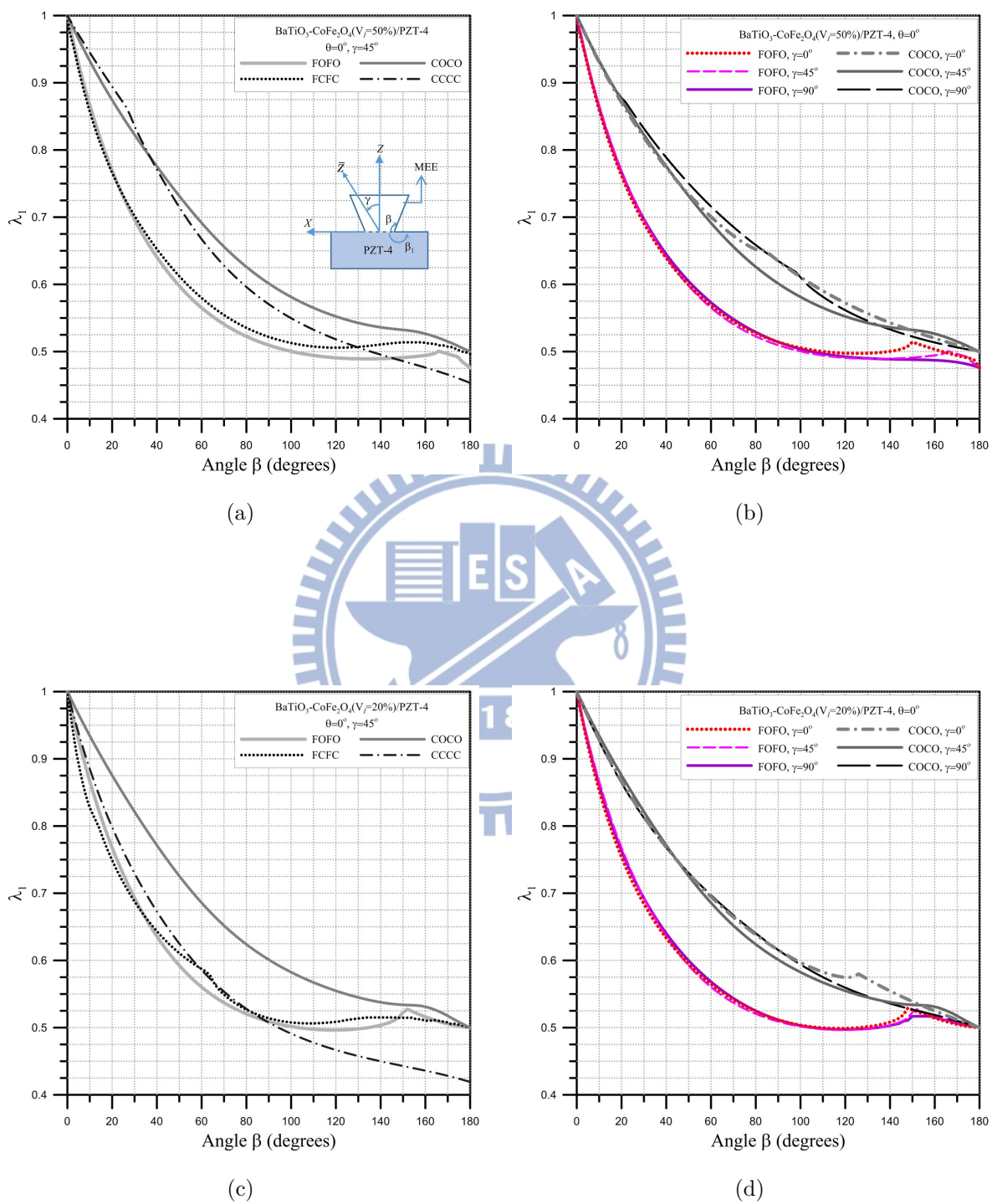


圖 3.17 不同邊界條件下 $\text{BaTiO}_3\text{-CoFe}_2\text{O}_4/\text{PZT-4}$ 迴轉體 $\text{Re}[\lambda_1]$ 隨 β 之變化

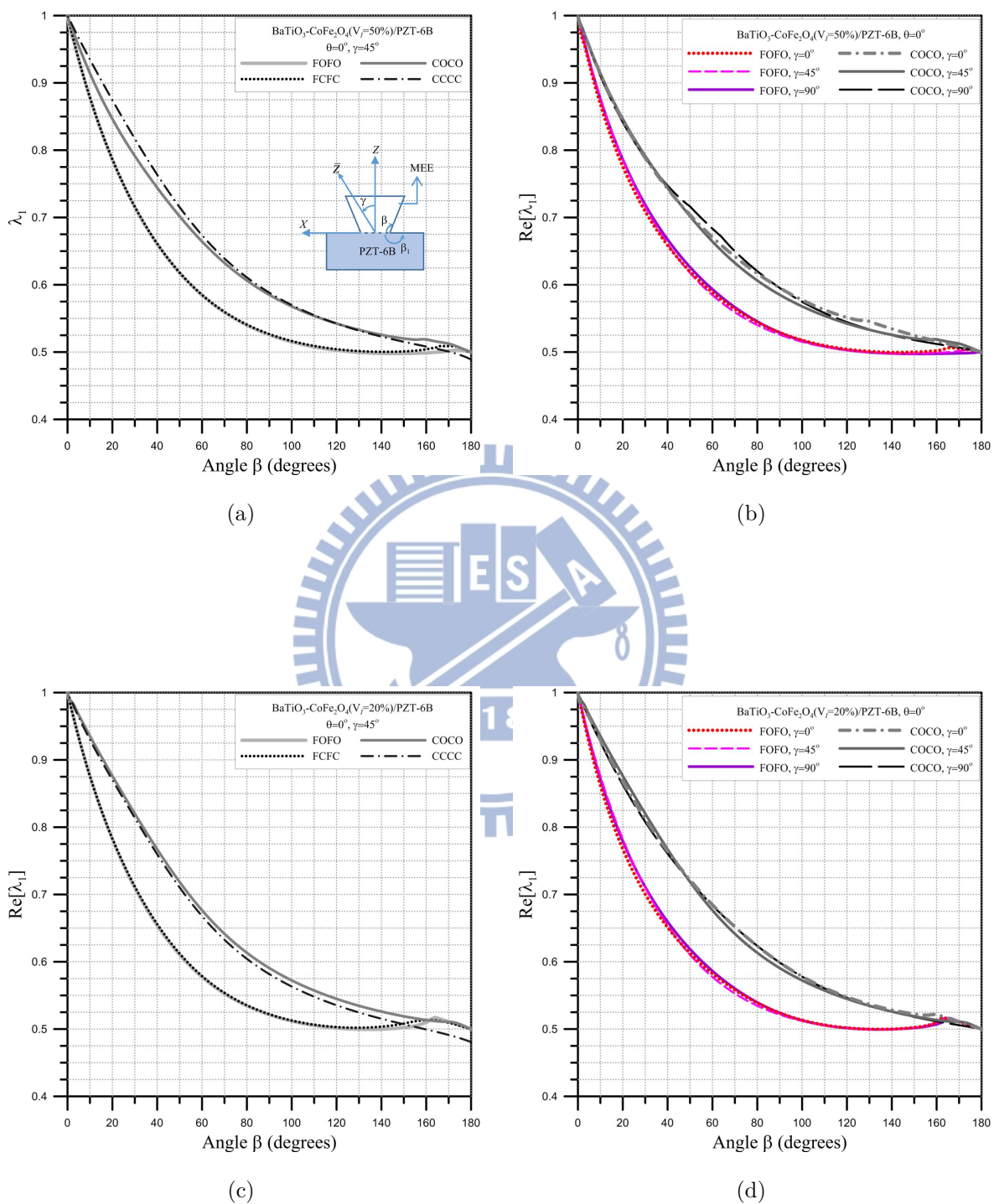


圖 3.18 不同邊界條件下 $\text{BaTiO}_3\text{-CoFe}_2\text{O}_4/\text{PZT-6B}$ 迴轉體 $\text{Re}[\lambda_1]$ 隨 β 之變化

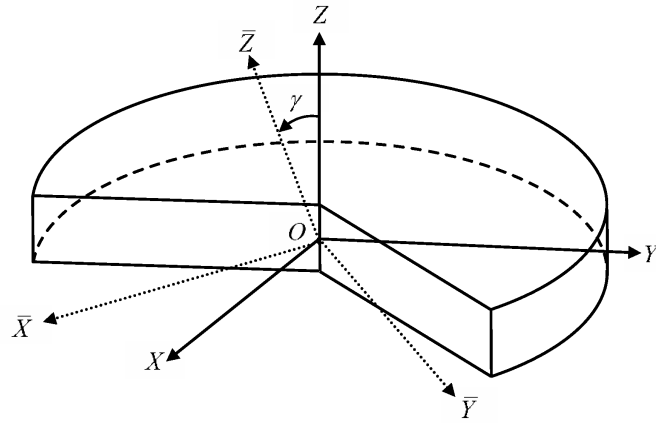


圖 4.1 楔形體示意圖

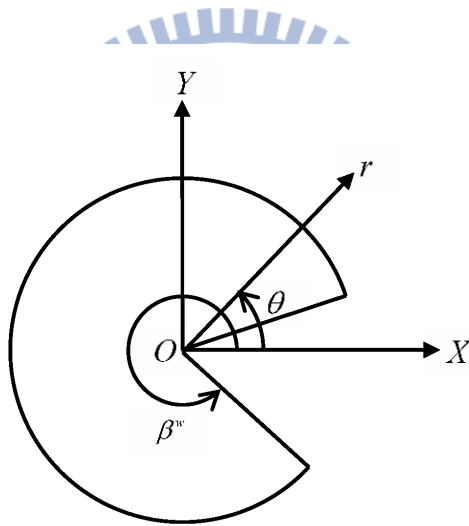


圖 4.2 楔形體 (r, θ) 座標系統

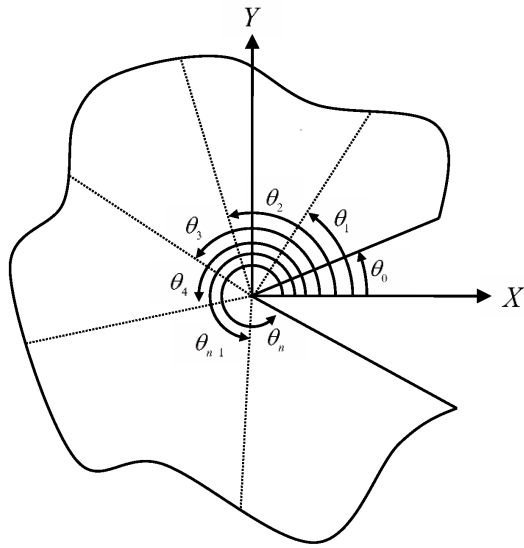


圖 4.3 楔形體子域 $\theta \in [\theta_0, \theta_n]$

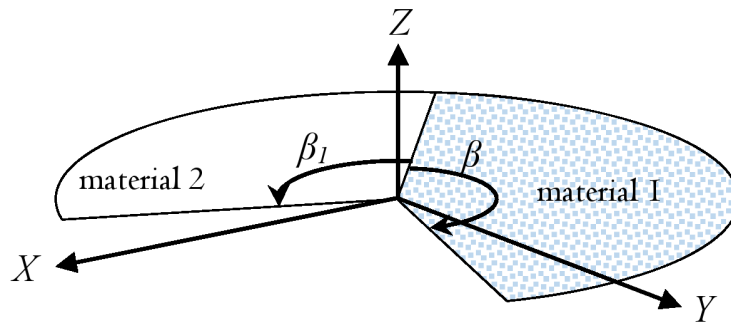
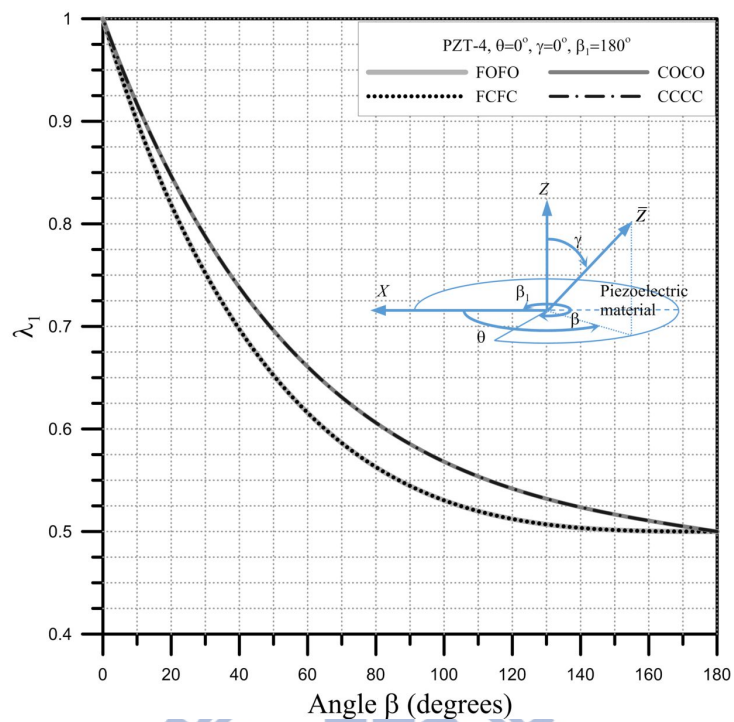
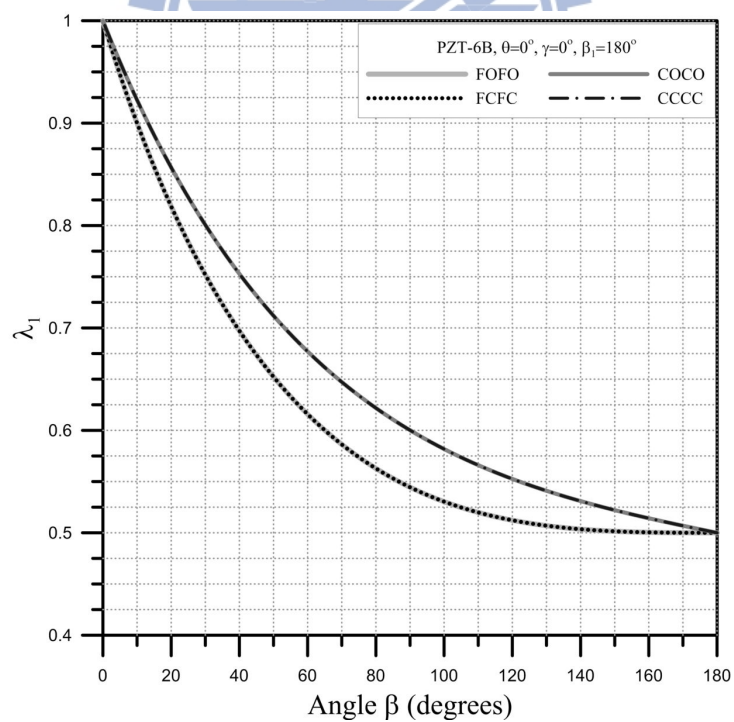


圖 4.4 楔形體幾何示意圖

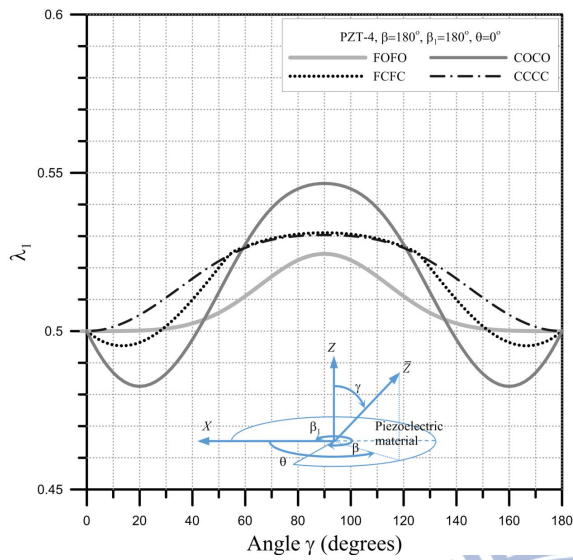


(a)

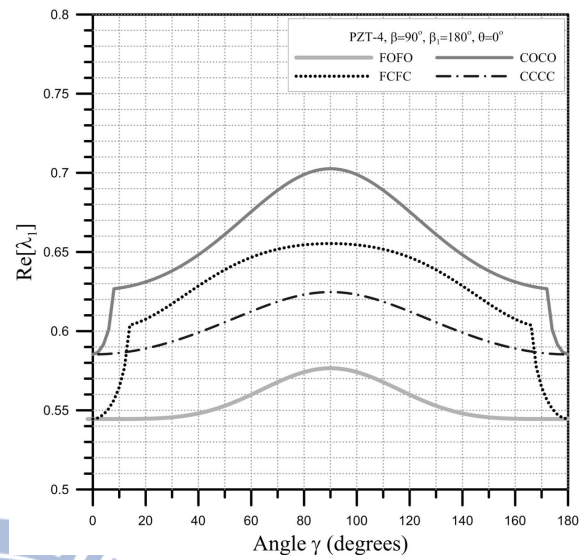


(b)

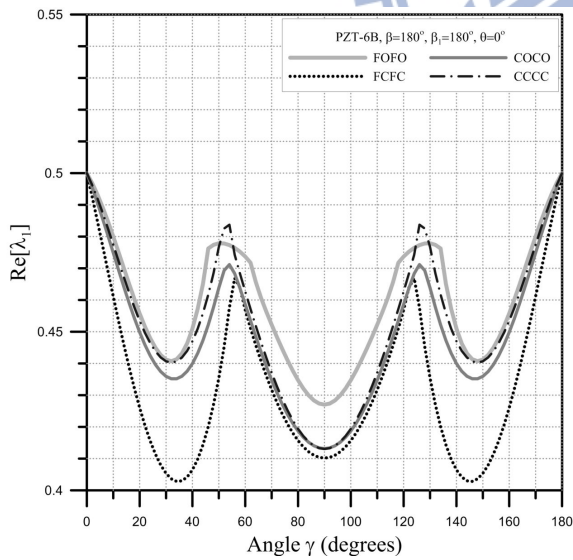
圖 5.1 不同邊界條件下單壓電材料楔形體 λ_1 隨 β 之變化



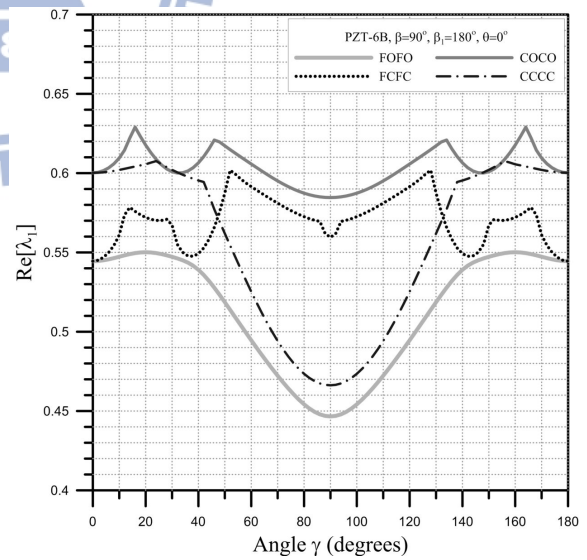
(a)



(b)



(c)



(d)

圖 5.2 不同邊界條件下單壓電材料楔形體 $Re[\lambda_1]$ 隨 γ 之變化

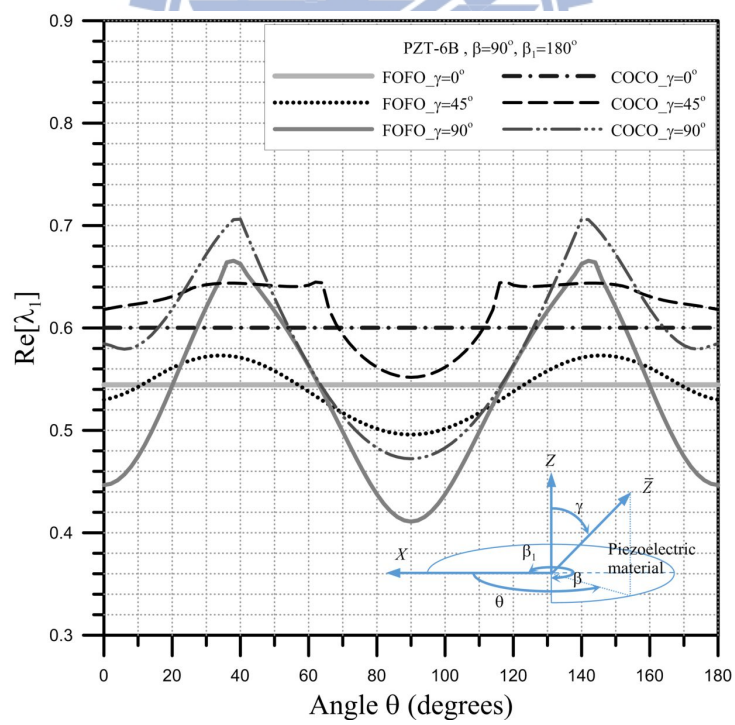
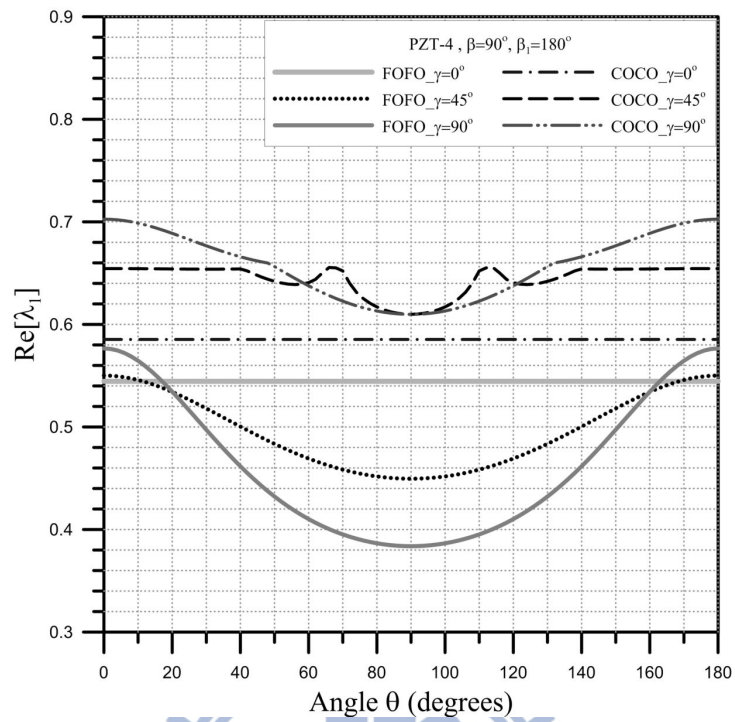
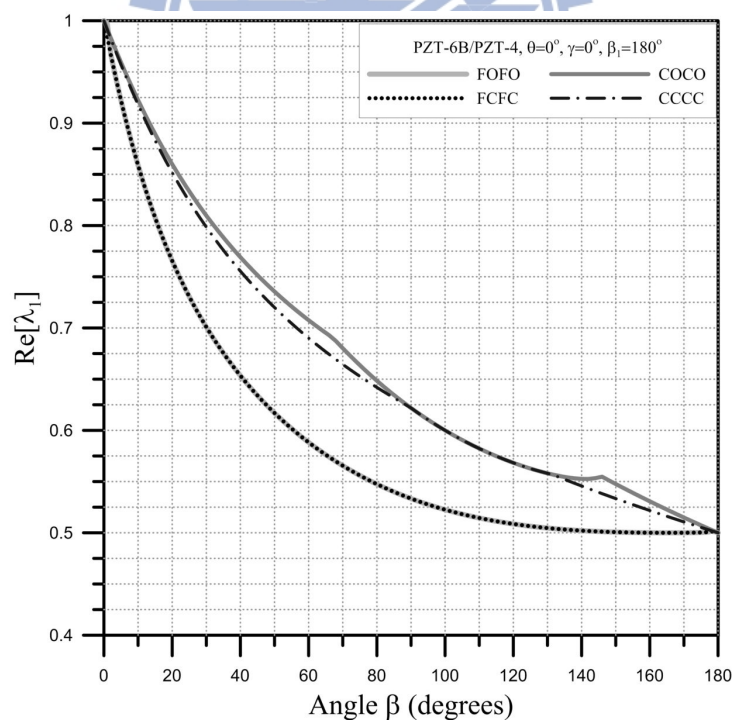
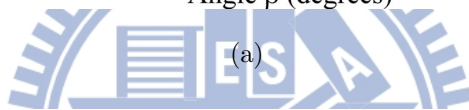
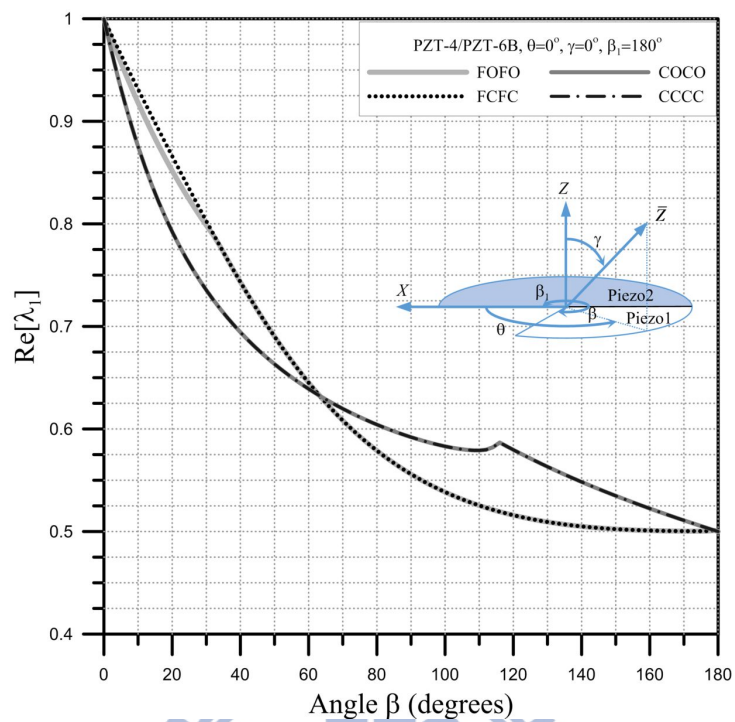
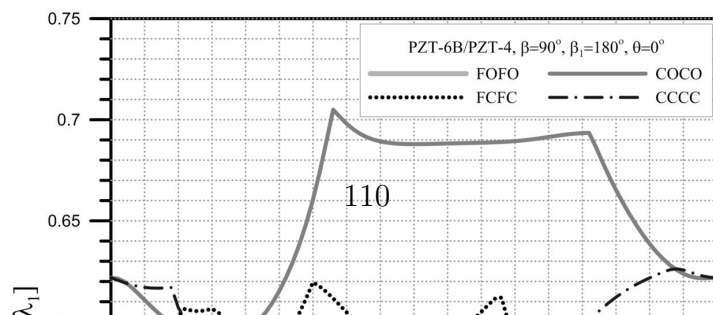
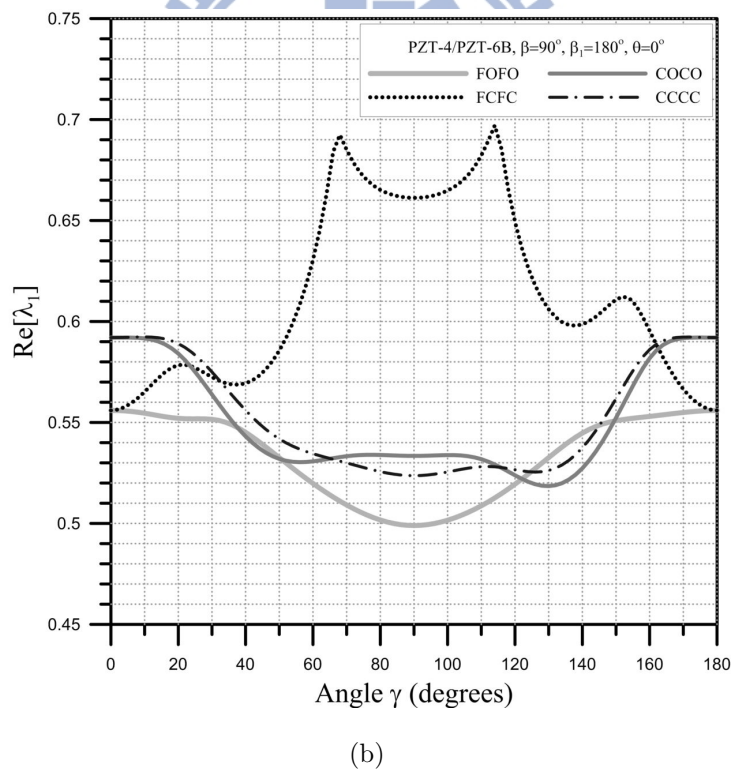
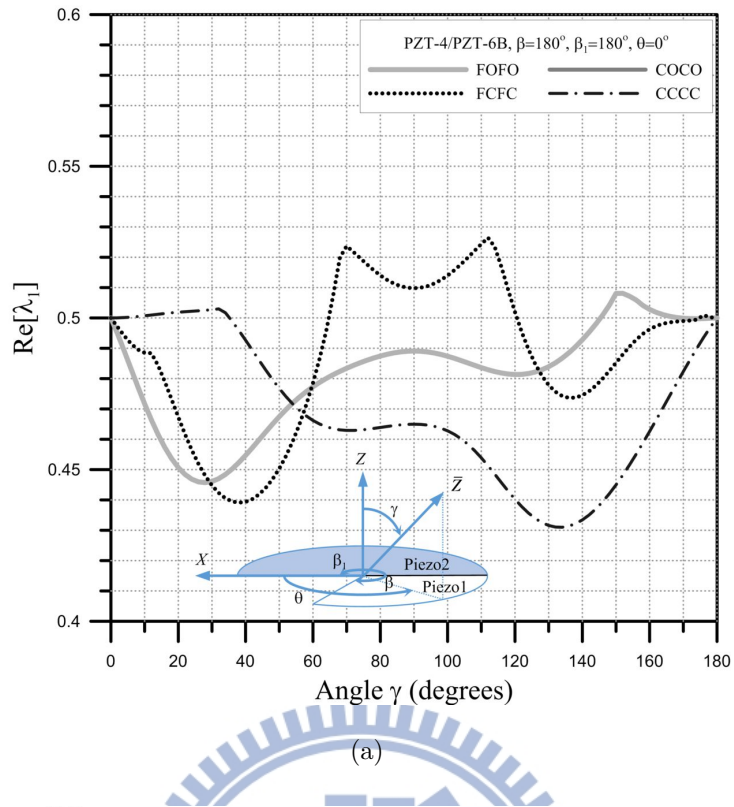


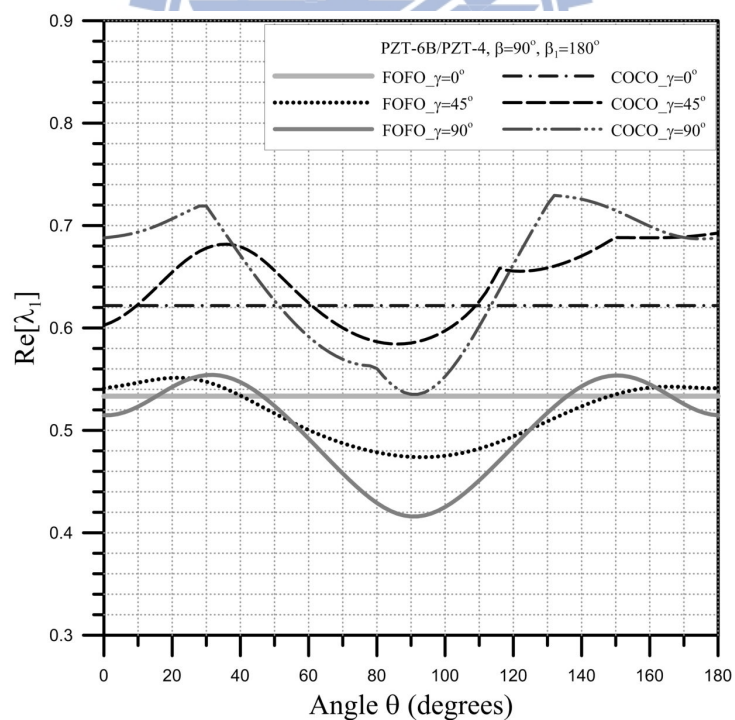
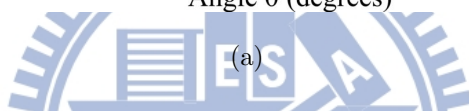
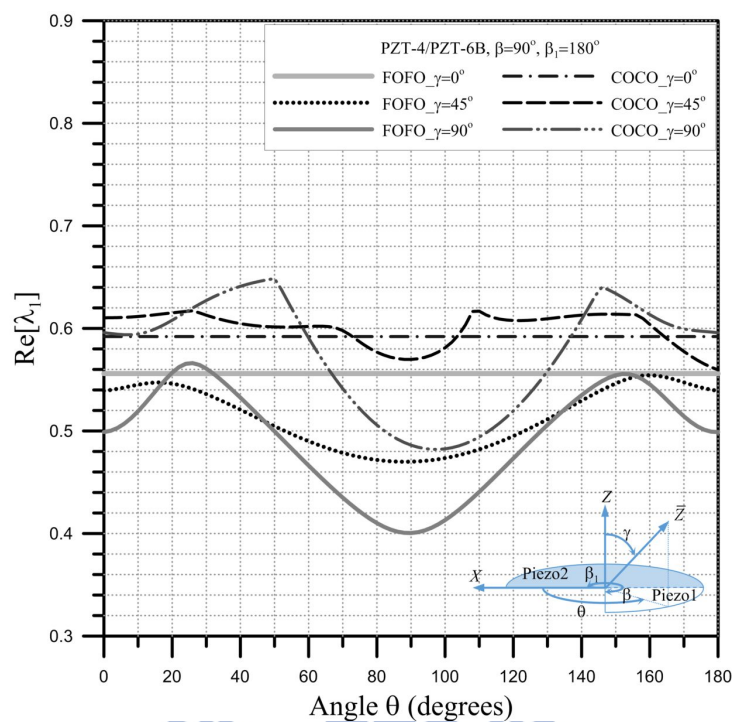
圖 5.3 不同邊界條件下單壓電材料楔形體 $\text{Re}[\lambda_1]$ 隨 θ 之變化



(b)

圖 5.4 不同邊界條件下雙壓電材料楔形體 $\text{Re}[\lambda_1]$ 隨 β 之變化





(b)

圖 5.6 不同邊界條件下雙壓電材料楔形體 $Re[\lambda_1]$ 隨 θ 之變化

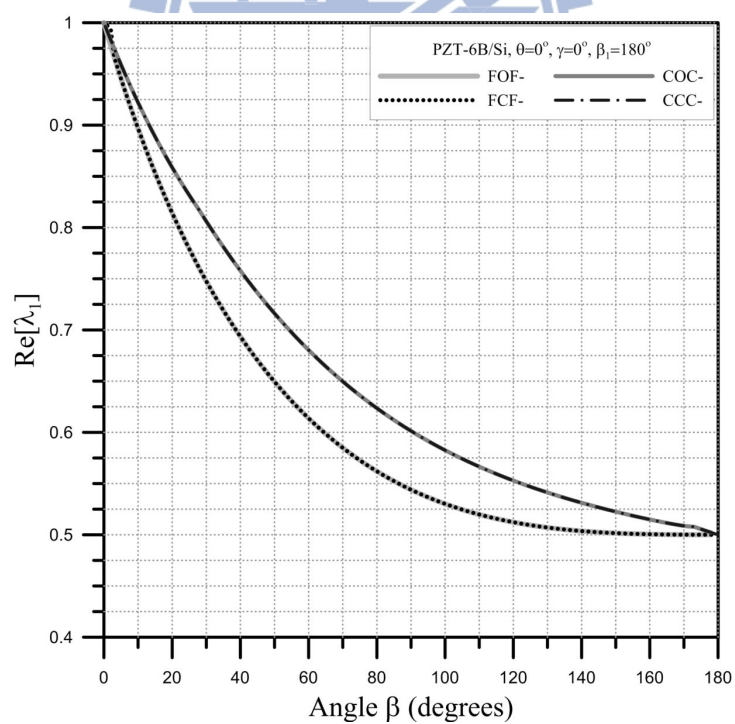
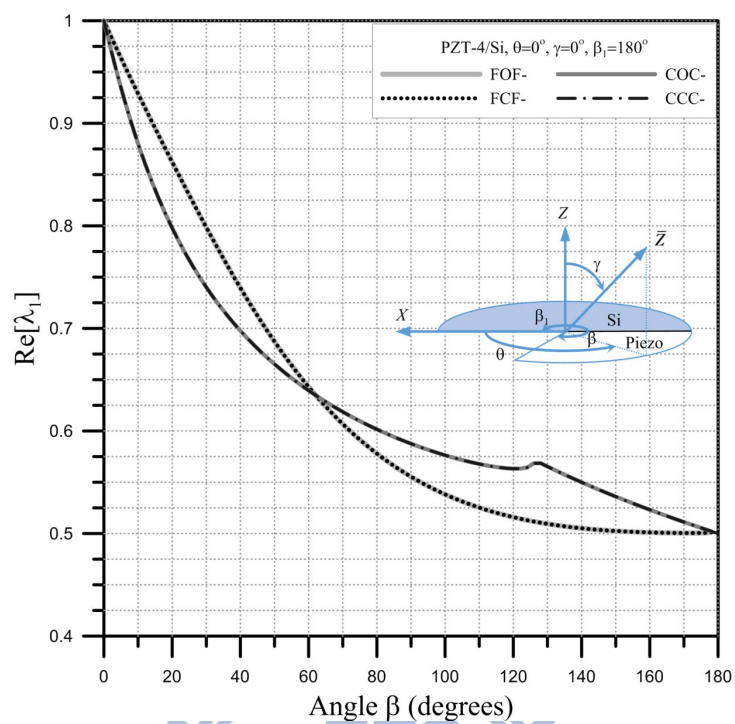
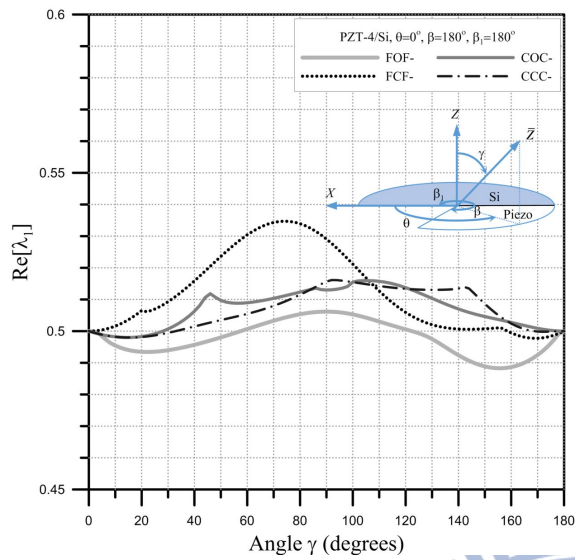
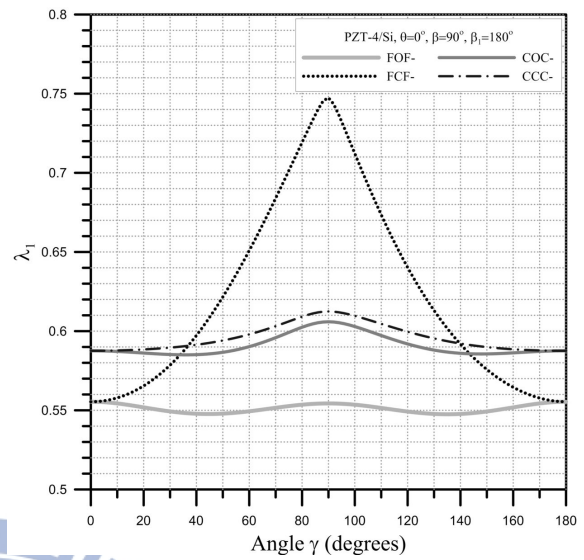


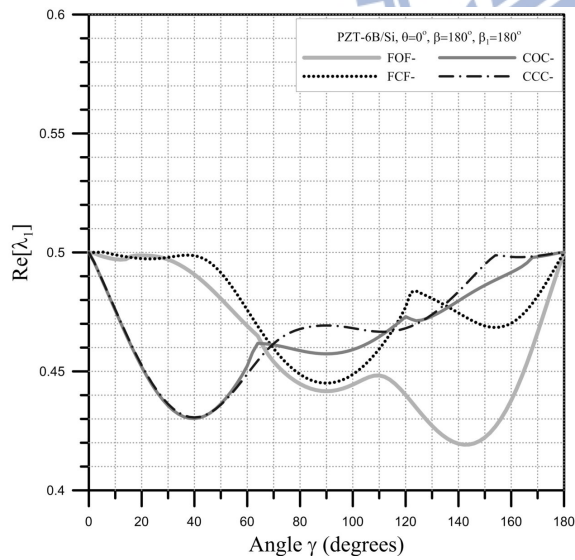
圖 5.7 不同邊界條件下壓電材料/Si 楔形體 $\text{Re}[\lambda_1]$ 隨 β 之變化



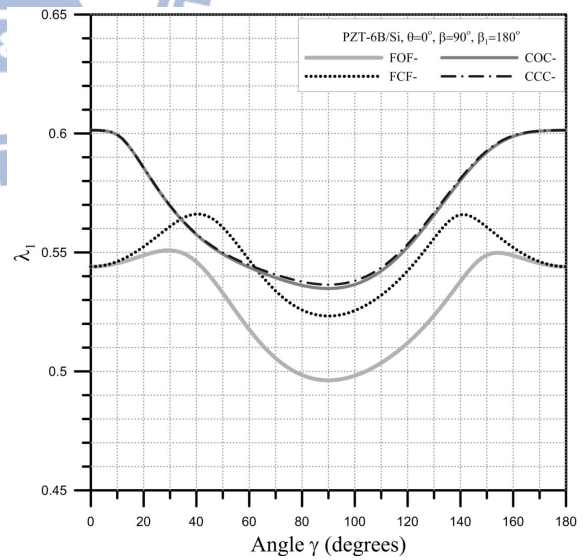
(a)



(b)

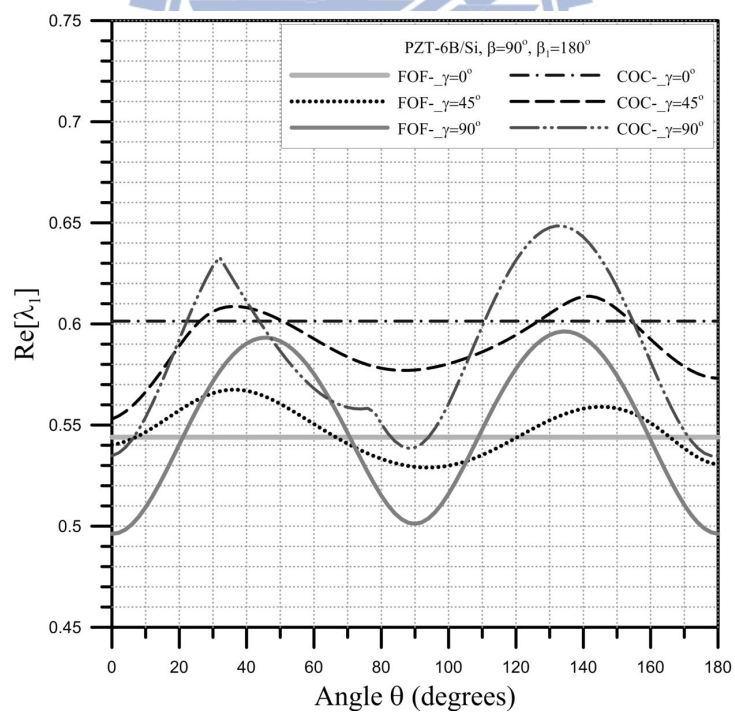
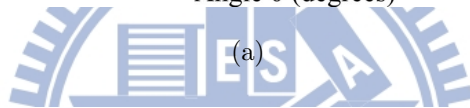
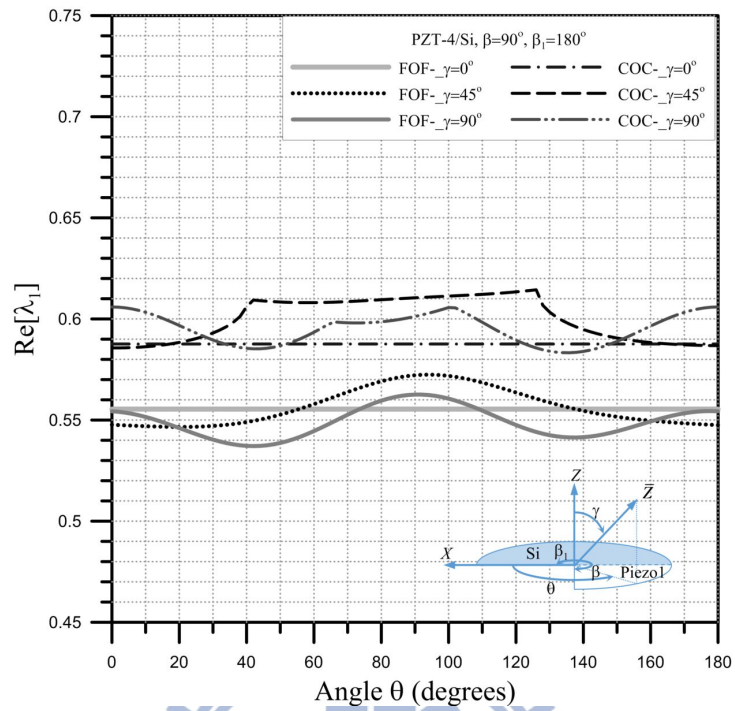


(c)



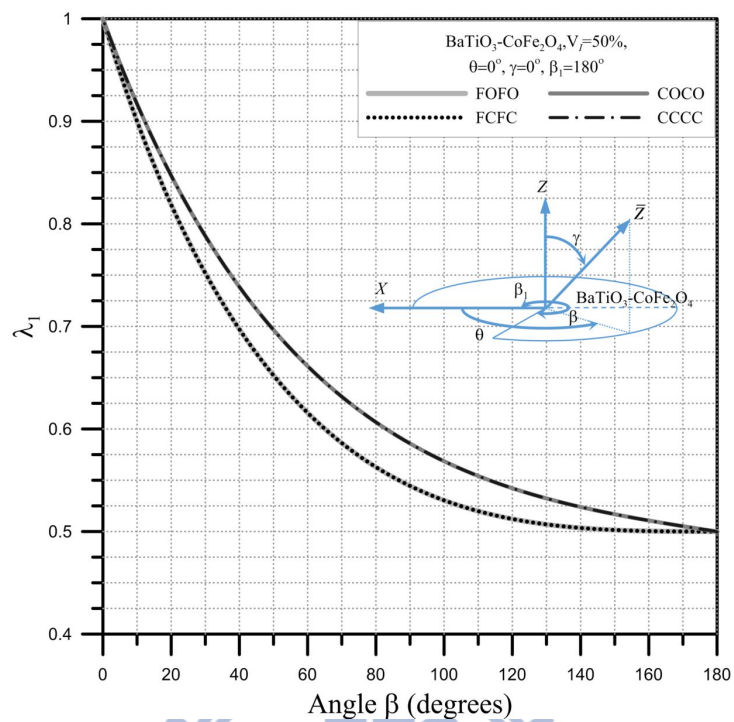
(d)

圖 5.8 不同邊界條件下壓電材料/Si 楔形體 $\text{Re}[\lambda_1]$ 隨 γ 之變化

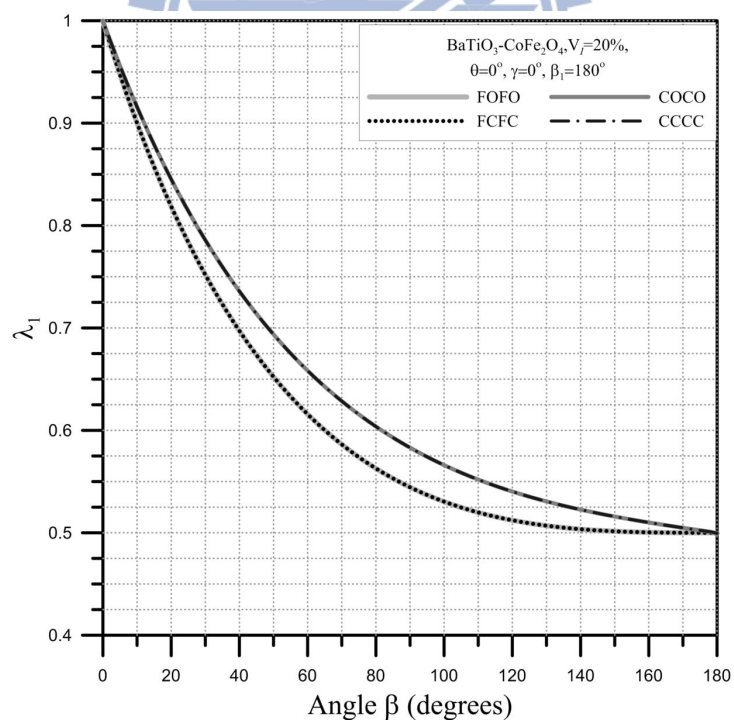


(b)

圖 5.9 不同邊界條件下壓電材料/Si 楔形體 $\text{Re}[\lambda_1]$ 隨 θ 之變化

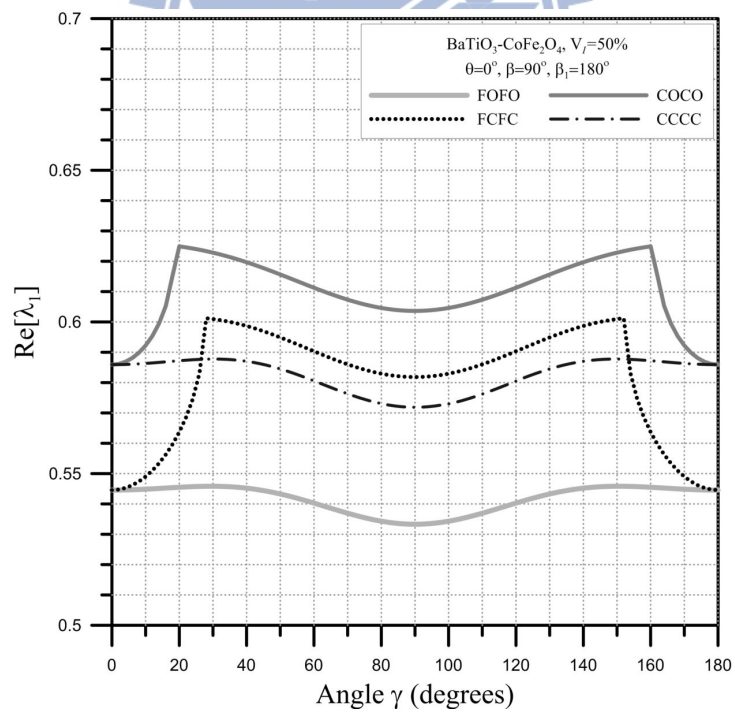
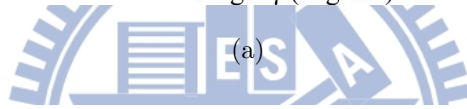
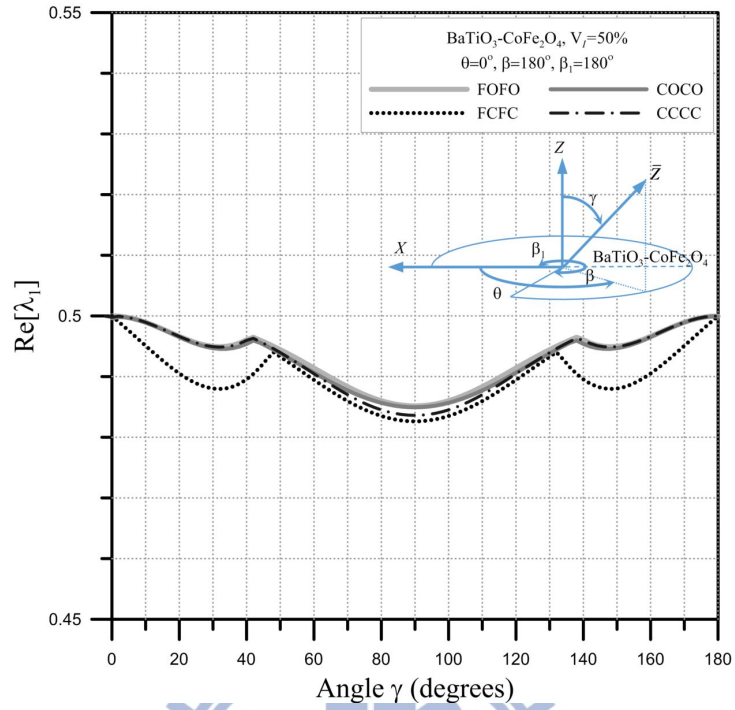


(a)



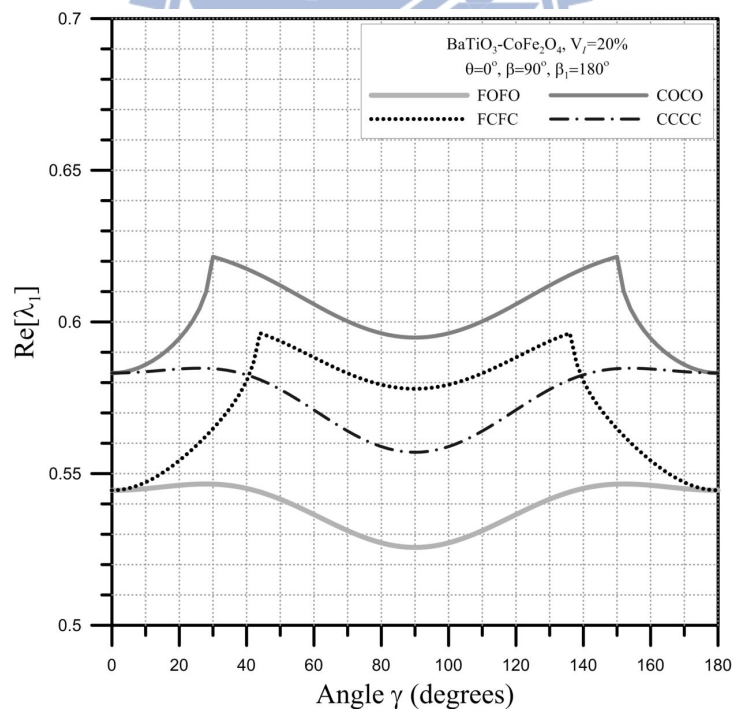
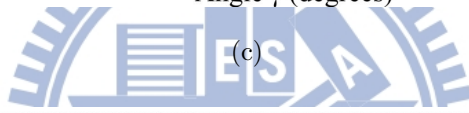
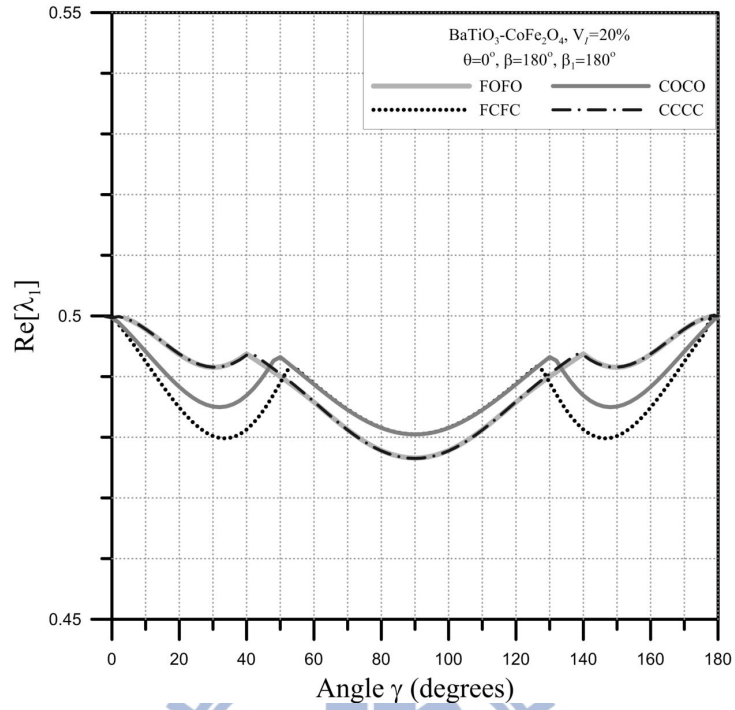
(b)

圖 5.10 不同邊界條件下單 $\text{BaTiO}_3\text{-CoFe}_2\text{O}_4$ 楔形體 λ_1 隨 β 之變化



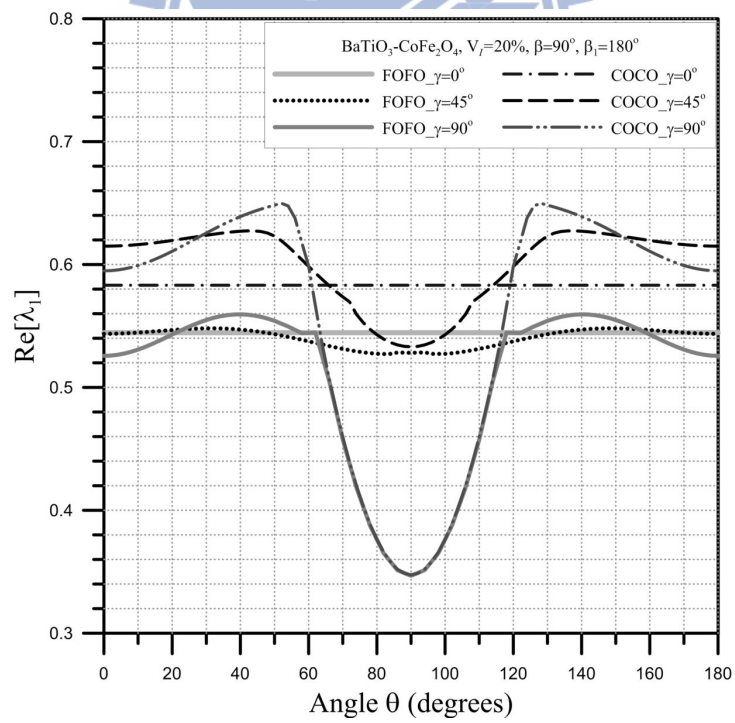
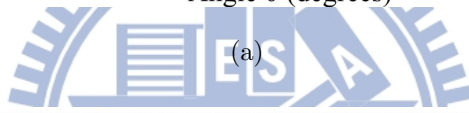
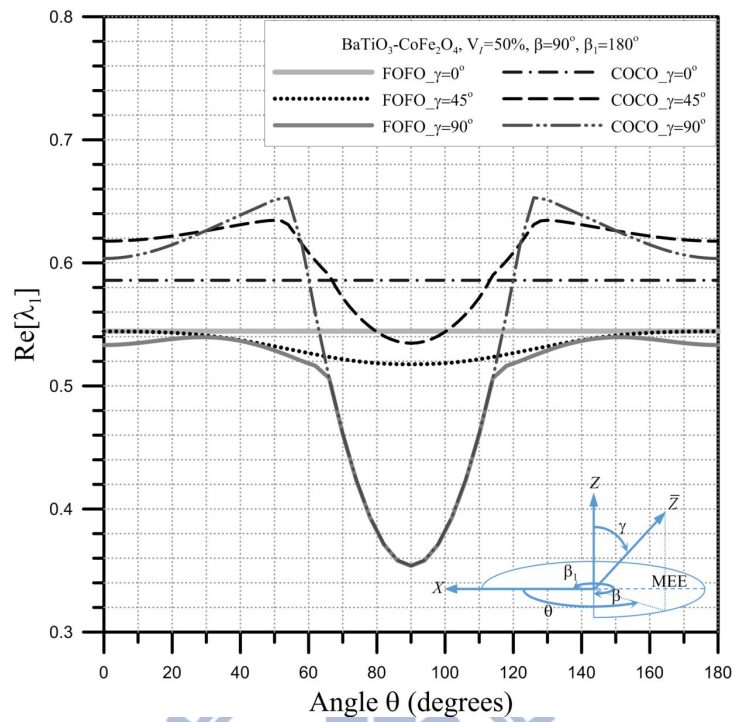
(b)

圖 5.11 不同邊界條件下單 $\text{BaTiO}_3\text{-CoFe}_2\text{O}_4$ 楔形體 $\text{Re}[\lambda_1]$ 隨 γ 之變化



(d)

圖 5.11 不同邊界條件下單 BaTiO₃-CoFe₂O₄ 楔形體 $Re[\lambda_1]$ 隨 γ 之變化



(b)

圖 5.12 不同邊界條件下單 $\text{BaTiO}_3\text{-CoFe}_2\text{O}_4$ 楔形體 $\text{Re}[\lambda_1]$ 隨 θ 之變化

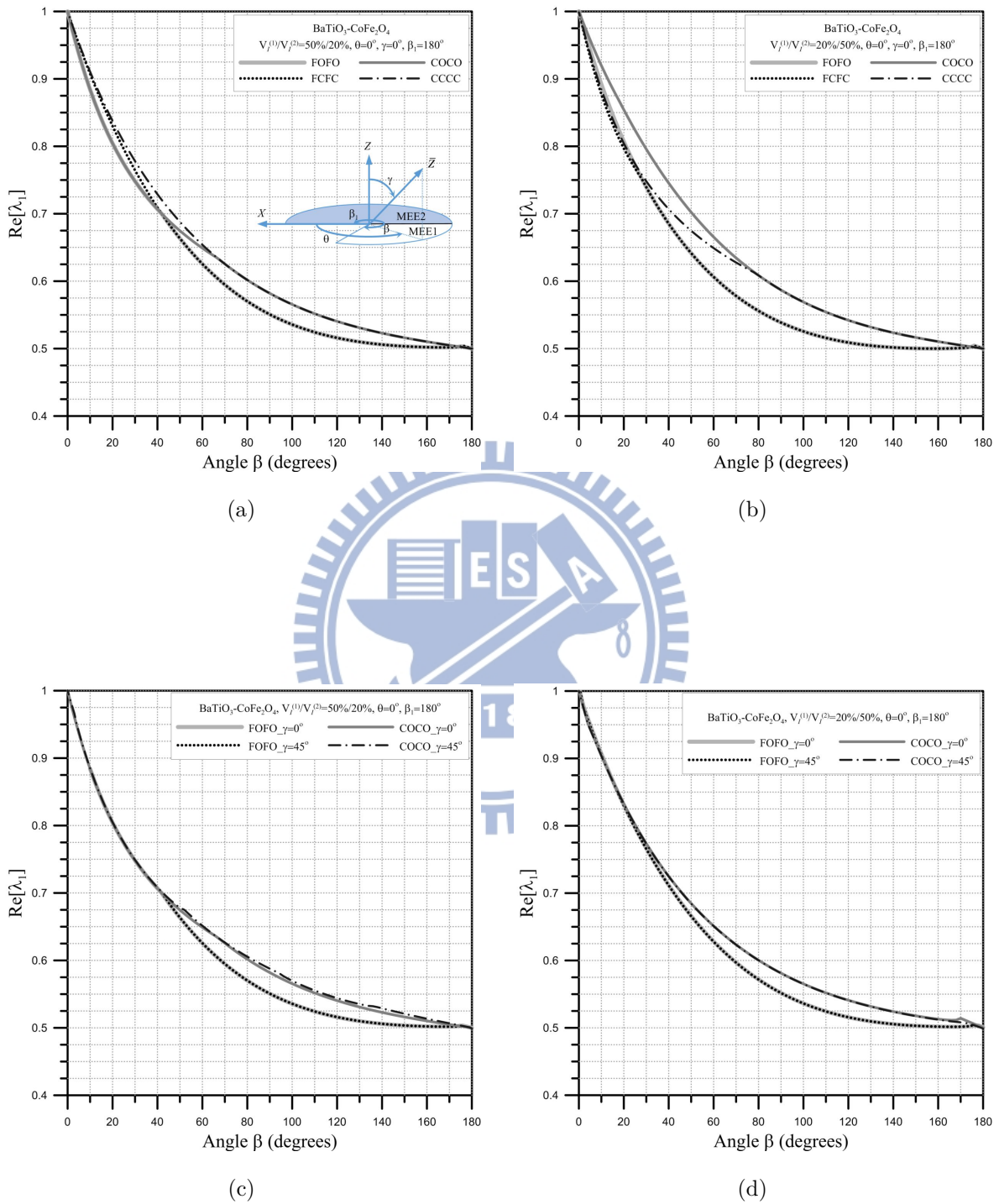
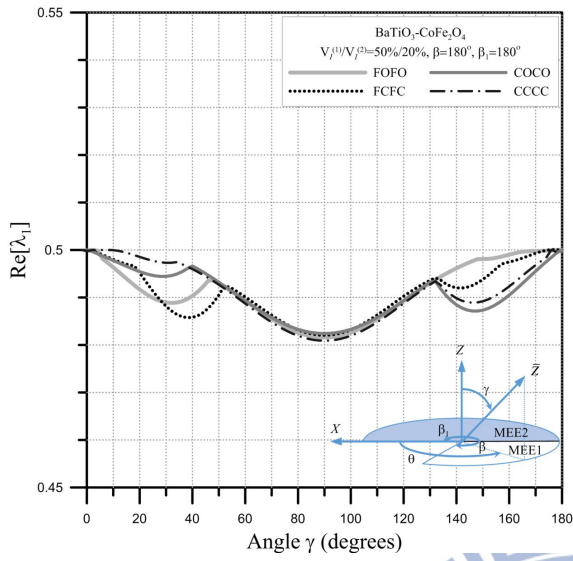
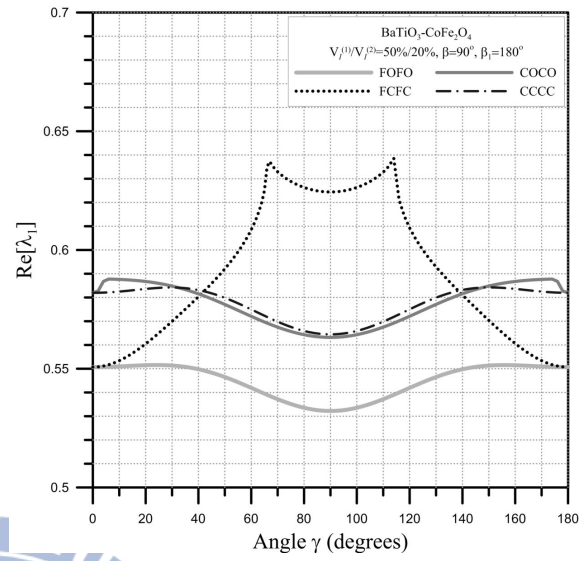


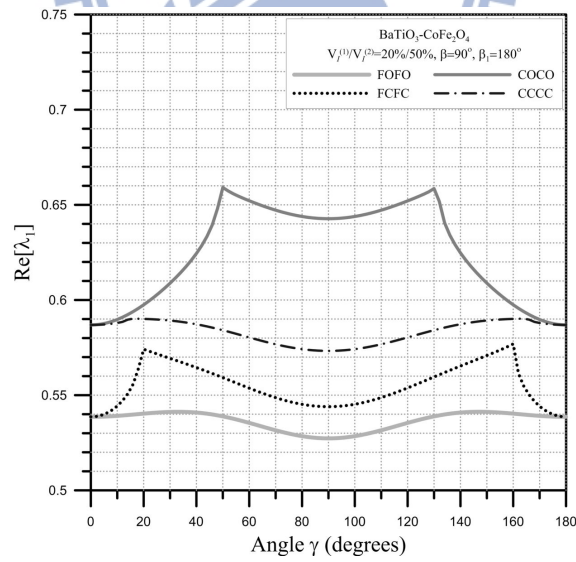
圖 5.13 不同邊界條件下雙 $\text{BaTiO}_3\text{-CoFe}_2\text{O}_4$ 楔形體 $\text{Re}[\lambda_1]$ 隨 β 之變化



(a)

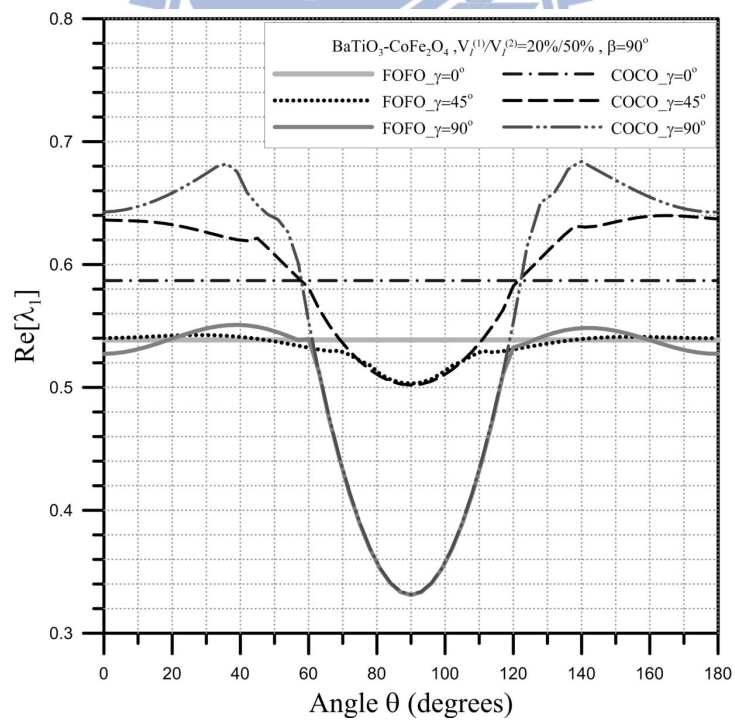
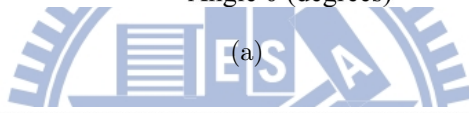
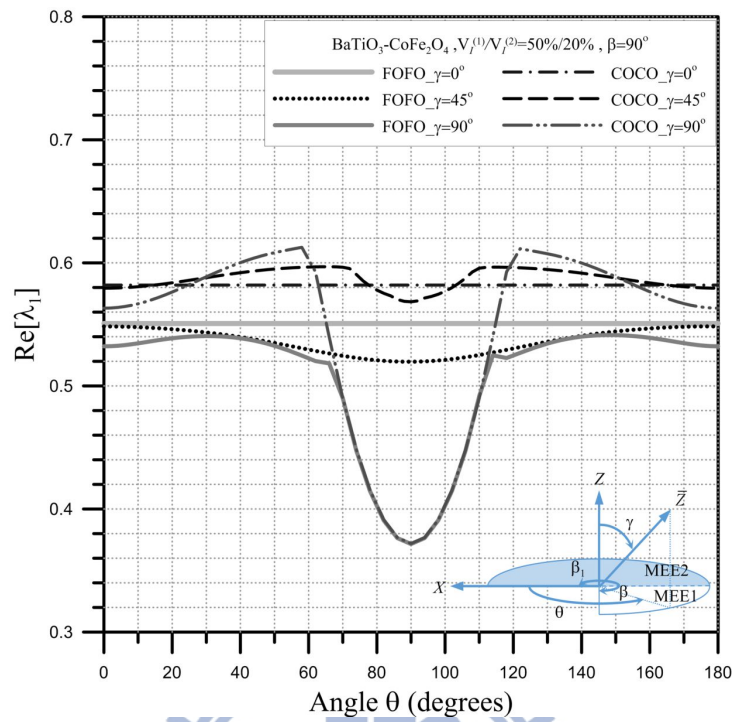


(b)



(c)

圖 5.14 不同邊界條件下雙 $BaTiO_3-CoFe_2O_4$ 楔形體 $Re[\lambda_1]$ 隨 γ 之變化



(b)

圖 5.15 不同邊界條件下雙 BaTiO₃-CoFe₂O₄ 楔形體 $\text{Re}[\lambda_1]$ 隨 θ 之變化

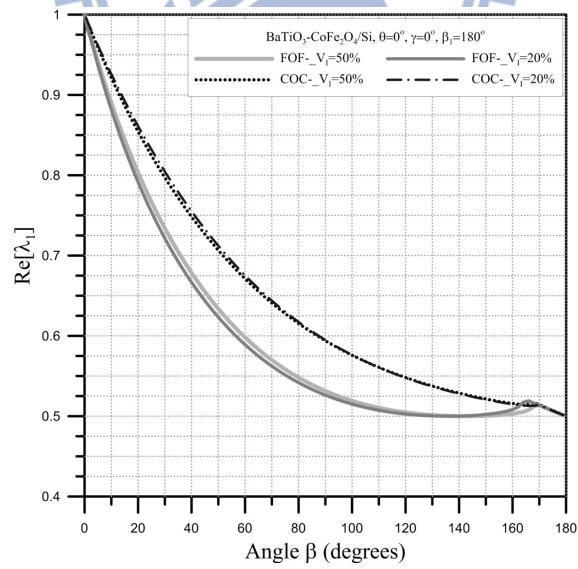
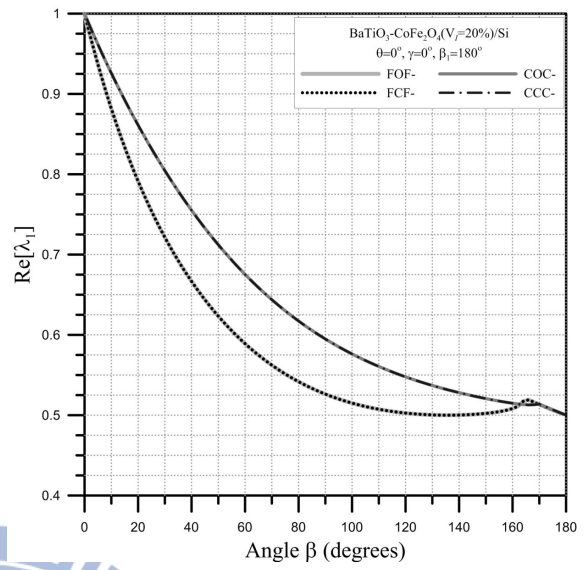
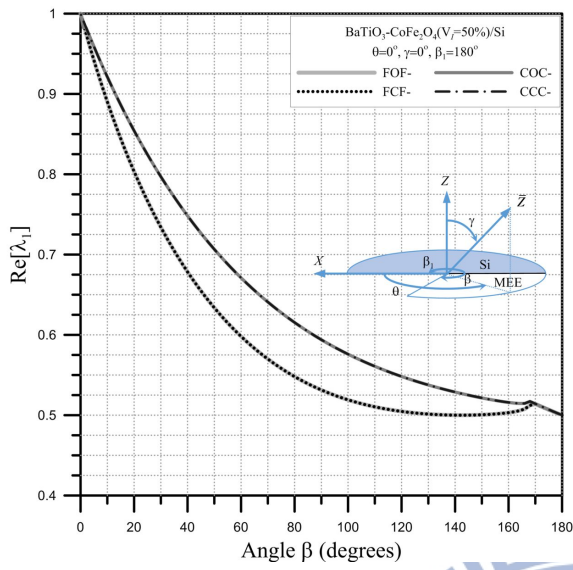
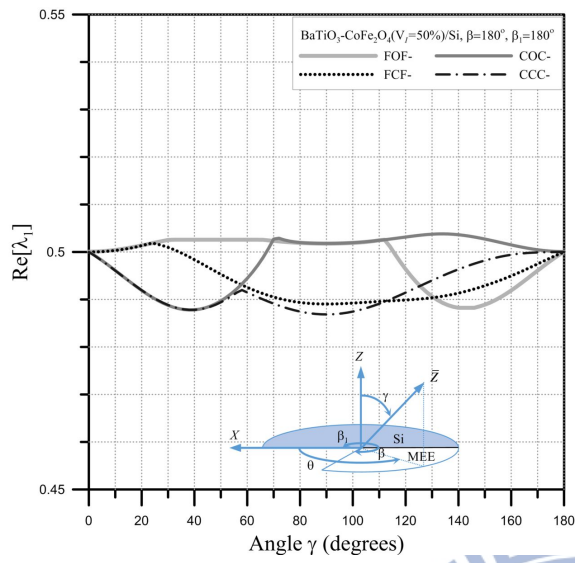
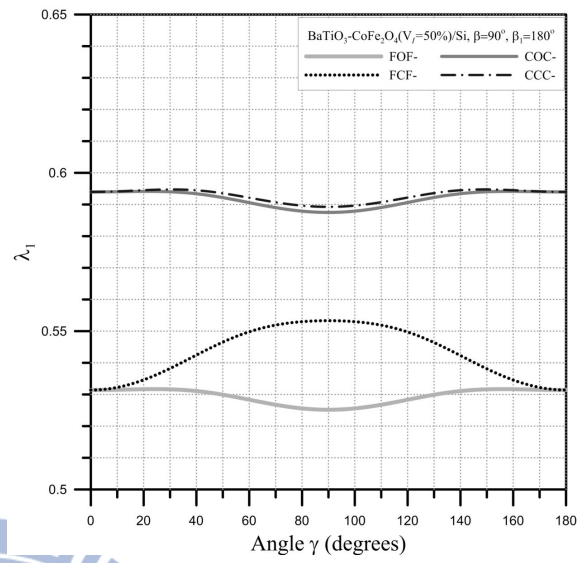


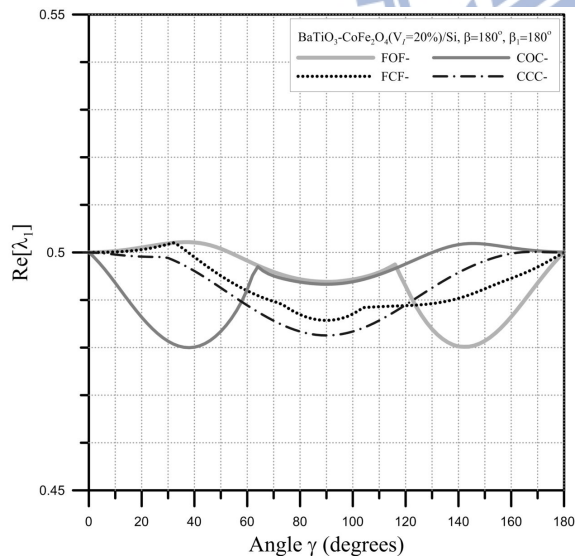
圖 5.16 不同邊界條件下 $\text{BaTiO}_3\text{-CoFe}_2\text{O}_4/\text{Si}$ 楔形體 $\text{Re}[\lambda_1]$ 隨 β 之變化



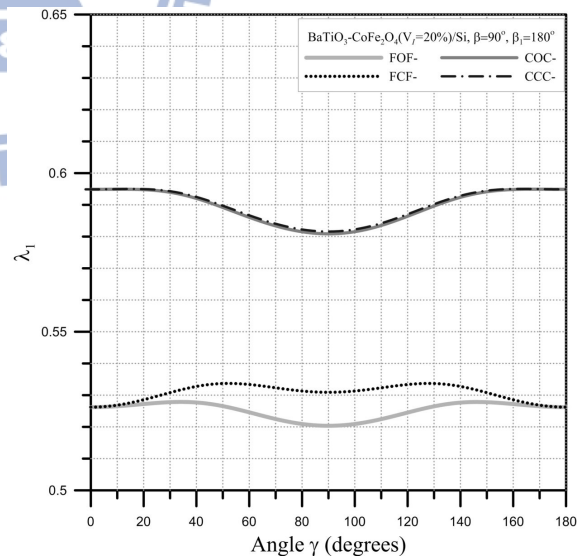
(a)



(b)

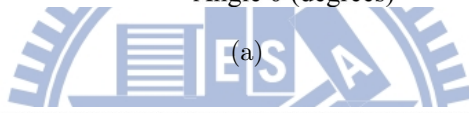
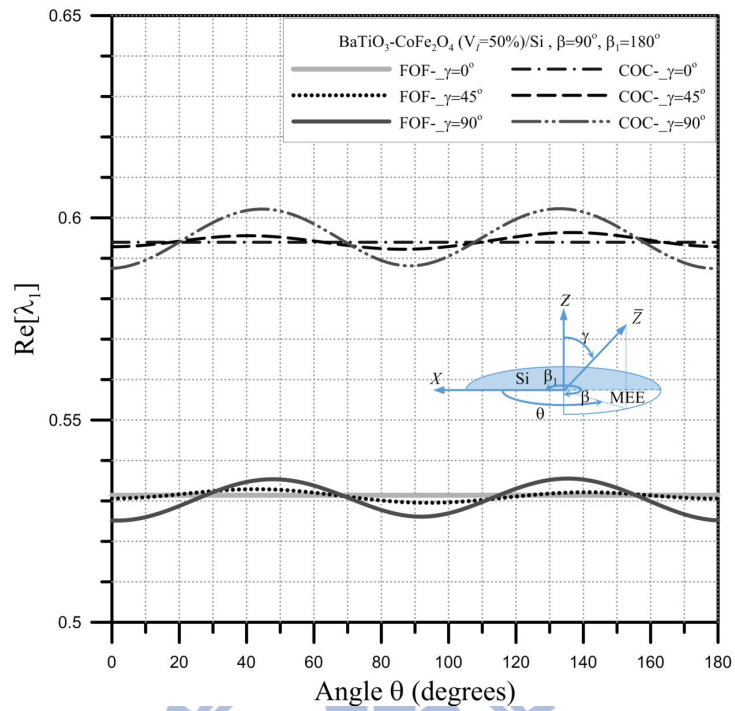


(c)

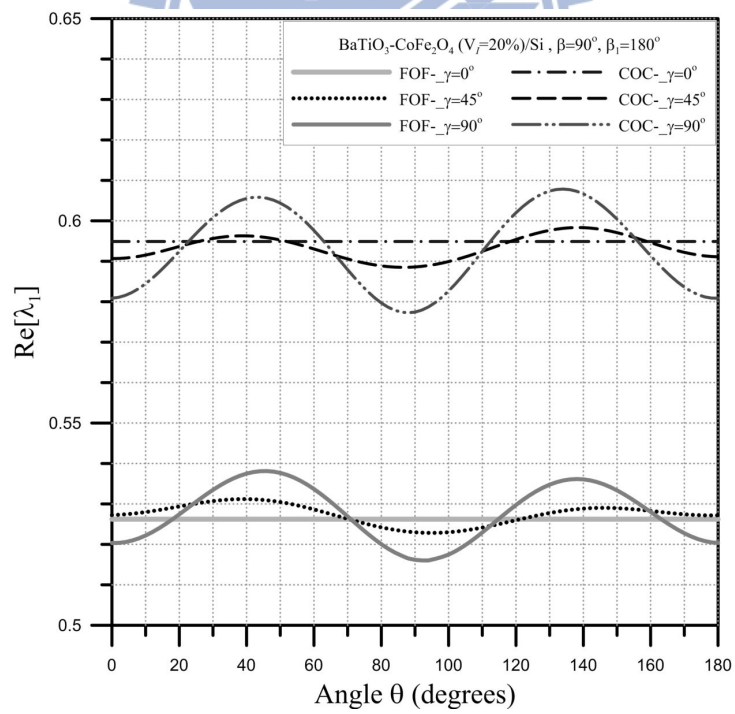


(d)

圖 5.17 不同邊界條件下 $\text{BaTiO}_3\text{-CoFe}_2\text{O}_4/\text{Si}$ 楔形體 $\text{Re}[\lambda_1]$ 隨 γ 之變化

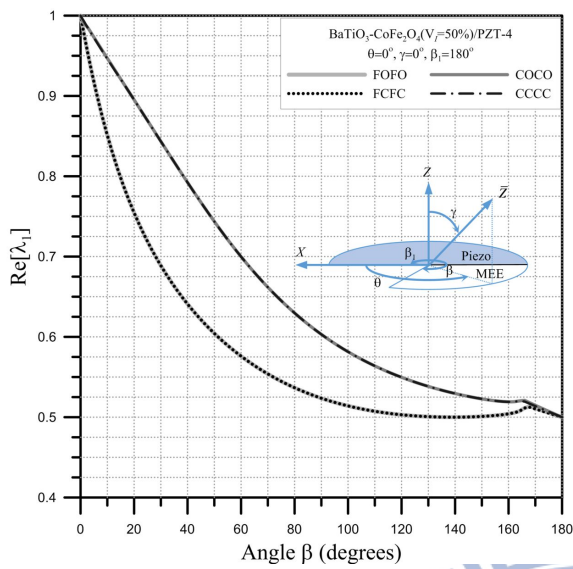


(a)

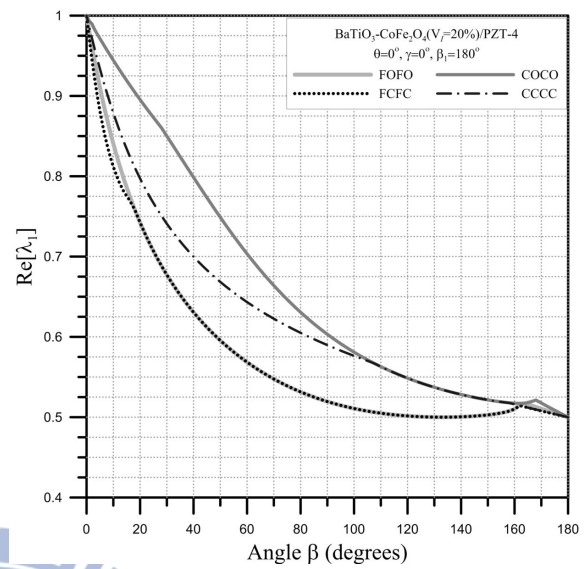


(b)

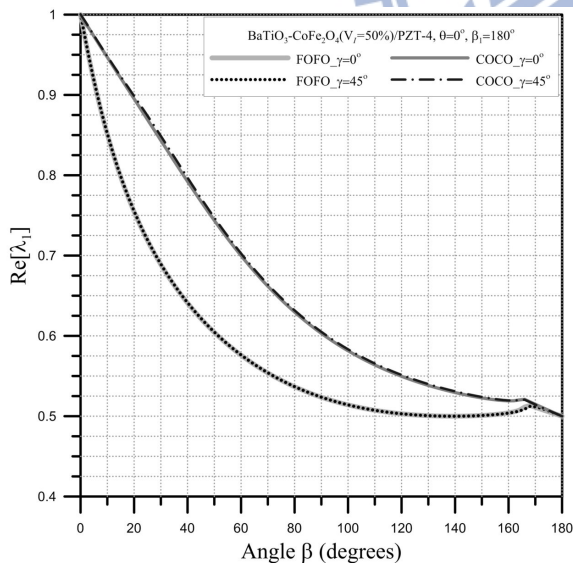
圖 5.18 不同邊界條件下 BaTiO₃-CoFe₂O₄/Si 楔形體 $\text{Re}[\lambda_1]$ 隨 θ 之變化



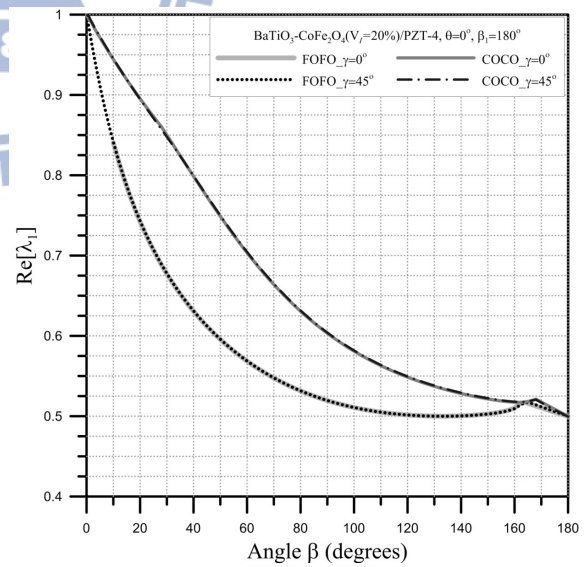
(a)



(b)



(c)



(d)

圖 5.19 不同邊界條件下 BaTiO₃-CoFe₂O₄/PZT-4 楔形體 Re[λ₁] 隨 β 之變化

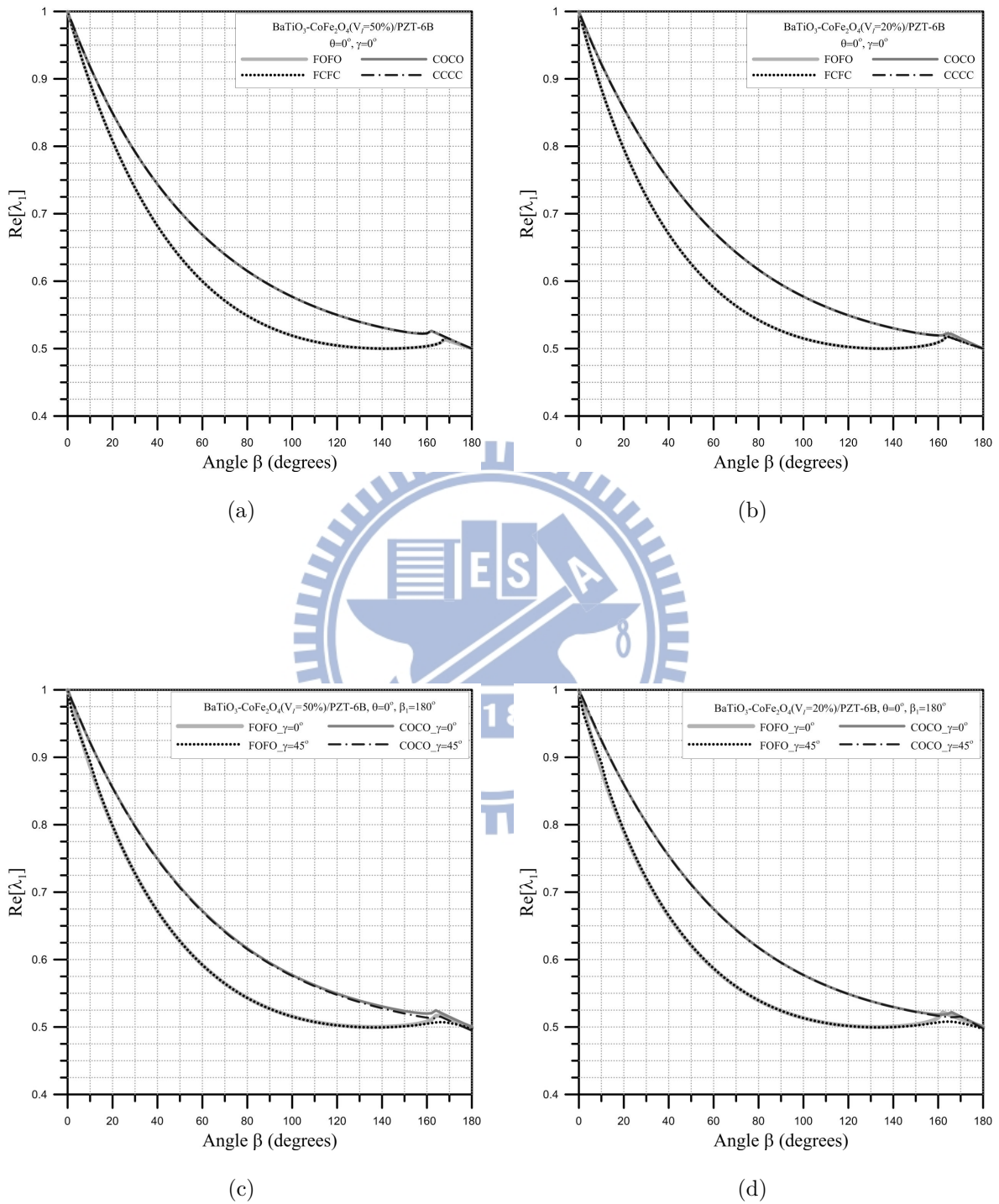


圖 5.20 不同邊界條件下 $BaTiO_3-CoFe_2O_4/PZT-6B$ 楔形體 $Re[\lambda_1]$ 隨 β 之變化

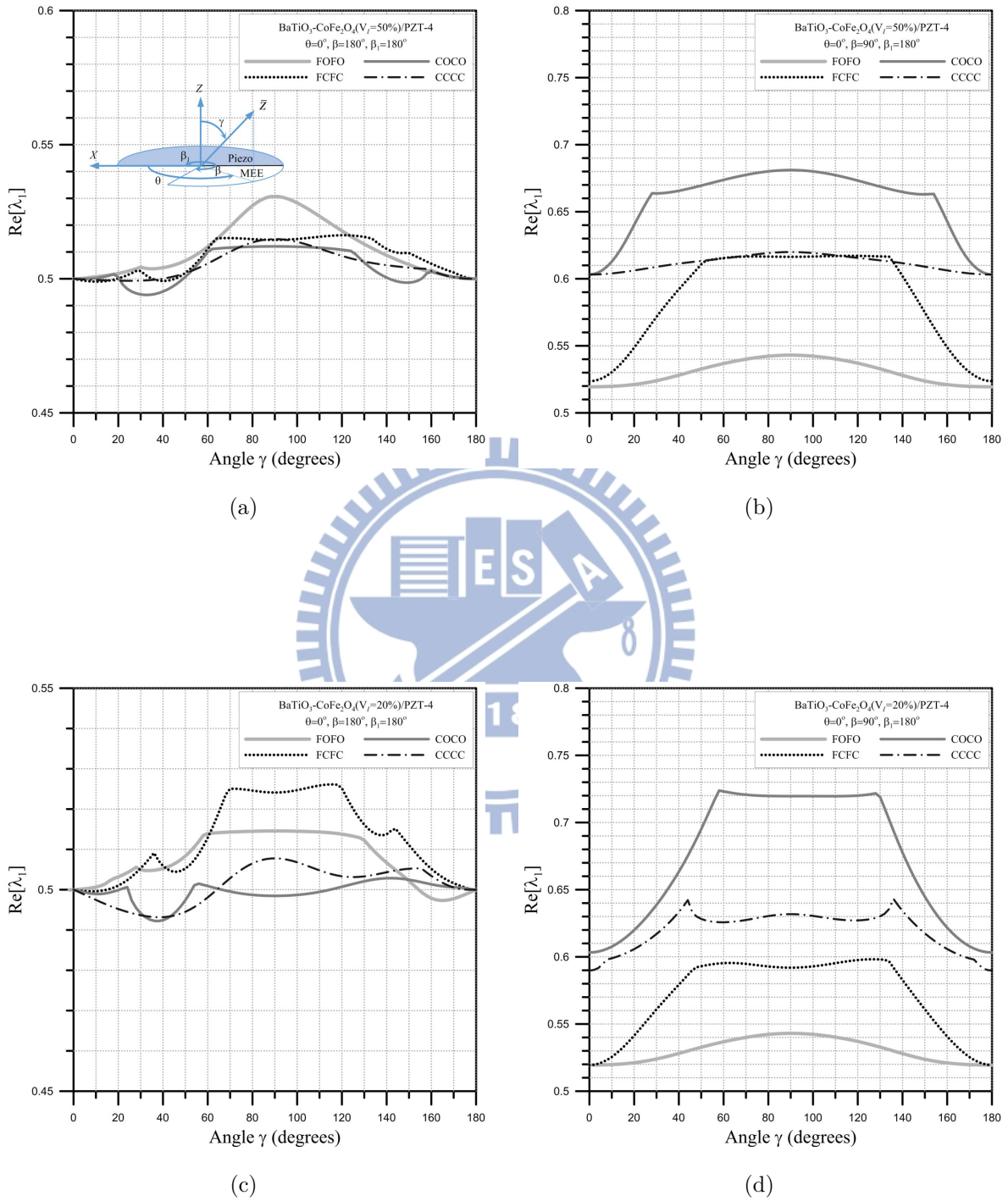


圖 5.21 不同邊界條件下 $BaTiO_3-CoFe_2O_4/PZT-4$ 楔形體 $Re[\lambda_1]$ 隨 γ 之變化

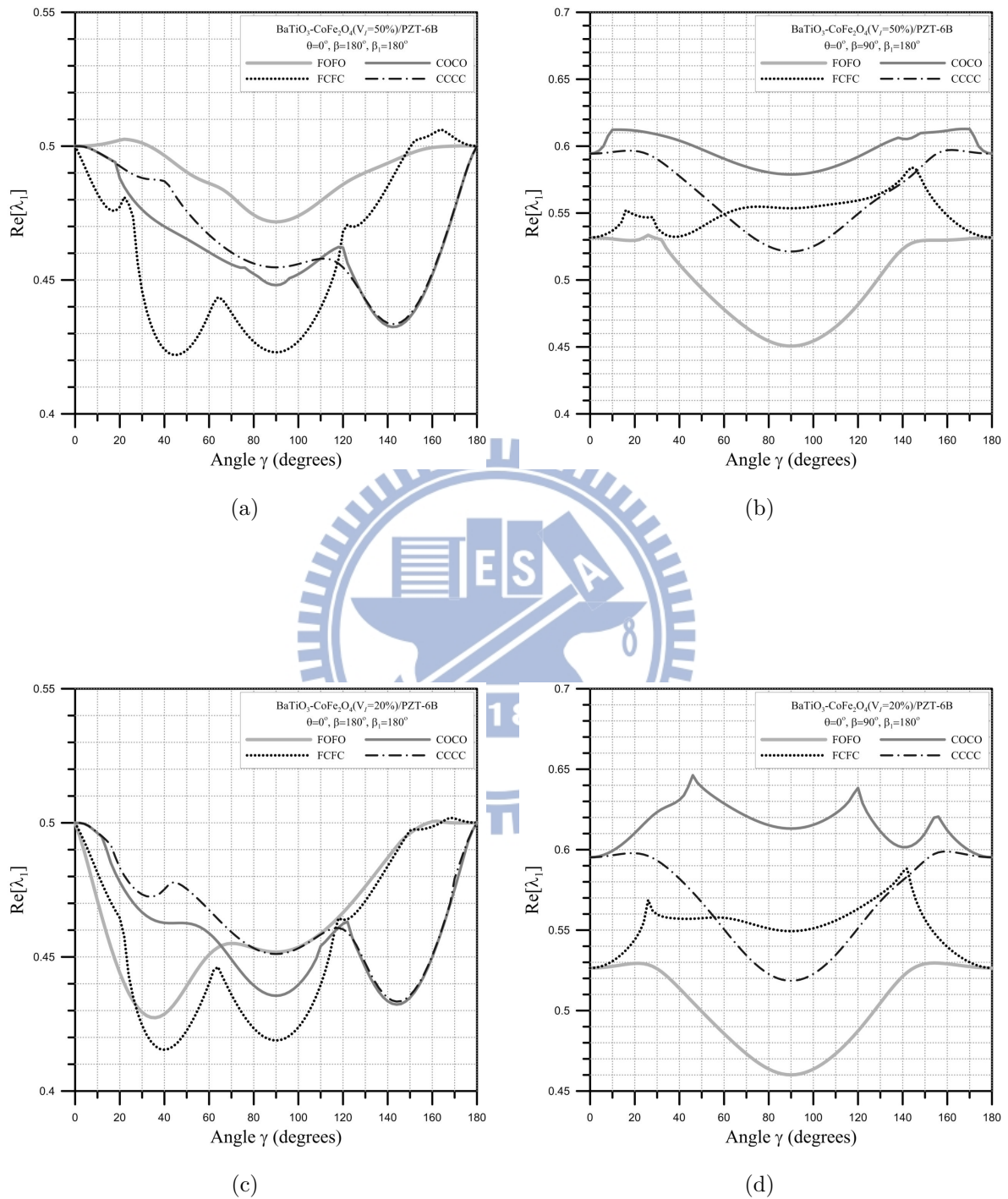
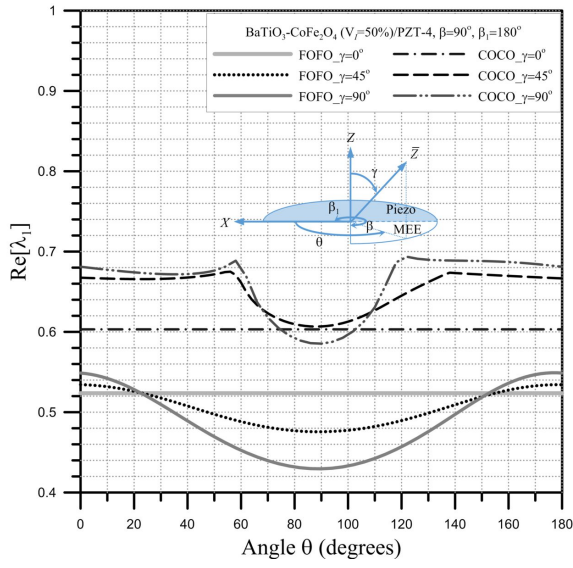
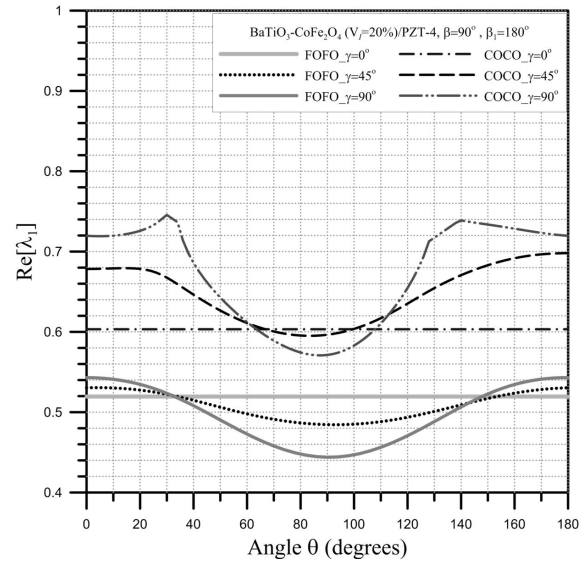


圖 5.22 不同邊界條件下 $\text{BaTiO}_3\text{-CoFe}_2\text{O}_4/\text{PZT-6B}$ 楔形體 $\text{Re}[\lambda_1]$ 隨 γ 之變化



(a)



(b)

圖 5.23 不同邊界條件下 $BaTiO_3-CoFe_2O_4$ / PZT-4 楔形體 $Re[\lambda_1]$ 隨 θ 之變化



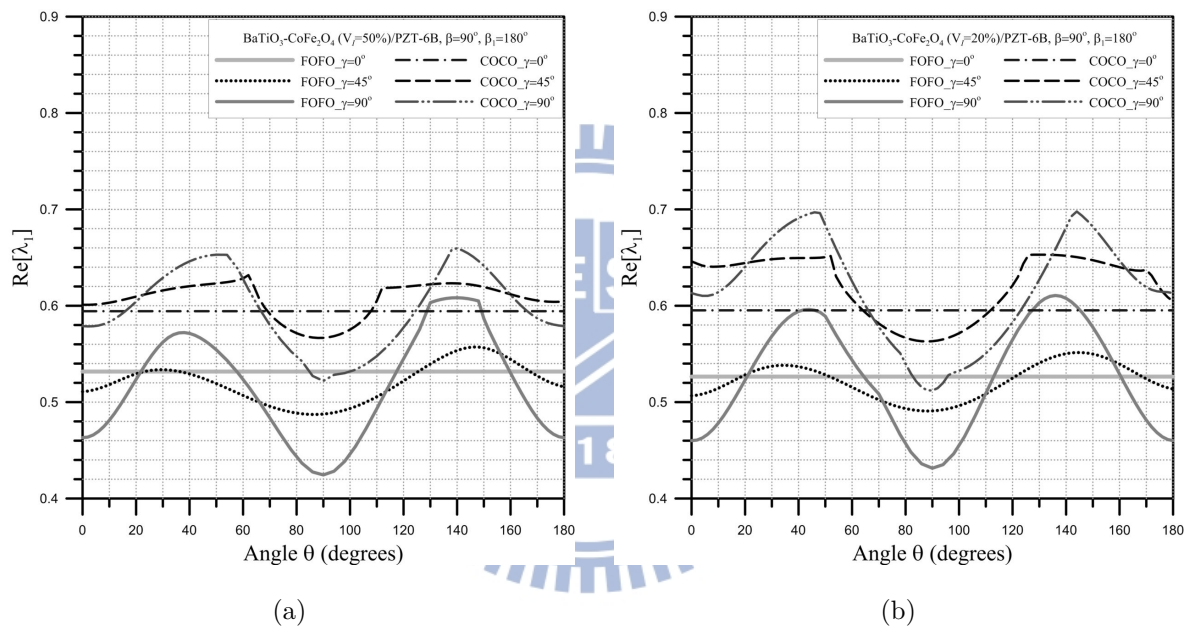


圖 5.24 不同邊界條件下 BaTiO₃-CoFe₂O₄/PZT-6B 楔形體 Re[λ₁] 隨 θ 之變化

附錄 A：座標系統轉換

$$[c] = [\mathbf{T}]_{\sigma} [\mathbf{K}] [\bar{c}] [\mathbf{K}]^T [\mathbf{T}]_{\varepsilon}^{-1}, \quad (\text{A.1})$$

$$[e] = [\mathbf{T}]_{\text{D}} [\mathbf{L}] [\hat{e}] [\mathbf{K}]^T [\mathbf{T}]_{\varepsilon}^{-1}, \quad (\text{A.2})$$

$$[d] = [\mathbf{T}]_{\text{B}} [\mathbf{L}] [\bar{d}] [\mathbf{K}]^T [\mathbf{T}]_{\varepsilon}^{-1}, \quad (\text{A.3})$$

$$[\eta] = [\mathbf{T}]_{\text{D}} [\mathbf{L}] [\bar{\eta}] [\mathbf{L}]^T [\mathbf{T}]_{\text{E}}^{-1}, \quad (\text{A.4})$$

$$[\mu] = [\mathbf{T}]_{\text{B}} [\mathbf{L}] [\bar{\mu}] [\mathbf{L}]^T [\mathbf{T}]_{\text{H}}^{-1} \quad (\text{A.5})$$

其中

$$[\mathbf{T}]_{\sigma} = \begin{bmatrix} \cos^2\theta & \sin^2\theta & 0 & 2\cos\theta\sin\theta & 0 & 0 \\ \sin^2\theta & \cos^2\theta & 0 & -2\cos\theta\sin\theta & 0 & 0 \\ 0 & 0 & 1 & 0 & 0 & 0 \\ -\cos\theta\sin\theta & \cos\theta\sin\theta & 0 & \cos^2\theta - \sin^2\theta & 0 & 0 \\ 0 & 0 & 0 & 0 & \cos\theta & \sin\theta \\ 0 & 0 & 0 & 0 & -\sin\theta & \cos\theta \end{bmatrix}$$

$$[\mathbf{T}]_{\varepsilon} = \begin{bmatrix} \cos^2\theta & \sin^2\theta & 0 & \cos\theta\sin\theta & 0 & 0 \\ \sin^2\theta & \cos^2\theta & 0 & -\cos\theta\sin\theta & 0 & 0 \\ 0 & 0 & 1 & 0 & 0 & 0 \\ -2\cos\theta\sin\theta & 2\cos\theta\sin\theta & 0 & \cos^2\theta - \sin^2\theta & 0 & 0 \\ 0 & 0 & 0 & 0 & \cos\theta & \sin\theta \\ 0 & 0 & 0 & 0 & -\sin\theta & \cos\theta \end{bmatrix}$$

$$[\mathbf{T}]_E = [\mathbf{T}]_D = [\mathbf{T}]_B = [\mathbf{T}]_H = \begin{bmatrix} \cos \theta & \sin \theta & 0 \\ -\sin \theta & \cos \theta & 0 \\ 0 & 0 & 1 \end{bmatrix}$$

$$[\mathbf{L}] = \begin{bmatrix} l_{11} & l_{12} & l_{13} \\ l_{21} & l_{22} & l_{23} \\ l_{31} & l_{32} & l_{33} \end{bmatrix} = \begin{bmatrix} \sin \theta & \cos \gamma \cos \theta & -\cos \theta \sin \gamma \\ -\cos \theta & \cos \gamma \sin \theta & \cos \theta \sin \gamma \\ 0 & \sin \gamma & \cos \gamma \end{bmatrix}, \quad [\mathbf{K}] = \begin{bmatrix} K_1 & 2K_2 \\ K_3 & K_4 \end{bmatrix}$$

$$\mathbf{K}_1 = \begin{bmatrix} l_{11}^2 & l_{12}^2 & l_{13}^2 \\ l_{21}^2 & l_{22}^2 & l_{23}^2 \\ l_{31}^2 & l_{32}^2 & l_{33}^2 \end{bmatrix}, \quad \mathbf{K}_2 = \begin{bmatrix} l_{12}l_{13} & l_{13}l_{11} & l_{11}l_{12} \\ l_{22}l_{23} & l_{23}l_{21} & l_{21}l_{22} \\ l_{32}l_{33} & l_{33}l_{31} & l_{31}l_{32} \end{bmatrix}$$

$$\mathbf{K}_3 = \begin{bmatrix} l_{21}l_{31} & l_{22}l_{32} & l_{23}l_{33} \\ l_{31}l_{11} & l_{32}l_{12} & l_{33}l_{13} \\ l_{11}l_{21} & l_{12}l_{22} & l_{13}l_{23} \end{bmatrix}, \quad \mathbf{K}_4 = \begin{bmatrix} l_{22}l_{33} + l_{23}l_{32} & l_{23}l_{31} + l_{21}l_{33} & l_{21}l_{32} + l_{22}l_{31} \\ l_{32}l_{13} + l_{33}l_{12} & l_{33}l_{11} + l_{31}l_{13} & l_{31}l_{12} + l_{32}l_{11} \\ l_{12}l_{23} + l_{13}l_{22} & l_{13}l_{21} + l_{11}l_{23} & l_{11}l_{22} + l_{12}l_{21} \end{bmatrix}$$

附錄 B：以位移、電勢與磁勢表示應力、電位移

與磁感應強度

$$\begin{aligned}
 \sigma_{rr} = & c_{11} \frac{\partial u_r^*}{\partial r} + c_{12} \left(\frac{1}{r} \frac{\partial u_\theta^*}{\partial \theta} + \frac{u_r^*}{r} \right) + c_{13} \frac{\partial u_z^*}{\partial z} + c_{14} \left(\frac{\partial u_\theta^*}{\partial z} + \frac{1}{r} \frac{\partial u_z^*}{\partial \theta} \right) + c_{15} \left(\frac{\partial u_z^*}{\partial r} + \frac{\partial u_r^*}{\partial z} \right) \\
 & + c_{16} \left(\frac{1}{r} \frac{\partial u_r^*}{\partial \theta} + \frac{\partial u_\theta^*}{\partial r} - \frac{u_\theta^*}{r} \right) + e_{11} \frac{\partial \phi^*}{\partial r} + e_{21} \frac{1}{r} \frac{\partial \phi^*}{\partial \theta} + e_{31} \frac{\partial \phi^*}{\partial z} \\
 & + d_{11} \frac{\partial \psi^*}{\partial r} + d_{21} \frac{1}{r} \frac{\partial \psi^*}{\partial \theta} + d_{31} \frac{\partial \psi^*}{\partial z}
 \end{aligned} \tag{B.1}$$

$$\begin{aligned}
 \sigma_{\theta\theta} = & c_{12} \frac{\partial u_r^*}{\partial r} + c_{22} \left(\frac{1}{r} \frac{\partial u_\theta^*}{\partial \theta} + \frac{u_r^*}{r} \right) + c_{23} \frac{\partial u_z^*}{\partial z} + c_{24} \left(\frac{\partial u_\theta^*}{\partial z} + \frac{1}{r} \frac{\partial u_z^*}{\partial \theta} \right) + c_{25} \left(\frac{\partial u_z^*}{\partial r} + \frac{\partial u_r^*}{\partial z} \right) \\
 & + c_{26} \left(\frac{1}{r} \frac{\partial u_r^*}{\partial \theta} + \frac{\partial u_\theta^*}{\partial r} - \frac{u_\theta^*}{r} \right) + e_{12} \frac{\partial \phi^*}{\partial r} + e_{22} \frac{1}{r} \frac{\partial \phi^*}{\partial \theta} + e_{32} \frac{\partial \phi^*}{\partial z} \\
 & + d_{12} \frac{\partial \psi^*}{\partial r} + d_{22} \frac{1}{r} \frac{\partial \psi^*}{\partial \theta} + d_{32} \frac{\partial \psi^*}{\partial z}
 \end{aligned} \tag{B.2}$$

$$\begin{aligned}
 \sigma_{zz} = & c_{13} \frac{\partial u_r^*}{\partial r} + c_{23} \left(\frac{1}{r} \frac{\partial u_\theta^*}{\partial \theta} + \frac{u_r^*}{r} \right) + c_{33} \frac{\partial u_z^*}{\partial z} + c_{34} \left(\frac{\partial u_\theta^*}{\partial z} + \frac{1}{r} \frac{\partial u_z^*}{\partial \theta} \right) + c_{35} \left(\frac{\partial u_z^*}{\partial r} + \frac{\partial u_r^*}{\partial z} \right) \\
 & + c_{36} \left(\frac{1}{r} \frac{\partial u_r^*}{\partial \theta} + \frac{\partial u_\theta^*}{\partial r} - \frac{u_\theta^*}{r} \right) + e_{13} \frac{\partial \phi^*}{\partial r} + e_{23} \frac{1}{r} \frac{\partial \phi^*}{\partial \theta} + e_{33} \frac{\partial \phi^*}{\partial z} \\
 & + d_{13} \frac{\partial \psi^*}{\partial r} + d_{23} \frac{1}{r} \frac{\partial \psi^*}{\partial \theta} + d_{33} \frac{\partial \psi^*}{\partial z}
 \end{aligned} \tag{B.3}$$

$$\begin{aligned}
 \sigma_{z\theta} = & c_{14} \frac{\partial u_r^*}{\partial r} + c_{24} \left(\frac{1}{r} \frac{\partial u_\theta^*}{\partial \theta} + \frac{u_r^*}{r} \right) + c_{34} \frac{\partial u_z^*}{\partial z} + c_{44} \left(\frac{\partial u_\theta^*}{\partial z} + \frac{1}{r} \frac{\partial u_z^*}{\partial \theta} \right) + c_{45} \left(\frac{\partial u_z^*}{\partial r} + \frac{\partial u_r^*}{\partial z} \right) \\
 & + c_{46} \left(\frac{1}{r} \frac{\partial u_r^*}{\partial \theta} + \frac{\partial u_\theta^*}{\partial r} - \frac{u_\theta^*}{r} \right) + e_{14} \frac{\partial \phi^*}{\partial r} + e_{24} \frac{1}{r} \frac{\partial \phi^*}{\partial \theta} + e_{34} \frac{\partial \phi^*}{\partial z} \\
 & + d_{14} \frac{\partial \psi^*}{\partial r} + d_{24} \frac{1}{r} \frac{\partial \psi^*}{\partial \theta} + d_{34} \frac{\partial \psi^*}{\partial z}
 \end{aligned} \tag{B.4}$$

$$\begin{aligned}
 \sigma_{zr} = & c_{15} \frac{\partial u_r^*}{\partial r} + c_{25} \left(\frac{1}{r} \frac{\partial u_\theta^*}{\partial \theta} + \frac{u_r^*}{r} \right) + c_{35} \frac{\partial u_z^*}{\partial z} + c_{45} \left(\frac{\partial u_\theta^*}{\partial z} + \frac{1}{r} \frac{\partial u_z^*}{\partial \theta} \right) + c_{55} \left(\frac{\partial u_z^*}{\partial r} + \frac{\partial u_r^*}{\partial z} \right) \\
 & + c_{56} \left(\frac{1}{r} \frac{\partial u_r^*}{\partial \theta} + \frac{\partial u_\theta^*}{\partial r} - \frac{u_\theta^*}{r} \right) + e_{15} \frac{\partial \phi^*}{\partial r} + e_{25} \frac{1}{r} \frac{\partial \phi^*}{\partial \theta} + e_{35} \frac{\partial \phi^*}{\partial z} \\
 & + d_{15} \frac{\partial \psi^*}{\partial r} + d_{25} \frac{1}{r} \frac{\partial \psi^*}{\partial \theta} + d_{35} \frac{\partial \psi^*}{\partial z}
 \end{aligned} \tag{B.5}$$

$$\sigma_{r\theta} = c_{16} \frac{\partial u_r^*}{\partial r} + c_{26} \left(\frac{1}{r} \frac{\partial u_\theta^*}{\partial \theta} + \frac{u_r^*}{r} \right) + c_{36} \frac{\partial u_z^*}{\partial z} + c_{46} \left(\frac{\partial u_\theta^*}{\partial z} + \frac{1}{r} \frac{\partial u_z^*}{\partial \theta} \right) + c_{56} \left(\frac{\partial u_z^*}{\partial r} + \frac{\partial u_r^*}{\partial z} \right)$$

附錄 C：式 (4.3) 之變係數

$$\begin{aligned}
 p_1(\theta) &= \frac{1}{c_{66}} \left(2\lambda_m c_{16} + \frac{\partial c_{66}}{\partial \theta} \right), & p_2(\theta) &= \frac{1}{c_{66}} \left(-c_{22} + \lambda_m \left(\lambda_m c_{11} + \frac{\partial c_{16}}{\partial \theta} \right) + \frac{\partial c_{26}}{\partial \theta} \right), \\
 p_3(\theta) &= \frac{c_{26}}{c_{66}}, & p_4(\theta) &= \frac{1}{c_{66}} \left(\lambda_m c_{12} - c_{22} + (\lambda_m - 1) c_{66} + \frac{\partial c_{26}}{\partial \theta} \right), \\
 p_5(\theta) &= \frac{1}{c_{66}} (\lambda_m - 1) \left(\lambda_m c_{16} - c_{26} + \frac{\partial c_{66}}{\partial \theta} \right), & p_6(\theta) &= \frac{c_{46}}{c_{66}}, \\
 p_8(\theta) &= \frac{\lambda_m}{c_{66}} \left(\lambda_m c_{15} - c_{25} + \frac{\partial c_{56}}{\partial \theta} \right), & p_9(\theta) &= \frac{e_{26}}{c_{66}}, \\
 p_{10}(\theta) &= \frac{1}{c_{66}} \left(\lambda_m (e_{16} + e_{21}) - e_{22} + \frac{\partial e_{26}}{\partial \theta} \right), & p_{11}(\theta) &= \frac{1}{c_{66}} \lambda_m \left(\lambda_m e_{11} - e_{12} + \frac{\partial e_{16}}{\partial \theta} \right), \\
 p_{12}(\theta) &= \frac{d_{26}}{c_{66}}, & p_{13}(\theta) &= \frac{1}{c_{66}} \left(\lambda_m (d_{16} + d_{21}) - d_{22} + \frac{\partial d_{26}}{\partial \theta} \right), \\
 p_{14}(\theta) &= \frac{1}{c_{66}} \lambda_m \left(\lambda_m d_{11} - d_{12} + \frac{\partial d_{16}}{\partial \theta} \right), & & \tag{C.1}
 \end{aligned}$$

$$\begin{aligned}
 q_1(\theta) &= \frac{1}{c_{22}} \left(2\lambda_m c_{26} + \frac{\partial c_{22}}{\partial \theta} \right), & q_2(\theta) &= \frac{1}{c_{22}} (\lambda_m - 1) \left[(\lambda_m + 1) c_{66} + \frac{\partial c_{26}}{\partial \theta} \right], & q_3(\theta) &= \frac{c_{26}}{c_{22}}, \\
 q_4(\theta) &= \frac{1}{c_{22}} \left(c_{22} + c_{66} + \lambda_m (c_{12} + c_{66}) + \frac{\partial c_{26}}{\partial \theta} \right), \\
 q_5(\theta) &= \frac{1}{c_{22}} \left(c_{26} + \lambda_m \left((\lambda_m + 1) c_{16} + c_{26} + \frac{\partial c_{12}}{\partial \theta} \right) + \frac{\partial c_{22}}{\partial \theta} \right), & q_6(\theta) &= \frac{c_{24}}{c_{22}}, \\
 q_7(\theta) &= \frac{1}{c_{22}} \left(\lambda_m (c_{25} + c_{46}) + c_{46} + \frac{\partial c_{24}}{\partial \theta} \right), & q_8(\theta) &= \frac{1}{c_{22}} \lambda_m \left((\lambda_m + 1) c_{56} + \frac{\partial c_{25}}{\partial \theta} \right), \\
 q_9(\theta) &= \frac{e_{22}}{c_{22}}, & q_{10}(\theta) &= \frac{1}{c_{22}} \left(\lambda_m (e_{12} + e_{26}) + e_{26} + \frac{\partial e_{22}}{\partial \theta} \right), & q_{11}(\theta) &= \frac{1}{c_{22}} \lambda_m \left((\lambda_m + 1) e_{16} + \frac{\partial e_{12}}{\partial \theta} \right), \\
 q_{12}(\theta) &= \frac{d_{22}}{c_{22}}, & q_{13}(\theta) &= \frac{1}{c_{22}} \left(\lambda_m (d_{12} + d_{26}) + d_{26} + \frac{\partial d_{22}}{\partial \theta} \right), & q_{14}(\theta) &= \frac{1}{c_{22}} \lambda_m \left((\lambda_m + 1) d_{16} + \frac{\partial d_{12}}{\partial \theta} \right), \\
 & & & & & \tag{C.2}
 \end{aligned}$$

$$\begin{aligned}
 r_1(\theta) &= \frac{1}{c_{44}} \left(2\lambda_m c_{45} + \frac{\partial c_{44}}{\partial \theta} \right), & r_2(\theta) &= \frac{1}{c_{44}} \lambda_m \left(\lambda_m c_{55} + \frac{\partial c_{45}}{\partial \theta} \right), & r_3(\theta) &= \frac{c_{46}}{c_{44}}, \\
 r_4(\theta) &= \frac{1}{c_{44}} \left(c_{24} + \lambda_m (c_{14} + c_{56}) + \frac{\partial c_{46}}{\partial \theta} \right), & r_5(\theta) &= \frac{1}{c_{44}} \left(\lambda_m \left(\lambda_m c_{15} + c_{25} + \frac{\partial c_{14}}{\partial \theta} \right) + \frac{\partial c_{24}}{\partial \theta} \right),
 \end{aligned}$$

$$\begin{aligned}
r_6(\theta) &= \frac{c_{24}}{c_{44}}, & r_7(\theta) &= \frac{1}{c_{44}} \left(\lambda_m c_{25} + (\lambda_m - 1) c_{46} + \frac{\partial c_{24}}{\partial \theta} \right), & r_8(\theta) &= \frac{1}{c_{44}} (\lambda_m - 1) \left(\lambda_m c_{56} + \frac{\partial c_{46}}{\partial \theta} \right), \\
r_9(\theta) &= \frac{e_{24}}{c_{44}}, & r_{10}(\theta) &= \frac{1}{c_{44}} \left(\lambda_m (e_{14} + e_{25}) + \frac{\partial e_{24}}{\partial \theta} \right), & r_{11}(\theta) &= \frac{1}{c_{44}} \lambda_m \left(\lambda_m e_{15} + \frac{\partial e_{14}}{\partial \theta} \right), \\
r_{12}(\theta) &= \frac{d_{24}}{c_{44}}, & r_{13}(\theta) &= \frac{1}{c_{44}} \left(\lambda_m (d_{14} + d_{25}) + \frac{\partial d_{24}}{\partial \theta} \right), & r_{14}(\theta) &= \frac{1}{c_{44}} \lambda_m \left(\lambda_m d_{15} + \frac{\partial d_{14}}{\partial \theta} \right),
\end{aligned} \tag{C.3}$$

$$\begin{aligned}
s_1(\theta) &= \frac{1}{\eta_{22}} \left(2\lambda_m \eta_{12} + \frac{\partial \eta_{22}}{\partial \theta} \right), & s_2(\theta) &= \frac{1}{\eta_{22}} \lambda_m \left(\lambda_m \eta_{11} + \frac{\partial \eta_{12}}{\partial \theta} \right), & s_3(\theta) &= -\frac{e_{26}}{\eta_{22}}, \\
s_4(\theta) &= -\frac{1}{\eta_{22}} \left(e_{22} + \lambda_m (e_{16} + e_{21}) + \frac{\partial e_{26}}{\partial \theta} \right), & s_5(\theta) &= -\frac{1}{\eta_{22}} \left(\lambda_m \left(\lambda_m e_{11} + e_{12} + \frac{\partial e_{21}}{\partial \theta} \right) + \frac{\partial e_{22}}{\partial \theta} \right), \\
s_6(\theta) &= -\frac{e_{22}}{\eta_{22}}, & s_7(\theta) &= -\frac{1}{\eta_{22}} \left(\lambda_m e_{12} + (\lambda_m - 1) e_{26} + \frac{\partial e_{22}}{\partial \theta} \right), \\
s_8(\theta) &= -\frac{1}{\eta_{22}} (\lambda_m - 1) \left(\lambda_m e_{16} + \frac{\partial e_{26}}{\partial \theta} \right), & s_9(\theta) &= -\frac{e_{24}}{\eta_{22}}, & s_{10}(\theta) &= -\frac{1}{\eta_{22}} \left(\lambda_m (e_{14} + e_{25}) + \frac{\partial e_{24}}{\partial \theta} \right), \\
s_{11}(\theta) &= -\frac{1}{\eta_{22}} \lambda_m \left(\lambda_m e_{15} + \frac{\partial e_{25}}{\partial \theta} \right), & s_{12}(\theta) &= \frac{g_{22}}{\eta_{22}}, & s_{13}(\theta) &= \frac{1}{\eta_{22}} \left(2\lambda_m g_{12} + \frac{\partial g_{22}}{\partial \theta} \right), \\
s_{14}(\theta) &= \frac{1}{\eta_{22}} \lambda_m \left(\lambda_m g_{11} + \frac{\partial g_{12}}{\partial \theta} \right),
\end{aligned} \tag{C.4}$$

$$\begin{aligned}
t_1(\theta) &= \frac{1}{\mu_{22}} \left(2\lambda_m \eta_{12} + \frac{\partial \mu_{22}}{\partial \theta} \right), & t_2(\theta) &= \frac{1}{\mu_{22}} \lambda_m \left(\lambda_m \eta_{11} + \frac{\partial \eta_{12}}{\partial \theta} \right), & t_3(\theta) &= -\frac{d_{26}}{\mu_{22}}, \\
t_4(\theta) &= -\frac{1}{\mu_{22}} \left(d_{22} + \lambda_m (d_{16} + d_{21}) + \frac{\partial d_{26}}{\partial \theta} \right), & t_5(\theta) &= -\frac{1}{\mu_{22}} \left(\lambda_m \left(\lambda_m d_{11} + d_{12} + \frac{\partial d_{21}}{\partial \theta} \right) + \frac{\partial d_{22}}{\partial \theta} \right), \\
t_6(\theta) &= -\frac{d_{22}}{\mu_{22}}, & t_7(\theta) &= -\frac{1}{\mu_{22}} \left(\lambda_m d_{12} + (\lambda_m - 1) d_{26} + \frac{\partial d_{22}}{\partial \theta} \right), \\
t_8(\theta) &= -\frac{1}{\mu_{22}} (\lambda_m - 1) \left(\lambda_m d_{16} + \frac{\partial d_{26}}{\partial \theta} \right), & t_9(\theta) &= -\frac{d_{24}}{\mu_{22}}, & t_{10}(\theta) &= -\frac{1}{\mu_{22}} \left(\lambda_m (d_{14} + d_{25}) + \frac{\partial d_{24}}{\partial \theta} \right), \\
t_{11}(\theta) &= -\frac{1}{\mu_{22}} \lambda_m \left(\lambda_m d_{15} + \frac{\partial d_{25}}{\partial \theta} \right), & t_{12}(\theta) &= \frac{g_{22}}{\mu_{22}}, & t_{13}(\theta) &= \frac{1}{\mu_{22}} \left(2\lambda_m g_{12} + \frac{\partial g_{22}}{\partial \theta} \right), \\
t_{14}(\theta) &= \frac{1}{\mu_{22}} \lambda_m \left(\lambda_m g_{11} + \frac{\partial g_{12}}{\partial \theta} \right).
\end{aligned} \tag{C.5}$$

個人簡歷

胡政甯 Cheng-Ning Hu

出生日期：1984.05.24

電子郵件：chengning.cv91@nctu.edu.tw

學歷

台北縣私立南山高級中學 普通科	1999.09 ~ 2002.06
國立交通大學 土木工程學系 大學部	2002.09 ~ 2005.06
國立交通大學 土木工程學系 結構工程組 碩士班	2005.09 ~ 2006.06
國立交通大學 土木工程學系 結構工程組 博士班	2006.09 ~ 2013.06

經歷

國立交通大學 材料科學與工程學系 兼任講師	2013.03 ~ 2013.07
-----------------------	-------------------

證照

民國 101 年 公務高考 結構工程高考	及格
民國 101 年 專技高考 結構工程技師	錄取

獲獎紀錄

92 學年度 第一學期 土木工程學系	書卷獎
92 學年度 第一學期 土木工程學系	書卷獎
93 學年度 財團法人榮民榮譽基金會	績優學生獎學金
94 學年度 第一學期 土木工程研究所	書卷獎
99 學年度 第二學期 財團法人中興工程顧問社	優秀學生獎學金
101 學年度 財團法人中華工程顧問司	第九屆工程科技獎學金

發表期刊

- 1 C.S. Huang, C.N. Hu, Geometrically induced stress singularities in a piezoelectric body of revolution, Computers and Structures, pp1681-1696, 2011.
- 2 C.S. Huang, C.N. Hu, Three-Dimensional analyses of stress singularities at the vertex of a piezoelectric wedge, Applied Mathematical Modelling, pp 4517-4537, 2013.
- 3 C.S. Huang, C.N. Hu, Singularity Analysis for a Magneto-electro-elastic Body of Revolution, Composite Structures, pp 55-70, 2013

研討會論文

- 1 C.C. Chen, W.M. Yu, C.N. Hu, Self-Centering steel moment resisting frames with supplemental column, 2006
- 2 王榮進、陳誠直、翁正強、蘇晴茂、胡政甯、蔡煒銘，Ductile behavior of steel beam to encased steel reinforced concrete column connections, 中華民國第九屆結構工程研討會，2008